Oxidative stress and metal homeostasis at the air-lung interface in Chronic Obstructive Pulmonary Disease

Leong-Smith, Pheneatia Yat Hwa

Awarding institution:
King's College London

Title: Oxidative stress and metal homeostasis at the air-lung interface in Chronic Obstructive Pulmonary Disease

Author: Phe Leong-Smith

Oxidative stress and metal homeostasis at the air-lung interface in Chronic Obstructive Pulmonary Disease

Miss Pheneatia Leong-Smith

Department of Forensic Science and Drug Monitoring

Pharmaceutical Sciences Research Division

School of Biomedical and Health Sciences

King's College London

Thesis submitted to the University of London in fulfillment of the requirements for the degree of Doctor of Philosophy

November 2012

Declaration

I, Pheneatia Leong-Smith, declare that all of the work submitted in this thesis is my own, with the following exceptions; bronchial instillation and subsequent bronchial wash were carried out within the Department of Respiratory Medicine and Allergy, University Hospital, Umeå, Sweden.

Signed: _____ (Student)

Signed: _____ (Supervisor)

Date: _____

Acknowledgements

This is probably the easiest section that I have had the pleasure of writing. Whilst there are many that may have contributed in a small way (and are still very much appreciated), there are two people that have truly been amazing. I will be forever grateful for the continued support given by both Dr. Ian Mudway and Dr. Mark Parkin. They have been unshakeable in their dedication and honesty with me throughout this intensely demanding process. I would also like to extend my thanks to Dr. Vincenzo Abbate for sneaking me into his laboratory so that I could synthesise my compound in peace and Dr. Leon Barron for helping me preserve my sanity.

In addition to the academic staff acknowledgements, thanks must also be given to my Mother who provided me with the financial means in order to complete my research as well as my Grandmother. Both have managed to pass on tenacious, dedicated and resistant traits which have served me well. You can take the girl out of the East End but you can't take the East End out of the girl.

I would also like to thank my friends and my special man Layne, who have been neglected for quite some time and have had to endure the mood-swings (which I have since discovered are perfectly normal). It feels like a century has passed since I began at King's and our shared office was without a doubt the best I've ever worked in! After all this, the beers and rum buckets are on me (and the Bols too if I can find enough).

Contents

Tables

Figures

Abstract

Background: Chronic obstructive pulmonary disease (COPD) represents a spectrum of disorders encompassing chronic bronchitis and emphysema, associated with cough, excess mucus and exercise-related dyspnoea and characterized by a progressive reduction in airflow. Development of these symptoms is associated with chronic exposure to noxious particles or gas, most commonly from tobacco smoking, which triggers abnormal inflammation in the lung. Consistent with this increased inflammatory burden, oxidative stress has been demonstrated in COPD patients, largely through determination of antioxidant and oxidative damage marker concentrations in exhaled breath condensate and induced sputum. Whilst these samples are easier to obtain than bronchoscopy-based lavage, there remains contention concerning how well they reflect the distal airway lining fluids and hence the actual disease state. In the present study, I therefore investigated the oxidative status of bronchoalveolar lavage fluids (BAL) from well defined groups of COPD patients; current and ex-smoker, as well as aged and smoking matched controls. In addition, as COPD has been argued to be a disease of accelerated ageing a group of young controls was included to examine the extent to which age influences the endpoints under consideration.

Chapter 2: In the first experimental chapter I investigated the evidence for oxidative stress in the airways of subjects with COPD (smokers and ex-smoking) relative to age and smoking matched controls. In addition, young healthy non-smokers and mild asthmatics were included to investigate the impact of age on the examined parameters, as well as to compare antioxidant defences in the context of acute and chronic inflammation. In this chapter, I examined respiratory tract lining fluid antioxidants sampled in bronchoalveolar lavage fluid, focusing on low molecular weight antioxidants (glutathione, urate and ascorbate) and their oxidation products (glutathione disulphide and dehydroascorbate), the lipid oxidation product 4-hydroxy-2-nonenal and the endogenous metal transport and storage proteins (transferrin, lactoferrin and ferritin). I found no simple evidence of oxidative stress related to the

presence of COPD, but observed smoking-related increases in glutathione and ferritin, and age-related increases in dehydroascorbate and 4-hydroxy-2-nonenal.

Chapter 3: In the second experimental chapter I attempted to understand the age-related increase in oxidation markers observed in the lavage samples from chapter 2. Pro-oxidant metal (Fe and Cu) concentrations were determined in the lavage samples from each of the groups used in chapter 2, by inductively coupled plasma mass spectrometry and a novel assay was developed based on metal catalysed oxidation of ascorbate, to provide a functional measure of the catalytically active metal pools at the surface of the lung. Through the use of selective chelators, the relative contribution of labile Fe and Cu pools was assessed. In this chapter I was able to demonstrate that respiratory tract lining fluid Cu concentrations increased with age, in parallel to an increased pro-oxidant status in the RTLF and evidence of a non-transferrin bound Fe pool. These indices appeared related to the concentration of oxidation markers reported in chapter 2.

Chapter 4: Given the failure to detect increases in gross measures of oxidative damage in COPD patients, it was decided that the focus should shift toward a more refined focus on specific oxidations to proteins functionally related to the pathogenesis of the disease. I decided based on the pre-existing literature, that there was merit in focusing on 4-hydroxy-2-nonenal adduction of proteins. To achieve this, I attempted to develop a mass spectrometry-based method for the identification of adducted proteins and protein sequences. This was an ambitious undertaking and unfortunately I was only able to take these experiments so far, but at least was able to demonstrate the feasibility of the method. The methodology developed was sufficiently promising to warrant further investigation after the completion of my PhD.

Short conclusion: In this study I was unable to demonstrate any evidence of oxidative stress in the airways of patients with COPD, either ex- or current smokers. I did however, observe evidence of increased oxidative damage, catalytic metal (Cu) concentrations and pro-oxidant metal activities (Cu and non-transferrin bound Fe) with age. At the end of this thesis, despite the attempt to investigate markers of

oxidative stress in a relevant compartment (the distal lung) and in carefully controlled groups (aged and smoking matched), the role of oxidative processes in COPD remains oblique.

Abbreviations

4-HNE	4-hydroxy-2-nonenal
AA	Ascorbic acid
AAT	α_1-antitrypsin
ACN	Acetonitrile
AGC	Automatic Gain Control
AH_2	Ascorbate / Ascorbic acid
AP-1	Activator protein-1
ASCII	American Standard Code for Information Interchange
AT	Angiotensin
BAL	Bronchoalveolar lavage
BCA	Bicinchoninic acid
BHT	Butylated hydroxytoluene
BSA	Bovine Serum Albumin
BW	Bronchial wash
CID	Collision-Induced Dissociation
COPD	Chronic Obstructive Pulmonary Disease / Disorder
CT	Computed tomography
D_3-4-HNE	Deuterated 4-hydroxy-2-nonenal
DEE	Diethylether
DEP	Diesel exhaust particles
DES	Desferal (deferoxamine mesylate)
DNA	Deoxyribonucleic acid
DNPH	Dinitrophenylhydrazine
DTNB	5,5'-dithiobis(2-nitrobenzoic acid)
DTPA	Diethylene triamine pentaacetic acid
DTT	Dithiothreitol
ECD	Electron-Capture Dissociation
ECSOD	Extra-cellular superoxide dismutase
EDTA	Ethylenediaminetetraacetic acid

ELISA	Enzyme-linked immunosorbent assay
ESI	Electrospray ionisation
ETD	Electron-Transfer Dissociation
FEV_1	Forced Expiratory Volume in one second
FVC	Forced Vital Capacity
GC	Gas chromatography
GM-CSF	Granulocyte-macrophage colony-stimulating factor
GOLD	Global Initiative for Chronic Obstructive Lung Disease
GPx	Glutathione peroxidase
GSH	Glutathione (reduced)
GSSG	Glutathione disulphide (oxidised glutathione)
GSTM1	Glutathione-S-transferase 1
HDAC-2	Histone deacetylase II
HO-1	Heme oxygenase
IAM	Iodoacetamide
ICAM	Intercellular adhesion molecule
IgA	Immunoglobulin A
IgG	Immunoglobulin G
IL	Interleukin
INOS	Inducible nitric oxide synthase
LC	Liquid chromatography
LRTI	Lower respiratory tract infections
LTB_4	Leukotriene B4
MALDI-TOF	Matrix Assisted Laser Desorption - Time of Flight
MCPBA	3-chloroperoxybenzoic acid
MMP	Matrix metalloprotease
MPA	Metaphosphoric acid
MS	Mass spectrometry
MW	Molecular weight
NAB	N-nitrosoanabasine
NAT	N-nitrosoanatabine
NF-κB	Nuclear factor-κB

NMR	Nuclear Magnetic Resonance spectroscopy
NNK	4-(methylnitrosamino)-1-(3-pyridyl)-1-butanone
NNN	N-nitrosonornicotine
Nrf2	Nuclear erythroid-related factor-2
NT	Neurotensin
NTA	Nitrilotriacetate
PBS	Phosphate buffer solution
PMN	Polymorphonuclear leukocytes
PTM	Post-translational modification
RNS	Reactive nitrogen species
ROS	Reactive oxygen species
RTLF	Respiratory tract lining fluid
SHS	Second hand smoke
SIRT	Sirtuin
SMOC2	Secreted modular calcium-binding protein 2
SNP	Single nucleotide polymorphism
SRM	Selected reaction monitoring
TCEP	Tris(2-carboxyethyl)phosphine
TFE	Trifluoroethanol
(TGF)-β	Transforming growth factor
TIC	Total ion count
TMS	Tetramethylsilane
TNF-α	Tumour necrosis factor-α
UA	Urate / Uric acid
UHPLC	Ultra high performance liquid chromatography
UV	Ultraviolet
VCAM	Vascular cell adhesion molecule
VEGF	Vascular endothelial growth factor
WHO	World Health Organisation

Chapter 1:

Introduction

1.1 Definition and diagnosis of Chronic Obstructive Pulmonary Disease

Chronic Obstructive Pulmonary Disease (COPD) is defined as a disease state characterized by chronic, progressive airflow limitation, which is not fully reversible (through bronchodilator treatment) and exhibits an abnormal inflammatory response of the lungs to irritant stimuli. In addition to its pulmonary pathology, it is also associated with significant extra-pulmonary effects and important co-morbidities (GOLD 2008). This definition can be further expanded to include a pathophysiologic spectrum of diseases including chronic bronchitis, emphysema and small airways disease. Symptomatically COPD is associated with chronic cough, sputum production, wheezing and shortness of breath, related to underlying airway pathology.

The diagnosis of COPD is confirmed by spirometry, based on Forced Vital Capacity (FVC) and the Forced Expiratory Volume in one second (FEV_1). To distinguish between asthma and COPD a bronchodilator test is performed with lung function commonly measured following inhalation of Salbutamol. In COPD a bronchodilator response is often absent. The 2006 GOLD (Global Initiative for Chronic Obstructive Lung Disease) report classified COPD into four main diagnostic stages from mild to very severe, reflecting disease progression/severity and based on post-bronchodilator spirometry (**Table 1.1**). As a normal function of ageing, lung volumes are expressed as FEV_1/FVC ratio decreases, so to avoid the problematic fixed ratio of 0.7 the values

obtained are related to population reference values to prevent an over-diagnosis of COPD. These functional cut-offs, however, are not clinically validated in the absence of additional presenting symptoms such as general breathlessness and reduced exercise capacity (Calverley, 2004). The spirometry tests are however useful as a guide to disease progression and in assessing the effectiveness of disease management.

1.2 Prevalence, morbidity and mortality

COPD is a major cause of premature mortality worldwide, with current estimates indicating that 80 million individuals suffer from moderate to severe disease globally (Rabe, 2007). Placed as the sixth most prevalent cause of death in 1990 (Raherison, 2009), The World Health Organization (WHO) issued statistics in 2004 placing it as the fourth leading cause of mortality, with an estimated 3.02 million deaths attributable to this condition (WHO, 2008). With an increasing mortality rate, largely related to rates of cigarette and biomass smoke exposure, it is estimated that this spectrum of obstructive pulmonary disorders will become the third most common cause of chronic disability and death by the year 2020, following ischaemic heart disease and stroke (Gudmundsson, 2006).

Table 1.1: GOLD classification of COPD severity.

COPD stages	**FEV_1/FVC value**	**% predicted FEV_1**
Stage I: Mild	<0.7	≥80%
Stage II: Moderate	<0.7	≤50-80%
Stage III: Severe	<0.7	≤30-50%
Stage IV: Very Severe	<0.7	≤30-50% plus chronic respiratory failure

FEV_1 = forced expiratory volume in 1 second and FVC = forced vital capacity.

In the UK alone, approximately 900,000 individuals have been diagnosed with COPD. This does not take into account the acknowledged under-diagnosis of this condition, with the actual figure estimated to be in excess of 1.5 million (Devereux, 2006). Often escaping diagnosis until clinically advanced, death often occurs from secondary causes such as heart failure (Kon, 2008), resulting in COPD not being detailed as the cause of death. This misclassification of the precipitating cause of death also contributes toward the lack of public awareness of this condition, with almost half of all newly diagnosed patients unaware of the disease. COPD is also associated with other co-morbidities such as diabetes mellitus, malnutrition, depression, osteoporosis, gastro-oesophageal reflux, normocytic anaemia and lung cancer (Barnes, 2009), which mask its true prevalence in official statistics. This issue is further exacerbated by methodological issues relating to the absence of standardised spirometry protocols between countries for COPD diagnosis (Halbert, 2006). Even with these limitations it is evident that the prevalence of COPD is increasing, and that it is appreciably higher in current and ex-smokers over 40 years of age (Rabe, 2007).

Based on the current literature, global COPD mortality attributable to cigarette smoking is estimated at 54% for men and 24% for women, aged between 30-69 years (Ezzati, 2003). For those aged 70 or older, the estimates are similar; 52% and 19% for men and women respectively. Cigarette smoking makes a substantially greater contribution to COPD rates in industrialised countries; 84% for men and 62% for women aged 30-69. Studies carried out in developed countries have shown that the prevalence of COPD is almost equal between the two sexes which is believed to be as a direct consequence of increased tobacco smoking amongst women in general since

the 1960's (Rabe, 2007). Using primary health care data from the UK covering the period 1990 to 1997, Soriano *et al.* (2000) found that whilst more men were diagnosed with COPD than women, the annual prevalence rates for women had increased from 0.80% to 1.36%. By the mid 1990's, the prevalence of COPD in women aged 20-44 years had surpassed the figure for men; prevalence for women between 45-65 years was broadly equivalent to the male rates.

1.3 Aetiology

In the developed world over 90% of patients with COPD are reported to have a history of smoking (Lokke, 2006). Correspondingly, the occurrence of COPD among those who have never smoked is estimated to be between 3-15% in various populations (Buist, 2007; Menezes, 2005), suggesting that other inhaled irritants can play a role in the aetiology of obstructive airway disease. Globally however, as illustrated in the previous section the exposure of individuals to indoor air pollution derived from the combustion of biofuels for space heating and cooking in poorly ventilated housing, is also a significant contributor to the global burden of COPD. The role of cigarette smoking and occupational/environmental exposure to inhaled irritants will be discussed in the following sections.

1.3.1 Tobacco smoking

Tobacco smoke can be divided into "sidestream" and "mainstream" smoke, with the former attributable to the burning tip of a cigarette and the latter the smoke inhaled through the mouth piece. Cigarette smoke consists of a highly complex combustion-derived aerosol, including 95 known carcinogenic compounds (Fowles,

2000). The full toxicological profile of cigarette smoke has not been fully characterised, with data only available for a fraction of its constituents. The gaseous phase contains; carbon monoxide, ammonia, dimethylnitrosamine, formaldehyde, hydrogen cyanide and acrolein; whilst the particulate phase consists of metals, nicotine, tar, benzene, benzo[a]pyrene, nitrosamine, minor alkaloids, N-nitroso derivatives and polycyclic aromatic hydrocarbons (PAHs) (Cohen, 2007). A non-exhaustive list of the compounds associated with unburnt tobacco is presented in **Table 1.2**.

The role of cigarette exposure in COPD is well illustrated by the Fletcher curve (**Figure 1.1**), which illustrates a longitudinal series of lung function measurements in a cohort of men, including current, ex- and never smokers. The study by Fletcher (1977) demonstrated that age-related declines in lung function were accelerated in cigarette smokers, with clear differences between individuals in relation to their susceptibility to this response. Smoking cessation in this cohort of smokers was found to reduce the rate of functional decline to that seen in healthy non-smokers, but without restoration of the long-term loss in lung function.

1.3.2 Second-hand smoke exposure and the risk of COPD

The noxious irritants within tobacco smoke have also been shown to adversely affect the pulmonary function of individuals through second-hand smoke (SHS) exposure (Eisner, 2005; Jayet, 2005; Leuenberger, 1994). Studies have found that cumulative lifetime exposure to SHS, both at home and at work (Yin, 2007; Sezer, 2006) presents a greater risk for the development of COPD in later life. Consistent

with SHS having a detrimental effect on the lungs of non-smokers, worldwide studies on bar and hospitality workers, who have traditionally experienced high SHS exposures, have shown a significant reduction in cough and expectorate following the introduction of non-smoking laws in public buildings and workplaces (Menzies, 2006; Skogstad, 2006; Allwright, 2005).

Table 1.2: Representative cigarette constituents (non brand specific) and their approximate weight ranges per cigarette.

Constituents in unburned tobacco per cigarette	Approximate weight range of constituent per cigarette
Alkaloids	
Nicotine	mg
Nornicotine	µg
Anabasine	µg
Anatabine	µg
Metals	
Arsenic	ng
Nickel	ng
Lead	ng
Cadmium	ng
Chromium	ng
Selenium	ng
Mercury	ng
Iron	µg/ng
Copper	µg
Nitrosamines	
NNN	ng
NNK	ng
NAT	ng
NAB	ng
Other	
Benzo[*a*]pyrene	ng
Triacetine	µg
Nitrate	mg
Ammonia	µg
Glycerol	mg
Propylene glycol	mg

NNN (N-nitrosonornicotine); NNK (4-(methylnitrosamino)-1-(3-pyridyl)-1-butanone); NAT (N-nitrosoanatabine); NAB (N-nitrosoanabasine).

1.3.3 Outdoor air pollution (traffic and other sources)

Outdoor air pollutants are derived from a variety of combustion sources including industrial, traffic and heating sources. Unlike other risk factors, exposure to

air pollution is continuous, occurring throughout our lifetime. Weather conditions and changes in pollutant emissions result in variable daily exposures over time, with strong evidence indicating a correlation with acute exacerbations of COPD (Sunyer, 2001).

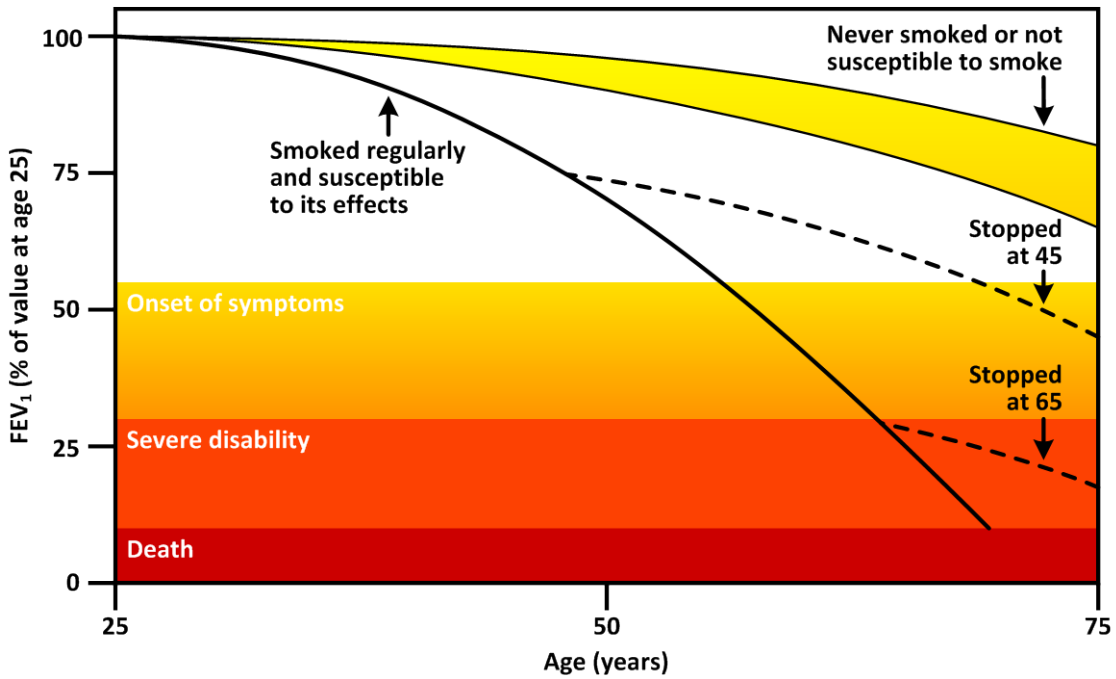

Figure 1.1: The Fletcher curve relating age related declines in lung function to cigarette smoking and illustrating the beneficial role of smoking cessation. The yellow/orange/red shaded areas illustrate how reductions in lung capacity are related to the onset of COPD symptoms.

Causal relationships between outdoor pollutant concentrations (including nitrogen dioxide, ozone and inhalable particulate matter, i.e. with a median aerodynamic diameter of <10, or 2.5µm, and decreased lung function have been shown in numerous cross-sectional studies (Holguin, 2007; Hogervorst, 2006). In support of a causal link between air pollution and poor lung function, studies have demonstrated improvements in respiratory health following reduction in ambient pollutant concentrations (particularly in ambient particulate matter) in cross-sectional

analyses (Sugiri, 2006; Frye, 2003). A further study demonstrated greater black carbon content (as a biomarker of exposure to particulate matter from fossil combustion) in sputum macrophages from individuals living near traffic and demonstrated that high black carbon loadings were associated with reduced FEV_1 (Kulkarni, 2006). Several longitudinal studies in children have also produced evidence that traffic derived pollutants may retard the lung development (Gauderman, 2007; Gauderman, 2000; Peters, 1999). Other large-scale cohort studies performed in Mexico and Europe have also associated impaired lung growth with chronic exposure to ambient particulate matter and nitrogen dioxide (a marker of traffic-related pollution) (Rojas-Martinez, 2007; Ihorst, 2004; Frischer, 1999). Whilst there is clear evidence from numerous cohort studies of a link between air pollutant exposure and impaired lung function (Downs, 2007; Schikowski, 2005) and retarded lung growth (Gauderman, 2007; Rojas-Martinez, 2007; Horak, 2002), at this time there is no definitive evidence linking outdoor pollutant exposure to the development of COPD.

1.3.4 Occupational exposure and the risk of COPD

As many workers with COPD have concurrent exposure to direct and indirect cigarette smoke, the role of occupational exposures in the aetiology of the disease is often difficult to distinguish from other risk factors. In addition, many studies are limited due to the difficultly in tracking job-leavers which effectively results in the under estimation of the role of these exposures. Nevertheless, a considerable body of literature exists linking specific occupational exposures to the development of COPD including: in miners of coal (Seixas, 1993; Attfield, 1992) and hard-rock minerals (Hnizdo, 1990; Holman, 1987), as well as tunnel (Ulvestad, 2001), concrete-

manufacturing (Meijer, 2001) and non-mining workers (Kauffmann, 1982). Toxicological studies also support the potential linkage between many of these exposure scenarios with lung pathology consistent with the induction of COPD. Agents such as endotoxin, sulphur dioxide, mineral dusts and vanadium have been shown to induce pathologically defined chronic bronchitis in animal models (Bonner, 2000; Harkema, 1993) and are known to be associated with chronic bronchitis in humans. Additionally, cadmium, coal and silica dusts (Shapiro, 2000) have been shown to induce emphysema in experimental animal models.

1.3.5 Biomass smoke and the risk of COPD

A significant proportion of COPD cases have been identified amongst never-smokers in developing countries, particularly in women who utilise open-fire stoves indoors for cooking and space heating, often in poorly ventilated homes. The fuel typically used in such stoves largely consists of wood, animal dung or crop residues collectively referred to as biomass. The combustion of such biomass results in particulate emissions far exceeding the concentrations observed in outdoor air (Smith, 1987). In the developing world, such exposure to biomass smoke begins *in utero* and spans an entire lifetime. The exposure during infancy has been shown to impair pulmonary function and defence, leading to the increased risk of developing respiratory infections and tuberculosis (Fullerton, 2008; Mudway, 2005; Smith, 2000). Numerous case-control and cross-sectional studies have demonstrated chronic bronchitis and/or airflow obstruction associated with biomass exposure in developing countries (Orozco-Levi, 2006; Kiraz, 2003). In a Mexican study a 4% decrease in FEV_1/FVC was observed in female never-smokers who cooked regularly with indoor

open-fire stoves (Regalado, 2006). A further study from Colombia demonstrated a greater risk of COPD development (defined by spirometry as per the GOLD criteria) upon use of biomass stoves for 10 or more years (Caballero, 2008). Countries such as China and India also use soft coal or “smoky coal” as fuel for domestic use, which is more polluting than conventional biomass fuels. The use of soft coal has been associated with COPD diagnosis in China (Zhou, 1995) and improved indoor ventilation with reduced incidents of COPD diagnosis (Chapman, 2005).

1.3.6 Chronic asthma and COPD

The development of asthma in later adulthood (≥65 years of age) is associated with less airway obstruction than that observed in subjects with early-onset asthma (Braman, 1991). This suggests a causal linkage between the effects of asthma and chronic airway obstruction; with prolonged asthma sufferers displaying more severe airway obstruction. Computed tomography (CT) of the thoracic region carried out on adults diagnosed with asthma and irreversible airway obstruction combined, have revealed a thickening of the bronchial wall (Vignola, 2004). Such scans also observed emphysema in some non-smoking asthmatic patients, in particular, those who had suffered long-standing asthma, irreversible airway obstruction and asthma of a greater severity (Kondoh, 1990).

As a normal function of ageing, lung capacity generally declines at approximately 20 ml/yr from the age of 25 onwards (Lange, 1998). The Copenhagen City Heart Study revealed an association between asthma and an accelerated decline in pulmonary function in both smoking and non-smoking subjects (Ulrik, 1994). Other

factors contributing towards an excess decline in pulmonary function for those with asthma included: low FEV_1 (Ulrik, 1992), decreased reversibility to β_2-agonists (Ulrik, 1999), increased severity in bronchial hyper-responsiveness (Van Schayck, 1991), excess mucus production (Lange, 1998), frequent exacerbations (Bai, 2007) and being male (Ulrik, 1994). In addition, evidence suggests lung function impairment observed in adulthood is closely linked with childhood asthma (Tennant, 2008). In the Tucson study, asthmatic phenotypes such as persistent wheezing observed in 3-6 year old children was associated with a lower FEV_1 in 16 year olds (early adulthood) (Morgan, 2005).

In summary, chronic airway obstruction and accelerated loss of pulmonary function are associated with chronic asthma. As airway obstruction can lead directly to the progression to COPD, asthma (both in the presence and absence of other risk factors) can therefore be assumed as a predisposition to the development of COPD. It is not confirmed, however, whether asthmatic adults meet COPD criterion such as the GOLD spirometric values or are similar or distinct in phenotype and pathology from clinically encountered COPD. Asthma, although an allergic airway disease, may display an increased neutrophil infiltration into the airways related to disease severity, which is more aligned with COPD (Wenzel, 1999). In order to establish a definitive causal link, further studies are required to elucidate the sub-phenotypes of COPD.

1.3.7 Tuberculosis and the risk of COPD

Tuberculosis has been strongly associated with a greater risk of developing COPD (Caballero, 2008; Menezes, 2007). An increased risk of tuberculosis has also

been linked with exposure to cigarette (Lowe, 1956) and biomass smoke (Pérez-Padilla, 2001; Mishra, 1999), illustrating the complex interactions between smoke inhalation and altered lung function.

1.3.8 Genetic factors and COPD

Whilst the development of COPD has been associated with exposure to tobacco smoke, only around 15% of smokers develop the disease (ATS, 1996). Thus an individual's genetic background is clearly important in determining whether the disease will occur and subsequently the rate at which it progresses, and/or responds to treatment (Silverman, 2006; Young, 2006). The first and only proven genetic risk factor for COPD is the α_1-antitrypsin gene (SERPINA1), which is estimated to be present in 1% of individuals with COPD (DeMeo, 2006). This gene, SERPINA1, located on chromosome 14 encodes a serine protease inhibitor which provides protection against proteolytic damage in the lung (Ekeowa, 2011). Deficiency in α_1-antitrypsin (AAT) is an established genetic risk factor for COPD in non-smoking individuals and is an autosomal recessive-inherited deficiency (Bossé, 2009). Two common alleles (S and Z) are associated with AAT deficiency, with individuals homozygous for the Z allele at high risk of COPD. Recently, evidence has emerged that the MZ genotype is also associated with lung function decline in the general population and smokers (Dahl, 2002; Sandford, 2001), as well as airway obstruction in COPD patients (Sandford, 1999). A more comprehensive discussion of AAT deficiency is provided in section 1.5.6.

Other rare genetic disorders implicated in the possible pathogenesis of COPD in non-smokers include Cutis Laxa, a rare hereditary disorder of the elastic fibres, caused by mutations in the elastin gene (Rodriguez-Revenga, 2004). This condition has been linked with emphysema during childhood and adolescence in non-smoking subjects, as well as in those who smoke (Van Maldergem, 1988; Turner-Stokes, 1983). Marfan syndrome (Wood, 1984), Ehlers-Danlos syndrome (Dowton, 1996) and Birt-Hogg-Dube syndrome (Ayo, 2007) have also been proposed as possible risk factors for the development of COPD, however, no definitive association has been observed to date.

A number of linkage studies have been performed to identify genes involved in COPD and impaired lung function. Amongst these is the Framingham study, which employed >300 families and identified a region on chromosome 6q as being potentially related to an increased risk of COPD (Joost, 2002). In addition, a number of chromosomal regions influencing lung function (FEV_1 and FVC) were also identified. One candidate gene on chromosome 6, SMOC2 (secreted modular calcium-binding protein 2), which contains a serine protease inhibitor domain has been studied in detail, with significant associations noted between a number of single-nucleotide polymorphisms (SNPs) and lung function in never-smokers (Wilk, 2007). A smaller linkage study of 72 families found evidence for linkage between mild obstructive lung disease in smokers with a region on chromosome 12 containing microsomal glutathione-S-transferase 1 (GSTM1) (Silverman, 2002).

Alternative approaches to gene identification include candidate gene association studies. A number of candidate genes involved in inflammation, immune response, antioxidant defence, protease/anti-protease imbalance and xenobiotic metabolism have been investigated in the quest to elucidate the genetic determinants of COPD, along with related phenotypes of the disease. Around 57 genes have been reported as having a positive association with COPD and lung function (Bossé, 2009); however, there are notable disparities and inconsistencies in the results (Hersh, 2005). Higher SERPINE2 expression has been reported in subjects with moderate to severe emphysema, independent of α_1-antitrypsin deficiency, compared with controls (DeMeo, 2006) and five significant SNPs have been reported in this gene related to a range of COPD phenotypes (DeMeo, 2006; Zhu, 2007). Similarly, a study by Joos *et al.* (2002) associated various SNPs in the MMP1 gene and promoter region and MMP12 to rapid lung function decline in a group of 284 smokers.

The low activity haplotype (His113–His139) in the gene for phase two xenobiotic enzyme microsomal epoxide has also been identified as being related to rapid lung function decline in smokers (Sandford, 2001). In addition, possession of this haplotype combined with a family history of COPD was associated with a six-fold increase in the risk of enhanced lung function decline in these smokers (Sandford, 2001). The His113 genotype in this gene has also been associated with COPD (Yoshikawa, 2000; Cheng, 2004).

In terms of inflammatory genes, the Q551R genotype in the gene for the IL-4 receptor (IL4RA, 5q31) has been associated with rapid decline in lung function in

smokers (He, 2003), as have the IL1β/IL1RN haplotypes (Joos, 2002). Specifically with respect to COPD, medium sized (53-182 patients versus 65-454 matched controls) association studies have shown an increased frequency in the IL-13 promoter polymorphism C-1055T (Van der Pouw, 2002) and IL-8RA G2044A SNPs (Stemmler, 2005) in patients than controls.

A recent genome-wide association study, examining 823 COPD subjects (current and ex-smoking) with 810 smoking control subjects, identified two single-nucleotide polymorphisms at the α-nicotinic acetylcholine receptor (CHRNA 3/5) as being associated with COPD (Pillai, 2009). The CHRNA 3/5 locus has previously been associated with increased smoking intensity, increased airflow obstruction and emphysema in COPD patients. Similarly, this locus has been identified a genetic risk factor for nicotine dependence and carcinoma of the lung (Spitz, 2008). Pillai *et al.* (2009) also identified a consistent replication of the hedgehog interacting protein (HHIP) locus and FAM13A locus on chromosome 4, although this was not shown to be significant genome-wide (Boezen, 2009). The HHIP locus has also been associated with both the systemic components of COPD and the frequency of COPD exacerbations, whilst the FAM13A locus is associated with airflow obstruction in COPD patients.

In summary, AAT deficiency and Cutis Laxa have been clearly associated with the development of COPD in non-smokers, whilst CHRNA 3/5, HHIP and FAM13A have been unequivocally associated with COPD amongst smokers (Pillai, 2010). These genetic epidemiology studies have confirmed the important influence of genetics in the development of COPD. Nonetheless, inconsistencies remain in the results of these

genetic association studies highlighting the need for further work to identify genetic variations causally linked to the development of COPD.

1.3.9 Diet and the risk of COPD

Dietary intake may affect pulmonary development, maintenance, function and response to injury (Aniwidyaningsih, 2008; Romieu, 2001). As an imbalance between oxidant production and endogenous antioxidant concentrations has been argued to predispose individuals to developing COPD, one might contend that a diet rich in antioxidants may proffer a protective defence against airway disease characterised by chronic and/or acute inflammation (Romieu, 2001).

A considerable body of evidence has demonstrated the beneficial effects of vitamin C on pulmonary function, with diets rich in this antioxidant being associated with greater FEV_1. Other antioxidants have also been evaluated and found to have beneficial effects on lung function, including: vitamin E, β-Carotene (Bonner, 2000; Churg, 1989), lutein (Harkema, 1993) and catechin (Shapiro, 2000). The importance of a good intake of dietary antioxidants was highlighted by a 25-year longitudinal investigation of 793 healthy middle-aged men in Zutphen, Netherlands, where an inverse relationship was established between the intake of fruits such as apples and pears and the incidence of chronic lung disease (Miedema, 1993). In contrast, randomised placebo-controlled trials using vitamin supplements C, E and β-carotene on a daily basis for 3 and 7 years have failed to demonstrate a positive impact upon the rate of decline of FEV_1 (Heart Protection Study Collaborative Group, 2002; Rautalahti, 1997). The effects of omega-3 polyunsaturated fatty acids and fish intake

have not been definitively established and whilst some studies have shown protective effects (Schunemann, 2001; Chuwers, 1997), others have found none (Guenegou, 2006; Kelly, 2003). Vitamin D has been positively associated with a potential effect on tissue remodelling and a higher mean FEV_1 in relation to a higher intake (Black, 2005).

In stark contrast, the intake of foods such as cured and processed meats has been shown to have deleterious effects (Varraso, 2007; Ricciardolo, 2006). Higher consumptions of such foods has been linked to lower FEV_1 and incidence of COPD, although it has been noted that these individuals are more likely to smoke, either actively or passively, have a higher body mass index, have reduced physical activity and consume a higher calorie vitamin deficient diet (Jiang, 2008; Jiang, 2007).

1.4 Pathology of COPD

The symptoms experienced by patients with COPD reflect long-term chronic remodelling of their airways due to their prolonged exposure to inhaled xenobiotics, particularly in the industrialised world to cigarette smoke. The recurrent cycles of injury, inflammation and repair over many years result in a range of pathologies leading to the development of mucus hyper-secretion, tissue destruction, and disruption to the normal repair and defence mechanisms. The results of these changes are increased airway resistance in small conducting airways, altered lung compliance, and the premature collapse of airways during expiration. The characteristic pathologies associated with COPD are described in the following sections.

1.4.1 Heterogeneity of COPD

As a condition, COPD encompasses several different diseases including chronic bronchitis, emphysema and small airways disease. These will be considered in the proceeding sections with a focus on the underlying tissue pathology and its impact on lung function. It should be noted however, that there is considerable overlap between these conditions and it is often difficult to dissect out the relative contribution of chronic bronchitis and emphysema to the clinical presentation of the disease. In addition, there can be substantial overlap with other obstructive lung diseases.

Although a clinically separate entity, long-standing chronic asthma (non-atopic intrinsic asthma) that fails to respond to treatment and becomes relatively irreversible also contributes towards COPD and is often clinically indistinguishable, causing diagnostic uncertainty. Whilst asthma is generally characterised by variable airflow obstruction, this is generally reversible upon administration of inhaled steroids. In long-standing chronic asthma, extensive remodelling of the airway including hypertrophy of the bronchial smooth muscle as well as collagen deposition in the basement membrane and submucosa can result in a degree of fixed airflow obstruction (Bellamy and Booker, 2005). As a result, the airways become unable to fully bronchodilate, similar to the situation in COPD.

1.4.2 Chronic bronchitis

Chronic bronchitis is classified as a chronic inflammation of the mucus membranes of the bronchi, associated with persistent cough and production of

sputum from the tracheobronchial tree for three or more consecutive months, over two successive years (Sethi, 1999). Clinically, as the condition worsens patients display a more chronic and persistent cough, exceptional dyspnoea and cyanosis. The presence of oedema, together with cyanosis secondary to cor pulmonale has resulted in the labelling of these patients as 'blue bloaters'.

The major pathologic feature of bronchitis is an increase in the mucus secreting apparatus of the airways, characterised by hyperplasia and hypertrophy of mucus cells and an increased number of goblet cells in the bronchial epithelium. The resultant excess mucus production observed in bronchitis contributes towards a decline in lung function as it obstructs the upper airways. Notably, inflammatory cells in the airways of patients with chronic bronchitis have been shown to release serine proteases and reactive oxygen species that act as secretagogues for mucus production exacerbating airway obstruction further (Sommerhoff, 1990; Shao, 2004). This obstruction through the expansion in the mucus secretory apparatus is also exacerbated by airway oedema. Damage to the airway epithelium, both through direct interaction with the toxic components of cigarette smoke and collateral injury arising from airway inflammation, is also apparent, reflected by squamous metaplasia of the bronchial epithelium and thickening of the basement membrane. Loss of ciliated epithelial cells also impairs the mucociliary elevator, promoting lower respiratory tract infections (LRTI). This results in further injury with irreversible damage to the smaller peripheral airways, where narrowing and distortion are observed (Barnett, 2006). Not all individuals develop COPD following bronchitis; approximately 80% of smokers do not exhibit an accelerated decline in their lung functions and can be diagnosed as

having ‘simple bronchitis’ (Bellamy and Booker 2005). A generalised illustration of the major pathologic features of the airway in chronic bronchitis is presented in **Figure 1.2**.

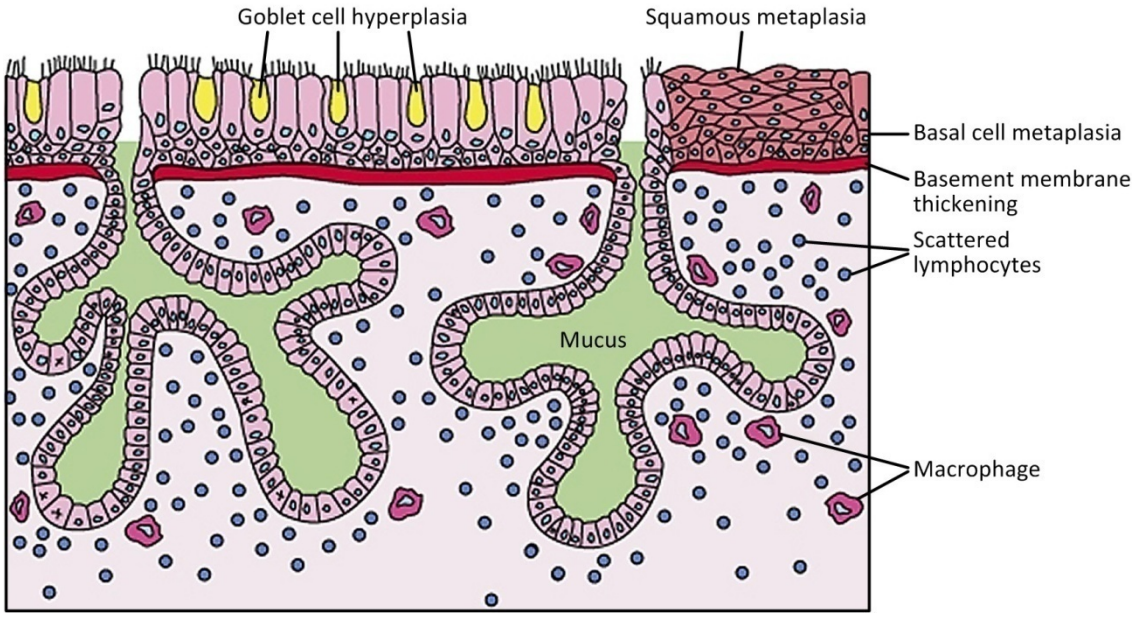

Figure 1.2: Illustration of the typical airway morphology in chronic bronchitis. Modified from a figure in Rubin “Essentials of Pathology” (Rubin, 2009).

1.4.3 Small airways disease

Bronchiolitis reflects pathologic changes to the bronchioles of the small airways (<2mm diameter), and is long-established as being a major cause of the obstruction characteristic of COPD (Hogg, 1968). Small airway obstruction has been associated with a remodelling (fibrosis and limited smooth muscle hypertrophy) and a thickening of the airway wall, allied to dysfunction of mucociliary clearance mechanisms (Hogg, 2004; Bellamy and Booker, 2005). The basis for this pathologic tissue adaptation has been proposed to be related both to the ongoing inflammation in the small airways (Saetta, 1998), with increased release of transforming growth factor (TGF)-β (Churg, 2006) as well as aberrant repair (Zandvoort, 2008).

1.4.4 Emphysema

Emphysema is defined as the abnormal and irreversible dilation of the terminal air spaces distal to the terminal bronchioles, accompanied by the destruction of their walls and loss of lung elasticity, in the absence of obvious fibrosis (Currie, 2007). Patients are characterised by the presence of a non-productive cough, in contrast to chronic bronchitis, associated with exertional dyspnoea. Radiologically they demonstrate hyperinflation of the lung, characterised by a depressed diaphragm and a barrel chest. Due to the higher ventilation rate in these patients they are able to maintain blood oxygenation and are therefore referred to as 'pink puffers'. It is a long-term progressive disease, with the rate of functional decline and the extent of pulmonary injury associated with an individual's smoking history. Approximately 40% of heavy smokers develop substantial emphysema (Hogg, 2004).

The protease-mediated destruction of alveolar walls in emphysema results in reduced maximal expiratory airflow via decreased elastic recoil. This occurs as a secondary consequence of the inflammation in the lung, due to the release of elastin, as well as by the apoptosis of endothelial cells and type I pneumocytes (Majo, 2001). The role of protease-antiprotease imbalance in the tissue destruction characteristic of emphysema is highlighted in subjects with α_1-antitrypsin enzyme deficiency, who display emphysemic pathologies even in the absence of exposure to inhaled xenobiotics, although this condition contributes toward just 2% of premature COPD.

Morphologically, emphysema is classified according to the location of the lesions within the acinus: panacinar (panlobular) or centriacinar (centrilobular) as

illustrated in **Figure 1.3**. The former classification is in reference to the mid-to-lower half of the lungs where distension and destruction are seen; the latter in reference to the upper lobes in the apex region of the lungs, where the respiratory bronchioles are damaged. In addition, a third classification exists, localised or paraseptal emphysema, in which the injury to the acinus occurs sporadically throughout the lung, with the remainder of the pulmonary parenchyma remaining largely unaffected. The lesions are often located at the apex of the upper lobes, where their progression can result in the formation of bulla; large areas of destruction.

1.4.5 Co-morbidities

It is now widely accepted that COPD is a systemic disease and that its morbidity and mortality is strongly related to co-morbid conditions (Sinden, 2010). For example, it is well-established that low FEV_1 is a risk factor for cardiovascular diseases and events and that chronic bronchitis can result in cor pulmonale (Sin, 2005). In addition to the established link with cardiovascular disease (Sin, 2005), associations have also been noted with lung cancer (Mannino, 2003), obesity and exercise intolerance (Sundh, 2011), diabetes (Song, 2010), osteoporosis (Dam, 2010), and anxiety/depression (Eisner, 2010). Mechanistically, presence of systemic inflammation in COPD provides a link between the pulmonary manifestations of COPD and the extra-pulmonary complications of this disease. This systemic inflammation has been hypothesised to reflect 'overspill' of inflammatory mediators produced in the lung into the circulation, though to date there is little firm evidence to support this contention (Zeng, 2009).

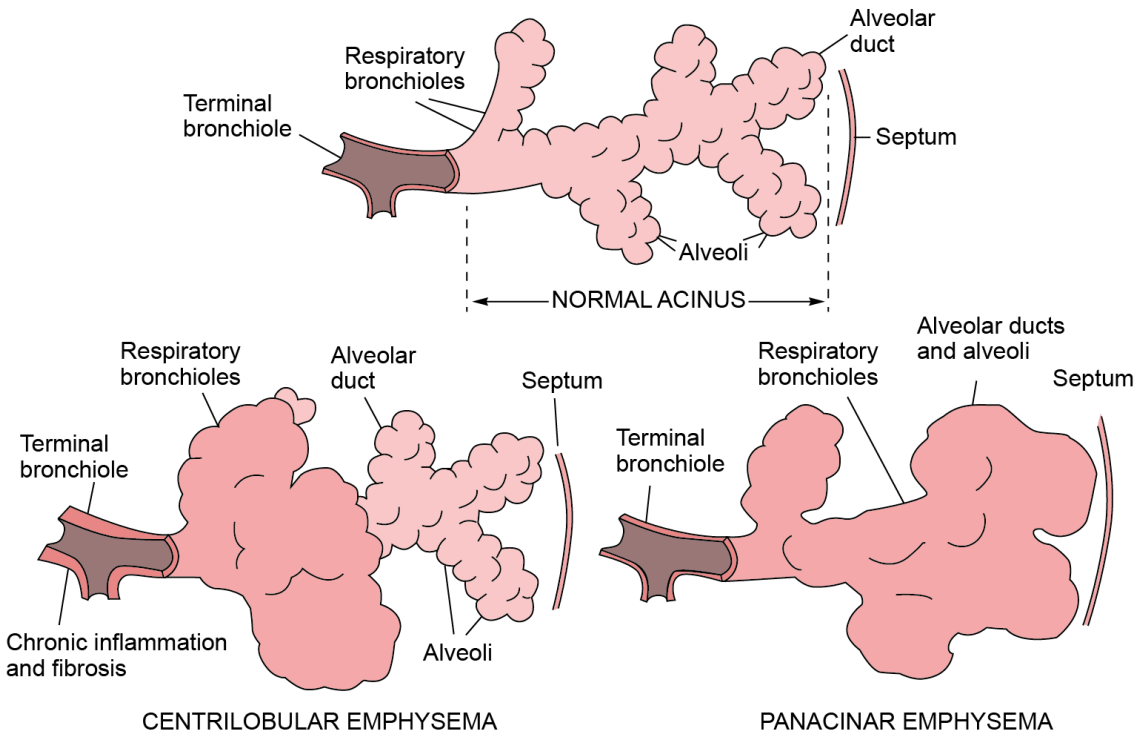

Figure 1.3: Morphologic features of emphysema. The upper panel illustrates a normal acinus distal to the terminal bronchiole, with the lower left and right hand panels demonstrating the sites of injury associated with centrilobular (injury to the respiratory bronchioles) and panacinar emphysema (affecting the whole acinus). Modified from a figure in Rubin's "Essentials of Pathology" (Rubin, 2009).

1.5 Mechanisms of injury in COPD

The pathologic features of COPD, and the characteristic remodelling of the airway leading to the irreversible obstruction, reflect the chronic impact of recurrent episodes of inflammation on the lung. The following sections will review three key areas that have been related to the aetiology and progression of COPD: pulmonary and extra-pulmonary inflammation, oxidative stress and protease/anti-protease imbalance. Each of these processes are inter-related and all contribute significantly to the evolution of chronic bronchitis and emphysema.

1.5.1 Neutrophilic inflammation in COPD

COPD is characterised by a chronic inflammation of the small airways and lung parenchyma, with elevated numbers of macrophages, neutrophils and T lymphocytes observed (Barnes, 2003). The role of neutrophils has been highlighted by increased cell numbers, as well as enhanced concentrations of neutrophil degranulation products (such as elastase and proteinase-3) in lavage samples obtained from COPD patients relative to age-matched controls (Lacoste, 1993; Linden, 1993). Consistent with these findings, increased concentrations of neutrophil chemoattractants (TNF-α, IL-8 and IL-6) have been reported in induced sputum samples from patients with COPD, with their levels seemingly related to the degree of obstruction (Hacievliyagil, 2006). Significantly, the number of neutrophils in BAL fluid and sputum appears to increase as FEV_1 declines (Di Stefano, 1998; Stanescu, 1996) suggesting a link between neutrophilia and airflow limitation. In support of this contention, increased submucosal neutrophil numbers have been reported in severe COPD relative to smoking controls (Di Stefano, 2001), and increased neutrophilic inflammation has been observed during COPD exacerbations, associated with increased concentrations of LTB_4 (Sapey, 2006), TNF-α, GM-CSF and neutrophil elastase (Fujimoto, 2005).

1.5.2 The role of airway macrophages in COPD

Macrophages play a central coordinating role in the pathophysiology of COPD with evidence of increased numbers in the bronchial submucosa (Di Stefano, 1996; Saetta, 1993), bronchial glands (Saetta, 1998) and small airway epithelium (Turato, 2002) of COPD patients, and an apparent relationship between their number and the

extent of tissue destruction (Finkelstein, 1995) and disease severity (Russell, 2002). Their role in the aetiology of the condition has been inferred from the observation of increased numbers of macrophages in the respiratory bronchioles of the autopsied lungs of young accident victims, who were known smokers (Niewoehner, 1974). Macrophages release a number of compounds including inflammatory cytokines, reactive oxygen species, chemotactic factors, mucus gland activators, extracellular matrix proteins and a variety of matrix metalloproteases such as MMP-1 (*Interstitial collagenase*), MMP-2 (*Gelatinase-A*), MMP-7 (*Matrilysin*), MMP-9 (*Gelatinase-B*) and MMP-12 (*Macrophage metalloelastase*) (O'Donnell, 2006; Montano, 2004), capable of degrading a similar spectrum of proteins to those targeted by the neutrophilic neutral proteases (*Neutrophil elastase, Cathepsin G, Proteinase-3, Lysozyme, Collagenase and Gelatinase*) (Tetley, 1993) and therefore potentially relevant to the injury profile observed in COPD (Kumagai, 1999). Whilst the potential to induce mucus hypersecretion exists, through the secretagogue activity of products such as leukotriene B4 (LTB_4) and interleukin 1 (IL-1), the main focus on the role of macrophages in COPD and specifically emphysema, has centred on their capacity to degrade the extracellular matrix. *In vitro* studies have shown increased concentrations of MMP-1 and MMP-9 in the cultured alveolar macrophages harvested from the lungs of COPD patients (Finlay, 1997), whilst *in vivo* studies have demonstrated increased MMP-2, MMP-9 (Segura-Valdez, 2000) and MMP-12 immunoreactivity in airway biopsies from COPD subjects compared with healthy controls (Molet, 2005; Montano, 2004).

Macrophages harvested from the lungs of COPD patients have also been shown to have impaired phagocytosis, internalising fewer *E. coli* (Prieto, 2001) and *H. Influenza* (Berenson, 2006) than cells from relevant control groups. This deficiency is highly significant as almost half of all hospitalisations for exacerbations in COPD are related to bacterial infections, and bacterial colonisation of the lower airways is apparent in many patients (Weinreich, 2008). A recent study by Taylor *et al.* (2010) confirmed this reduced phagocytic activity to bacteria in monocyte derived macrophages from COPD patients and demonstrated that this was not related to patient medication, or the expressions of cell surface receptors involved in bacterial recognition: toll-like receptors 2 and 4, CD163, CD36 or the mannose receptor.

1.5.3 Lymphocytes in COPD

Airway lymphocytosis has also been reported in patients with COPD, with expansion of cytotoxic and helper T-cell numbers reported compared with both 'healthy' age-matched smokers and never-smokers. Cytotoxic T-cells ($CD8^+$) are understood to be the predominant subtype in COPD, with increased numbers observed in the large (O'Shaughnessy, 1997; Di Stefano, 2009) and small (Saetta, 1998) airway mucosa, as well as the smooth muscle (Baraldo, 2004) and bronchial arteries (Saetta, 1999). Significantly, a relationship has been demonstrated between the number of airway $CD8^+$ cells and lung function decline in COPD (O'Shaughnessy, 1997; Saetta, 1998), suggesting a functional role for these cells in the pathogenesis of the disease. Whilst the key function of this cell is to defend against viruses, via cytolysis of infected cells or the induction of apoptosis, collateral tissue damage may

occur during periods of inflammation (Cannon, 1988). The mechanism of damage to the lung parenchyma has not been fully resolved, but likely involves direct injury related to the release of the lytic substances perforin and granzyme (Garcia-Sanz, 1988). This contention found recent support with the observation that $CD8^+$ cells recovered from the sputum of COPD patients showed increased perforin expression and cytotoxic activity compared with cells extracted from control subjects (Chrysofakis, 2004). This is consistent with the evidence of activation of $CD8^+$ cells in both smokers and patients with COPD (Roos-Engstrand, 2009).

Along with CD8+ cells, increased numbers of T-helper cells (CD4+) have been reported in the small airways of smokers with COPD (Turato, 2002). Increased CD4+ cell numbers have also been observed in the large airways of smoking COPD patients relative to ex-smokers (Lapperre, 2006). T-helper cells contribute in the inflammatory process through the production of a variety of pro-inflammatory mediators including; the Th1 cytokines, TNF-α, granulocyte-macrophage colony-stimulating factor (GM-CSF), IFN-γ and IL-2, as well as members of the Th2 family (IL-4, IL-5 and IL-6). In addition to CD4+ and CD8+ cells, natural killer (NK) T lymphocytes have also been proposed as playing a role in COPD, with increased numbers reported in the large airway submucosa of COPD smokers, and their recruitment thought to occur as a consequence of repetitive cycles of viral and bacterial infection (Di Stefano, 1998).

1.5.4 Evidence of eosinophilic inflammation in COPD

Eosinophilic inflammation, although usually considered a feature of asthma and often used as a distinguishing factor, has been demonstrated in patients with COPD. Induced sputum samples from patients with stable COPD have reportedly shown the presence of eosinophilic inflammation in 20-40% of cases (Brightling, 2005; Pizzichini, 1998), mildly overlapping with the 50% of cases noted for asthmatic patients (Douwes, 2002). The recruitment of such cells is selectively mediated by Th2 cytokine-producing T cells and whilst the origin of eosinophilic inflammation in COPD is not well understood, it is assumed that its presence is indicative of an asthmatic component in fixed airway obstruction (Barnes, 1998). However, most studies on COPD patients exclude subjects with airflow obstruction and those with asthmatic features, thereby suggesting that eosinophil influx into the airway mucosa may be as a result of smoking and other mechanisms (Saha, 2006). Bronchial biopsies sampled from patients during acute COPD exacerbations have shown a 30-fold increase in eosinophil counts compared with samples from stable COPD patients (Saetta, 1994).

1.5.5 Mast cells in COPD

Mast cells have also been considered in the pathology of COPD, with greater numbers reported in smokers compared to ex-smokers (Mortaz, 2011). The activation of mast cells results in the coordinated release of pro-inflammatory mediators such as IL-4 and IL-3 which can influence the response of T cells, as well as histamine and cysteinyl leukotrienes which activate lung macrophages causing the generation of nitric oxide, lysosomal enzymes and cytokines. Mast cell-mediated injury in smokers

has been demonstrated in a number of studies; with histamine and tryptase concentrations elevated in bronchoalveolar lavage samples from smokers compared to healthy controls (Yamamoto, 1997; Kalenderian, 1988), and increased numbers of degranulated mast cells in lavage and bronchial tissue from smokers (He, 2004). Additionally, an increase in mast cell numbers has been observed in the airways and lung parenchyma of COPD patients in several human studies (Rahman, 2002). However, it remains unclear whether mast cells play a leading or supporting role in the pathogenesis of COPD.

1.5.6 Protease/antiprotease imbalance

The observation of emphysema in the lungs of non-smokers with α_1-antitrypsin deficiency (Laurell, 1963), coupled with the induction of emphysemic pathology in the lungs of rats following the intra-tracheal instillation of the cysteine protease papain (Gross, 1965), led to the contention that protease-antiprotease imbalance in the lung may be critical to the development of COPD. It is hypothesised that an imbalance between proteases and antiproteases in the lungs may occur either as a consequence of increased release of proteases from activated neutrophils and macrophages recruited to the airway, inhibition, or down-regulation of their corresponding antiproteases, or a combination of both. A list of the major proteases and their associated antiproteases from neutrophils and macrophages are summarised in **Table 1.3**.

Acute exposure to cigarette smoke has been shown to result in the recruitment and activation of neutrophils in the lung, associated with the release of neutrophil elastase (see section 1.5.1). Under normal circumstances α_1-antitrypsin (AAT) inhibits the activity of unbound neutrophil elastase and provides in excess of 90% of the protection against this protease within the lower respiratory tract (Vogelmeier, 1996). Therefore in individuals deficient in α_1-antitrypsin, tissue destruction as a result of unopposed proteolysis has been conjectured to be related to rapid lung function decline and the premature onset of COPD. Cigarette smoke-induced injury can also be seen in COPD patients without AAT deficiency, with evidence that elastase activity in bronchoalveolar lavage samples from these subjects is positively correlated with both the degree of emphysema, as assessed by computed tomography and airway diffusing capacity (Fujita, 1999). In this study the extent of tissue destruction was also found to be negatively associated with lavage AAT activity, again supporting the importance of protease-antiprotease imbalance in COPD. Cigarette smoke itself has been reported to directly inhibit AAT activity (Gadek, 1979), though this finding remains contentious (Stone, 1983). In addition to this enhanced degradation of elastin, severe AAT deficiency results in Z antitrypsin polymerisation in the lung, which acts as a neutrophil chemoattractant, enhancing neutrophil recruitment to the lung (Parmar, 2002).

Table 1.3: The main proteases associated with neutrophils and macrophages, with their corresponding antiproteases.

	Proteases	**Antiproteases**
Neutrophils	Serine proteases Neutrophil elastase Cathepsin G Proteinase-3	α_1-Antitrypsin Secretory leucoprotease inhibitor Elafin
Macrophages	Cysteine proteases Cathepsins A,B,E, K,L,S Matrix metalloproteases (MMP-8, MMP-9, MMP-12)	Cystatins Tissue inhibitors of MMP (TIMP1-4)

The relationship between elastase-induced injury and the expression of AAT is also not straight forward as lavage from COPD patients with severe AAT deficiency was found to retain significant elastase inhibitory activity, implying that other antiproteases may compensate for the loss of AAT activity (Morrison, 1987). Further to this, once AAT is bound to elastin it no longer appears to be significantly inhibited (Morrison, 1990).

It has also been argued that alveolar macrophages contribute to protease-antiprotease imbalance in COPD. Airway macrophage numbers are elevated in COPD patients and are rich sources of MMPs (as reviewed in section 1.5.2), the excess production of which has been argued to contribute to the accelerated breakdown of connective tissue (Kim, 2004). In support of this view, increased elastolytic activity is evident from the cultured macrophages from COPD patients relative to healthy controls (Mulley, 1994). Increased expression of MMP1, 9 and 12 has been observed

in macrophages harvested from the lungs of COPD patients relative to controls (Finlay, 1997; Molet, 2005), and increased MMP1, 2, 8 and 9 have been reported in airway biopsies by immunohistochemistry (Segura-Valdez, 2000). Importantly, alveolar macrophages from COPD patients have been shown to release less TIMP1 (tissue inhibitor of metalloproteinases and a major inhibitor of most MMPs) than controls (Pons, 2005), which would support an imbalance between protease and antiprotease activity *in vivo*.

Human secretory leucoprotease inhibitor (SLPI) also serves to protect the lung from protease-induced degradation, in conjunction with its antimicrobial and anti-inflammatory properties. A dominant serine protease inhibitor, SLPI is a cationic protein of 11.7 kDa found in the upper respiratory tract at the mucosal surface (Weldon, 2009). Neutrophils, macrophages, acinar cells of submucosal glands and epithelial cells have all been shown to be rich sources of SLPI. Proteases such as elastase, cathepsin G and trypsin (neutrophil derived), chymase and tryptase (mast cell derived) are all released during an inflammatory response (Doumas, 2005) and their detrimental actions are inhibited in part by the subsequent release of SLPI. In addition, SLPI has also been shown to possess immunomodulatory activity through the suppression of neutrophil elastase and IL-8 in the lung (Vogelmeier, 1996). Lavage studies targeting the physiological role of SLPI have suggested its main function is as a neutrophil elastase inhibitor, thus providing protection within the upper and lower respiratory tract. In contrast to α_1-antitrypsin, SLPI is capable of inhibiting neutrophil elastase that is bound to elastin and can therefore protect against both its free and bound forms.

The interaction between airway inflammation and protease/antiprotease imbalance is illustrated in **Figure 1.4**. This figure demonstrates how these processes contribute to the pathological features of the disease (reviewed in section 1.4), through the promotion of tissue injury and airway remodelling, as well as the induction of mucus hypersecretion.

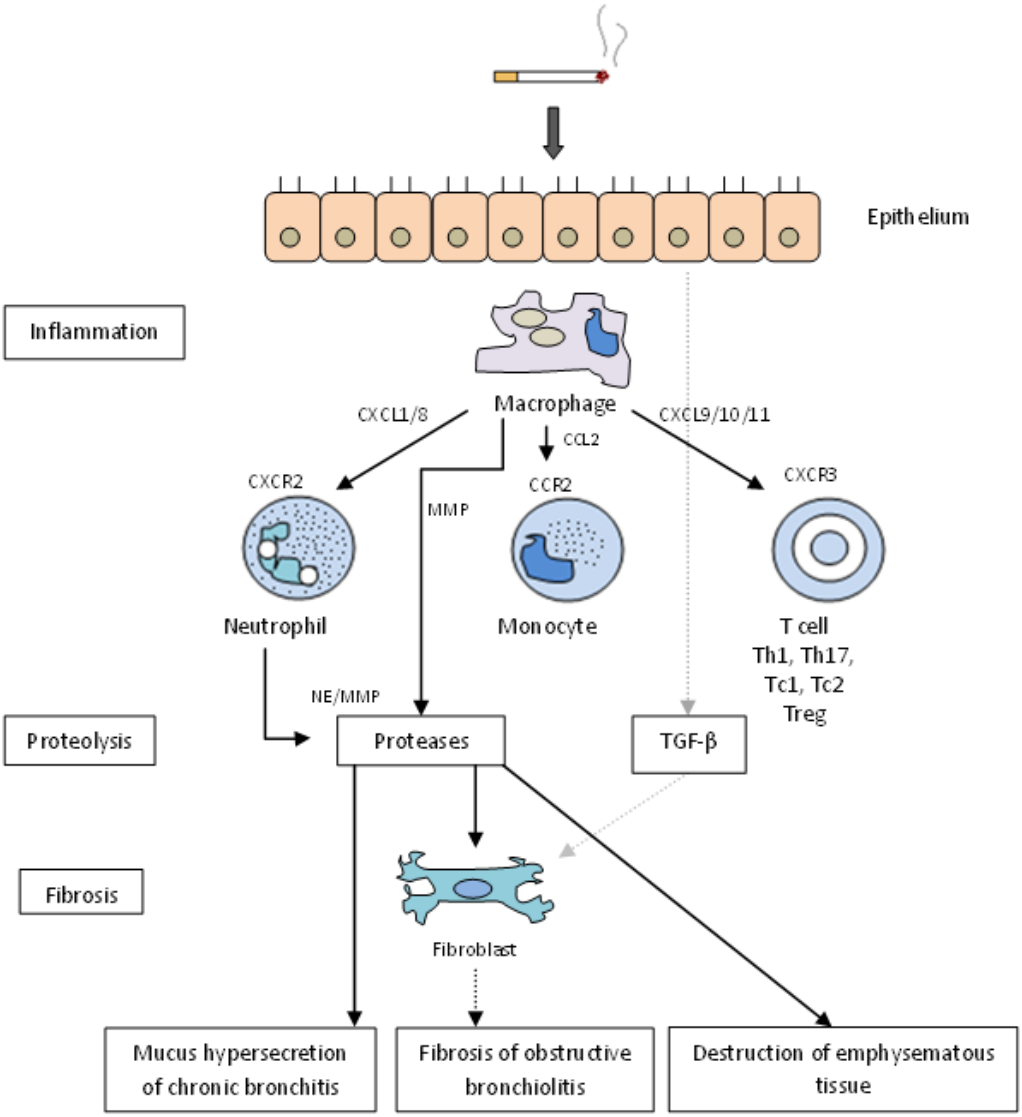

Figure 1.4: Inflammation, proteolysis and fibrosis in the lung caused by cigarette smoke. This figure illustrates the protease/antiprotease imbalance induced by cigarette smoke and the resulting injuries such as inflammation, mucus hypersecretion, fibrosis and damage of emphysematous tissue. CCL2 = C-C motif ligand 2 which is a monocyte chemoattractant protein-1 chemokine; CXCL1= C-X-C motif ligand which activates neutrophils (CXCL8 recruits neutrophils, CXCL9/10/11 are T-cell chemoattractants induced by interferon-γ); CCR2 = chemokine C-C motif receptor 2 which is a receptor for CCL2; CXCR2 = C-X-C motif receptor 2 which is a receptor for CXCL8 (CXCR3 is a receptor for CXCL9/10/11); MMP = matrix metalloproteinases; NE = neutrophil elastase; TGF-β = transforming growth factor beta; Th1 = T helper cell which is a lymphocyte (Th17 is a T helper cell that produces interleukin-17); Tc1 = cytotoxic T cell that secretes interferon-γ, interleukin-2 and tumour necrosis factor-α (Tc2 secretes interleukin-4); T reg = regulatory T cells that suppress the activation of the immune system.

1.5.7 Oxidative Stress

Biological systems are continuously exposed to free radicals and oxidants generated both endogenously and exogenously. Free radicals are defined as "any species capable of existing independently and which contain one or more unpaired electrons" (Halliwell and Gutteridge, 2007). Reactive oxygen species may contain non-radical derivatives of oxygen which have the capacity to participate in redox reactions, such as hydrogen peroxide, hypochlorous acid and ozone. Endogenous reactive oxygen species (ROS) are generated through normal cellular processes such as electron leakage from the mitochondrial electron transport chain during respiration and the activation of phagocytes during inflammation. Exogenous oxidants, or pro-oxidants (species that can promote reactive oxygen species generation *in vivo*) can be directly inhaled from the environment as a result of smoking, as well as exposure to ambient gaseous (ozone and nitrogen dioxide) and particulate pollutants (Rahman and MacNee 1996).

The gas and tar phases of cigarette smoke are known to contain high concentrations of reactive oxygen (ROS) and reactive nitrogen species (RNS) underpinning its capacity to elicit oxidative stress, both within the lung and systemically. Gas phase smoke alone has been conjectured to contain in excess of 10^{14} carbon- and oxygen-centred radicals per puff, including alkyl peroxynitrite, peroxynitrate esters, nitric oxide (NO) and nitrogen dioxide (NO_2) (Pryor, 1983; Cueto, 1994). The tar phase has also been shown to contain semiquinones (Pryor, 1997) and catalytic metals such as Fe, Cu, Ni and Cr (Stavrides, 2006) capable of redox cycling at the air-lung interface. This 'initial' oxidative insult is subsequently exacerbated by the

induction of inflammation, with further ROS produced via the activation of the phagocytic nicotinamide adenine dinucleotide phosphate (NADPH) oxidase (Kon, Hansel *et al.* 2008) – **Figure 1.5**.

The toxicity of exogenous oxidants to the lung, especially those present in cigarette smoke, needs to be viewed in the context of the endogenous antioxidant defences present at the air-lung interface, both within the extracellular respiratory tract lining fluid as well as intracellularly within the airway epithelial and resident inflammatory cell populations. These defences will be reviewed in section 1.6. The imposition of oxidative stress *in vivo* requires that the balance between the endogenous generation of oxidant species and the protective antioxidant pool is perturbed, either by increased production of the former, or decreases in the latter. This shift not only promotes damage to cellular components through lipid peroxidation, protein and DNA oxidation, but is also sufficient to trigger the up-regulation of redox sensitive transcription factors, such as nuclear factor kappa-light-chain-enhancer of activated B cells (NF-κB) which promotes the transcription of pro-inflammatory mediators, such as interleukin 8 (IL8) and IL6. The subsequent activation of airway phagocytes results in further production of ROS amplifying the damage and resulting in a detrimental cycle of inflammation and injury. In smokers and patients with COPD, the increased burden of oxidants arising from smoking and airway inflammation has been shown to result in oxidative stress, evidenced through increased concentrations of oxidative damage markers in the alveolar space, blood, breath and urine (MacNee, 2000). The intimate association between oxidative damage and inflammation is illustrated in **Figure 1.6**.

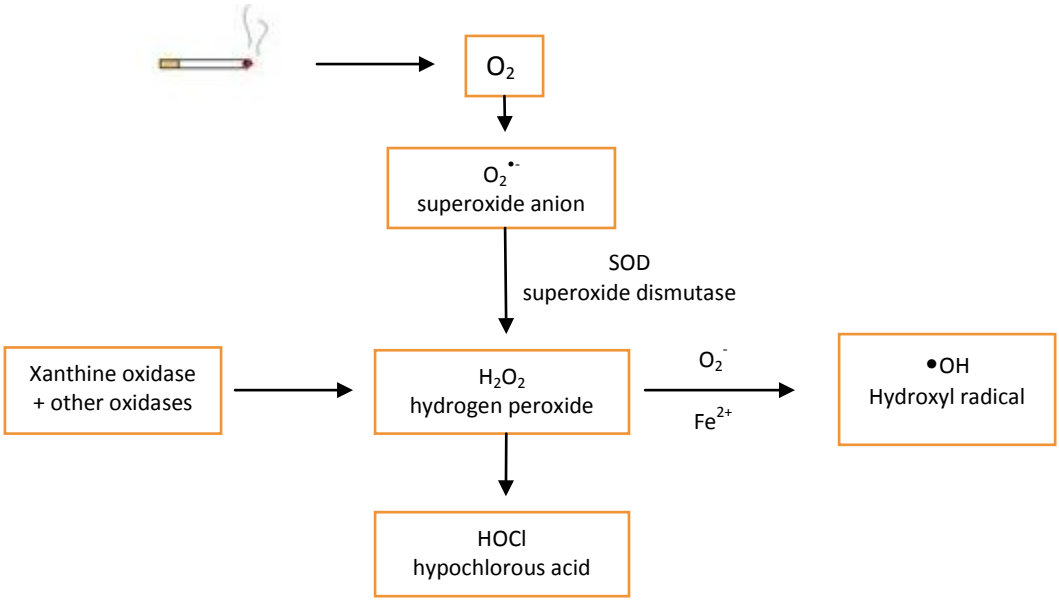

Figure 1.5: ROS induction by cigarette smoke and COPD airways. This simple scheme illustrates the initial formation of superoxide, via the reduction of oxygen and its subsequent transformation *in vivo* into more reactive species (hydroxyl radical), either via Fenton-type chemistry, or conversion to reactive halides, such as hypochlorous acid (HOCl).

1.6 Defence mechanisms of the lung

As the primary entry route of inhaled xenobiotics, the lung has evolved into a comprehensive antioxidant network at the air-lung interface, both within airway epithelial cells and the thin liquid layer that bathes the surface of the lung: the respiratory tract lining fluid (RTLF). The primary antioxidants found within the RTLF include the low molecular weight antioxidants glutathione, urate and ascorbate; the metal chelators lactoferrin, transferrin, ferritin and caeruloplasmin and the antioxidant enzymes extracellular superoxide dismutase and plasma glutathione peroxidase. These will be discussed in detail in the following sections.

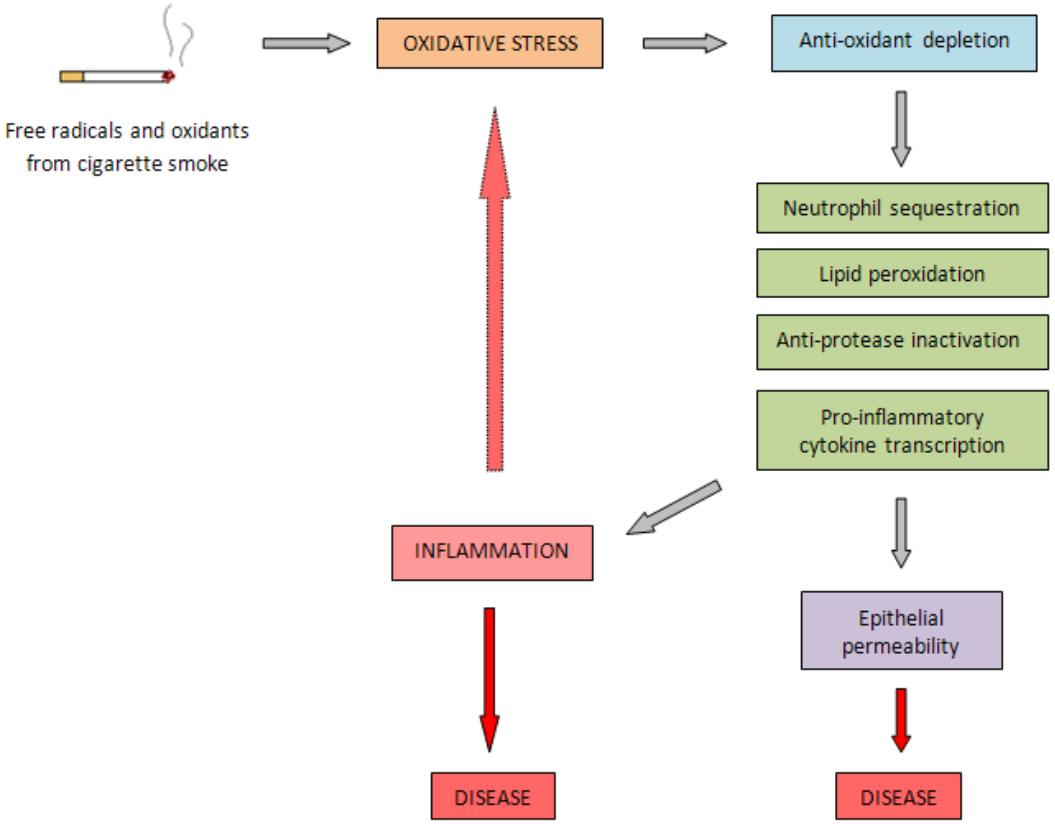

Figure 1.6: Oxidant-mediated lung injury in smokers.

1.6.1 Antioxidant defences within the RTLF

The RTLF exists as a bi-layered structure, with an upper mucus (Gel phase) and the lower aqueous layer (Sol phase), derived from plasma exudation and local synthesis from the lung epithelium and resident immune cells. It is believed to be continuous from the nasal airway to the alveolar region of the lung, though its thickness decreases from 10 µm in the former region to around 1 µm in the latter. This compartment therefore represents the first physical interface encountered by inhaled particulates and gases, and as such, is critical in mitigating against oxidative injury to the underlying epithelium. Importantly, there are marked regional variations in the concentrations of antioxidants contained within this compartment, with urate and

lactoferrin purported to be high in the upper versus lower airways, and glutathione thought to be enriched within the distal airway RTLFs (Kelly, 2003; Cross, 1994 – **Figure 1.7**).

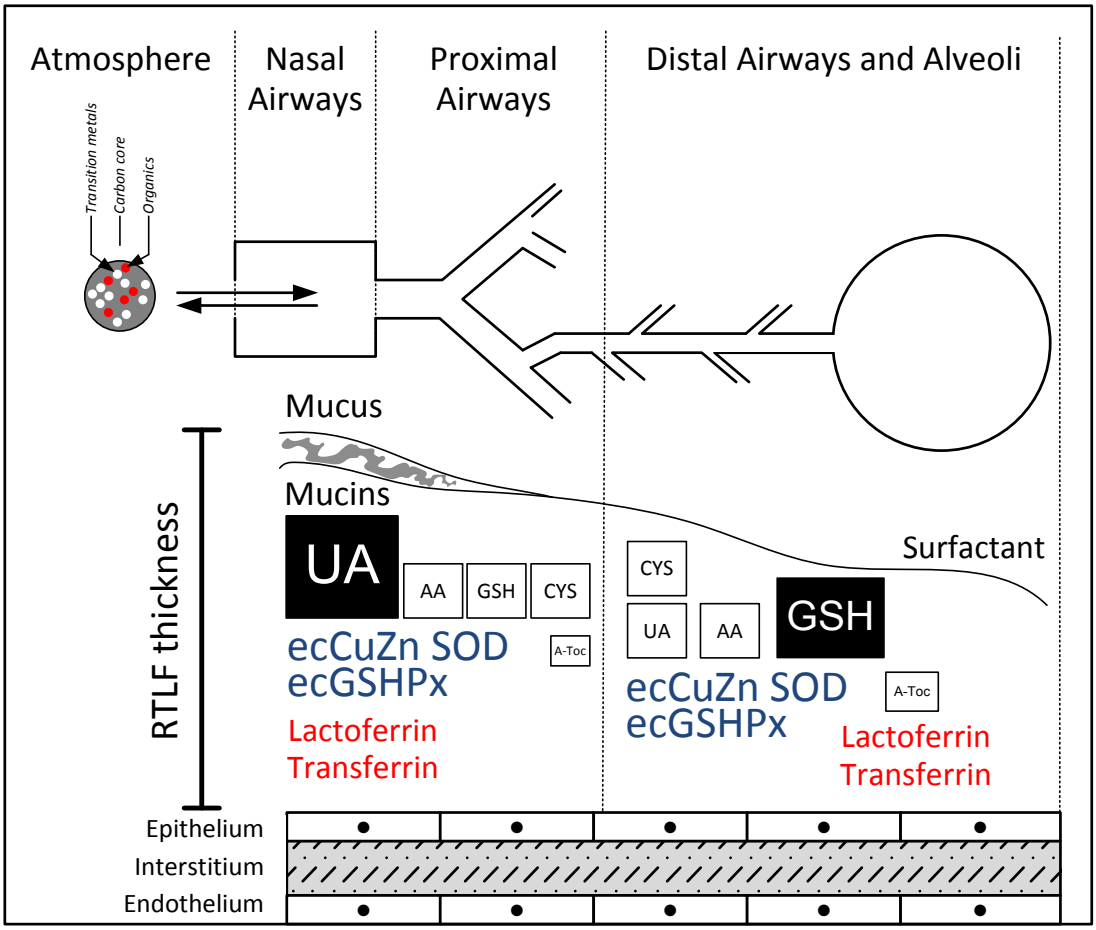

Figure 1.7: Regional variation in the composition of human RTLFs. UA, urate; AA, ascorbate; GSH, glutathione; A-Toc, alpha-tocopherol (vitamin E), ecCuZn SOD, extracellular Cu, Zn superoxide dismutase; ecGSHPx, extracellular (plasma) glutathione peroxidase.

Much of our knowledge about the composition of this compartment has arisen from the use of bronchoscopy based lavage. Bronchoalveolar lavage (BAL) involves the instillation of saline into defined lung segments, which is then recovered by aspiration. Despite its importance, there is little agreement on the best way to account for the variable dilution of the RTLFs which is inherent with the technique and consequently

the literature values for the concentration of RTLF components are expressed with a high degree of uncertainty. In addition to this issue, the lavage dwell time prior to aspiration, the location sampled and sampling handling/storage issues also complicate the determination of accurate RTLF reference values. Common approaches used by research groups to correct for lavage dilution include the use of endogenous markers such as urea or instilled dyes such as methylene blue (Van der Vliet, O'Neill *et al.* 1999). However, the value of both these methods has been questioned (Haslam and Baughman 1999).

The urea method, which has been the most widely applied correction in the literature, is based on the assumption that this low molecular weight molecule is freely diffusible across the blood-air barrier. Therefore, by calculating the ratio between the plasma and lavage concentrations a dilution factor can be generated that can be applied to other measured constituents. One criticism of this approach is that lavage urea concentrations will be augmented as it moves down the imposed concentration gradient from the plasma to the instilled saline bolus in the airway, with this effect becoming magnified with longer saline dwell times in the lung. In an attempt to overcome this problem and generate meaningful reference values for RTLF low molecular weight antioxidants, Van der Vliet and colleagues (1999) developed a single-cycle BAL technique in which 60 mL of saline was instilled and immediately aspirated (<1 minute) into four 15 mL syringes. Based on this study, following urea correction, the predominant low molecular weight antioxidant present in RTLF from the distal airways was urate at 207 ± 167 μM followed by glutathione (GSH), ascorbate

and α-tocopherol at 109 ± 64, 40 ± 18 and 0.7 ± 0.3 respectively. These data are presented in **Table 1.4**, with plasma and nasal lavage values included for reference.

Table 1.4: Single-cycle BAL and nasal lavage performed on 12 healthy volunteers.

	ELF		
Antioxidant (μM)	**Nasal**	**Bronchoalveolar**	**Plasma**
Urate	225 ± 105	207 ± 167	387 ± 132
GSH	<0.5	109 ± 64	1.0 ± 0.7
Ascorbate	28 ± 19	40 ± 18	67 ± 25
α-tocopherol	ND	0.7 ± 0.3	16.5 ± 5
Total protein (mg/mL)	ND	9.5 ± 6.1	74 ± 19

Footnote: Protein levels were calculated from urea values and compared with the relevant plasma reading. Bronchoalveolar concentrations were determined from the final 2 fractions. ND = not determined. Table adapted from Van der Vliet *et al.* (1999).

1.6.2 Low molecular weight antioxidants

In the following section I will review the major low molecular weight antioxidants found within the healthy RTLF and provide information concerning changes in their concentration in relation to smoking status and the presence of COPD. These antioxidants, predominately by order of concentration; ascorbate, urate and glutathione, are often thought of simplistically as acting as sacrificial substrates for ROS/RNS that are introduced or generated at the air-lung interface. In this view they react with ROS/RNS forming non-toxic products and by doing so spare more

critical targets. This view is however a little too simplistic and I will also develop the theme in the proceeding sections of how components of cigarette smoke may actually subvert their protective function, to actually promote radical generation and airway injury.

1.6.2.1 Urate

Urate is formed as the end product of purine metabolism and represents one of the most abundant antioxidants within human plasma and RTLFs. It has the capacity to neutralise free radicals (including hydroxyl and peroxyl radicals), singlet oxygen (Cross and Motchnik, 1992) and MPO-derived hypochlorous acid (Winterbourn, 1985) through single-electron oxidation. During this process urate (UA) is irreversibly oxidised to allatonin, oxonic/oxaluric and parabanic acids along with several other unidentified oxidation products (Kaur and Halliwell, 1990). Urate has also been shown to be a powerful scavenger of O_3 and NO_2 suggesting that it is one of the major defences in the airways against these common ambient pollutant gases (Mudway, 2000). The capacity to scavenge the NO_2 radical is clearly important with regard to cigarette smoke, as is its neutralising reaction with peroxynitrate (Whiteman, 2002). These protective actions against RNS are potentially of major relevance in COPD, both because α_1-antitrypsin is protected from nitration and inhibition by UA *in vitro* (Whiteman, 2002), but also because of the negative role nitration is thought to play in the inactivation of histone deacetylase 2 in COPD (Osoata, 2009). Urate has also been proposed to inhibit the transition metal-catalysed oxidation of ascorbate, through the formation of non-catalytic stable complexes with iron (Davies, 1986). Again, this is a

potentially significant protective role given the presence of catalytic metals in cigarette smoke aerosol.

Relatively few studies have examined the role of urate in COPD and those that have tend to focus on plasma concentrations. Two studies have reported conflicting results relating plasma/serum urate concentrations with lung function in COPD (Garcia-Pachon, 2007; Hageman, 2003). Garcia-Pachon and colleagues (2007) demonstrated an association between high serum UA with low FEV_1, whilst an earlier study reported lower plasma UA concentrations in COPD patients (Hageman, 2003). In a recent larger scale study investigating 500 smokers (367 with COPD) low plasma urate was associated with more severe COPD, based on airflow obstruction (Nicks, 2011). Urate concentrations have been shown to be elevated in the saliva, but not BAL fluid from COPD smokers and ex-smokers relative to aged and smoking status matched controls (Yigla, 2007).

1.6.2.2 Ascorbate

Ascorbate is not synthesised within the human body (due to the lack of gluconolactone oxidase) and as such our nutritional needs are met through the diet, which may account for the wide inter-individual variation in reported lavage concentrations (Kelly, 1999). Ascorbate is highly water soluble and extensively distributed around the aqueous regions of the body. Its function as an antioxidant lies in its ability to scavenge •OH, H_2O_2, O_2•-, hypochlorous acid and singlet oxygen. Ascorbate is an unstable molecule and can be readily oxidised, with the rate being dependent upon the pH of the environment and the presence of catalytic metals

(Favier, 1995). During its oxidation the ascorbyl radical is formed. The unpaired electron belonging to the ascorbyl radical is found in the delocalised π-system and as such remains relatively unreactive. If no further oxidation occurs, a disproportionation reaction will take place between two ascorbyl radicals, leading to the regeneration of one ascorbate and one dehydroascorbate (DHA) molecule (Roginsky and Stegmann, 1994). The DHA formed in this reaction, or directly via a two step oxidation, is highly unstable under physiological conditions and will rapidly undergo hydrolysis to 2,3-diketo-L-gulonic acid and a range of further degradation products such as oxalic and L-threonic acid. There is evidence that DHA can be recycled back to ascorbate, following uptake into cells via facilitated glucose transporters, GLUT1, GLUT3 and GLUT4, (Liang, 2001). Once internalised, the DHA is rapidly reduced to ascorbate by NADPH-dependent dehydroascorbate reductases (Wilson, 2002). Whether such recycling occurs within the extracellular RTLF compartment is currently not known, although the high concentrations of GSH reported within this compartment (Van der Vliet, 1999) would support some reduction of DHA to ascorbate (Winkler, 1994). This is a critical issue as it implies that ascorbate lost from this compartment as a function of its radical scavenging capacity must be replenished by redistribution from other compartments, either from transduction from the plasma pool or the airway cells themselves. Ultimately, the intake of dietary ascorbate should dictate the extent of protections observed.

As with urate, the majority of the studies examining ascorbate (vitamin C) in lung function decline, smoking and COPD are based on plasma concentrations or estimated dietary intakes. There is currently an absence of studies examining RTLF

ascorbate concentrations in patients with COPD. The study cited above by Yigla *et al.* (2007) did not examine ascorbate in the lavage samples from their COPD patients, and only a limited literature exists demonstrating cigarette smoke induced decreases in lavage ascorbate in rats, as well as in smokers versus non-smokers (Ghio, 2008).

It has long been established that high plasma concentrations of nutritional antioxidants (vitamins C and E) and high intakes of foods rich in these vitamins are associated with better indices of lung function (FEV_1 and FVC) in the general population (Britton, 1995; Grievink, 1998; Schwartz, 1994; McKeever, 2008). However, recent studies have demonstrated a similar relationship in populations with airways disease. A study of 218 asthmatic and COPD patients found that estimated dietary intakes of ascorbate was positively associated with FEV_1 and FVC (Ochs-Balcom, 2006). In broad agreement with this, low intakes of vitamin C and E were associated with more wheezing, phlegm production and dyspnoea (Schwartz, 1990; Grievink, 1998). Furthermore an increase of 20 micromol/L in plasma vitamin C has been associated with a 13% reduction in the risk of developing obstructive airway disease OR: 0.87 (Sargeant, 2000).

1.6.2.3 Glutathione

As the most fundamental nonprotein sulphydryl in cells, GSH (L-γ-glutamyl-L-cysteinylglycine) is integral in maintaining the cellular redox status. Its effectiveness as an antioxidant has been demonstrated *in vitro*, where it has been shown to scavenge a broad spectrum of ROS including •OH, HOCl, RO• and RO_2•. In addition to its direct ROS scavenging properties and its role as a substrate for peroxidase and transferase

enzymes, GSH can also protect against oxidative stress by chelating copper ions (Jimenez and Speisky, 2000), regenerating vitamin C (May, Qu *et al.* 2001) and preventing the oxidation of protein thiols (-SH) (Kelly and Mudway 2003). Many of these processes result in the oxidation of GSH to glutathione disulphide (GSSG), or the formation of mixed protein disulphides. GSH is an integral component of the antioxidant network and therefore it is essential to maintain high GSH/GSSG ratios in cells and extracellular fluids. This is achieved either by the enzymatic regeneration of GSH from GSSG or by de novo GSH synthesis. The synthesis of GSH is performed in two enzymatic steps that are catalysed by glutamate cysteine ligase (the rate-limiting enzyme) and glutathione synthetase. Regeneration of GSSG occurs via the action of glutathione reductase and other reductase enzymes, at the expense of NADPH, which is in turn regenerated by the pentose-phosphate shunt (Filosa, Fico *et al.* 2003).

Typical GSH concentrations within plasma range from 1-3 µM and between 40-200 µM in BAL (Halliwell and Gutteridge, 2007) although some research groups have reported ranges of 90-500 µM in BAL obtained from healthy subjects (Van der Vliet, O'Neill *et al.* 1999). Human lavage studies have demonstrated a 2-4-fold increase in GSH concentrations in the RTLFs of chronic smokers compared to non-smokers (Morrison, 1999; Cantin, 1987). In chronic smokers this extracellular increase in GSH was not matched by increased concentrations in airway leukocytes and was in fact associated with a decreased expression of γ-GCS (Neurohr, 2003). This suggests that the increased extracellular GSH concentrations observed are unlikely to be protective against chronic exposure to cigarette smoke. These *in vivo* results are somewhat at odds with the reported induction of γ-GCS activity and γ-GCS heavy subunit mRNA in

cultured immortalised human type II alveolar epithelial cells (A549) treated with cigarette smoke condensate (Rahman, 1996).

In COPD the data on RTLF and airway cell GSH concentrations are somewhat conflicting and difficult to interpret due to the influence of patient smoking status. Increased RTLF GSH concentrations have been reported in COPD patients, though this may simply have reflected their smoking status and concentrations were reported to fall significantly during exacerbations (Drost, 2005).

1.6.3 Enzymatic antioxidants

The most important enzymatic antioxidants within the RTLFs are extracellular superoxide dismutase (ECSOD) and plasma glutathione peroxidase (plGPx). While reports exist of other enzymatic antioxidants within this extracellular compartment including catalase (Ulker, 2007) and glutathione disulphide reductase (Smith, 1997), these data are contentious and likely reflect contamination of the extracellular sample with intracellular material, arising from damage to the airway epithelium during the bronchoscopy. The following section will therefore focus only on the data on ECSOD and plGPx.

1.6.3.1 Extracellular SOD

Three SOD enzymes (CuZnSOD [SOD1], MnSOD [SOD2], and ECSOD [SOD3]) have been characterized in mammalian cells (Arcaroli, 2009). Of these forms only extracellular SOD (ECSOD) exists in the RTLF in close association with the epithelial surface through its interaction with collagen, hyaluronan and heparin sulphate (Gao,

2008). ECSOD is a tetrameric glycoprotein with each subunit containing a copper and zinc atom which functions to catalyse the conversion of superoxide radicals (O_2•-) to H_2O_2 (Halliwell and Gutteridge, 2007). Mice lacking ECSOD have been shown to have increased sensitivity of a range of insults characterised by the induction of oxidative stress, including hyperoxia (Carlsson, 1995) and asbestos (Fattman, 2006), as well as cigarette smoke and elastase-induced emphysema (Yao, 2010). Consistent with this enzyme protecting against oxidative stress, its over-expression appears protective against hyperoxia (Folz, 1999) and cigarette smoke in experimental murine models (Tollefson, 2010). The importance of ECSOD in COPD has been emphasised by recent genetic studies demonstrating that polymorphisms in this gene, especially the Arg213Gly polymorphism, associated with increased circulating levels of this enzyme are protective against COPD in smokers (Young, 2006; Oberley-Deegan, 2009).

There are few reports examining ECSOD in human subjects after smoking or in patients with COPD. In a recent study, plasma, sputum and bronchoalveolar lavage fluid concentrations of ECSOD were compared in smokers with and without COPD to non-smoking controls. Whilst plasma ECSOD concentrations were equivalent in the groups examined, increased concentrations were apparent in induced sputum supernatants obtained from current smokers and COPD patients compared with non-smoking controls. This apparent increase in the upper airways was not apparent in bronchoalveolar lavage fluid, reflective of lower airway lining fluids, and decreases in ECSOD immunoreactivity were observed around blood vessels and bronchioles in COPD lungs (Regan, 2011).

There is somewhat more data available regarding the intracellular SODs, though much of this information is limited to peripheral blood leukocytes. Red blood cell (RBC) SOD activity has been reported in stable COPD patients relative to non-smoking controls, parallel to increased plasma concentrations of lipid (malondialdehyde) and protein oxidation (carbonyls) markers (Nadeem, 2005). In this study RBC SOD activities were not related to the extent of airway obstruction in the COPD patients, and there was no difference between patients at disease stage II or III. In contrast, patients undergoing exacerbation demonstrated increased RBC SOD activities while the activities of glutathione disulphide reductase and glutathione peroxidase fell (Gumral and Nazirolglu, 2009).

1.6.3.2 Plasma glutathione peroxidase

Glutathione peroxidases (GPx) are a family of selenium-dependent and independent antioxidant enzymes located in both intracellular and extracellular compartments (Mak, 2008). These tetrameric proteins catalyse the reduction of H_2O_2 to water through the oxidation of glutathione. The glutathione disulphide (GSSG) formed in this reaction is subsequently reduced back to GSH by glutathione reductase at the expense of NADPH (Rahman and Biswas, 2006), though the extent to which this occurs extracellularly is debatable. Certain isoforms of GPx can also break down lipid hydroperoxides (LOOH) in tandem with the oxidation of glutathione producing GSSG, LOH and OH^-. Eight different isoforms of glutathione peroxidase (GPx1-8) have been identified in humans, which vary in cellular location and substrate specificity. The most abundant form is glutathione peroxidase 1 (GPx1), which is present in nearly all mammalian tissues and catalyses the reduction of H_2O_2. Glutathione peroxidase 2

(GPx2) is an extracellular enzyme located in the intestine, while glutathione peroxidase 3 (plGPx) has been shown to be present in human plasma and RTLF (Avissar and Reed, 2000). Glutathione peroxidase 4 (GPx4) like GPx1 is cytosolic and widely distributed throughout the body, albeit at lower levels, where it plays a significant role in the reduction of lipid hydroperoxides.

Much of the work investigating glutathione peroxidases in COPD has focused on plasma/erythrocyte enzyme activities. Erythrocytic GPx1 activity has been shown to be significantly decreased between GOLD Stages II, III and IV in COPD patients relative to controls, with the residual activity inversely related to systemic indices of inflammation (Tkacova, 2007). The observation of decreased GPx1 activity in peripheral blood was recently confirmed in a study of 109 stable COPD patients and 51 controls, though notably with no incremental difference between patients at different disease stages (Biljak, 2010). This study also demonstrated increased glutathione reductase activities in the peripheral blood from these subjects, parallel to the reduction in GPx1. In contrast to peripheral blood, few studies have investigated GPx in the airways of COPD patients, and there are no reports specifically addressing plGPx (GPx3). GPx3 has been reported within healthy human RTLFs and been shown to decrease acutely following exposure to the oxidant gas ozone (Avissar and Reed, 2000), suggesting that it may be prone to oxidative inactivation. However, recent data suggests that expression of GPx1 is reduced in airway cells in subjects with emphysema, related to reduced nuclear localisation of the nuclear factor (erythroid-derived 2)-like 2 (Nrf2) transcription factor (Goven, 2008). In this study the expression of GPx1 was inversely correlated with the degree of airway obstruction

1.6.4 Chelator proteins

The RTLF also contains endogenous metal chelators (transferrin, lactoferrin, ferritin and caeruloplasmin), which perform the important antioxidant role of sequestering redox active metals, to prevent the formation of highly reactive radicals via Fenton-like chemistry. These proteins will be discussed in the following sections.

1.6.4.1 Transferrin

Transferrin is an iron-binding glycoprotein, predominantly synthesised by hepatocytes, but which can also be produced by pulmonary epithelial cells and submucosal glands within the lung (Shigemura and Nasuhara, 2010). In healthy individuals, transferrin is only loaded with 20-30% iron and therefore has 70% of its binding capacity available for the uptake of iron (Halliwell and Gutteridge, 2007). Transferrin levels, expressed as a percentage of total protein, are significantly higher in BAL (4-5.6%) than in plasma, suggesting that transferrin is locally synthesised within the lung and is not purely derived from plasma through transudation (Mateos, 1998). Decreased levels of transferrin in BAL has been observed in patients with COPD (Shigemura and Nasuhara, 2010), whilst smoking alone does not appear to alter BAL fluid concentrations of transferrin, despite the influx of iron.

Transferrin functions as an iron transport protein as two ferric irons (Fe^{3+}) can be reversibly bound; one binds to the N-terminal domain and one binds to the C-terminal domain. CD71 is a transferrin receptor which mediates the cellular uptake of iron. B and T lymphocytes along with macrophages within the alveolar region express CD71, clearly indicating that the iron transport capabilities of transferrin are required

for the maintenance of metabolic function within such cells. Transferrin is a recyclable protein and the affinity of iron to bind with transferrin is largely pH-dependent as transferrin cannot effectively bind iron at a pH of less than 4.5. The transferrin receptors bind transferrin at the cell surface at a biological pH of approximately 7.4 and then internalises it within endocytic vesicles. The release of iron from the transferrin upon endosomal acidification (pH of less than 4.5) then follows and the newly formed apotransferrin-transferrin receptor complex undergoes dissociation which sees the release of the apotransferrin from the receptors (Ponka, 1999). The pH-dependent binding of Fe is significant as studies have shown the RTLF (based on the pH of exhaled breath condensate) of asthmatics to be 5.3 ± 0.21 (Hunt and Fang, 2000), which would limit the uptake and sequestration of Fe and hence indirectly promote a pro-oxidant state in this compartment. It should be noted that this is a highly contentious observation that has largely failed to be corroborated in the subsequent literature. Whilst the pH of exhaled breath condensate from COPD patients has been shown to be lower compared with age and smoking status matched controls, and to decrease with disease stage, the differences are minor and near neutrality and therefore unlikely to impact on metal handling (Papaioannou, 2011).

1.6.4.2 Lactoferrin

Lactoferrin is a monomeric, cationic iron-binding glycoprotein that is synthesised by the secretory epithelium and myeloid cells (Ghio and Stonehuerner, 2008). It possesses a high affinity for iron at low pH, a property that transferrin lacks, and can effectively bind two iron (Fe^{3+}) molecules. It is found in nasal secretions, bile, tears, seminal fluid, mucosal secretions and saliva (Bournazou and Mackenzie, 2010)

and is present in the secondary granules of neutrophils. During an inflammatory response, lactoferrin transports iron across the cell membrane after which follows its deposition into ferritin. Within BAL, the mean concentration of lactoferrin is approximately 10 times lower than the concentration of transferrin. The lactoferrin present in BAL is sourced predominantly from the airway as opposed to the alveolar region offering an explanation as to why smokers exhibit increased levels of lactoferrin in BAL (Mateos, 1998).

1.6.4.3 Ferritin

Ferritin is an iron storage protein that can essentially store up to 4500 iron ions (Halliwell and Gutteridge, 2007) and can detoxify intracellular non-functional iron (Ponka, 1999). It exerts an antioxidant effect through the sequestration of iron but also serves as an iron source. It is present in mitochondria but is mainly cytosolic. Iron enters ferritin as Fe^{2+} and undergoes oxidation by the protein to form Fe^{3+}. Ferritin can release iron through its degradation within lysosomes where iron is released and the protein shell is converted into an insoluble product known as haemosiderin (Halliwell and Gutteridge, 1984). Instillation of iron-containing particles into human volunteers has been shown to result in an increase in lavage ferritin (Ghio and Carter, 1998). This occurred in parallel to increased lavage lactoferrin and decreased transferrin concentrations. This induction of a protective response was subsequently confirmed in cultured human bronchial epithelial (NHBE) cells challenged with residual oil fly ash (rich in transition metals) where increased ferritin protein was observed, parallel to increased lactoferrin mRNA and protein (Ghio *et al.* 1998). Similar increases have been reported in rat and human respiratory epithelial cells exposed to cigarette smoke

and/or condensate (Ghio *et al.* 2008). In this paper, these *in vitro* findings were confirmed in airway lavage samples from smokers and patients with COPD, which displayed elevated concentrations of iron and ferritin relative to healthy non-smoking controls.

1.6.4.4 Caeruloplasmin

Caeruloplasmin is a copper transport protein that also exhibits ferroxidase activity. It is synthesised within the lung and secreted into the surrounding lining fluids (Halliwell and Gutteridge, 2007). It aids in the loading of Fe into transferrin, and possibly ferritin by oxidising Fe^{2+} to Fe^{3+}. This protein also serves as a peroxidase which in the presence of GSH is capable of removing H_2O_2 and lipid peroxides. Caeruloplasmin also has the capability of binding to myeloperoxidase, thus inhibiting the formation of HOCl without hindering its ferroxidase function.

1.7 Evidence of oxidative stress in COPD

Evidence of increased oxidative stress in the airways of smokers and patients with COPD is largely based on the measurement of ROS or markers of oxidative damage in exhaled breath condensate, due to the difficulty in obtaining lavage samples from these subjects. Smokers and patients with COPD have been shown to display higher levels of exhaled H_2O_2 than non-smokers, with concentrations further elevated during exacerbations (Kharitonov, 2001; Montuschi *et al.* 2000). Similarly, the concentrations of lipid oxidation products such as 8-iso-prostaglandin F2α (8-isoprostane) and thiobarbituric acid-reactive substances (TBARS) have been shown to be elevated in the EBC in healthy smokers relative to non-smokers and more markedly

in patients with COPD (Montuschi *et al.* 2000; Nowak *et al.* 1999). Urinary concentrations of 8-iso-prostaglandin have also been shown to be increased in COPD patients relative to age-matched controls, consistent with the presence of systemic oxidative stress (Pratico, 1998). Actual oxidative damage to the airway epithelium, endothelium and neutrophils has been observed in lung tissue specimens obtained during lung resections from patients with and without COPD. In these specimens, increased staining for 4-hydroxy-2-nonenal (4-HNE)-modified proteins was observed in COPD patients (Rahman, van Schadewijk *et al.* 2002) providing direct evidence of increased oxidative stress in the airway, with some evidence that this was related to lung function in these subjects.

1.7.1 The oxidative stress response model in COPD

In the previous sections I have discussed evidence supporting antioxidant dysregulation and the presence of oxidative stress in the airways of subjects with COPD. These observations need, however, to be placed into the context of how the lung responds to oxidative stress in order to understand how this imbalance contributes to the genesis and progression of the pathologies associated with COPD. In addition to the inherent protection of the airway against acute oxidative insults, via the extensive antioxidant network both within the RTLF and airway epithelium, the lung is also able to adapt to acute insults to mitigate injury. This in part is achieved through the action of the redox sensitive transcription factors, activator protein-1 (AP-1) and nuclear erythroid-related factor-2 (Nrf2), which bind to antioxidant response elements and drive the transcription of cytoprotective genes related to antioxidant

defence, xenobiotic metabolism and metal handling (Biswas and Rahman, 2009; Cho and Kleeberger, 2010). In a healthy airway the combination of these endogenous antioxidant defences and inducible protective mechanisms are usually sufficient to protect the airway, but if the insult is sufficiently large or chronic, the capacity of these defences may be overwhelmed resulting in oxidative stress and injury to the lung. The imposition of oxidative stress, often described in the literature as an increase in the cellular GSH:GSSG ratio (Rahman *et al.* 2005), has been associated with the induction of inflammation, ostensibly through the activation and nuclear mobilisation of nuclear factor-κB (NF-κB) and ultimately with cell proliferation, arrest and death as the magnitude of the oxidative insult increases further (Halliwell, 2000). More recently this graded response to oxidative stress has been defined in the hierarchical response model by the group of Nel (2006), specifically in relation to nanoparticle toxicity and summarised in **Figure 1.8**. This model in its original form defined the response to oxidative stress into three tiers: adaption, inflammation and cell death. The transition through these stages in response to oxidative stress was confirmed by this group *in vitro* using immortalised macrophages (THP-1) challenged with increasing doses of diesel exhaust particles (DEP). At the lowest dose employed, greater expression of heme oxygenase (HO-1) was observed, with increases in the secretion of IL-8 protein only apparent as the DEP dose and GSH:GSSG ratio increased. At the highest dose, evidence of apoptosis was seen using annexin V staining and flow cytometry (Li, 2003). This scheme has been illustrated in **Figure 1.8**, but modified to include an additional tier of protection related to the endogenous antioxidant defences at the air-lung interface, which were not integrated into the model by Nel (2006). In addition, the expanded model includes information of the major transcription factors regulating the

transition from adaption to inflammation, as well as important gene products relevant to the airway response to oxidative stress.

1.7.2 Redox activation of Nrf2 in COPD

Nuclear erythroid-related factor-2 (Nrf2) is a basic-region leucine zipper transcription factor, which binds to the cis-regulatory antioxidant response element and transcriptionally up-regulates a variety of cytoprotective enzymes including HO-1, glutamate cysteine ligase (the rate-limiting enzyme of GSH synthesis), as well as detoxifying enzymes such as NADPH:quinone oxidoreductase 1 (NQO1) and glutathione-S-transferase (Cho, 2006). Under normal cellular conditions Nrf2 is held in the cytoplasm in a complex with Kelch-like ECH-associated protein 1 (Keap1), which contains a Kelch repeat domain that anchors Nrf2 by binding to both the transcription factor and actin filaments of the cytoskeleton (Itoh, 2010; Kobayashi, 2004). Several cysteine residues within Keap1 are responsible for the maintenance of the Nrf2-Keap1 complex (Dinkova-Kostova *et al.* 2002). In addition, Keap1 forms a bridge between Nrf2 and the cullin-3 (CUL-3) E3 ubiquitin ligase complex thereby promoting Nrf2 proteasomal degradation, limiting its accumulation (Jeong, 2006). Upon the imposition of oxidative stress, Nrf2 dissociates from Keap1 and translocates to the nucleus, where it accumulates and binds to AREs in a heterodimeric complex with one of a subset of the small Maf-family of transcription factors (Blank, 2008), resulting in the transactivation of phase 2 detoxifying and antioxidant genes (Jeong, 2006).

Recent literature proposes that electrophilic modification of critical cysteine residues in Keap1, particularly C151 in the BTB domain, leads to de-ubiquitination of Nrf2 in favour of ubiquitination of Keap1 (Eggler, 2005). Thus, Nrf2 protein is stabilized and the turnover of Keap1 is increased. He *et al.* (2007) demonstrated that cells lacking Nrf2 expression exhibited elevated ROS production and apoptosis compared to control cells when exposed to chromium (VI). Additionally, Marzec *et al.* (2007) observed a higher risk of acute lung injury in a limited population with a single-nucleotide polymorphism located in the promoter region of Nrf2.

Recent studies have demonstrated impaired Nrf2 transcriptional activity in patients with COPD, with reduced Nrf2 protein concentrations in lung tissue and alveolar macrophages reduced in patients with COPD and emphysema compared to age-matched controls (Goven *et al.* 2008). This occurred in parallel to increased Keap1 and Bach1 (a cap'n'collar type of basic region leucine zipper factor that inhibits the expression of MAF proteins) protein expression, associated with decreased HO-1, NQO1 and glutathione peroxidase 2 mRNA. This suggests that Nrf2 could be regarded as a candidate susceptibility gene for COPD and illustrates its critical role in antioxidant defence in the lung (Boutten, 2011; Sykiotis, 2010; Malhotra, 2008).

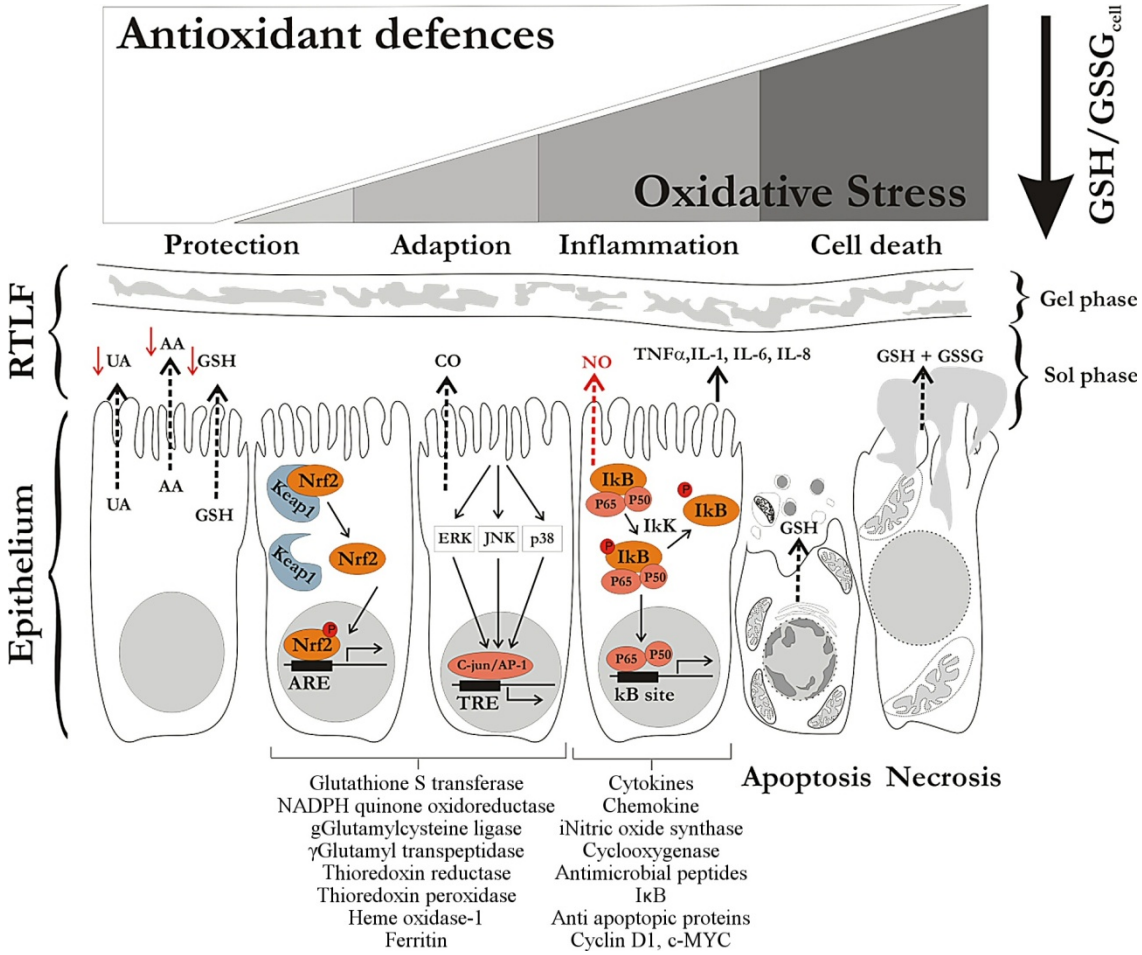

Figure 1.8: Diagrammatic representation of the hierarchical response of cells to PM-induced oxidative stress at the air-lung interface. This diagram represents an extension of the earlier model proposed by Nel *et al.* (2006), to include the influence of the antioxidant defences within the respiratory tract lining fluids which overlay the epithelium. In this modified model, the initial defence against PM-induced oxidative stress resides within the RTLFs, initially characterised by acute early losses of ascorbate (AA), urate (UA) and glutathione (GSH). In light of the findings in the present study we suggest this initial loss is partially offset by movements of these antioxidants, particularly GSH, from the epithelium to the extracellular compartment. When these defences are overwhelmed the underlying cells initially induce adaptive strategies, under the regulation of Nrf2 and AP-1 to deal with the oxidative stress, or process the inhaled xenobiotics. The figure illustrates a number of genes known to be up-regulated in these adaptive responses, under the regulation of Nrf2 and AP-1, including the glutathione S transferase and heme oxygenase-1. Further oxidative stress, reflected by a decrease in the cellular GSH/GSSH ratio, leads to the transcription of genes under the regulation of NFκB, such as pro-inflammatory cytokines and inducible nitric oxide. Further oxidative stress subsequently leads to cell arrest and induction of cell death, either by apoptosis or necrosis. These later two processes can also be associated with either regulated (apoptosis) export of intracellular GSH, or its unregulated release by necrosis associated with its subsequent oxidation to GSSG.

1.8 The ageing hypothesis in COPD

COPD has long been recognised as sharing many features with the aged lung, summarised in **Table 1.5**. This is perhaps not surprising given that the majority of COPD sufferers are of late middle-age to elderly. In addition, many COPD co-morbidities are also degenerative diseases of accelerated senescence, including heart failure, atherosclerosis, osteoporosis, and diabetes. Recently however, it has been proposed that the normal physiologic ageing of the lung, associated with degraded homeostatic and repair mechanisms and the accumulation of molecular damage, is accelerated in COPD due to recurrent episodes of inflammation and airway remodelling, driving mitotic cells toward senescence (Ito, 2009). In support of this view, shortened telomeres have been observed in the alveolar type II cells and endothelial cells (Tsuji, 2006), peripheral mononuclear blood cells (Morla, 2006) and fibroblasts (Muller, 2006) from the lungs of COPD subjects compared to age-matched non-smoking subjects. The development of emphysematous pathology is also seen to occur early in the lungs of animal models of accelerated ageing, such as the Klotho and the SMP30 mice, concurrent with increased oxidative stress (Sato *et al.* 2007; Sato *et al.* 2007).

Antioxidant enzyme activity, the expression of anti-ageing molecules such as the protein deacetylase sirtuin 1 (SIRT1) and sensitivity to corticosteroids are all decreased with age, with further declines apparent in COPD patients (reviewed in Ito, 2009). These changes occur against a background of increased basal age-related inflammation characterised by increased neutrophilia and pro-inflammatory cytokines (IL-1β, IL-6, IL-8 and TNF-α) production. This immuno-ageing effect also appears to be

exacerbated in COPD in comparison to age-matched controls (reviewed in Ito, 2009). The activity of enzymes such as superoxide dismutase has also been reported as being lower in aged smokers and stable COPD patients than in healthy age-matched controls (Kirkil, 2008) although there is still a degree of uncertainty surrounding these data (Nadeem, 2005).

Table 1.5: Comparison table of normal aged lung and COPD lung, adapted from a publication by Ito (2009).

Variables	Aging	COPD
Lung function	↓	↓↓
Alveolar spaces	↑	↑↑, with alveolar wall destruction
Neutrophils	↑	↑↑
Basophils	↑	?
IL-6	↑	↑
IL-8, TNF-α, IL-1β	↑	↑↑
IL-2	↓	→
VEGF	↑	↓
iNOS	↑	↑↑
Hemoxygenase-1	↑	↑
Manganese superoxide dismutase, catalase	↓	↑↓→?
Adhesion molecules (E-selectin, P-selectin, L-selectin, VCAM, ICAM)	↑	↑
NF-κB activation	↑	↑↑
Histone deacetylase 2	Slight reduction	↓
Corticosteroid sensitivity	↓	↓↓↓
Reactive oxygen species	↑	↑↑
Nitrated and oxidized proteins	↑	↑↑

VCAM = vascular cell adhesion molecule; iNOS = inducible nitric oxide synthase; ICAM = intercellular adhesion molecule; VEGF = vascular endothelial growth factor; ↑ indicates degree of increase; ↓ indicates degree of decrease; → indicates no change; ? indicates unknown.

A reduced expression of sirtuins (anti-ageing molecules), in particular SIRT1 and SIRT6, have been reported in the lung tissue and peripheral blood mononuclear

cells of COPD patients (Vuppusetty, 2007; Rajendrasozhan, 2008) and with SIRT1 being a major inhibitory regulator of MMP-9, a decline in its expression may lead to structural changes of the lung such as emphysema. A reduction in SIRT6 expression (Meyer, 1998) leaves DNA vulnerable to damage. Additionally, a reduction in the activity and expression of histone deacetylase II (HDAC-2) in the peripheral lung tissue and alveolar macrophages of COPD patients has been attributed to enhanced inflammation and corticosteroid insensitivity (Ito, 2005; Ito, 2006).

1.9 Overview

The presence of oxidative stress in the COPD lung has been proposed to be critical in the development of the underlying disease pathology. There is however, a paucity of data concerning the status of the antioxidant defences present at the air-lung interface in COPD to support this contention, with much of the published data related to markers determined in blood and exhaled breath condensate. The extent to which the latter can be employed as a surrogate for actual sampling of the lower airway RTLFs remains a highly contentious issue. The aim of the studies described in this thesis were therefore to present a comprehensive analysis of antioxidant defences, including metal homeostasis at the surface of the lung, specifically within the respiratory tract lining fluids of patients with COPD. This was achieved by comparing antioxidant and oxidative damage marker concentrations in bronchoalveolar lavage fluid samples from COPD patients (both smokers and ex-smokers) with those determined in age and smoking status matched control subjects. I hypothesised that there would be clear evidence of oxidative stress within the RTLF of COPD patients and that the extent of antioxidant depletion, or macromolecule

oxidation, would be quantitatively related to the extent of airway inflammation and the functional impairment of the lung. The experimental data in this thesis are presented in three chapters, which deal with the following areas: (**1**) evidence of oxidative stress in COPD; (**2**) quantification of a catalytically active metal pool in COPD patients, consistent with the propagation of damaging oxidation reactions within this compartment, and (**3**) the development of a novel mass spectrometry based method to assess specific protein oxidative modifications *in vivo*. This final chapter is limited only to a consideration of the early developmental stages of establishing a robust quantitative method, but provides the basis for future work as discussed in the final concluding chapter (**chapter 5**).

1.9.1 Experimental chapter synopsis

Chapter 2 is presented in two parts; the first (**I**) providing a detailed account of the antioxidant defences present at the air-lung interface (measured in bronchoalveolar lavage) in patients with COPD, both within current and ex-smokers, versus their appropriate age and smoking status matched controls. This includes data on both the major low molecular weight antioxidants (ascorbate, urate and glutathione) and endogenous chelator proteins (ferritin, lactoferrin and transferrin) within this compartment. The formation of 4-HNE-protein adducts is also discussed. In order to place these results into context and in part to address the accelerated ageing hypothesis in COPD, I then addressed a more restricted list of oxidative stress markers in young adult non-smokers and subjects with mild atopic asthma. These analyses presented in part **II**, permitted a comparison of young and aged healthy adults as well

as a comparison of antioxidant status in two airway diseases characterised by differing modes of airway inflammation. The data presented in this chapter are novel and this study represents the first comprehensive assessment of oxidative stress in COPD within distal airway RTLFs.

Chapter 3 employed the same clinical samples as the previous chapter (COPD and asthma studies) but sought to quantify the concentration of 'catalytically' active metals in the recovered lavage fluid samples (Cu and Fe), together with a panel of non-redox metals (Zn) and metals reflective of cigarette smoke inhalation (Cd and As). Here, I hypothesised that increased rates of biologically damaging oxidation reactions would be observed in COPD patients and smokers, related to the presence of non-transferrin bound and hence catalytically active Fe and Cu pools in their RTLFs. To establish this, both inductively coupled plasma mass spectrometry and a novel functional assay of metal catalysis in biological fluids was employed. This latter method is novel and employs exogenous metal chelators (diethylene triamine pentaacetic acid – DTPA and nitrilotriacetic acid - NTA) to isolate whether a pro-oxidant signal can be related to Fe or other redox active metal, likely in biological systems to be Cu. This methodology is again novel and the data presented in this chapter represent the first attempt to examine this question in asthma and COPD.

Whilst chapters 2 and 3 addressed global markers of oxidative stress or altered metal homeostasis at the air-lung interface, **chapter 4** focused on the requirement for more precise mass spectrometry based tools to interrogate oxidative post-translational modifications to functional proteins within the RTLF. One could

speculate, for example, that selective oxidations to key functional proteins such as proteases or antiproteases in COPD, may play a significant role in the pathophysiology of the condition, even in the absence of global changes in the redox environment of the lung. Based on the available literature at the time, I decided to focus this exploratory method development on the identification and quantification of 4-HNE-protein adducts considering the Michael additions of 4-HNE to lysine, histidine and cysteine residues, with the ultimate objective of employing this technology in human lavage fluid samples. This was a highly ambitious undertaking and the data presented in this chapter is best viewed as exploratory, presenting a work-up of the method using simple peptides and albumin 4-HNE adducts, to a limited examination in the more complex lavage samples. This chapter provides data that justifies further investment in this approach but at this time the data can only be described as preliminary.

Chapter 2:

Is oxidative stress at the air-lung interface characteristic of the COPD phenotype?

2.1 Introduction

Oxidative stress is believed to play a central role in the aetiology and progression of inflammatory airway diseases such as asthma and COPD. This contention is supported by evidence of antioxidant deficiencies and increased oxidative damage marker concentrations within the respiratory tract lining fluids (RTLF) (Xie *et al.* 2009; Kelly *et al.* 1999), induced sputum (Kinnula *et al.* 2007; Beeh *et al.* 2004), exhaled gases (Montuschi P *et al.* 2001; Horváth *et al.* 1998; Zayasu *et al.* 1997) and exhaled breath condensate (Nowak *et al.* 1999; Montuschi *et al.* 1999; Loukides *et al.* 2002) of these patient groups (see **Table 2.1)**. Evidence of increased signalling through redox sensitive pathways (Di Stefano *et al.* 2002; Goven *et al.* 2008; Hart *et al.* 1998) and oxidative damage within the respiratory epithelium (Ricciardolo *et al.* 2005; Rahman *et al.* 2002) has also been reported and related to disease severity (also illustrated in **Table 2.1**). The increased oxidant burden within the lungs of patients with these conditions has been related to the accumulation and activation of inflammatory cells such as neutrophils, eosinophils and macrophages in the distal and proximal airways, with evidence of exaggerated generation of reactive oxygen species from these cells during the oxidative burst (Crystal, 1991). Generally speaking, the evidence for oxidative stress in RTLFs is greater for asthma than COPD with the data in the latter group largely derived from measurements in exhaled breath condensate

and induced sputum samples. There is considerable debate within the literature as to what extent measurements made using these methods accurately reflect changes in the bronchial airways and alveolar compartments of the lung, with some recent papers appearing to demonstrate some underlying relationship in certain markers (Vatrella *et al.* 2007; Antczak *et al.* 2011).

Table 2.1: Published evidence of oxidative stress in a variety of biological samples taken from patients suffering with COPD or asthma.

	COPD	**Asthma**
EBC	↑ H_2O_2 [a] ↑ $PGF_{2\alpha}$ [b]	↑ H_2O_2 [c] ↑ $PGF_{2\alpha}$ [d, e]
Induced sputum	↑ $PGF_{2\alpha}$ [f] ↑ GSSG [g]	↑ 3-bromotyrosine [h] ↑$PGF_{2\alpha}$ [i] ↓ AA [j]
Exhaled gases	↑ CO [k] ↑ NO [k, l]	↑ CO [m,n]
Airway lavage	No data	↑ 8-isoprostane [o] ↓ AA, ↑ GSSG [p]
Airway tissue	↑ NFκB [q] ↓ IκB-α [r] ↓ Nrf2 [s] ↑ 4-HNE [t] ↑ 3-NT [u]	↑ NFκB [v] ↓ SOD [w, x]

Abbreviations: H_2O_2: hydrogen peroxide; $PGF_2\alpha$: prostaglandin F2alpha; GSSG: glutathione disulphide; AA: ascorbic acid; CO: carbon monoxide; NO: nitric oxide; NFκB : nuclear factor kappa light chain enhancer of activated B cells; IκB-α : nuclear factor of kappa light polypeptide gene enhancer in B-cells inhibitor, alpha; Nrf2: nuclear factor erythroid 2-related factor 2; 4-HNE: 4-hydroxynonenal; 3-NT: 3-nitrotyrosine; SOD: superoxide dismutase.

References: ‘a’, Nowak *et al.* 1999; ‘b’, Montuschi *et al.* 2000; ‘c’, Loukides *et al.* 2002; ‘d’, Montuschi *et al.* 1999; ‘e’, Zanconato *et al.* 2004; ‘f’, Kinnula *et al*. 2007; ‘g’, Beeh *et al.* 2004; ‘h’, Aldridge *et al.* 2002; ‘i’, Wood *et al.* 2005; ‘j’, Kongerud *et al.* 2003; ‘k’, Montuschi *et al.* 2001; ‘l’, Ansarin *et al.* 2001; ‘m’, Horváth *et al.* 1998; ‘n’, Zayasu *et al.* 1997; ‘o’, Xie *et al.* 2009; ‘p’, Kelly *et al.* 1999; ‘q’, Di Stefano *et al.* 2002; ‘r’, Szulakowski *et al.* 2006; ‘s’, Goven *et al.* 2008; ‘t’, Rahman *et al.* 2002; ‘u’, Ricciardolo *et al.* 2005; ‘v’, Hart *et al.* 1998; ‘w’, Smith *et al.* 1997; ‘x’, De Raeve *et al.* 1997.

Despite the wealth of data summarised in **Table 2.1**, there is a complete absence of information in the literature related to RTLF antioxidant concentrations in COPD patients, with much inferred from the alterations in redox status observed in the lungs of chronic smokers or in subjects after acute inhalation of cigarette smoke (reviewed in Rahman and MacNee, 1999). Such information is vital in assessing the sensitivity of individuals or disease groups to oxidative injury. At this time, despite the preliminary evidence of some association between inflammatory markers made in exhaled breath condensate and bronchoalveolar lavage, bronchoscopy based lavage still remains the 'gold standard' method of assessing airway immunopathology and redox status.

In the first part of this chapter, I will address whether antioxidant defences at the air-lung interface are depressed in COPD patients, both smokers and ex-smokers, relative to appropriate age and smoking status matched 'healthy' controls. These data are derived from bronchoscopy based lavages in these subject groups and therefore represent a unique examination of antioxidant defences (low molecular weight antioxidants: ascorbate, urate and glutathione; metal chelating proteins: transferrin, lactoferrin and ferritin; plus a range of oxidative damage markers: glutathione disulphide, dehydroascorbate, 4-hydroxynonenal) within the regions of the lung affected in this disorder. This information will then be compared against antioxidant measurements made in young healthy non-smokers and patients with mild atopic asthma. The inclusion of these additional groups in the second part of this chapter was to address the extent to which declines in airway antioxidant status, if seen in COPD patients, might be attributed to normal age-related declines in airway defences, as

well as a ‘generalised’ inflammatory state: allergic versus chronic. I hypothesised that COPD would be characterised by impaired antioxidant defences within the RTLF, relative to aged-matched controls, associated with the presence of chronic airway inflammation and that this would be apparent irrespective of smoking status. Current smoking, I conjectured, would further degrade the antioxidant defences at the air-lung interface. Further, I hypothesised that the extent of oxidative stress (more precisely defined as altered redox status) in the RTLF would be related to disease severity, the presence and extent of airway inflammation and measures of lung function.

2.2 Methods

2.2.1 Subject demographics

Subjects for all groups were invited to participate in the present study through advertisements in the local media. COPD patients (aged 50-75 years) had moderate to severe disease according to the GOLD criteria (FEV_1 30-80% of predicted, FEV_1/FVC less than 0.7) with a smoking history of at least ten pack-years and no evidence of other concomitant disease. All patients were required to be non-atopic and clinically stable, i.e. without any respiratory tract infection within a six-week period prior to and during the study, along with no history of frequent exacerbations during a period of at least 3 months prior to inclusion. The only medication permitted was short-acting β2-agonists and/or anti-cholinergic drugs. Neither long-acting bronchodilators nor inhaled corticosteroids were allowed. All subjects were also required to undergo a detailed medical consultation with an ECG and chest X-rays prior to inclusion. Healthy never-smoking volunteers were age-matched (50-75 years), had normal lung function (>80 FEV_1 % of predicted) and were all non-atopic. Similarly, aged 'healthy' smokers were required to have normal lung function, as previously defined, were age-matched (50-75 years) and had a smoking history of more than ten pack-years. They were all non-atopic and clinically stable.

Subjects recruited to the young healthy control group were required to meet the following inclusion criteria: age 18-40 years; never smokers; no history of allergy or asthma and normal lung function (FEV_1 >80% predicted). All mild asthmatics (FEV_1 >80% of predicted, age range 18-40 years) were required to have a history of allergy and at least one positive skin prick test to either Birch or Timothy grass pollen. Mild

asthmatics were also required to exhibit bronchial hyper-responsiveness (PC_{20} <8mg/ml metacholine). Exclusion criteria were: uncontrolled asthma; any airway infection within six weeks prior to the study and current use of medication other than inhaled corticosteroids or short-term β2-agonists. Exclusion criteria for all groups were the use of any medications other than those specifically stated in the inclusion criteria and any use of antioxidant supplementation, including iron supplements.

A total of 57 subjects were recruited into the first part of the study (the aged population with and without COPD); 13 healthy aged controls (all never-smokers); 16 aged smokers (with no evidence of chronic respiratory disease); 17 COPD patients (ex-smokers) and 11 patients who had continued to smoke following their diagnosis of COPD. The second part of the study included 16 young healthy and 16 mild asthmatic subjects. All subjects participated following submission of formal consent with study approval awarded by the local Ethics Committee of the University of Umeå, in accordance with the declaration of Helsinki. A summary of the subject demographics is provided in **Table 2.2** (aged controls, smokers and COPD patients) and **Table 2.3** (young adults and asthmatics).

2.2.2 Pulmonary function test

Dynamic spirometry variables (VC, FVC and FEV_1) were measured pre and 15-20 minutes post-bronchodilation with 1mg of terbutalin (Bricanyl® Turbuhaler®; AstraZeneca, Södertälje, Sweden) using a Vitalograph spirometer (Buckingham, UK) and reversibility calculated. At least three satisfactorily performed and well-

cooperated measurements of each variable were carried out according to the recommendations of the American Thoracic Society. The diffusion capacity of carbon monoxide (CO) was obtained by the single breath procedure (Ogilvie *et al.* 1954).

2.2.3 Collection and preparation of bronchoalveolar lavage samples

Bronchoscopy was performed on an outpatient basis, following an overnight fast, using a flexible video bronchoscope (Olympus BF IT240, Tokyo, Japan) inserted through the mouth with the subject in the supine position. Pre-medication with atropine (1 mg) was given subcutaneously 30 minutes prior to bronchoscopy to reduce airway mucus secretion, with Lidocain (5% and 1%) sprayed onto the airways to achieve topical anaesthesia. Bronchial wash (BW) was performed by infusing two aliquots of 20 mL sterile sodium chloride (NaCl), pH 7.3 at 37^{o}C into the lingular or middle lobe, which was gently sucked back after each infusion. These recovered aspirates were kept as separate aliquots on wet ice. Bronchoalveolar lavage (BAL) was performed immediately after these small volume infusions by the instillation and immediate aspiration of 3 consecutive aliquots of 60 mL saline. The recovered aspirates were pooled and placed on wet ice prior to transport to the laboratory for processing.

Both BW and BAL fluids were passed through a nylon filter (pore diameter 100 µM) to remove the mucus and the cellular content was isolated by centrifugation at 400 rpm for 15 minutes at 4˚C. The obtained pellets were then resuspended in phosphate buffer solution (PBS) to a concentration of 10^6 cells/ml. Total and

differential cell counts were carried out on cyto-centrifuge preparations stained with May-Grűnwald Giemsa, with a 400 total cell count per slide. Further description of these methods is available (Mudway 2001). The chilled bronchial wash (BW) and bronchoalveolar lavage (BAL) fluids were filtered through a nylon filter and centrifuged (400 rpm, 15 minutes, at 4˚C). After centrifugation, the cell pellet was separated from the supernatant and resuspended in PBS. The total number of cells was counted and adjusted to a final concentration of 10^6 cells/ml. The resultant supernatant was treated as follows: an aliquot of lavage fluid (450 µL) was treated with 50 µL of 50% metaphosphoric acid (MPA), vortexed for 30 seconds and centrifuged at 13,000 rpm for 5 minutes (4^oC) to remove protein. The resultant supernatant was then stored at -80^oC within 30 minutes of BAL collection until required for analysis. Samples for GSH and GSSG determination were treated with the metal chelator deferoxamine mesylate (DES) and the synthetic antioxidant butylated hydroxytoluene (BHT) both at 2 mM, 5 µl of each to 490 µl of lavage, prior to storage at -80°C. The remaining lavage was untreated but immediately aliquotted and stored at -80°C.

Table 2.2: Subject demographics for the aged population; with and without COPD, smokers, ex-smokers and never smokers.

	Age Control Never smoker *(n=13)*	**Aged Control Current smoker** *(n=16)*	**COPD patients Ex-smokers** *(n=17)*	**COPD patients Current smokers** *(n=11)*	**KW-test**
Age (*mean + range*)	66.9 (57-74)	60.6 (50-71)*a*	67.9 (53-77)	64.1 (55-75)	$P = 0.014$
Gender (*m/f*)	7/6	7/9	11/5	3/8	
Pack years (*mean + range*)	0	36.9 (18-95)*a*	33.5 (5-68)*c*	35.2 (13-80)	$P < 0.001$
FVC (median, IQR, L)	4.1 (3.6-4.7)	4.0 (3.1-4.9)	2.9 (2.3-3.0)*c*	2.4 (2.2-2.6)*b*	$P < 0.001$
FVC % of predicted (*median, IQR, L*)	104.0 (95.0-116.0)	114.5 (107.0-122.3)	73.0 (66.0-77.5)*c*	85.0 (67.5-91.0)*b*	$P < 0.001$
FEV_1 (*median, IQR, L*)	3.0 (2.2-3.4)	3.2 (2.6-3.8)	1.4 (1.0-1.9)*c*	1.3 (1.1-1.6)b	$P < 0.001$
FEV_1 % of predicted (*median, IQR, L*)	100.0 (91.0-118.0)	113.0 (104.0-115.8)	51.0 (42.0-64.0)*c*	60.0 (39.0-69.0)*b*	$P < 0.001$
Reversibility (*%*)	1.0 (-0.5-4.4)	2.7 (1.2-4.9)	17.1 (12.0-24.4)*c*	6.2 (1.9-15.1)*d*	$P < 0.001$
TLC (*median, IQR, L*)	nd	6.8 (5.4-8.1)	7.0 (6.1-7.6)	6.0 (5.3-6.5)	NS
IC (*median, IQR, L*)	nd	3.1 (2.7-3.6)	2.6 (2.2-3.0)	2.0 (1.7-2.5)b	$P = 0.006$
MEF_{50} (*median, IQR, L s^{-1}*)	nd	2.76 (2.15-3.64)	0.37 (0.28-0.70)	0.72 (0.40-0.79)*b*	$P < 0.001$
TL_{CO}^{SB} (*median, IQR, mmol min^{-1} kPa^{-1}*)	nd	7.4 (6.1-7.8)	5.7 (3.9-6.3)	5.2 (4.8-5.7)*b*	$P < 0.001$
BAL recovery (*%*)	50.0 (44.0-56.0)	53.0 (48.8-63.8)	36.0 (29.0-48.0)*c*	39.0 (29.0-48.0)	$P = 0.025$

All data are expressed as medians with either the inter-quartile or full range, as indicated. Significant differences across groups were assumed at the 5% level using the Kruskal–Wallis one-way analysis of variance by ranks (significance illustrated in the far right hand column), with post-hoc testing between specified groups performed using the Mann-Whitney U Test. Comparison of individual groups were restricted to healthy smokers versus never smokers (*a*, $P < 0.05$), healthy smokers and COPD current smokers (*b*, $P < 0.05$), never smokers versus COPD ex-smokers (*c*, $P < 0.05$) and COPD current and ex-smokers (*d*, $P < 0.05$). Lung function measurements are based on post-bronchodilator values, with evidence of % airway reversibility indicated. Pack years were calculated by multiplying the number of packs of cigarettes smoked per day by the number of years the person had smoked. FVC = Forced Vital Capacity; FEV_1 = Forced Expiratory Volume in 1 second; TLC = Total Lung Capacity; IC = Inspiratory Capacity; MEF_{50} = Maximum Expiratory Flow when 50% of the FVC has been exhaled; TL_{CO}^{SB} = lung carbon monoxide diffusing capacity in a Single Breath; % BAL recovery was based on a total instilled saline volume of 180 mLs.

Table 2.3: Subject demographics for the young healthy and mild asthmatic groups.

	Healthy controls *(n=16)*	**Mild asthmatics** *(n=16)*
Age (*mean + range*)	25 (19-39)	26 (20-36)
Gender (*m/f*)	11/5	6/10
FVC (median, IQR, *L*)	4.51 (4.08-5.74)	4.00 (3.44-5.03)
FVC % of predicted	107.0 (98.0 – 112.5)	99.0 (90.0 – 104.0)
FEV_1 (median, IQR, *L*)	3.95 (3.45-4.86)	3.29 (2.97-4.06)
FEV_1 % of predicted	106.0 (98.0 – 111.8)	95.0 (90.0-102.0)
Skin prick test	No	Yes
PC20 (*mg/ml*)	nd	1.1 (0.65 – 4.14)

All data are expressed as medians with either the inter-quartile or full range, as indicated.

2.2.4 Differential cell counts

Cytocentrifuged specimens were prepared by centrifugation at 450 rpm for 5 minutes. The slides were stained with May-Grünwald Giemsa for cell differential counts. 500 cells per slide were counted using a light microscope at 100x magnification and the proportion of non-epithelial cells including macrophages, neutrophils, eosinophils and lymphocytes was established. Mast cells were analyzed on slides stained with basic toluidine blue and counterstained with Mayer´s acid haematoxylin, counting a minimum of 12 visual fields at 20x magnification. Based on the total cell concentration and the differential cell counts, the concentration of each cell type was determined as cell/ml.

2.2.5 Antioxidant and oxidative damage marker analyses

2.2.5.1 Ascorbate and urate

All chemicals used in this and subsequent analyses were obtained from Sigma-Aldrich Chemical Company Ltd (Poole, UK) unless otherwise stated. Ascorbate (AA) and urate (UA) were measured simultaneously by reversed-phase HPLC with electrochemical detection (Iriyama, Yoshiura et al. 1984). Pre-acidified and deproteinated samples stored at -80^{o}C in 5% MPA were thawed on wet ice. Lipid extraction was achieved by transferring 400 µl aliquots of these acidified samples to eppendorfs containing 50 µl of 5% MPA and 200 µl of heptane chilled to 4^{o}C, followed by vortexing for 60 seconds and centrifugation at 13,000 rpm for 5 minutes (4^{o}C). The resultant lower layer was then carefully decanted into amber HPLC vials for analysis. All sample processing was performed on wet ice with care taken to protect the samples from light at all times. A Gilson 234 auto-sampler was used to inject 20 µl aliquots of each sample for analysis on a 5 µm C18 column (4.6 x 150 mm) from Phenomenex, eluted with a 0.2 mM K_2HPO_4-H_3PO_4 mobile phase containing 0.25 mM octanesulphonic acid (pH 2.1) at a flow-rate of 1.5 ml/min. An E&EG amperometric electrochemical detector was used for detection with the voltage set at 400 mV and a current sensitivity of 0.2 µA. Ascorbate and urate concentrations were determined against appropriate standards (AA range: 0-12.5 µM; UA: 0-25 µM). Typical standard curves for both compounds are shown in **Figure 2.1**.

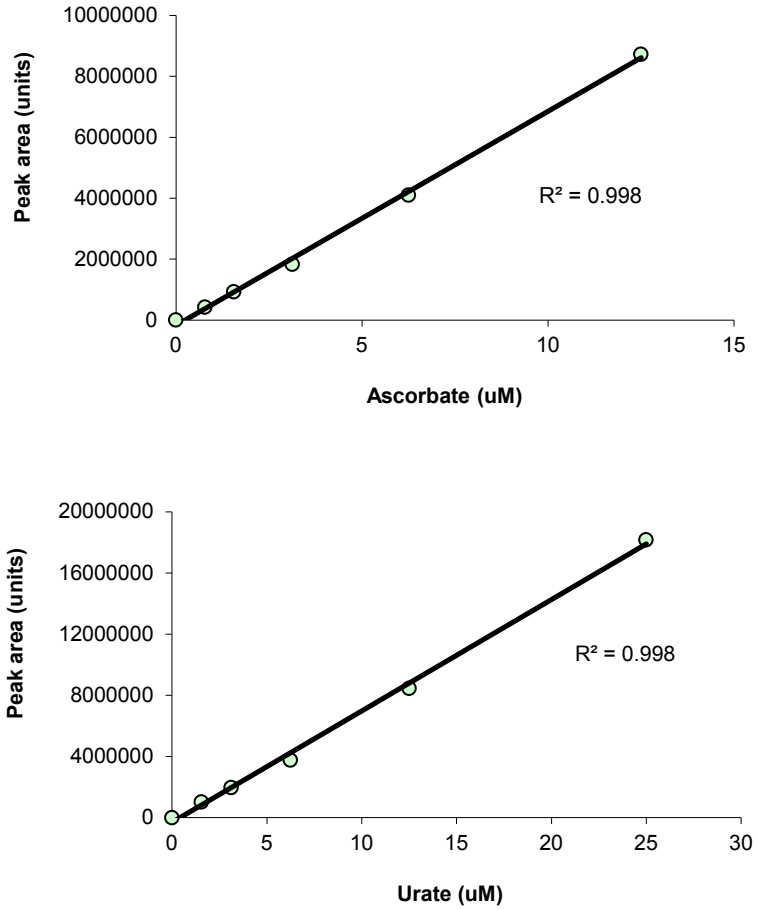

Figure 2.1: Typical standard curves of ascorbate (upper panel; concentrations: 0, 0.78, 1.56, 3.125, 6.25 and 12.5 µM; n = 1) and urate (lower panel; concentrations: 0, 1.56, 3.125, 6.25, 12.5 and 25 µM).

Total vitamin C (dehydroascorbate (DHA) + ascorbate) was also measured by pre-treating the 400 µl aliquots of acidified sample with 50 µl of 50 mM Tris(2-carboxyethyl)phosphine (TCEP) in 5% MPA (Molecular Probes, Eugene, Oregon USA) for 15 minutes and then performing the lipid extraction and HPLC analysis as described above. The DHA concentration was then calculated by subtracting the measured ascorbate concentration from the total vitamin C concentration.

Representative lavage ascorbate and vitamin C (following sample pre-treatment with the reductant dithiothreitol (DTT), an alternative to TCEP in un-acidified samples) traces are illustrated in **Figure 2.2**. Nasal lavage fluid was used for these illustrative chromatograms as the lavage procedure, described by Mudway *et al.* (1999), permits rapid sampling of the nasal epithelial lining fluids and therefore allows samples to be processed for analysis within 10-15 minutes, minimising the likelihood of artifactual oxidation of ascorbate. Nasal lavage was performed on a healthy male subject and the sample was processed for immediate determination of ascorbate and vitamin C content at 400 mV. The fresh lavage contained 0.43 µM of ascorbate and 3.63 µM of vitamin C following sample reduction with DTT (final concentration 5 mM), hence 3.2 µM DHA. The authenticity of this peak was confirmed relative to the retention time of a 3.125 µM ascorbate standard prepared in 5% MPA and by spiking a 400 µL aliquot of the lavage with 50 µL of a 5 µM ascorbate solution prior to the addition of 50 µL of 50% MPA. The subsequent concentration in the sample was 1.39 µM, indicating a 96% recovery of the added ascorbate. Samples were also incubated in the presence of ascorbate oxidase for 5 minutes at room temperature (5U/mL final concentration), which completely abolished the ascorbate peak. To confirm that the increase in the ascorbate peak following DTT reduction could not be attributed to the appearance of another signal with an identical retention time, we re-ran the sample at 810 mV, a potential at which thiols (cysteine, glutathione and homocysteine) are readily detectable in this assay. At this potential, following sample reduction with DTT, a cysteine peak was apparent, close to, but separate from the ascorbate peak. This peak was unaffected by the ascorbate oxidase treatment. To confirm that an ascorbate oxidation product other than DHA was not being recycled by DTT we

repeated the ascorbate oxidase treatment with the amendment that following the initial 5 minute incubation, the sample was transferred to an incubator at 37^{O}C for a further 10 minutes to promote the hydrolysis of DHA. Following DTT reduction and acidification of this sample no ascorbate was recovered, whilst the cysteine and uric acid peaks seen at 810 mV were unaffected.

2.2.5.2 Glutathione determinations

Total glutathione concentrations were measured using the GSSG-reductase-DTNB recycling method developed by Tietze (Tietze 1969) and subsequently modified for use on a plate reader by Baker *et al.* (Baker, Cerniglia et al. 1990). This is based on a kinetic assay in which glutathione causes a continuous reduction of 5,5'-dithiobis(2-nitrobenzoic acid) (DTNB) to TNB. Glutathione reductase and NADPH subsequently recycle the oxidised glutathione (GSSG) formed to regenerate reduced glutathione (GSH). The product, TNB, is assayed by measuring the absorbance at 405 nm, its production being proportional to the total glutathione present, and is expressed as GSH equivalents: total glutathione = GSH + (2 x GSSG).

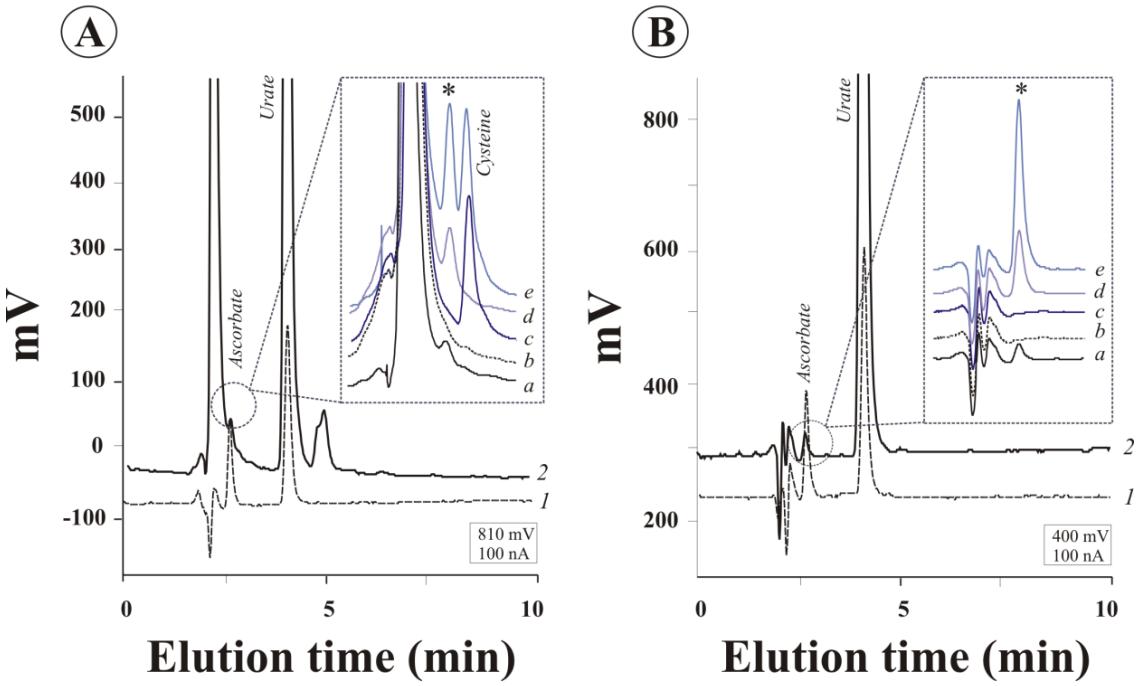

Figure 2.2: Typical chromatograms derived from freshly prepared nasal lavage fluid obtained from a healthy male subject. Panel 'A' illustrates a set of traces at 810 mV, with thiols (cysteine and reduced glutathione) and panel 'B' at 400 mV, without thiols. The ascorbate and urate peaks are highlighted. The trace labelled '1' in both diagrams corresponds to a standard containing ascorbate and uric acid at 3.125 and 6.25 µM respectively, prepared in 5% MPA. Trace '2' corresponds to the acidified (5% MPA final concentration) nasal lavage fluid sample. The inset panels illustrate a magnification of the circled section of the main trace with, 'a', corresponding to the acidified lavage sample; 'b', the sample treated with ascorbate oxidase; 'c', the sample treated as outlined previously, but subsequently incubated at room temperature for 10 minutes prior to sample reduction with 0.1% DTT (final concentration); 'd', the lavage fluid spiked with ascorbic acid; and 'e', the lavage fluid immediately reduced with DTT, prior to sample acidification. The position of the ascorbate peak is marked with an asterisk.

50 µl aliquots of DES/BHT-treated samples were added to a 96-well ELISA microplate (Greiner Bio-one, Stonehouse, UK) and 100 µl of DTNB reaction mix added to achieve final concentrations of 0.15 mM DTNB, 0.2 mM NADPH and 1 U glutathione reductase (from baker's yeast) in phosphate buffer (100 mM sodium phosphate containing 1 mM ethylenediaminetetraacetic acid (EDTA), pH 7.5) in each well. The plate was then transferred to a plate reader (SpectraMAX 190, Molecular Devices) and the immediate rate of change of absorbance at 405 nm followed for two minutes at 30°C, with absorbance measurements made every 10 seconds with mixing between measurements. Glutathione concentrations in samples were measured by comparison with a set of standards (GSSG: 0-6.6 µM). A typical standard curve for total glutathione is illustrated in **Figure 2.3**.

The GSSG concentration was measured by pre-treating samples with 2-vinyl pyridine for 1 hour. This reagent forms a conjugate with GSH and prevents it from reacting with the DTNB. Treated samples were analysed as outlined above. GSSG produces two molecules of TNB when it reacts with DTNB whereas reduced GSH produces only one molecule of TNB. Consequently, the reduced GSH concentration was calculated as:

$$\text{Total glutathione} - (2 \times \text{GSSG})$$

GSSG concentrations in samples were again measured by comparison with a set of standards (GSSG: 0-3.3 µM) also treated with 2-vinyl pyridine. A typical standard curve for GSSG ran with and without 2-vinyl pyridine treatment is shown in **Figure 2.3**. The sensitivity of this glutathione assay has been determined to be 0.025 µM and 0.01 µM

for GSH and GSSG respectively. Intra- and inter-assay variability for GSH was determined to be <5% and for GSSG <10%.

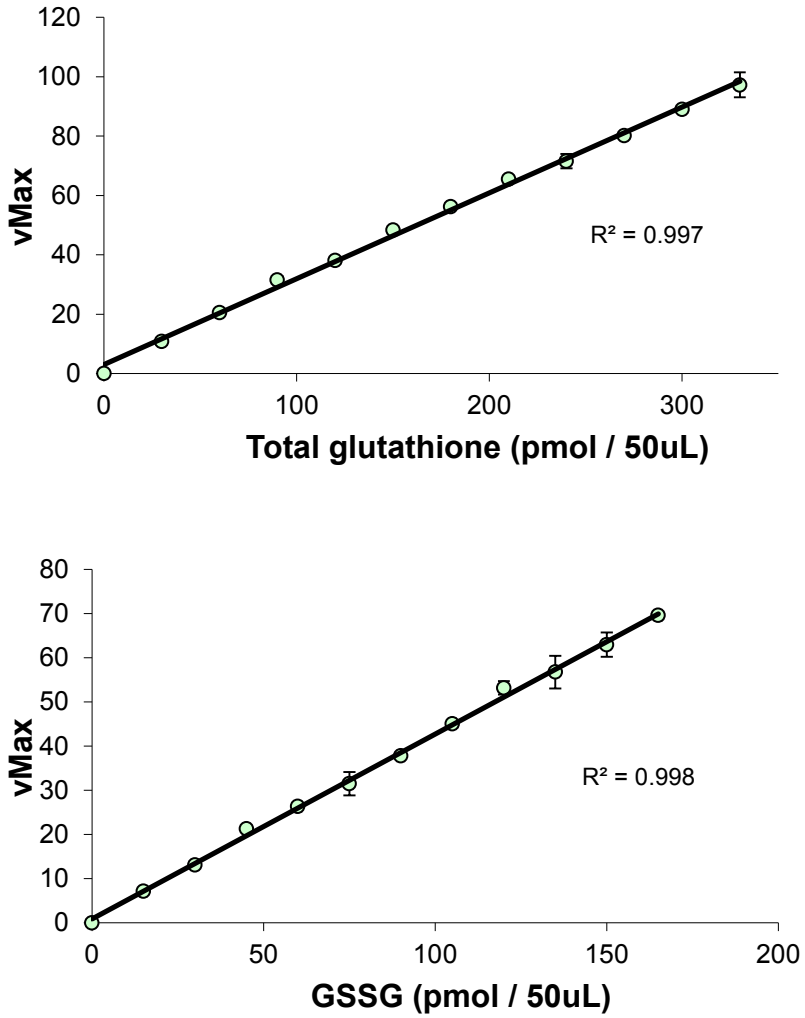

Figure 2.3: Typical standard curves of total glutathione (upper panel; concentrations: 0, 30, 60, 90, 120, 150, 180, 210, 240, 270, 300 and 330 ρmol/50 µl; n = 2) and glutathione disulphide (lower panel; concentrations: 0, 15, 30, 45, 60, 75, 90, 105, 120, 135, 150 and 165 ρmol/50 µl).

2.2.5.3 Total protein determinations

Total protein was measured by reaction with bicinchoninic acid (BCA) and 4% copper (II) sulphate against a set of bovine serum albumin (BSA) standards (Smith,

Krohn et al. 1985). This method is based on the reduction of Cu^{2+} by proteins in an alkaline medium, with the highly sensitive and selective colourimetric detection of Cu^{+} using BCA. The chelation of two molecules of BCA with each Cu^{+} ion forms a purple coloured product that exhibits a strong absorbance at 562 nm. A typical standard curve is illustrated in **Figure 2.4**.

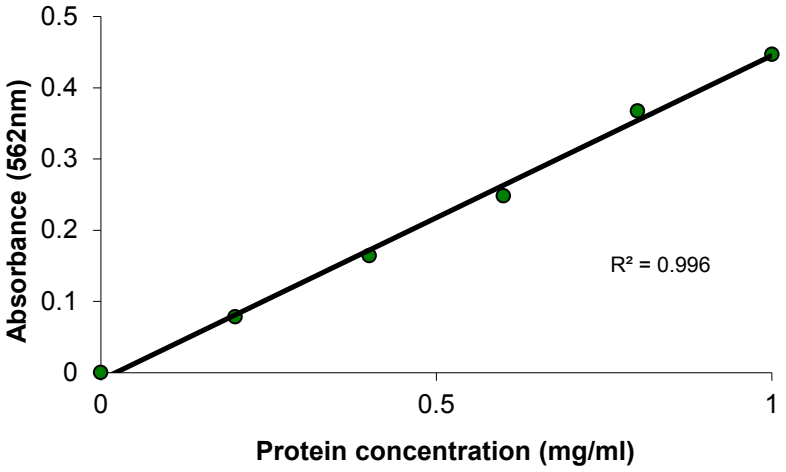

Figure 2.4: Typical standard curve of total protein concentration with BSA standard concentrations of 0, 0.2, 0.4, 0.6, 0.8 and 1.0 mg/ml.

2.2.5.4 Endogenous protein chelator measurements

Metal handling proteins were measured in untreated lavage using a variety of commercially available ELISA kits. Human transferrin (diluted 50-fold in the supplied assay buffer) and ferritin (undiluted) were quantified in BAL fluid samples with the use of ELISA kits from Alpha Diagnostic International, Inc., San Antonio, TX, USA. Human lactoferrin (undiluted) was quantified by ELISA kits from OXIS Research International, Inc., Portland, OR, USA.

2.2.5.5 Determination of protein bound 4-HNE

HNE-His protein adducts were quantified using the OxiSelect HNE-His Adduct ELISA Kit (Cell Biolabs, Inc., San Diego, CA) according to the manufacturer's instructions. HNE-His adduct concentrations in the lavage samples were established by comparing the sample absorbance against a known HNE-BSA standard curve: 0-10 μg/ml.

2.2.6 Statistics

Data were not normally distributed (Shapiro-Wilks test) and are therefore expressed throughout as medians with the 25th and 75th percentiles. Comparison of inflammatory cell numbers, antioxidant and oxidative damage markers concentrations across the various subject groups were performed using the Kruskal–Wallis one-way analysis of variance by ranks, with post-hoc testing between specific groups performed using the Mann-Whitney U test. In all cases significant differences were assumed at the 5% level. Correlation analysis for each individual group, plus compiled groups of COPD patients (current and ex-smokers) and smokers (both aged 'healthy' smokers and COPD smokers) were performed using the Spearman Rank Order Correlation. These analyses were restricted parameters that had been shown to differ significantly between groups to limit the likelihood of reporting spurious associations. All analyses were performed using SPSS, version 17.0 (SPSS Inc., Chicago, IL).

2.3 Results and Discussion

To investigate whether COPD patients exhibit oxidative stress at the surface of their airways, I performed measurements of the major low molecular weight

antioxidants and chelator proteins in airway lavage fluids recovered from current and ex-smoking patients, as well as age and smoking-history matched controls (details provided in **Table 2.5**). In addition, I examined the concentration of the lipid oxidation marker, 4-hydroxynonenal (as protein adducts), which had previously been reported to be elevated in lung tissue specimens obtained during lung resections of patients with COPD (Rahman *et al*. 2002). This is the first comprehensive study to examine RTLF antioxidant defences in lavage samples from COPD patients, as reviewed in **section 2.1**, and complements earlier work examining cellular antioxidant defences in airway leukocytes recovered by BAL in these subjects (Behndig *et al*. 2009). Data arising from these subject groups on lymphocyte subsets have been published previously by our collaborators at the University of Umeå (Roos-Engstrand *et al*. 2009, 2010 and 2011).

Of the subjects recruited into the study, bronchoscopy with bronchoalveolar lavage was successfully performed on 9/11 COPD smokers, 15/17 COPD ex-smokers, 13/13 healthy aged never-smokers and 16/16 'healthy' aged smokers, with recovery being significantly lower (36%) in the COPD ex-smoking group relative to the aged match never-smokers (50%, $P<0.05$) – **Table 2.2**. Overall recoveries were markedly lower than has previously been reported in younger populations of healthy volunteers and asthmatics, where in excess of 70-80% of the instilled volume is typically recovered (Mudway *et al*. 2001). Differential cell counts are presented for both BW and BAL fluid in **Table 2.4** and were performed by colleagues at the Division of Medicine/Respiratory Medicine and Allergy, Umeå University, Umeå, Sweden.

2.3.1 Differential cell counts

An increase in total airway leukocytes of smokers compared to never-smokers was observed, predominantly reflecting a 2.6 and 2.1-fold expansion in BAL fluid macrophage numbers in aged healthy and COPD smokers compared with their corresponding never-smoking or ex-smoking controls (P<0.001 in both cases – **Table 2.4**). These data therefore accord with other published studies showing an increase in total leukocytes in the airways of smokers with normal lung function (Wallace *et al*. 1992; Barcelo *et al*. 2008); with a similar expansion in airway macrophage numbers reported in the lungs of young smokers (Ohnishi *et al*. 1998). A similar smoking-related increase in macrophage numbers was not apparent in the more proximal BW sample. No increase in macrophage numbers was observed in the COPD patients, current or ex-smokers compared with their relevant control groups. This result is somewhat at odds with the literature reports of increased macrophage numbers in the bronchial sub-mucosa (Rutgers *et al*. 2000; Di Stefano *et al*. 1996; Saetta *et al*. 1993), bronchial glands (Saetta *et al*. 1997) and airway epithelium (Turato *et al*. 2002) of COPD patients. Furthermore, there is some evidence supporting a positive association between alveolar macrophage numbers and the severity of COPD (Finkelstein *et al*. 1995; Gorska *et al*. 2008). It is important to state that the COPD patients in the current study were all clinically stable, with no airway infection for a period of 3 months prior to the bronchoscopy, no recent exacerbations and were not taking anti-inflammatory medications. These tight recruitment criteria were adopted to minimise the influence of recent exacerbations and medication usage. Other studies examining airway inflammation in COPD have often provided limited information on the patient's recent history of infection, medication usage or smoking

history (examples being, Smyth *et al*. 2007; Saetta *et al*. 1993; Costabel *et al*. 1992), which makes a simple comparison of observations between studies difficult. This theme will be discussed in greater detail in the later section examining the absence of a clear neutrophilia in COPD patients examined in this study.

Table 2.4: Differential white blood cell counts in BW and BAL fluids from COPD patients and aged and smoking matched controls. Cell numbers are presented as cell/mL*10^4.

	Age Control Never smoker *(n=13,13≠,13§)*	Aged Control Current smoker *(n=16, 16≠,16§)*	COPD patients Ex-smokers *(n=17, 15≠,15§)*	COPD patients Current smokers *(n=11, 8≠,9§)*	KW-test
			Bronchial wash		
Total Cells	7.0 (5.6-11.2)	9.7 (7.9-19.9)	3.8 (2.1-10.2)	9.7 (3.4-14.5)	NS
Macrophages	6.2 (3.4-9.3)	8.7 (6.5-17.0)	2.0 (1.6-6.6)*c*	8.9 (3.2-13.0)	$P = 0.031$
Neutrophils	1.2 (0.3-1.4)	0.4 (0.2-0.7)	0.6 (0.2-1.4)	0.5 (0.2-0.6)	NS
Lymphocytes	0.6 (0.3-0.8)	0.7 (0.4-0.9)	0.3 (0.1-0.5)*c*	0.2 (0.1-0.4)*b*	$P = 0.016$
Eosinophils	0.0 (0.0-0.1)	0.1 (0.0-0.1)	0.0 (0.0-0.1)	0.0 (0.0-0.2)	NS
Mast cells	0.00 (0.00-0.01)	0.03 (0.01-0.04)*a*	0.00 (0.00-0.01)	0.00 (0.00-0.01)	$P = 0.027$
			Bronchoalveolar lavage fluid		
Total Cells	17.1 (11.1-26.9)	39.7 (34.0-48.3)*a*	17.7 (14.7-23.8)	29.7 (27.4-45.6)*d*	$P < 0.001$
Macrophages	14.1 (9.8-16.6)	36.6 (30.7-45.5)*a*	14.0 (11.3-20.7)	29.0 (26.1-39.3)*d*	$P < 0.001$
Neutrophils	0.1 (0.1-0.2)	0.5 (0.3-0.8)*a*	0.3 (0.1-0.4)	0.1 (0.1-0.6)	NS
Lymphocytes	1.7 (0.9-3.9)	2.3 (1.5-3.2)	2.3 (1.1-3.2)	1.3 (0.6-1.5)	NS
Eosinophils	0.0 (0.0-0.1)	0.1 (0.0-0.1)	0.1 (0.0-0.2)	0.2 (0.1-0.3)	NS
Mast cells	0.01 (0.01-0.02)	0.06 (0.03-0.10)*a*	0.01 (0.00-0.02)	0.03 (0.03-0.07)	$P = 0.013$

All data are expressed as medians with either the inter-quartile or full range, as indicated. Significant differences across groups were assumed at the 5% level using the Kruskal–Wallis one-way analysis of variance by ranks (significance illustrated in the far right hand column), with post-hoc testing between specified groups performed using the Mann-Whitney U Test. Comparison of individual groups were restricted to healthy smokers versus never smokers (*a*, $P < 0.05$), healthy smokers and COPD current smokers (*b*, $P < 0.05$), never smokers versus COPD ex-smokers (*c*, $P < 0.05$) and COPD current and ex-smokers (*d*, $P < 0.05$). Subject numbers given in parenthesis represent the subjects recruited, plus the number of subjects from which BW or BAL was recovered for differential cell counts.

Whilst I observed no evidence of increased macrophage numbers associated with COPD, the smoking related increase was clear cut. It was also notable at the gross level that the aspirates obtained from the lungs of smoking subjects were discoloured (**Figure 2.5**), with corresponding cytospin preparations demonstrating the presence of carbon inclusions in many of the macrophages, consistent with previous observations (Brody *et al*. 1975). This increase in macrophage numbers in the distal lung in response to cigarette smoke could reflect increased recruitment or proliferation within the lung, or reduced cell death. In support of the first of these options, monocyte-selective chemokine (MCP-1) and GRO-α have been shown to be increased in induced sputum and BAL samples from COPD patients, including current smokers (Traves *et al*. 2002; Capelli *et al*. 1999), associated with increased alveolar and airway macrophage numbers (de Boer *et al*. 2000). Evidence of increased macrophage proliferation or reduced cell death has been inferred from the observation that inclusion bodies containing particles from cigarette smoke can be detected within the airway macrophages at least 2 years after smoking cessation (Marques *et al*. 1997). Macrophages themselves appear to have relatively low proliferative capacity within the lung, though some evidence of proliferation has been noted in the lungs of smokers relative to healthy and asthmatic subjects (Tomita *et al*. 2002; Bitterman *et al*. 1984; Barbers *et al*. 1991). There is however, increasing evidence that alveolar macrophages from smokers exhibit a reduced rate of cell death (Tomita *et al*. 2002) related to increased expression of anti-apoptotic proteins, such as Bcl-xL and redox sensitive induction of p21CIP1/WAF1, a key regulator of the cell cycle (Yin *et al*. 1999). Recently, a significant reduction in the proportion of sputum

neutrophils undergoing spontaneous apoptosis has also been reported in healthy smokers and individuals with COPD compared with non-smokers (Brown *et al*. 2009).

Cigarette smoke has also been reported to activate alveolar macrophages stimulating the release of inflammatory mediators such as tumour necrosis factor (TNF)-[alpha], IL-8, LTB4 and interleukin-1 (IL-1) (Sarir *et al*. 2009; Ito *et al*. 2000) as well as reducing their capacity to phagocytose apoptotic epithelial cells (Hodge *et al*. 2003), *Escherichia coli* (Prieto *et al*. 2001) and *H. influenzae* (Berenson *et al*. 2006). Whilst I did not explore cellular function in this thesis in relation to disease severity or smoking status, it is significant that there is increasing evidence of aged and functionally impaired macrophages in the lungs of aged smokers. Previous work by Behndig *et al.* (2009) examining the antioxidant enzymes in airway leukocytes (predominately alveolar macrophages) harvested from the same subjects as employed in this analysis demonstrated an apparent age related decline in their activities, which appeared independent of disease state or smoking status. Given that many of the non-smoking COPD patients were recent quitters, it is tempting to speculate that the presence of aged cell macrophages in the lung with degraded defences may contribute to the pathology of COPD, though one would want to see evidence of increased oxidative stress in these individuals in support of this contention.

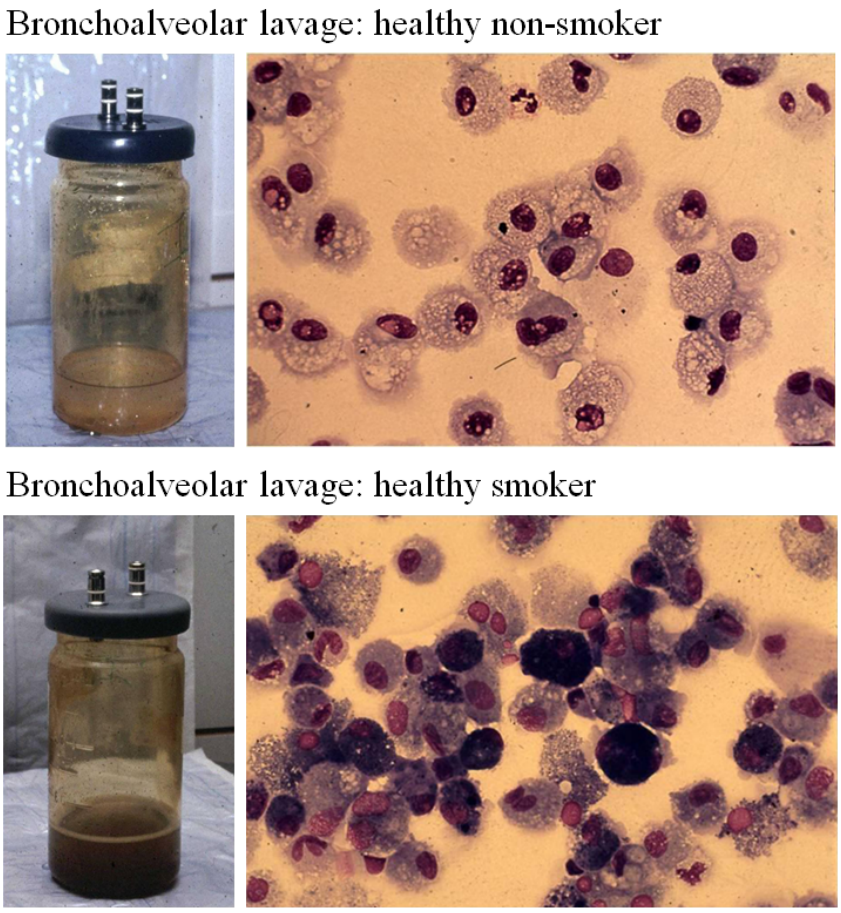

Figure 2.5: Bronchoalveolar lavage aspirates from a healthy never-smoker (upper left hand panel), and a current smoker (lower left hand panel) from the aged control groups of the current study. The corresponding May-Grűnwald Giemsa stained cytospins are illustrated to the right, illustrating the preponderance of macrophages, and in the lower panel the presence of carbon inclusions in the darkly stained cells.

No evidence of neutrophilia in COPD smokers and ex-smokers was observed relative to their control groups (**Table 2.4**). This observation differs markedly from the published literature where increased BAL neutrophils have been reported in both smoking and ex-smoking COPD patients (Babusyte *et al*. 2007; Barnes *et al*. 2003). Moreover, this increase in neutrophil numbers has been reported to persist even after smoking cessation (Louhelainen *et al*. 2009). The basis for this cellular recruitment to the airways has been associated with the increased release of chemotactic factors such as interleukin 8 (IL-8) and leukotriene B_4 (LTB_4), which have been shown to be

elevated in the airways of patients with COPD (Corhay *et al*. 2009; Sarir *et al*. 2009). Again, the discrepancy between the absence of overt inflammation in the COPD patients in the current study versus the existing literature may reflect the clinical status of the mild to moderate COPD patients examined in the present study. Previous studies have reported increased airway neutrophilia to be associated with more severe disease (Hodge *et al*. 2004) or exacerbations (Fiorini *et al*. 2000).

Increases in BAL mast cell numbers were also observed in aged 'healthy' smokers (0.06 (0.03-0.10) cell/mL*10^4) relative to the aged non-smokers (0.01 (0.01-0.02) cell/mL*10^4, P=0.002), with a similar increase also apparent in the more proximal BW sample (P=0.017). A similar increase was not observed in the COPD smokers relative to the ex-smoking patients. Recently, it has been demonstrated that the numbers of mast cells were significantly increased in the sputum of smokers compared to ex-smokers (Wen *et al*. 2010). Moreover, CXCL-10, which has recently been implicated in mast cell migration to the airway smooth muscle cells bundles (Brightling *et al*. 2005) has been shown to be elevated in the airways of smokers compared to control groups (Clarke *et al*. 2010). Mast cell activation has also been demonstrated in the distal lung of smokers, with increased concentrations of histamine and tryptase reported in bronchoalveolar lavage fluid recovered from these subjects (Yamamoto *et al*. 1997). Overall therefore, I observed little evidence of upper or lower airway inflammation in relation to the presence of COPD itself, rather the increased numbers of macrophages and mast cells were related to smoking status.

2.3.2 Low molecular weight antioxidants

Consideration of the antioxidant defences within the respiratory tract lining fluids of the volunteers was restricted to the major low molecular weight antioxidants (glutathione, urate and ascorbate) and chelator proteins (transferrin, lactoferrin and ferritin). Due to the limited recovery of lavage samples from the bronchial airways, especially from the COPD patients, these analyses were restricted to the more distal bronchoalveolar lavage fluid samples. These data are summarised in **Table 2.5**. Significantly increased concentrations of GSH were noted in both the aged 'healthy' (5.1-fold increase, $P<0.001$) and COPD smokers (2.3-fold increase, $P=0.019$) relative to their non-smoking control groups (**Figure 2.6)**. These increases were not associated with enhanced concentrations of glutathione disulphide in the smoking subjects. In addition, I observed no evidence of increased GSH or GSSG concentrations related to the presence of COPD. The observation of an increase in respiratory tract lining fluid GSH concentrations following acute smoking, or in active smokers, accords with previous observations (Cantin, North *et al.* 1987; Linden, Hakansson *et al.* 1989; Morrison, Rahman *et al.* 1999; MacNee 2000). Similar increases in GSH at the air-lung interface have also been reported in human subjects following inhalation of gaseous oxidants (nitrogen dioxide - Kelly *et al*. 1996; ozone -Mudway *et al*. 2006), or diesel exhaust (Mudway *et al*. 2004) suggesting that the transient up-regulation of GSH following acute exposures to these aerosols may act to counteract the increased oxidant burden at the air-lung interface.

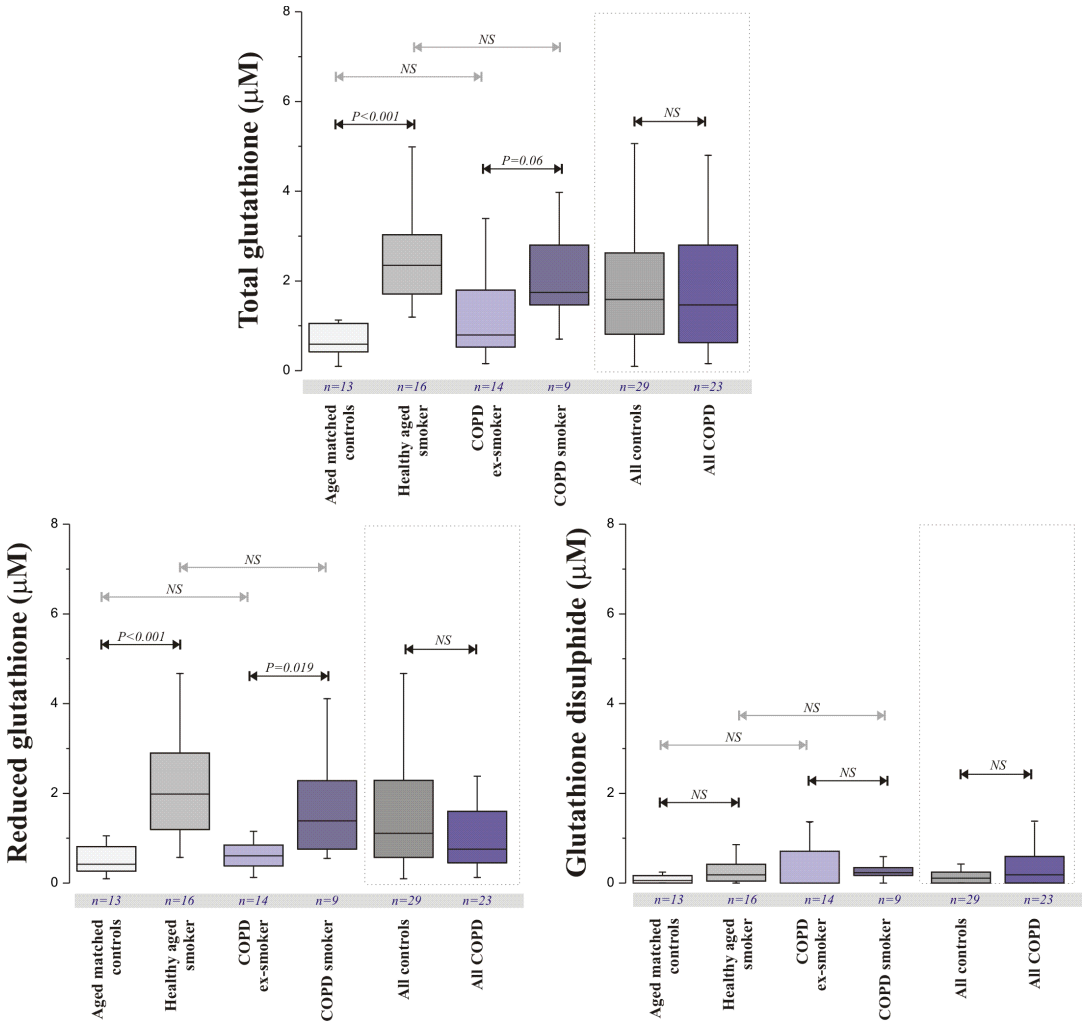

Figure 2.6: Total and reduced glutathione, plus glutathione disulphide concentrations in bronchoalveolar lavage fluids recovered from COPD patients (both current and ex-smokers) and aged matched controls (current and never smokers). Data are summarised as box plots, with the central line illustrating the median values, the upper and lower boundaries of the box, the 75th and 25th percentiles respectively, and the whiskers, the 95% confidence intervals. Comparisons between groups were performed using the Mann-Whitney U Test, with *P*-values illustrated. NS = no significant difference between the indicated groups.

Table 2.5: Antioxidant and oxidative damage marker concentrations on BAL fluid from COPD patients and age-match controls.

	Age Control Never smoker *(n=11-13)*	Aged Control Current smoker *(n=13-15)*	COPD patients Ex-smokers *(n=12-14)*	COPD patients Current smokers *(n=8-9)*	KW-test
Total glutathione (GSx, µM)	0.59 (0.42-1.05)	2.41 (1.74-3.23)*a*	0.82 (0.54-1.73)	1.74 (1.47-2.80)	$P < 0.001$
Reduced glutathione (GSH, µM)	0.42 (0.27-0.81)	2.14 (1.46-2.91)*a*	0.61 (0.38-0.84)	1.38 (0.76-2.28)*d*	$P < 0.001$
Glutathione disulphide (GSSG, µM)	0.06 (0.00-0.16)	0.19 (0.05-0.42)	0.04 (0.00-0.68)	0.23 (0.17-0.34)	*NS*
Vitamin C (µM)	0.37 (0.27-0.51)	0.66 (0.46-0.75)*a*	0.31 (0.27-0.52)	0.66 (0.54-0.76)	$P = 0.026$
Ascorbate (AA, µM)	0.00 (0.00-0.09)	0.09 (0.01-0.22)	0.02 (0.00-0.09)	0.16 (0.08-0.39)*d*	$P = 0.016$
Dehydroascorbate (DHA, µM)	0.29 (0.26-0.37)	0.46 (0.36-0.67)	0.21 (0.17-0.56)	0.43 (0.25-0.65)	NS
Urate (UA, µM)	0.48 (0.32-0.68)	0.41 (0.31-0.79)	0.54 (0.36-0.72)	0.66 (0.44-0.78)	NS
Total protein (mg/mL)	0.16 (0.13-0.19)	0.12 (0.12-0.16)	0.16 (0.14-0.18)	0.14 (0.13-0.16)	*NS*
4-hydroxynonenal (4-HNE,mg/mL)	1.81 (1.47-2.39)	1.32 (0.90-2.60)	0.84 (0.45-2.08)	1.29 (0.85-2.07)	NS
4-hydroxynonenal (4-HNE,µg/mg protein)	425 (384-489)	363 (301-510)	289 (212-456)	359 (292-455)	NS
Transferrin (mg/mL)	5.2 (2.7-9.3)	5.5 (4.8-8.1)	4.8 (3.5-6.5)	5.4 (1.8-6.7)	*NS*
Lactoferrin (ng/mL)	20.11 (10.58-24.44)	17.90 (14.83-32.20)	30.52 (15.02-91.14)	23.8 (18.2-26.3)	*NS*
Ferritin (ng/mL)	4.2 (4.1-6.4)	27.8 (20.9-51.0)*a*	6.5 (4.3-12.4)	74.8 (38.8-104.5)*d*	$P < 0.001$

All data are expressed as medians with inter-quartile range. Significant differences across groups were assumed at the 5% level using the Kruskal–Wallis one-way analysis of variance by ranks (significance illustrated in the far right hand column), with post-hoc testing between specified groups performed using the Mann-Whitney U Test. Comparison of individual groups were restricted to healthy smokers versus never smokers (*a*, $P < 0.05$), healthy smokers and COPD current smokers (*b*, $P < 0.05$), never smokers versus COPD ex-smokers (*c*, $P < 0.05$) and COPD current and ex-smokers (*d*, $P < 0.05$).

It remains unclear from the literature, as reviewed in Chapter 1 (**section 1.6.2.3**) whether this is a transient or sustained increase, or indeed whether it reflects a regulated export mechanism that could be defined as an adaptation or passive release from dying cells, hence reflecting injury. For example, it is long established that cells induced to undergo apoptosis demonstrate a rapid and specific efflux of GSH (van den Dobbelsteen *et al*. 1996) that can be delayed by the provision of GSH-diethylesters to boost intracellular GSH concentrations. This export process appears to involve multidrug resistance-associated protein 1 (MRP1), with export retarded by knocking down the expression of this transporter by RNA interference (Hammond *et al*. 2007). This channel also appears to play a role in the basal export of glutathione to the extracellular environment (Marchan *et al*. 2008), though it remains unclear from the existing literature how its expression is affected by oxidative stress. In addition to MRP1, multidrug resistance-associated protein 2 (MRP2) and the cystic fibrosis transmembrane conductance regulator (CFTR) have been demonstrated to play a role in GSH export (Gao *et al*. 1999; Ballatori *et al*. 2005), though once again their regulation in response to oxidative stress is poorly defined. This discussion on the potential source of the GSH moving into the RTLFs in smokers will be developed later, following consideration of the other antioxidants and relation of these findings to those obtained in young adults and asthmatic subjects.

Vitamin C (ascorbate, plus dehydroascorbate) concentrations were also found to be significantly augmented in healthy smokers, compared with the aged-matched non-smoking controls (1.8-fold, P=0.025 – **Table 2.5**, **Figure 2.7**). An increase (2.1-fold) was also observed in the COPD smoking group compared with the ex-smokers

but this failed to attain statistical significance (*P*=0.06). These increases again only appeared to relate to the subjects smoking status and not the presence of COPD. In the COPD patients the significant increase in BAL fluid vitamin C concentrations with smoking, reflected an increase in ascorbate (*P*=0.016) though it was notable that ascorbate itself contributed only a small fraction of the measured vitamin C pool and was often not measureable in the ex-, or never-smoking subjects.

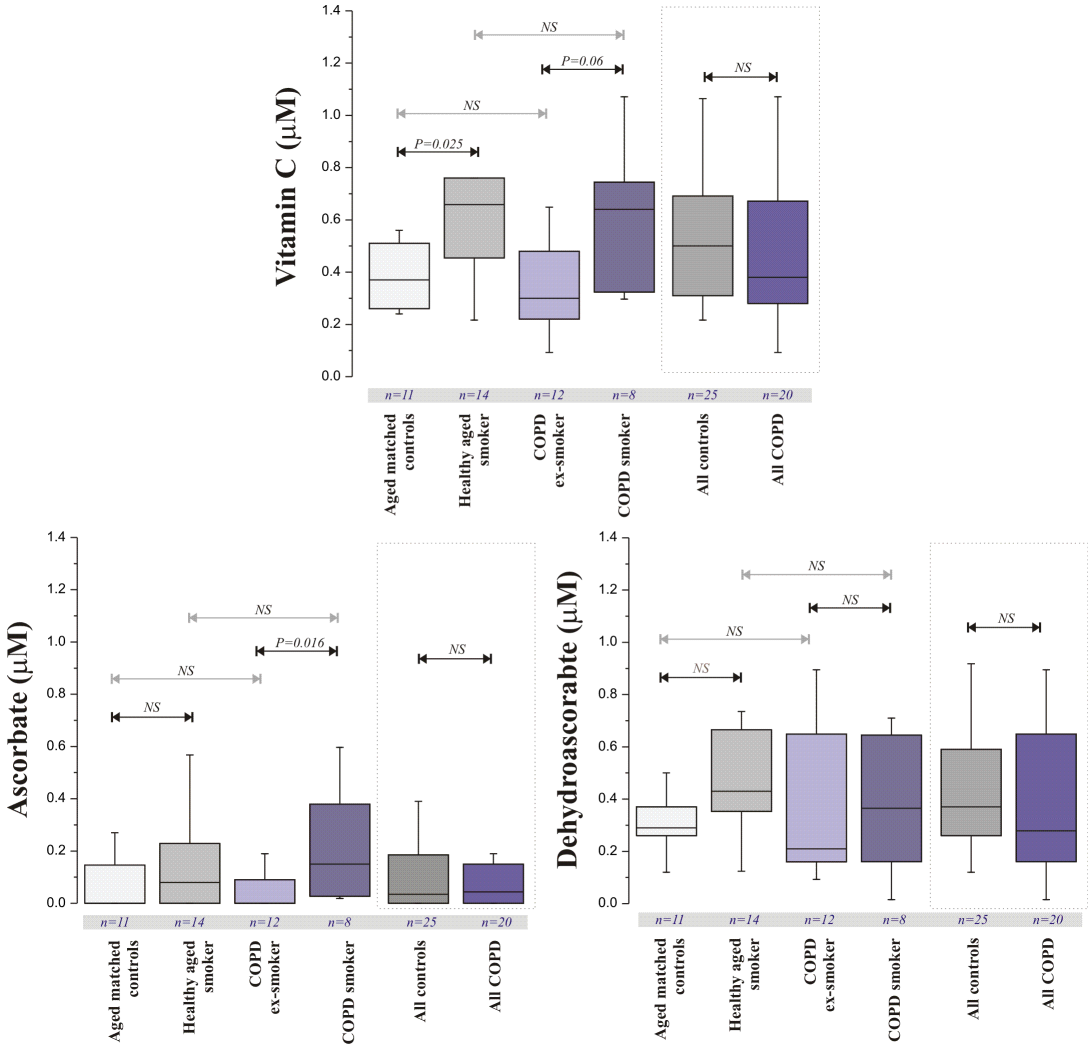

Figure 2.7: Total Vitamin C, ascorbate and dehydroascorbate concentrations in bronchoalveolar lavage fluids recovered from COPD patients (both current and ex-smokers) and aged matched controls (current and never smokers). All other data details are as outlined in the legend to figure 2.6.

The presence of high concentrations of dehydroascorbate (DHA) in the BAL fluid samples is a contentious observation. DHA is inherently unstable under physiological conditions and rapidly hydrolyses to a variety of irreversible oxidation products including 2,3-diketo-L-golonic, oxalic and threonitic acids (Deutsch, 2000). Its presence at baseline therefore raises numerous conceptual problems; if ascorbate within airway RTLFs were inherently unstable this would constitute a significant drain on the body's vitamin C reserves. Thus one has to first address the question of whether erroneous oxidation has occurred in the samples. All lavages were performed with unbuffered saline (pH 5.4) to limit oxidation during the collection and then immediately acidified with metaphosphoric acid after the isolation of the cell free fraction (see section **2.2.3**). These precautions, together with rapid sample processing at 4^{o}C and storage at -80^{o}C would be considered sufficient to preserve the *in vivo* ratio of ascorbate to DHA. It should also be noted that conditions likely to promote the oxidation of ascorbate would also result in hydrolysis of DHA, and that the ratio of GSH to GSSG (**Table 2.5**) in the samples did not support the view that there was generic oxidation of lavage aspirates.

In contrast to the intracellular environment, which is maintained in a reducing state, there is increasing evidence that the respiratory tract lining fluids of the lung may represent a more oxidising environment. Studies have demonstrated that ascorbate is rapidly oxidised by induced sputum in an azide inhibitable manner suggesting that endogenous peroxidases may contribute to the oxidative losses observed (Schock, 2004). The RTLF has also been shown to contain appreciable concentrations of non-transferrin bound iron, especially in chronic inflammatory

diseases (Gutteridge, 1996). Thus, if substantial losses of vitamin C from the RTLF are to be prevented, either regenerative pathways must exist to reduce DHA back to ascorbate, or the half-life of DHA in this compartment must be sufficient to permit its uptake by epithelial or resident inflammatory cells with its subsequent reduction back to ascorbate. Whilst the high concentrations of GSH within the RTLF will reduce a small fraction of the DHA back to ascorbate (Winkler *et al*. 1994), the rate at which this occurs over the RTLF concentration range, 200-400 μM, is insufficient to prevent substantial hydrolysis of DHA. There is also no solid evidence of dehydroascorbate reductase activity within this extracellular compartment to catalyse such a reduction. In contrast, the rapid uptake of DHA into a variety of cell types (neutrophils, lymphocytes, epithelial cells) via facilitated glucose transporters GLUT1, GLUT3 and GLUT4 has been demonstrated (Vera *et al*. 1993; Rumsey *et al*. 1997; Liang *et al*. 2001), with evidence that once internalised the DHA is rapidly reduced to ascorbate by NADPH-dependent dehydroascorbate reductases (Park *et al*. 1996; Wilson *et al*. 2002).

The major route of ascorbate uptake into cells occurs through the high affinity Na^{+-}dependent vitamin C transporters, SVCT1 and SVCT2 (Tsukaguchi *et al*. 1999). It has been argued that the uptake of DHA is only likely to be significant during episodes of oxidative stress where high local concentrations of DHA occur near to cells producing reactive oxygen species (ROS). This DHA may be taken up by the ROS producing cells, as is the case for neutrophils (Wang *et al*. 1997) as well as by other cells near the site of production (Nualart *et al*. 2003). This view is based on a number of assumptions: that vitamin C is maintained in its reduced state *in vivo* through the

action of DHA-reductases and the effective chelation of iron, and that glucose will block DHA transport.

Little is known about the regulation of vitamin C at the lung surface. Traditionally it has been assumed that RTLF ascorbate is derived by passive diffusion from the plasma pool, but there is little experimental evidence to support this view. Attempts to correlate basal human plasma and RTLF ascorbate concentrations have proven inconclusive (Behndig *et al*. 2009). Assuming that diffusion from the blood does contribute to RTLF levels it is tempting to speculate that the rapid oxidation of ascorbate not only provides DHA for cellular uptake, but also promotes further movement of ascorbate into this compartment down its concentration gradient. If ascorbate is not derived directly from the plasma pool, it might be assumed that an export mechanism exists from respiratory epithelial cells. Whilst a considerable body of work has investigated ascorbate and DHA uptake, relatively little is known about cellular export. Both the addition of ascorbate to cells and intracellular reduction of DHA to ascorbate have been shown to stimulate efflux (Wilson, 2005), though the transporters involved have not been characterised. In addition, volume sensitive anion channels have been shown to be permeable to ascorbate (Furst *et al*. 2002) but again the molecular identities of these channels are not known. Whilst there is little data on ascorbate exporters, the airway epithelium has been shown to express both SVCT1 and 2 (Tsukaguchi *et al*. 1999) in the apical membranes of tracheal, bronchial and alveolar epithelium (Jin *et al*. 2005). Thus it would seem that rather than exporting ascorbate into this compartment, the epithelium may actively take up this antioxidant.

This, coupled to the instability of ascorbate within this compartment, may partially explain why the measured ascorbate concentrations were low in the current study. The basis for the relatively small increase observed in the smoking subjects, as with the GSH response, remain elusive and will be considered later in this chapter.

Urate represents one of the major low molecular weight antioxidants within the RTLF (reviewed in section **1.6.2.1**). Whilst previous studies have demonstrated low plasma urate concentrations to be associated with COPD severity (Nicks, 2011), in the present study I observed no evidence of altered BAL fluid urate concentrations associated with either smoking status or the diagnosis of COPD (**Table 2.5)**. This accords with the only other published study addressing lavage urate concentrations in COPD, which demonstrated elevated concentrations in saliva but not BAL fluid from COPD smokers and ex-smokers relative to aged and smoking status matched controls (Yigla, 2007).

2.3.3 Chelator proteins

In addition to the low molecular weight antioxidants, I also considered the concentration of transferrin, lactoferrin and ferritin within the lavage returns. These data (summarised in **Table 2.5** and **Figure 2.8**) demonstrated a marked smoking-related increase in ferritin concentrations in both the aged healthy and COPD smokers relative to their non-smoking controls. This response appeared to parallel the increased concentrations of glutathione and vitamin C reported in the smoking groups. As ferritin is predominately an intracellular Fe storage protein, one explanation of this finding is that ferritin is being released into the respiratory tract

lining fluids as a function of cell death, with an associated release of intracellular antioxidants which possibly suggests that the response is not a regulated adaptation, as discussed previously. A previous study by Ghio *et al*. (1998) demonstrated a similar increase in ferritin in human volunteers following instillation of an iron-containing particle. In contrast to the present study however, Ghio also observed a parallel increase in lavage lactoferrin and decreased transferrin concentrations. In the present study, the concentration of these proteins was equivalent across the considered groups. Similar increases in ferritin have been reported in rat and human respiratory epithelial cells exposed to cigarette smoke and/or condensate with ferritin also reported to be elevated in airway lavage samples from smokers and patients with COPD, relative to healthy non-smoking controls (Ghio, 2008).

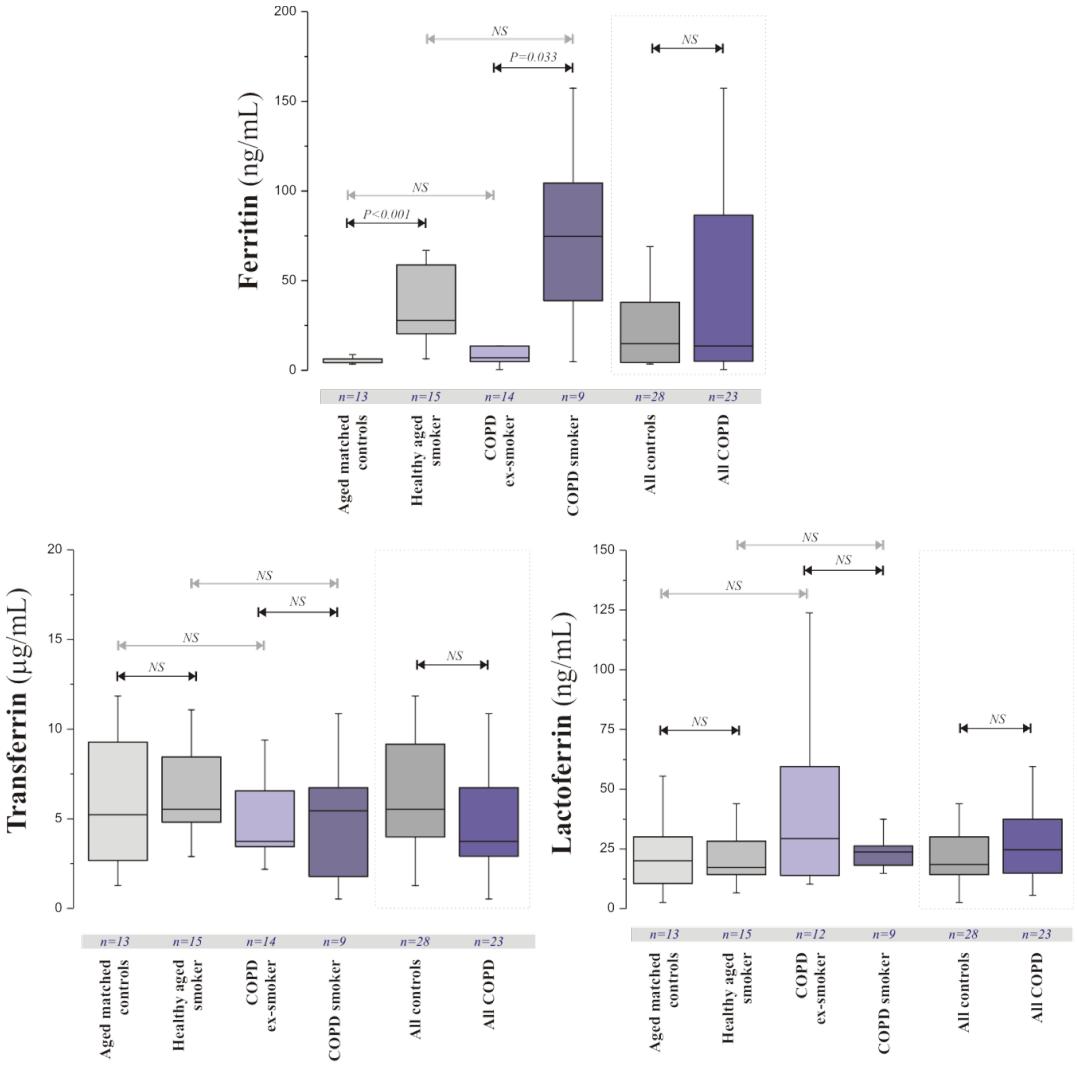

Figure 2.8: Ferritin, transferrin and lactoferrin concentrations in bronchoalveolar lavage fluids recovered from COPD patients (both current and ex-smokers) and aged matched controls (current and never smokers). All other data details are as outlined in the legend to figure 2.6.

2.3.4 Protein bound 4-HNE

In addition to respiratory tract lining fluid antioxidant concentration, I also examined the concentration of 4-hydroxy-2-nonenal (4-HNE) protein adducts **Table 2.5**, **Figure 2.9** (data are expressed per unit volume of recovered BAL, or per unit protein). The focus on this oxidative post-translational modification was based on previously published data in which increased staining for 4-HNE-modified proteins was

observed in the airway epithelium, endothelium and neutrophils in lung tissue specimens obtained during lung resections, from patients with and without COPD (Rahman, *et al*. 2002). I observed no evidence of increased adduct concentrations in the lavage samples in relation to subject smoking status, or the presence of COPD (**Figure 2.9**). Rather, there was evidence of decreased concentration of 4-HNE-modified proteins in COPD ex-smokers relative to their aged-matched non-smoking controls, though this failed to attain statistical significance (P=0.06) unless the comparison was performed between the combined groups of smoking and non-smoking controls and COPD patients on a per unit protein basis (P=0.04).

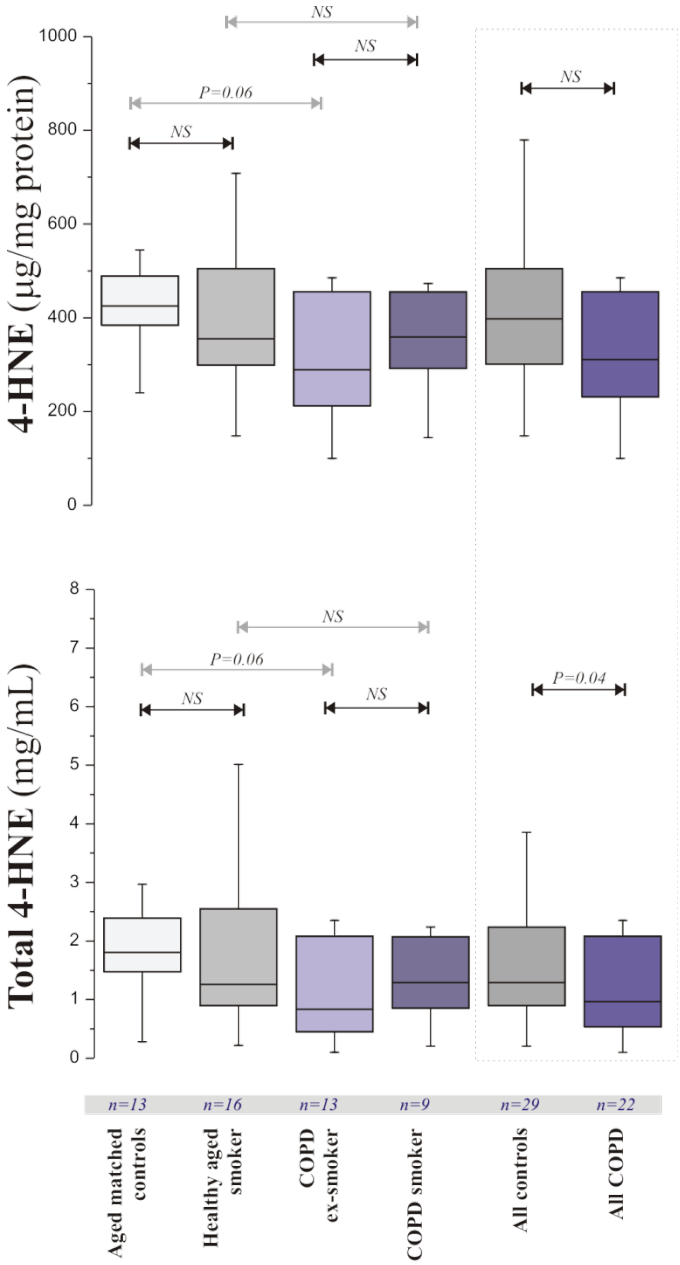

Figure 2.9: Protein bound 4-hydroxynonenal concentrations in bronchoalveolar lavage fluids recovered from COPD patients (both current and ex-smokers) and aged matched controls (current and never-smokers). Data are expressed per volume of recovered lavage and per mg of total protein. All other details are as outlined in the legend to figure 2.6.

2.3.5 Correlation data

Correlation analysis was performed between those antioxidant and oxidative damage marker concentrations which had been shown to differ between the patient groups and selected clinical endpoints related to impaired pulmonary function (FEV_1 and reversibility), gas exchange ($TL_{CO}SB$) and inflammation (BAL macrophage and neutrophil numbers). The results of these analyses are summarised in **Tables 2.6 – 2.9** for healthy never-smokers, healthy smokers, COPD ex-smokers and COPD current smokers respectively. Further correlation matrices related to all smoking subjects and all COPD patients are subsequently illustrated in **Tables 2.10** and **2.11**. Overall these analyses failed to show any coherent pattern of associations related to smoking status or the severity of COPD. Whilst there was evidence of a statistically significant association between BAL GSH and predicted FEV_1 (Spearmans rho (ρ)=0.74, *P*=0.003) and airway reversibility following bronchodilation with 1mg of terbutalin (ρ=0.62, *P*=0.019) in the COPD ex-smokers (**Table 2.8**), similar associations were not apparent following smoking continuation in these subjects (**Table 2.9**) or when all COPD subjects (n=28) were considered in the analysis (**Table 2.11**).

Table 2.6: Correlation (Spearman Rank Order Correlations) matrix for healthy aged never-smokers.

		Clinical parameters						Bal cells		Antioxidants						
		Age	Pack years	FEV_1% *predicted*	FVC% *predicted*	TL_{CO}^{SB}	Reversibility	Macrophages	Mast cells	GSx	GSH	GSSG	Vitamin C	Ascorbate	DHA	Ferritin
Age	Spearman rho (ρ)		.	-.336	-.607	.	.282	-.420	.077	.196	.188	.131	-.133	.218	-.469	.417
	P-value		.	.262	.063	.	.351	.153	.802	.521	.539	.670	.696	.520	.146	.156
Pack years	Spearman rho (ρ)			.	.	.	.	.	.	.	.	.	.	.	.	.
	P-value			.	.	.	.	.	.	.	.	.	.	.	.	.
FEV% *predicted*	Spearman rho (ρ)				.948	.	-.105	.486	.057	-.180	-.326	-.010	-.137	-.529	.307	-.330
	P-value				<0.001	.	.733	.092	.853	.557	.277	.974	.687	.094	.359	.271
FVC% *predicted*	Spearman rho (ρ)					.	-.474	.468	.280	-.170	-.237	-.148	.006	-.398	.042	-.525
	P-value					.	.166	.172	.434	.638	.510	.683	.989	.329	.921	.119
TL_{CO}^{SB}	Spearman rho (ρ)						.	.	.	.	.	.	.	.	.	.
	P-value						.	.	.	.	.	.	.	.	.	.
Reversibility	Spearman rho (ρ)							-.176	-.293	-.137	-.027	.099	-.323	-.379	.132	-.221
	P-value							.566	.331	.655	.929	.747	.332	.250	.699	.467
Macrophages	Spearman rho (ρ)								.225	-.011	.170	-.507	.697	.337	.487	.083
	P-value								.460	.972	.578	.077	.017	.311	.128	.788
Mast cells	Spearman rho (ρ)									.014	.390	-.487	.120	.239	-.290	-.232
	P-value									.963	.188	.092	.725	.478	.388	.445
GSx	Spearman rho (ρ)										.819	.620	.569	.769	.141	.620
	P-value										.001	.024	.067	.006	.679	.024
GSH	Spearman rho (ρ)											.150	.633	.832	.023	.382
	P-value											.625	.036	.001	.947	.198
GSSG	Spearman rho (ρ)												-.292	-.183	.125	.285
	P-value												.383	.591	.715	.345
Vitamin C	Spearman rho (ρ)													.781	.534	.508
	P-value													.005	.090	.111
Ascorbate	Spearman rho (ρ)														-.021	.677
	P-value														.951	.022
DHA	Spearman rho (ρ)															.105
	P-value															.758

Significant associations (Spearman rho and *P*-value, n=8-13) are highlighted in red text. Grey cells illustrate that one or both pairs of variable were not determined in this particular group.

Table 2.7: Correlation (Spearman Rank Order Correlations) matrix for 'healthy' aged smokers.

		Clinical parameters						Bal cells		Antioxidants						
		Age	Pack years	FEV_1% *predicted*	FVC% *predicted*	TL_{CO}^{SB}	Reversibility	Macrophages	Mast cells	GSx	GSH	GSSG	Vitamin C	Ascorbate	DHA	Ferritin
Age	Spearman rho (ρ)		.382	-.394	-.289	.240	-.387	-.003	-.166	.358	.163	.155	.327	.114	.206	.174
	P-value		.145	.131	.278	.370	.138	.991	.538	.174	.547	.566	.254	.698	.480	.534
Pack years	Spearman rho (ρ)			-.257	-.404	.322	.151	.477	.273	-.034	.165	-.504	.177	.482	-.208	.296
	P-value			.336	.121	.224	.578	.062	.306	.901	.540	.047	.544	.081	.476	.283
FEV% *predicted*	Spearman rho (ρ)				.814	-.224	.384	-.272	-.023	.251	.121	.329	.411	.407	.093	.017
	P-value				<0.001	.404	.142	.309	.932	.348	.655	.214	.144	.148	.752	.952
FVC% *predicted*	Spearman rho (ρ)					-.115	.131	-.334	-.345	.158	-.010	.407	.349	.244	.141	.008
	P-value					.672	.628	.206	.191	.560	.970	.118	.222	.401	.631	.977
TL_{CO}^{SB}	Spearman rho (ρ)						-.043	.346	-.057	.191	.222	-.069	.176	.231	.187	-.029
	P-value						.875	.189	.833	.478	.408	.800	.546	.426	.522	.919
Reversibility	Spearman rho (ρ)							.285	.333	.047	.141	-.145	.046	.462	-.288	.470
	P-value							.284	.208	.863	.602	.593	.875	.096	.318	.077
Macrophages	Spearman rho (ρ)								.426	-.041	.324	-.573	.306	.340	.354	.540
	P-value								.100	.880	.222	.020	.287	.234	.215	.038
Mast cells	Spearman rho (ρ)									-.190	.097	-.709	.012	.209	-.053	.144
	P-value									.481	.722	.002	.967	.472	.857	.609
GSx	Spearman rho (ρ)										.859	.498	.850	.469	.495	.148
	P-value										<0.001	.050	<0.001	.091	.072	.598
GSH	Spearman rho (ρ)											.097	.883	.633	.464	.290
	P-value											.719	<0.001	.015	.095	.295
GSSG	Spearman rho (ρ)												.174	-.162	.179	-.370
	P-value												.552	.580	.540	.174
Vitamin C	Spearman rho (ρ)													.580	.694	.405
	P-value													.030	.006	.151
Ascorbate	Spearman rho (ρ)														-.060	.321
	P-value														.839	.262
DHA	Spearman rho (ρ)															.233
	P-value															.422

Significant associations (Spearman rho and *P*-value, n=14-16) are highlighted in red text. Grey cells illustrate that one or both pairs of variable were not determined in this particular group.

Table 2.8: Correlation (Spearman Rank Order Correlations) matrix for COPD ex-smokers.

		Clinical parameters						Bal cells		Antioxidants						
		Age	Pack years	FEV_1% *predicted*	FVC% *predicted*	TL_{CO}^{SB}	Reversibility	Macrophages	Mast cells	GSx	GSH	GSSG	Vitamin C	Ascorbate	DHA	Ferritin
Age	Spearman rho (ρ)		-.117	-.048	-.137	-.135	.283	-.352	.015	.049	.329	-.259	-.305	.566	-.453	-.523
	P-value		.655	.856	.627	.605	.287	.199	.958	.869	.251	.371	.336	.055	.162	.055
Pack years	Spearman rho (ρ)			.492	.556	.215	.346	.218	.391	.238	.283	.174	.264	-.188	.560	-.295
	P-value			.045	.031	.408	.189	.434	.149	.412	.327	.551	.408	.559	.073	.305
FEV% *predicted*	Spearman rho (ρ)				.543	.146	.536	.219	-.049	.575	.735	.160	.455	.394	.183	-.262
	P-value				.036	.577	.032	.433	.863	.032	.003	.585	.137	.205	.591	.365
FVC% *predicted*	Spearman rho (ρ)					.007	.493	.274	.134	.733	.576	.515	.280	-.119	.261	-.228
	P-value					.980	.073	.365	.662	.007	.050	.087	.434	.743	.467	.476
TL_{CO}^{SB}	Spearman rho (ρ)						.285	.371	.077	-.077	-.022	-.021	.168	.337	.255	.174
	P-value						.284	.173	.785	.794	.940	.943	.601	.285	.450	.553
Reversibility	Spearman rho (ρ)							.218	.338	.341	.615	.096	.084	.486	.027	-.481
	P-value							.455	.238	.233	.019	.743	.795	.109	.937	.081
Macrophages	Spearman rho (ρ)								.110	.213	-.187	.242	-.270	.045	-.118	.481
	P-value								.696	.464	.522	.405	.397	.890	.729	.081
Mast cells	Spearman rho (ρ)									-.178	.070	-.173	-.262	.073	-.056	-.367
	P-value									.543	.812	.554	.410	.822	.871	.197
GSx	Spearman rho (ρ)										.687	.852	.550	.037	.336	-.077
	P-value										.007	<0.001	.064	.908	.312	.794
GSH	Spearman rho (ρ)											.388	.691	.482	.420	-.559
	P-value											.170	.013	.112	.198	.038
GSSG	Spearman rho (ρ)												.539	-.484	.550	.120
	P-value												.071	.111	.079	.684
Vitamin C	Spearman rho (ρ)													-.043	.834	-.102
	P-value													.894	.001	.753
Ascorbate	Spearman rho (ρ)														-.416	-.303
	P-value														.203	.339
DHA	Spearman rho (ρ)															-.036
	P-value															.915

Significant associations (Spearman rho and *P*-value, n=11-17) are highlighted in red text. Grey cells illustrate that one or both pairs of variable were not determined in this particular group.

Table 2.9: Correlation (Spearman Rank Order Correlations) matrix for COPD smokers.

		Clinical parameters						Bal cells		Antioxidants						
		Age	Pack years	FEV_1% *predicted*	FVC% *predicted*	TL_{CO}^{SB}	Reversibility	Macrophages	Mast cells	GSx	GSH	GSSG	Vitamin C	Ascorbate	DHA	Ferritin
Age	Spearman rho (ρ)		.000	-.296	.009	.036	-.005	-.633	.271	.367	.167	-.017	-.238	-.071	-.310	-.250
	P-value		1.000	.377	.979	.915	.989	.067	.480	.332	.668	.966	.570	.867	.456	.516
Pack years	Spearman rho (ρ)			-.164	-.301	-.409	.410	.150	.712	.467	.500	.150	.000	.190	-.167	.233
	P-value			.630	.368	.212	.210	.700	.031	.205	.170	.700	1.000	.651	.693	.546
FEV% *predicted*	Spearman rho (ρ)				.794	.041	-.324	.350	-.034	-.067	-.233	.483	.190	-.500	.595	-.200
	P-value				.004	.905	.331	.356	.931	.865	.546	.187	.651	.207	.120	.606
FVC% *predicted*	Spearman rho (ρ)					-.224	.021	.209	-.068	-.100	-.335	.494	.000	-.587	.455	-.360
	P-value					.508	.952	.589	.862	.797	.379	.177	1.000	.126	.257	.342
TL_{CO}^{SB}	Spearman rho (ρ)						-.446	-.250	-.254	-.583	-.450	-.683	.071	.000	.024	.383
	P-value						.169	.516	.509	.099	.224	.042	.867	1.000	.955	.308
Reversibility	Spearman rho (ρ)							.151	.170	-.134	-.184	-.109	-.667	-.286	-.500	.084
	P-value							.699	.661	.731	.635	.781	.071	.493	.207	.831
Macrophages	Spearman rho (ρ)								-.186	.083	.233	.067	.238	.238	.190	.483
	P-value								.631	.831	.546	.865	.570	.570	.651	.187
Mast cells	Spearman rho (ρ)									.627	.610	.220	.366	-.122	.390	.034
	P-value									.071	.081	.569	.373	.774	.339	.931
GSx	Spearman rho (ρ)										.900	.583	.214	-.095	.238	-.183
	P-value										.001	.099	.610	.823	.570	.637
GSH	Spearman rho (ρ)											.383	.524	.238	.333	.167
	P-value											.308	.183	.570	.420	.668
GSSG	Spearman rho (ρ)												.190	-.452	.405	-.350
	P-value												.651	.260	.320	.356
Vitamin C	Spearman rho (ρ)													.286	.810	.476
	P-value													.493	.015	.233
Ascorbate	Spearman rho (ρ)														-.286	.476
	P-value														.493	.233
DHA	Spearman rho (ρ)															.119
	P-value															.779

Significant associations (Spearman rho and *P*-value, n=8-11) are highlighted in red text. Grey cells illustrate that one or both pairs of variable were not determined in this particular group.

Table 2.10: Correlation (Spearman Rank Order Correlations) matrix for all aged smokers.

		Clinical parameters						Bal cells		Antioxidants						
		Age	Pack years	FEV_1% *predicted*	FVC% *predicted*	TL_{CO}^{SB}	Reversibility	Macrophages	Mast cells	GSx	GSH	GSSG	Vitamin C	Ascorbate	DHA	Ferritin
Age	Spearman rho (ρ)		.180	-.406	-.313	-.403	.192	-.250	-.084	.237	.048	.104	.062	.117	-.062	.094
	P-value		.379	.039	.120	.041	.347	.238	.695	.265	.824	.627	.790	.615	.791	.669
Pack years	Spearman rho (ρ)			-.004	-.068	.030	.281	.409	.344	.134	.311	-.356	.028	.396	-.343	.230
	P-value			.983	.741	.884	.164	.047	.100	.533	.139	.088	.905	.075	.127	.290
FEV% *predicted*	Spearman rho (ρ)				.942	.621	-.313	.048	.181	.378	.282	.203	.219	-.091	.255	-.241
	P-value				<0.001	.001	.119	.823	.398	.069	.182	.342	.339	.694	.264	.267
FVC% *predicted*	Spearman rho (ρ)					.510	-.203	-.030	.006	.339	.201	.269	.151	-.178	.250	-.291
	P-value					.008	.319	.888	.979	.105	.347	.204	.514	.440	.275	.178
TL_{CO}^{SB}	Spearman rho (ρ)						-.230	.248	.317	.128	.126	-.115	.114	.118	-.025	.187
	P-value						.258	.242	.131	.552	.557	.594	.621	.609	.915	.393
Reversibility	Spearman rho (ρ)							.222	-.156	-.093	-.105	-.090	-.176	.120	-.198	-.048
	P-value							.298	.467	.665	.624	.676	.444	.604	.389	.828
Macrophages	Spearman rho (ρ)								.361	-.003	.307	-.391	.388	.253	.339	.405
	P-value								.083	.989	.145	.059	.082	.269	.133	.055
Mast cells	Spearman rho (ρ)									.092	.332	-.593	.131	.121	.054	.083
	P-value									.668	.112	.002	.572	.601	.815	.705
GSx	Spearman rho (ρ)										.867	.411	.568	.198	.393	.046
	P-value										<0.001	.046	.007	.391	.078	.833
GSH	Spearman rho (ρ)											.031	.637	.351	.390	.200
	P-value											.886	.002	.119	.081	.361
GSSG	Spearman rho (ρ)												.145	-.138	.184	-.333
	P-value												.530	.550	.425	.121
Vitamin C	Spearman rho (ρ)													.529	.720	.468
	P-value													.014	<0.001	.032
Ascorbate	Spearman rho (ρ)														-.125	.579
	P-value														.590	.006
DHA	Spearman rho (ρ)															.063
	P-value															.786

Significant associations (Spearman rho and *P*-value, n=22-25) are highlighted in red text. Grey cells illustrate that one or both pairs of variable were not determined in this particular group.

Table 2.11: Correlation (Spearman Rank Order Correlations) matrix for all COPD patients.

		Clinical parameters						Bal cells		Antioxidants						
		Age	Pack years	FEV_1% *predicted*	FVC% *predicted*	TL_{CO}^{SB}	Reversibility	Macrophages	Mast cells	GSx	GSH	GSSG	Vitamin C	Ascorbate	DHA	Ferritin
Age	Spearman rho (ρ)		-.130	-.158	-.210	.173	.052	-.530	-.014	-.053	.031	-.217	-.391	.089	-.366	-.475
	P-value		.509	.421	.303	.388	.792	.008	.949	.812	.888	.320	.088	.709	.123	.022
Pack years	Spearman rho (ρ)			.197	.106	.064	.279	.080	.430	.309	.323	.119	.244	-.013	.197	-.081
	P-value			.316	.607	.753	.150	.710	.036	.151	.133	.589	.300	.955	.419	.713
FEV% *predicted*	Spearman rho (ρ)				.641	.308	-.116	.287	.031	.328	.294	.287	.347	.094	.405	-.152
	P-value				<0.001	.118	.558	.174	.885	.126	.173	.184	.134	.694	.085	.490
FVC% *predicted*	Spearman rho (ρ)					.089	-.138	.448	.159	.400	.188	.465	.232	-.048	.339	-.002
	P-value					.672	.500	.037	.479	.072	.415	.033	.354	.850	.169	.992
TL_{CO}^{SB}	Spearman rho (ρ)						.008	.111	.304	.050	.244	-.050	.105	.277	.104	-.267
	P-value						.969	.615	.158	.819	.261	.821	.661	.237	.670	.217
Reversibility	Spearman rho (ρ)							-.151	-.037	-.254	-.267	-.200	-.242	-.217	-.129	-.143
	P-value							.480	.864	.243	.217	.360	.305	.359	.599	.514
Macrophages	Spearman rho (ρ)								.299	.449	.392	.308	.394	.458	.173	.641
	P-value								.156	.032	.064	.152	.085	.042	.479	.001
Mast cells	Spearman rho (ρ)									.158	.355	-.105	.001	.201	.035	-.119
	P-value									.472	.096	.634	.996	.396	.887	.590
GSx	Spearman rho (ρ)										.795	.804	.673	.163	.490	.234
	P-value										<0.001	<0.001	.001	.492	.033	.282
GSH	Spearman rho (ρ)											.372	.720	.527	.387	.070
	P-value											.081	<0.001	.017	.101	.751
GSSG	Spearman rho (ρ)												.604	-.232	.599	.216
	P-value												.005	.325	.007	.323
Vitamin C	Spearman rho (ρ)													.290	.794	.281
	P-value													.215	<0.001	.230
Ascorbate	Spearman rho (ρ)														-.249	.184
	P-value														.305	.438
DHA	Spearman rho (ρ)															.047
	P-value															.847

Significant associations (Spearman rho and *P*-value, n=19-28) are highlighted in red text. Grey cells illustrate that one or both pairs of variable were not determined in this particular group.

Overall these results, similar to the inflammatory cell data, failed to provide any clear evidence of antioxidant perturbation or oxidative stress within the respiratory tract lining fluids of patients with COPD. Rather the responses observed were increased GSH, vitamin C and ferritin related to smoking status, though there was very little evidence that this was quantitatively associated to the subjects' reported smoking history (pack years) or clinical indices of pulmonary health.

2.3.6 Alternative control subjects (healthy young and mild asthmatics)

To further explore how the combination of COPD and smoking related inflammation and age impacted on the endogenous antioxidant defences in these subjects, further subject groups of healthy young and mild asthmatic non-smokers were recruited for bronchoscopy. The demographics of these subjects are provided in **Table 2.3**, with information on total and differential cell counts in recovered bronchial wash and bronchoalveolar lavage in **Table 2.12**. Inclusion of these subjects allowed me to address two supplementary issues in relation to COPD antioxidant defences at the air-lung interface: first, whether there was a degradation of antioxidant defences with evidence of increased oxidative stress with age, and second, whether general airway inflammation and acute allergic inflammation, as opposed to the more chronic pattern associated with COPD, was characterised by antioxidant adaptation to protect against oxidative stress. The former issue has recently gained prominence due to the accelerated ageing hypothesis of COPD that was proposed by the group of Barnes (reviewed in **section 1.8**), supported by evidence of shortened telomeres in alveolar type II and endothelial cells (Tsuji, 2006), peripheral mononuclear blood cells (Morla, 2006) and fibroblasts (Muller, 2006) from the lungs of COPD subjects. In addition,

antioxidant enzymes such as superoxide dismutase have also been reported to be lowered in aged smokers and stable COPD patients (Kirkil, 2008). To date, no comprehensive studies addressing human respiratory tract lining fluid antioxidant status with age have been published, though degradation of these defences has been speculated upon as potentially increasing the vulnerability of the aged lung to inhaled xenobiotics (Kelly *et al*. 2003).

Table 2.12: Differential white blood cell counts in BW and BAL fluids from healthy young and mild asthmatic subjects. Cell numbers are presented as cell/mL*10^4.

	Healthy controls *(n=16)*	**Mild asthmatics** *(n=16)*
	Bronchial wash	
Total Cells	7.8 (6.3-13.9)	6.2 (5.6-10.4)
Macrophages	7.2 (5.2-12.3)	5.3 (4.6-9.2)
Neutrophils	0.7 (0.3-1.0)	0.2 (0.1-0.6)
Lymphocytes	0.3 (0.2-0.7)	0.6 (0.3-0.9)
Eosinophils	0.0 (0.0-0.1)	0.1 (0.0-0.3)*a*
Mast cells	0.01 (0.00-0.02)	0.03 (0.01-0.04)*a*
	Bronchoalveolar lavage fluid	
Total Cells	15.1 (9.9-18.4)	13.2 (11.6-17.9)
Macrophages	13.9 (8.9-17.6)	12.0 (10.6-16.1)
Neutrophils	0.1 (0.0-0.2)	0.1 (0.0-0.2)
Lymphocytes	0.7 (0.5-1.0)	1.1 (0.6-1.4)
Eosinophils	0.0 (0.0-0.1)	0.1 (0.0-0.2)
Mast cells	0.01 (0.00-0.03)	0.02 (0.01-0.04)

All data are expressed as medians with inter-quartile. Significant differences across groups were assumed at the 5% level the Mann-Whitney U Test. Significant P values for '*a*' are 0.0012 (eosinophils) and 0.012 (mast cells).

Figures 2.10 (macrophages, neutrophils and lymphocytes) and **2.11** (eosinophils and mast cells) illustrate how the inflammatory cell populations observed in the young healthy and asthmatic populations relate to the previous observations in

the aged smokers and COPD patients. Macrophage numbers did not differ between the young healthy and asthmatic patients in either of the sampled compartments, but numbers in bronchial wash were significantly reduced (P<0.001) in the aged versus young healthy non-smokers. A similar contrast was not apparent in the more distal BAL fluid sample. In contrast, macrophage numbers were elevated above those seen in the young asthmatics in the aged smoking groups in both the BW and BAL samples. Neutrophil numbers in both the BW and BAL samples were broadly equivalent in the young healthy and asthmatic groups in contrast to previous studies that have reported neutrophilia in mild asthmatic subjects (Mudway *et al*. 2001). Indeed there was a trend suggesting decreased neutrophil numbers in the BW of asthmatics, which failed to attain statistical significance (P=0.06). Comparison of neutrophil numbers in BW and BAL between the young asthmatics with aged smokers and COPD patients produced mixed results with only a statistically significant increase in COPD smokers occurring in both compartments. Lymphocyte numbers were equivalent between young healthy and asthmatic subjects, and young healthy and aged non-smoking controls in both BW and BAL, with evidence of a significant depression in numbers in COPD patients (independent of smoking status) compared with the asthmatics. As expected, both eosinophil and mast cell numbers were increased in the BW of atopic mild asthmatics (**Figure 2.11**). Evidence of allergic inflammation was not apparent in the distal BAL fluid sample. Interestingly, there was some evidence of an expansion in mast cell numbers in BAL obtained from healthy and COPD smokers.

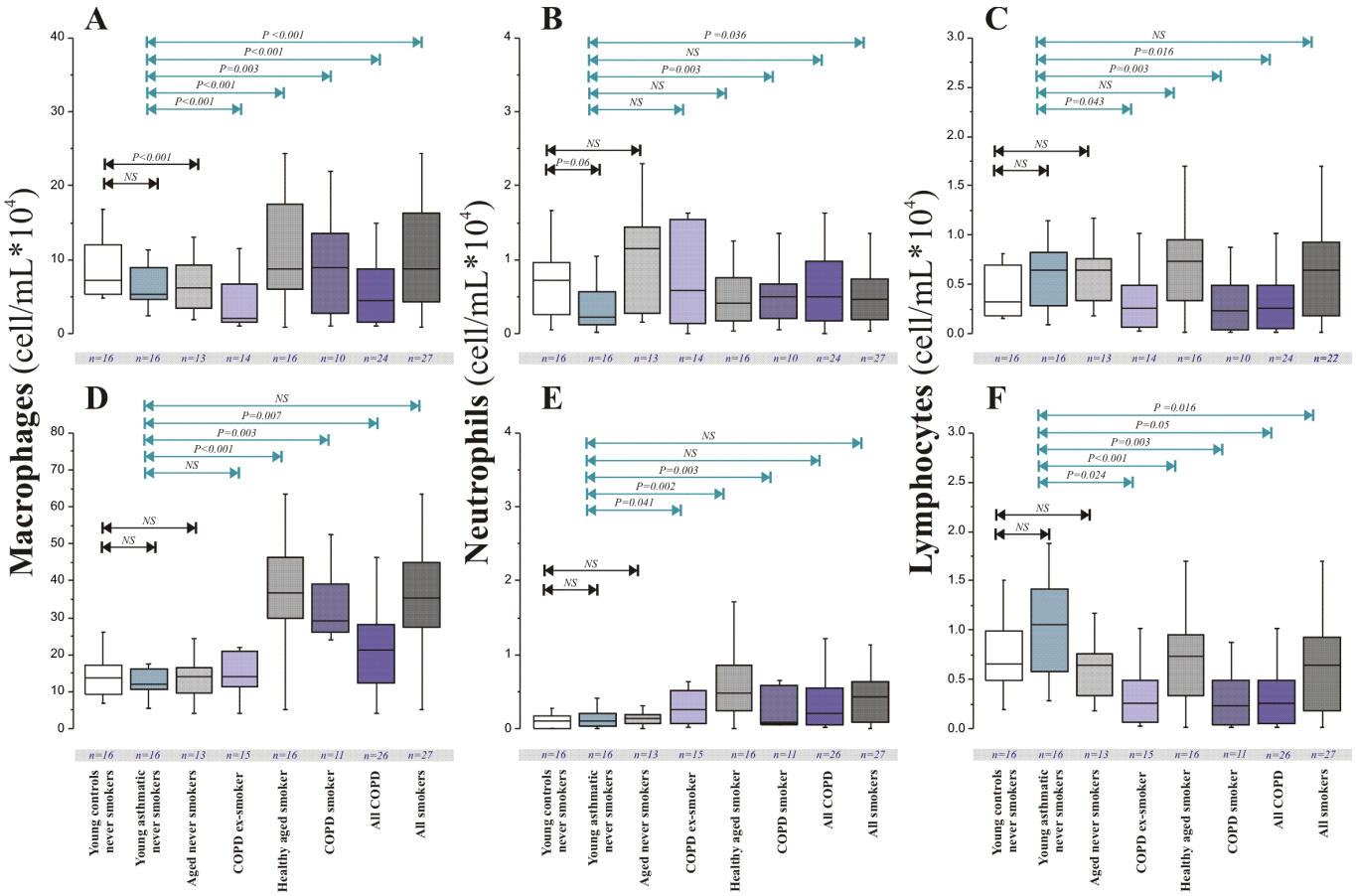

Figure 2.10: BAL fluid cell populations in young and aged adults (smokers and non-smokers), young mild asthmatics and COPD patients (smokers and non-smokers). Data are illustrated as box plots as outlined in the legend to figure 2.6. Statistical comparison (Mann-Whitney U tests) were restricted to young vs. aged adults; young health and mild asthmatic volunteers, and the asthmatic population vs. all COPD groups, plus all smokers irrespective of clinical status. *P*-values for all comparisons are illustrated.

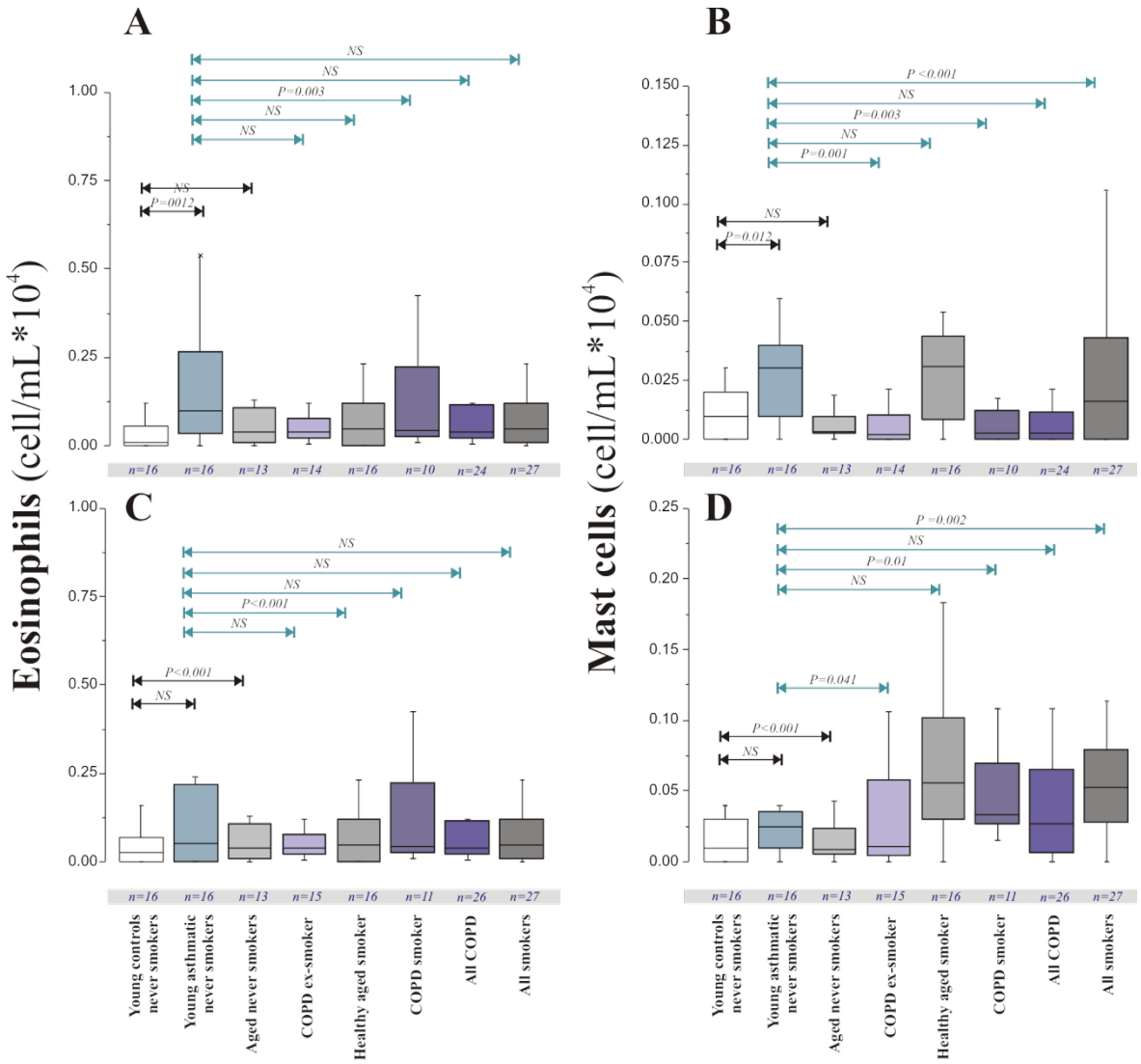

Figure 2.11: Eosinophil and mast cell numbers measured in BAL fluid recovered from young and aged adults (smokers and non-smokers), young mild asthmatics and COPD patients (smokers and non-smokers). All other details are as outlined in the legend to figure 2.10.

The concentration of BAL fluid antioxidants measured in the young healthy and mild asthmatic subjects are summarised in **Table 2.13**. Ferritin was not considered in these analyses as the previous results had demonstrated increases only in smokers and all of the subjects in these tow groups were never-smokers. Overall no significant differences were noted in any of the low molecular weight antioxidants or in transferrin concentration between the two groups. This contrasted significantly with

previous reports of compromised ascorbate concentrations within bronchial wash (Kelly *et al*. 1999), bronchoalveolar lavage (Kelly *et al*. 1999) and induced sputum (Kongerud *et al*. 2003) of asthmatic subjects. In these papers and others addressing antioxidant responses to inhaled xenobiotics (Mudway *et al*. 2004; Mudway *et al*. 2001), low basal ascorbate in the respiratory tract lining fluids of asthmatics was associated with increased GSH and GSSG concentrations, again absent in the present samples.

Table 2.13: Antioxidant and oxidative damage marker concentrations on BAL fluid from young atopic mild asthmatic and aged matched healthy controls.

	Healthy controls *(n=15-16)*	**Mild asthmatics** *(n=13-15)*
Total glutathione (GSx, μM)	0.90 (0.82-1.02)	0.83 (0.63-1.09)
Reduced glutathione (GSH, μM)	0.65 (0.60-0.90)	0.80 (0.53-0.92)
Glutathione disulphide (GSSG, μM)	0.07 (0.00-0.15)	0.09 (0.04-0.11)
Vitamin C (μM)	0.64 (0.48-0.82)	0.64 (0.50-0.74)
Ascorbate (AA, μM)	0.56 (0.43-0.71)	0.55 (0.38-0.67)
Dehydroascorbate (DHA, μM)	0.09 (0.06-0.12)	0.09 (0.08-0.10)
Urate (UA, μM)	0.48 (0.36-0.54)	0.60 (0.40-0.83)
Total protein (mg/mL)	0.07 (0.06-0.09)	0.09 (0.08-0.11)
Transferrin (μg/mL)	7.87 (3.63-10.93)	7.74 (6.95-11.48)

All data are expressed as medians with inter-quartile. No significant differences were noted in the quoted parameters between the two groups.

A review of these earlier papers reveals that in all cases where ascorbate was depressed and glutathione augmented, basal neutrophilia was present in the airways of the asthmatic subjects. Thus the argument developed in these papers, that compromised antioxidant defences at the air-lung interface of asthmatics were

characteristic of the disease, may be incorrect and the level of airway ascorbate may simply be a function of the degree of neutrophilic inflammation. Such a view would chime well with the DHA uptake model in which activated neutrophils oxidize ascorbate in their immediate vicinity to enable rapid uptake of DHA and subsequent reduction back to ascorbate to augment their intracellular concentrations (Wang et al, 1997). It was notable that in contrast to the aged subjects, the contribution of DHA to the measured vitamin C concentration was much reduced in the young subject groups.

The glutathione responses observed in the young healthy and mild asthmatic subjects are compared against the previous data obtained from the aged smokers and COPD patients in **Figure 2.12**. No evidence was observed of an age-related increase in either GSH or GSSG in the young versus aged never-smokers, or between the young asthmatics and the aged COPD ex-smokers. This contrasted markedly with the results obtained for ascorbate and dehydroascorbate, where there was a clear age-related decrease in the former ($P<0.001$) and elevation in the latter ($P<0.001$), **Figure 2.13.** This age-related increase in ascorbate oxidation within the asthmatic respiratory tract lining fluids was paralleled by a significant increase ($P<0.001$) in 4-HNE protein adducts with age, with no difference observed in concentrations between the young healthy and mild asthmatic subjects, **Figure 2.14**. To our knowledge, this is the first evidence of enhanced ascorbate oxidation with age, specifically within the context of the lung.

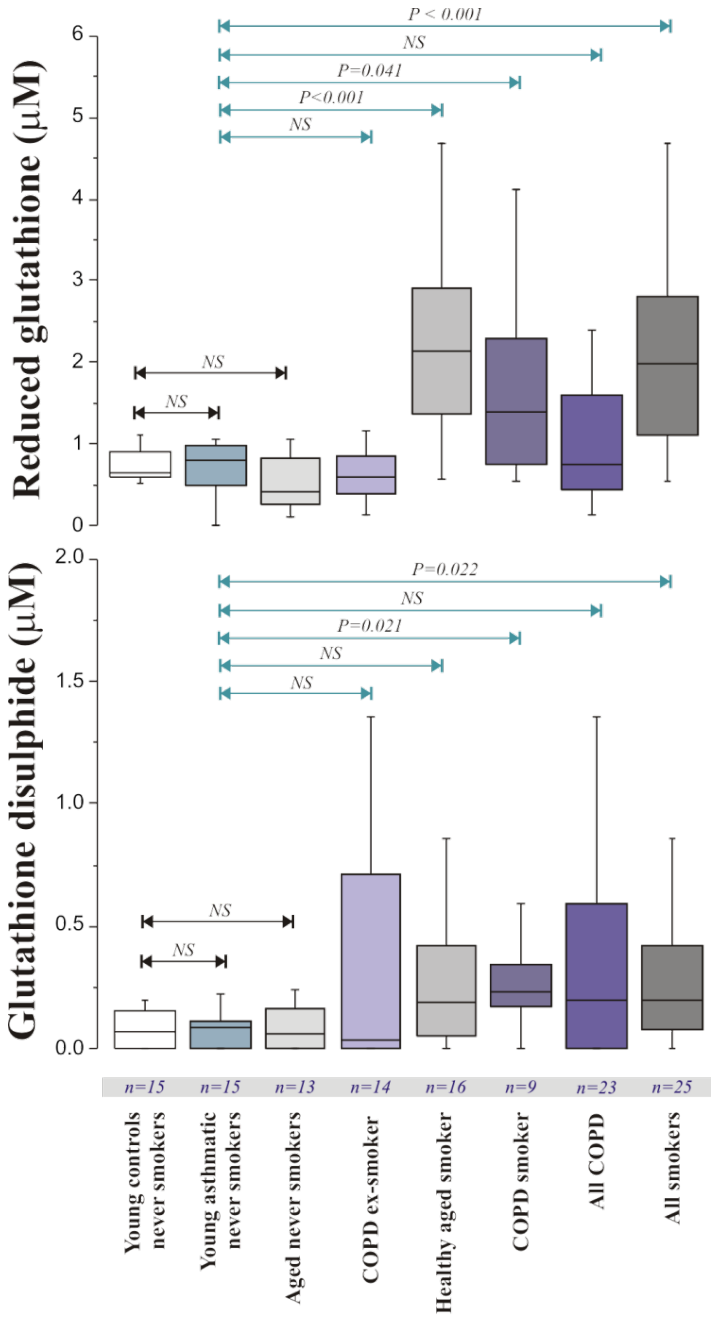

Figure 2.12: Reduced glutathione and glutathione disulphide concentrations in bronchoalveolar lavage fluids recovered; young never-smokers, mild asthmatics (never-smokers), aged never and 'healthy' smokers, plus COPD patients (current and ex-smokers). All other details are as outlined in the legend to figure 2.6. Comparisons between groups (*restricted to young vs. asthmatic adults, young vs aged controls, and asthmatics vs. all aged COPD and smoking groups*) were performed using the Mann-Whitney U Test, with *P*-values illustrated. NS = no significant difference between the indicated groups.

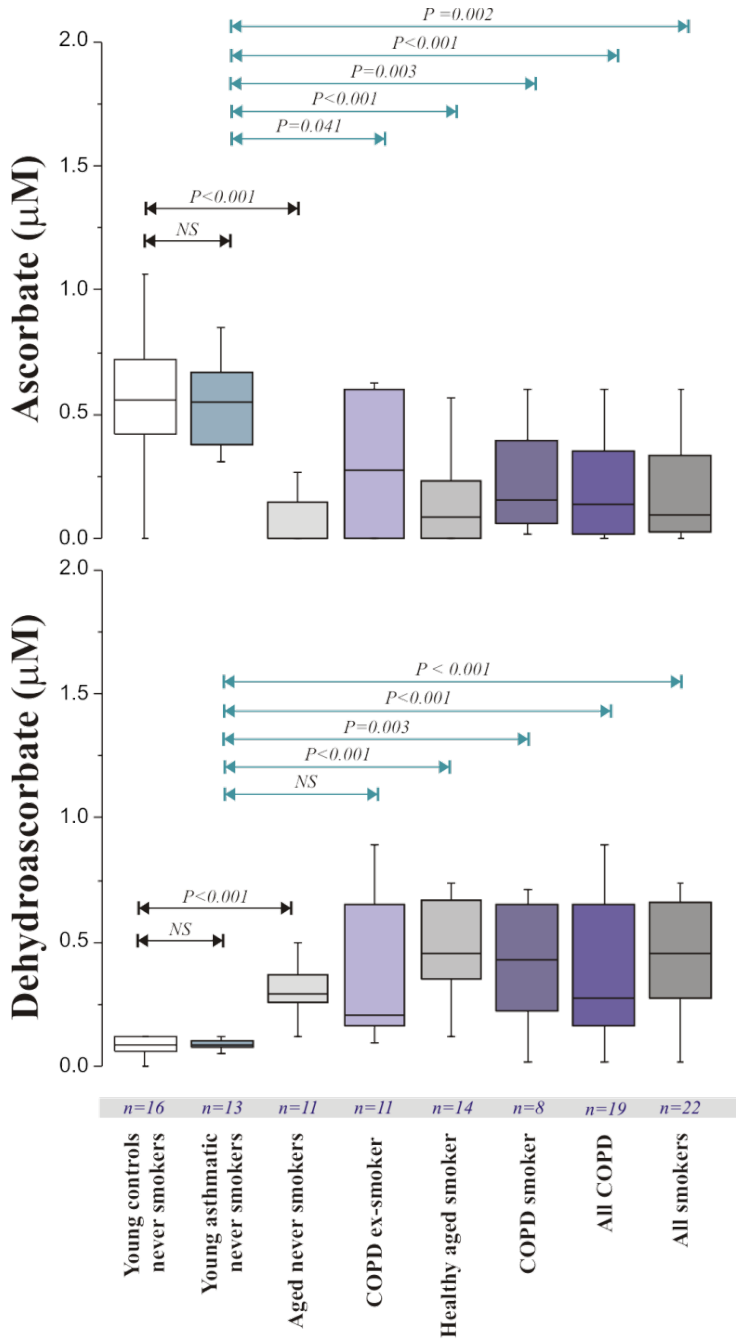

Figure 2.13: Ascorbate and dehydroascorbate concentrations in bronchoalveolar lavage fluids recovered; young never-smokers, mild asthmatics (never-smokers), aged never and 'healthy' smokers, plus COPD patients (current and ex-smokers). All other details are as outlined in the legend to figure 2.10.

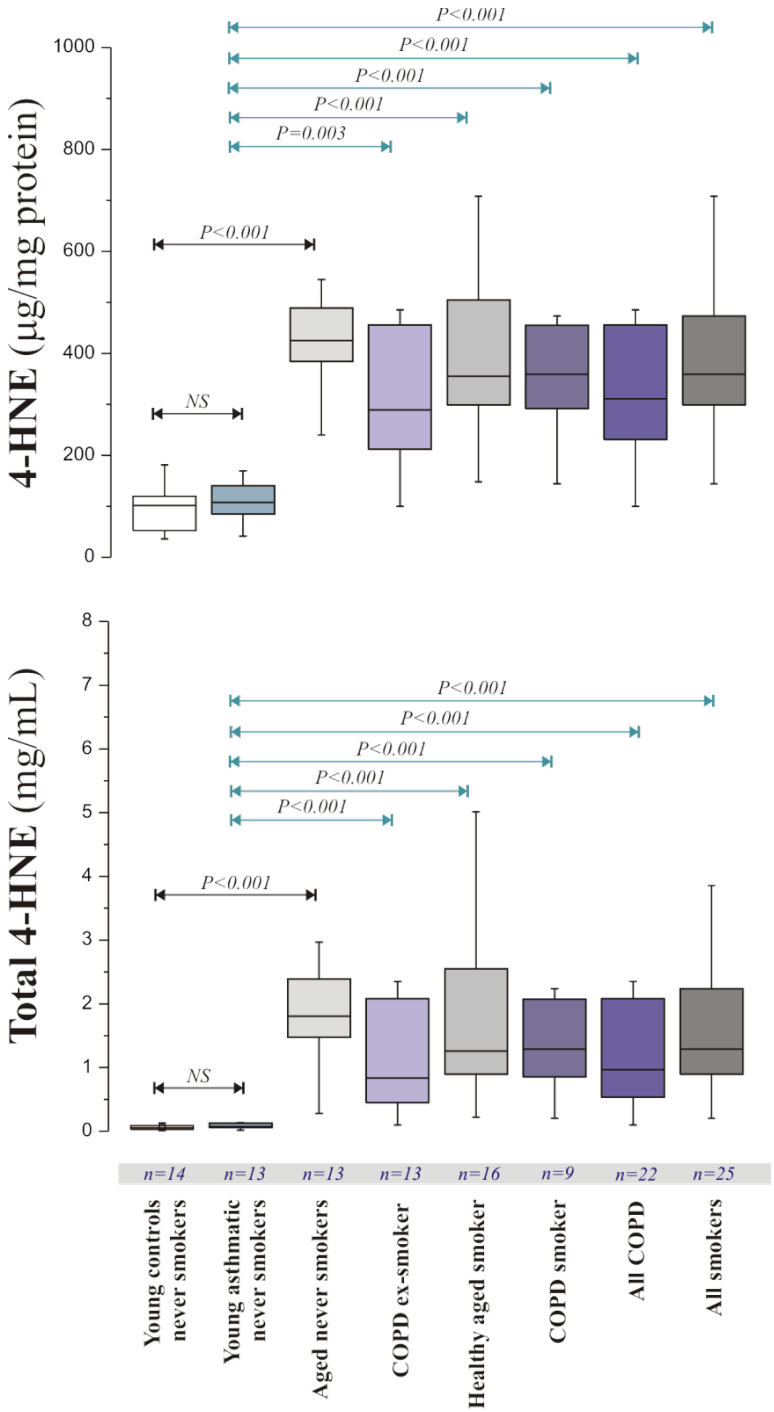

Figure 2.14: Protein bound 4-hydroxy-2-nonenal concentrations in bronchoalveolar lavage fluids recovered; young never-smokers, mild asthmatics (never-smokers), aged never and 'healthy' smokers, plus COPD patients (current and ex-smokers). All other details are as outlined in the legend to figure 2.10.

2.4 Conclusion

In the present study I sought to address whether increased inflammation and associated oxidative stress at the air-lung interface was associated with the presence and clinical severity of COPD. To achieve this I investigated the concentration of a range of antioxidants (both low molecular weight antioxidants and metal chelators) in lavage samples obtained from COPD patients, both current and ex-smokers, and compared these concentrations with those observed in aged and smoking history matched controls. I hypothesised that patients with COPD would have depressed concentrations of antioxidants at their air-lung interface, reflecting the presence of chronic inflammation and consistent with the sensitivity of this group of patients to inhaled xenobiotics.

In contrast to my expectations, I failed to show any evidence for oxidative stress or perturbed antioxidant status in the airways of COPD patients. Rather the changes in antioxidant concentrations observed were either related to smoking status or age-related changes in respiratory tract lining fluid redox, i.e. increased ascorbate oxidation and the presence of 4-HNE protein adducts. It also appeared likely that the increased concentrations of vitamin C and glutathione at the air-lung interface occurred as a consequence of cell lysis, based on the release of intracellular ferritin, though this would need further confirmation through the quantification of other wholly intracellular proteins within the extracellular compartment. This does not infer that oxidative stress does not play a role in the aetiology and progression of COPD, for example its relationship to cigarette smoking clearly demonstrates that this is the case, but in stable patients, in the absence of an inhaled oxidant challenge or

exacerbation, it appears extracellular defences are no worse than would be observed in a healthy aged subject. This study did not specifically address the extent to which adaptive mechanisms may be impaired in COPD, and clearly there is an increasing body of evidence supporting this view (Goven et al, 2009).

Therefore, with evidence of oxidative stress directly related to age and smoking status, I hypothesised that smoking and age-related responses could be related to the presence of an increased catalytic metal pool (predominately Fe and Cu) within the RTLF, either arising from the inhalation of a metal-rich cigarette smoke aerosol or dysregulation of metal handling at the air-lung interface which is explored in chapter 3.

Chapter 3:

Metal homeostasis at the air-lung interface in inflammatory airway diseases

3.1 Introduction

In the previous chapter I investigated whether COPD was associated with an impaired antioxidant defence network in the RTLFs of the distal lung. Contrary to my original hypothesis I found no evidence supporting the presence of oxidative stress in patients with COPD. The alterations observed in the RTLF antioxidant network were either related to smoking status (elevated glutathione and ferritin concentrations), or the age of the volunteers, with clear evidence of increased oxidative stress in the older patients/volunteers (increased dehydroascorbate and 4-HNE concentrations). To further explore these observations in this chapter, I hypothesised that the smoking and age-related responses were related to the presence of an increased catalytic metal pool (predominately Fe and Cu) within the RTLF, either arising from the inhalation of a metal-rich cigarette smoke aerosol (Pappas, 2011), or dysregulation of metal handling at the air-lung interface (Ghio, 2009). Under normal conditions Fe released into the RTLF from dying cells (Ghio, 2009), or incident from inhaled air (Gilmour, 1996; Happo, 2008), is rapidly bound by the extracellular protein transferrin and transported into cells via receptor-mediated endocytosis for storage in ferritin (Syed, 2006). In addition, Fe as well as other metal cations including Cu and Zn can be taken up into cells by the divalent metal transporter 1 (DMT1) (Wang, 2002), which has been shown to be expressed on both alveolar macrophages (Nguyen, 2006) and

airway epithelial cells *in vitro* (Wang, 2002) and *in vivo* (Ghio, 2003). Neutrophils also release secondary granules containing the glycoprotein lactoferrin which complexes with ferric iron, which can then be taken up by respiratory epithelial cells and macrophages for storage within ferritin (Markowetz, 1979). This emphasis on the rapid cellular sequestration of Fe, as well as other catalytically active metals in the lung, reflects both their deleterious effects promoting oxidative reactions in the lung (Jomova, 2011), as well as the need to limit the availability of these metals to bacteria, which require Fe for growth and proliferation (Oppenheimer, 2001; Fischbach, 2006). Correspondingly, transferrin levels expressed as a percentage of total protein, are significantly higher in RTLFs (4-5.6% of the total protein) than in plasma (Mateos and Brock 1998). In addition, there would appear to be a considerable functional Fe binding reserve in healthy individuals, with transferrin usually only 20-30% loaded with iron (Halliwell and Gutteridge, 2007).

The lung has therefore clearly evolved an array of mechanisms to prevent the accumulation of Fe as well as other divalent metals at the air-lung interface. One might therefore imagine that with the reserve metal binding capacity of transferrin, there would be a sufficient buffer against the appearance of 'free' unbound and hence catalytically active metals. There are a number of caveats however, that need to be considered: first, it is now clear that pools of non-transferrin bound iron can exist, even in the presence of unsaturated transferrin (Gutteridge, 1995; Aruoma, 1999; Gosriwatana, 1999); second, reductions in pH can significantly impact on the Fe binding capacity of transferrin (Wally, 2007); and finally, there is clear evidence of both up– and down-regulation of components of the metal sequestration system in a

variety of acute and chronic lung diseases: lung transplantation (Pugh, 2005); acute respiratory distress syndrome (Ghio, 2003); idiopathic pulmonary alveolar proteinosis (Ghio, 2008); and cystic fibrosis (Stites, 1999).

For metals to promote damaging oxidations at the air-lung interface they must therefore be unbound to any of the endogenous chelators (lactoferrin, transferrin) within the RTLF. These pools of unbound, or 'free' metals, usually assumed to be Fe only, have been given the name 'the non-transferrin iron (NTBI) pool.' For Cu, the term 'the caeruloplasmin-bound pool' has recently been proposed (Walshe, 2012). It is however, misleading to refer to 'free' pools of metals *in vivo* as they are never truly unbound in body fluids, where they exist complexed to a variety of molecules including albumin, citrate, DNA and phosphate (Nilsson, 2002). Thus, the central question is not whether it is 'free', but rather whether the bound form retains the capacity to catalyse free radical reactions. Numerous assays have been developed to quantify these 'catalytically' active metal pools, including the highly sensitive bleomycin and nitrilotriacetic acid assays (Gutteridge, 1981; Gosriwatana, 1999). These assays were first employed to demonstrate the presence of a NTBI pool in patients with thalassaemia (Graham, 1979) or haemochromatosis (De Valk, 2000). There is however, evidence of a non-transferrin bound iron (NTBI) pool at the lung surface in both healthy subjects and subsets of patients with adult respiratory distress syndrome (Gutteridge, 1996). This observation has never been followed up in the literature and has been widely questioned. This in part reflects the technical difficulty in making these measurements in dilute lavage returns, as opposed to in plasma, but also the apparent measurement of an unchelated Fe pool in healthy adults.

To address the hypothesis that the age-related increase in oxidation markers in the lavage returns might be related to altered metal homeostasis at the air-lung interface, I examined both the concentration of Fe and Cu in the recovered samples using ICP-MS, as well as the pro-oxidant status of the lavage samples. The later assay was based on a method designed to quantify contaminating Fe in biological buffers (Welch, 2002). This method, based on the capacity of metals to catalyse the oxidation of ascorbate, was preferred over a direct quantification of the NTBI pool as it provided a direct measure of catalytically active metals and is highly sensitive and suitable for use with dilute samples. In addition, through the use of selective chelators, either to augment (NTA) or inhibit (DTPA) the oxidation of ascorbate, it was possible to proportion pro-oxidant activity to metal and non-metal sources and through the interaction of NTA with Fe and Cu, to further discriminate their contribution to the observed rates.

3.2 Methods

3.2.1 Materials

All chemicals used were obtained from Sigma Chemical Company Ltd. (Poole, U.K.), Fluka (Dorset, U.K.) or Laboratory Supplies (Poole, U.K.) and were of analytical grade or better quality.

3.2.2 Chelex water preparation

Ultra pure water was employed to decrease background metal contamination when assessing the endogenous pro-oxidant activity of the lavage samples. Each litre of deionised Elga-stat water (18 Ώ) was treated with 30 grams of Chelex 100 resin (iminodiacetic acid-coated polystyrene beads). This solution was prepared in a polycarbonate beaker and after mixing for 24 hours at room temperature, the Chelex 100 resin was removed by vacuum filtration through a 0.45 µm cellulose nitrate membrane. The pH of the purified water was subsequently adjusted to 7 using 1M sodium hydroxide and 1M hydrochloric acid, both previously prepared in ultra pure water and stored at 4 °C for a maximum of one month.

3.2.3 Subject demographics

The subject demographics were as described in **section 2.2.1** with corresponding **tables 2.2** and **2.3**.

3.2.4 Determination of BAL metal concentrations

Trace metal concentrations (Fe, Cu, Zn, As, Cd and Y) in BAL fluid samples were established by inductively coupled plasma mass spectroscopy (ICP-MS) following an acid digestion in dilute nitric acid. Each lavage sample (0.5 mL) was added to 1.5 mL of 6.5% HNO_3 (10.83 ml of 60% HNO_3 + 89.17 ml of ultra pure Chelex resin treated water) and spiked with 20 µl of a 1 ppm yttrium solution (prepared in 6.5% HNO_3 from a 100 ppm yttrium stock (Lleeman Lab, Inc – Lowell, MA, USA). All digestions were performed in acid washed (2% HNO_3) Teflon vials following extensive rinsing in ultra pure water. The acidified samples were then vortexed for two minutes prior to heating in a hot water bath at 90 ºC for 90 minutes. All samples were ran in parallel to digestion blanks, at least 8 per run, containing 1500 µl of 6.5% Nitric acid and 20 µl of internal standard, plus 0.5 mL of Chelex 100 resin treated ultra pure water. The resultant digests were then allowed to cool to room temperature overnight in a fume cupboard prior to centrifugation at 4,000 rpm for 10 minutes. Where a precipitate was apparent (this was not observed with any of the digests) the resultant supernatant was transferred to a new tube prior to analysis. Samples were analysed (^{63}Cu (natural abundance 69.15%), ^{56}Fe (91.72%), ^{89}Y (100%), ^{111}Cd (12.80%), ^{75}As (100%), ^{66}Zn (66; 27.90%)) by ICP-MS using an ELAN DRC ICP-MS (MSF008) at the King's College London mass spectrometry facility. The selected isotopes were chosen to avoid known potential isotopic interferences. The potential ArO^+ interference for the major isotope of iron (^{56}Fe) was removed using the dynamic reaction cell, through its reaction with ammonia. Trace metal calibrations were conducted using dilutions of a certified multi-elemental standard solution (VI CertiPUR Merck, Lot. No.OC529648). Typical 7 point

standard curves are illustrated in **Figure 3.1**. In addition to the digestion blanks, repeat digestions of a single BAL fluid sample recovered from a healthy adult (24 year old male) were ran throughout each run to assess the intra-assay variability. The results of these analyses versus the background intensity measurements in the digestion blanks are illustrated in **Figure 3.2**.

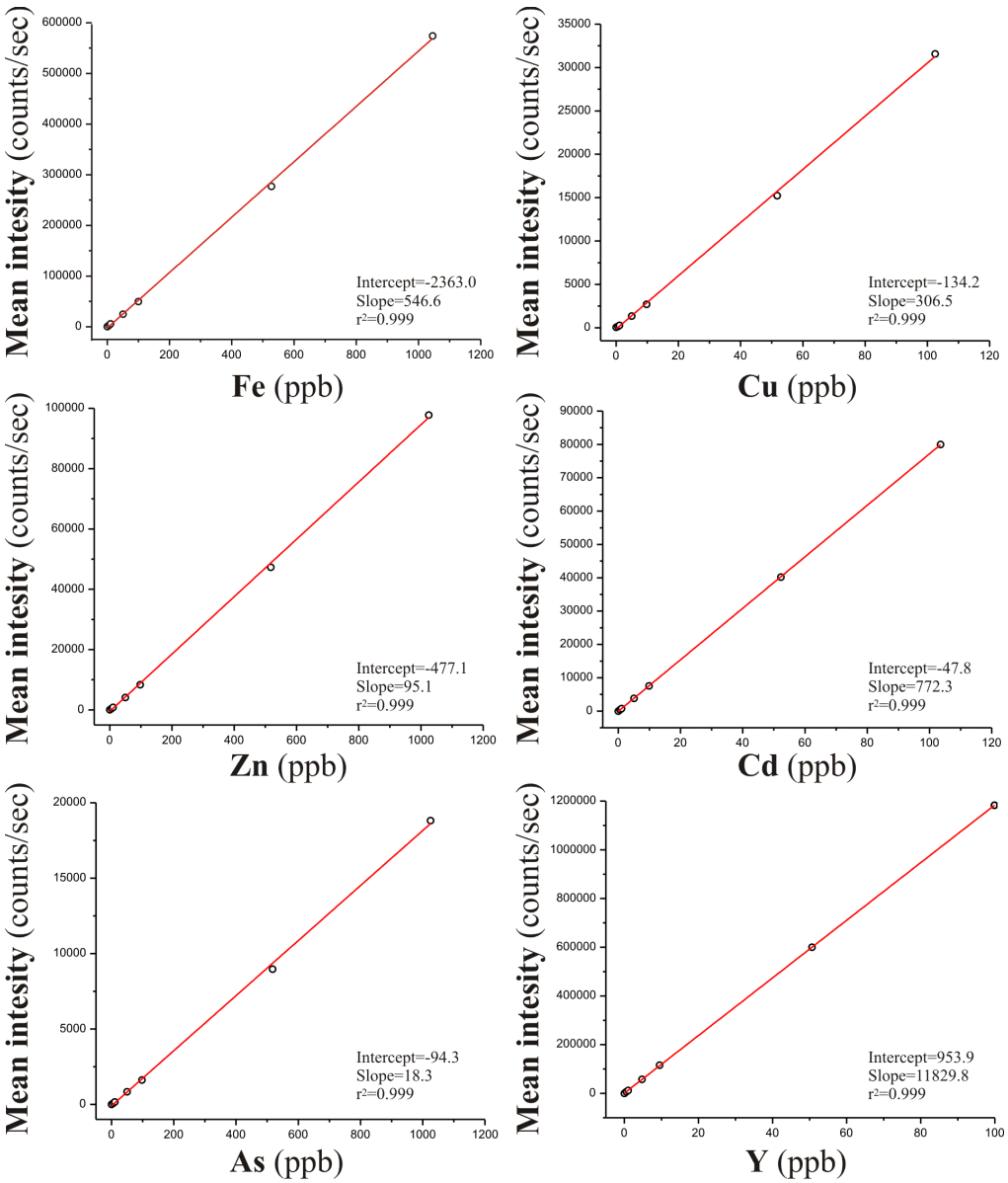

Figure 3.1: Typical elemental standard curves. Data points represent the mean intensity from triplicate readings.

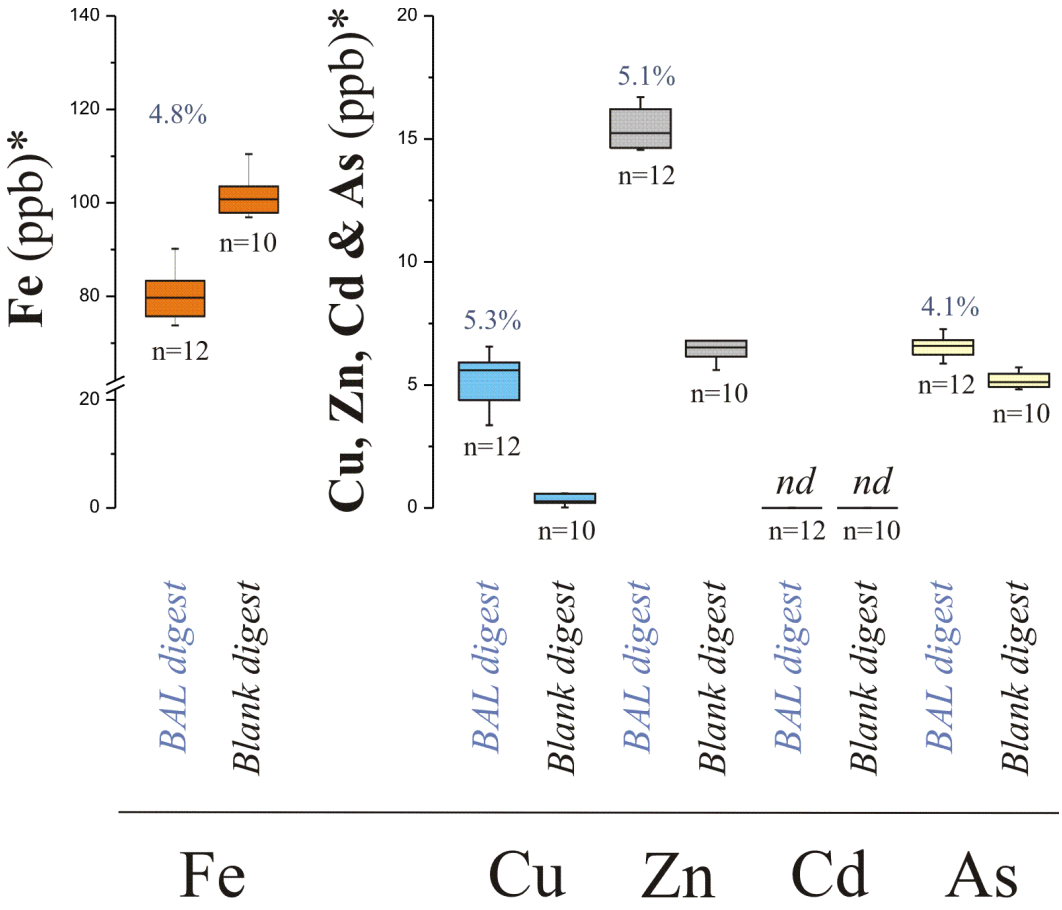

Figure 3.2: Raw concentrations (*corrected for the internal standard, not the final dilution, but equivalent for blanks and lavage samples) of the indicated elements in repeat lavage and blank digests. The number of repeat incubations and analyses are indicated, as is the coefficient of variation (standard deviation/mean x 100) for the measured concentrations in the BAL digests. Note: In the case of Fe, the values from the BAL digests were always less, or near equivalent to the concentrations measured in the blanks. Cd was below the detection limit of the assay: *nd*, not detected.

3.2.5 Ascorbate depletion assay

The pro-oxidant activity of the recovered BAL fluid samples was assessed with respect to their capacity to deplete ascorbate (AA) from a single 200 µM antioxidant solution. In this assay, greater ascorbate depletion rates were expected to occur in samples containing unchelated catalytic metals, predominately Fe or Cu. A stock AA solution was prepared at a concentration of 4 mM in Chelex treated water and

adjusted to pH 7.0. An aliquot of each lavage sample (90 µL) was diluted with 5 µL of Chelex-treated water and then incubated with the stock antioxidant solution (5 µL) at 37 °C for two hours in a plate reader (Spectra Max 190). Lavage fluid incubations with AA were performed in triplicate in UV 96-well flat-bottom plates (Greiner bio-one). The concentration of AA remaining in each well was quantified by measuring the absorbance at 265 nm every two minutes over the two hour incubation period. Duplicate blanks and standards (25 – 200 µM AA) were run in parallel with samples on the 96-well plate, such that a calibration curve was constructed for each two minute measurement; calibration curves are shown for a selection of the measurement time points in **Figure 3.3**.

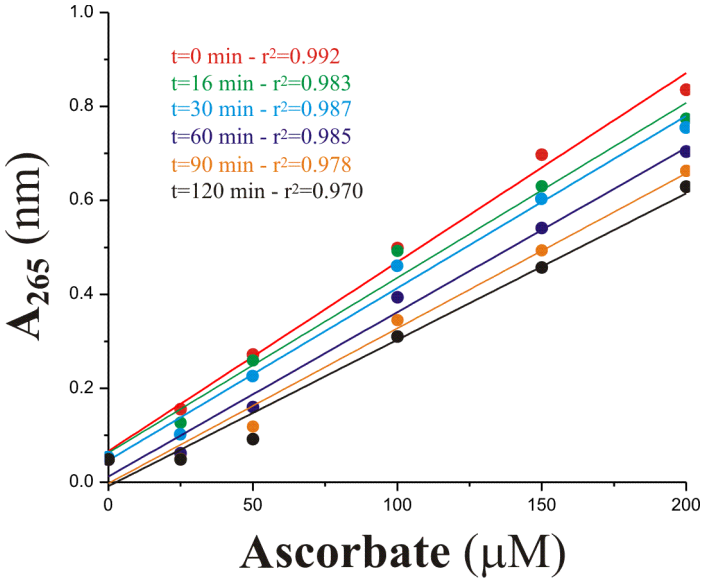

Figure 3.3: Example of a typical AA calibration curve for quantifying depletion in a single antioxidant solution. Note: the absorbance values at each concentration fall with time reflecting the auto-oxidation of ascorbate from the standard.

The AA concentration in sample wells at each time point was determined against its respective calibration curve and corrected for AA losses by auto-oxidation measured in the blank controls. The rate of AA depletion was determined over the

two hour incubation and expressed as µM second^{-1}. As the decline of this antioxidant was assumed to follow first order kinetics, only the linear portion of the measurement time course was considered. Rates were derived using Microcal Software Limited's OriginLab (version 5.0). To determine the influence of metals in the measured rate of AA depletion, samples were incubated with the metal cation chelators DTPA and NTA (structures illustrated in **Figure 3.4**). Incubations were conducted in a similar procedure as previously described above, however, instead of diluting the nasal lavage samples with 5 µL Chelex-treated water, samples were spiked with 4 mM DTPA (5 µL). The likely impact of these chelators on the observed rates is described in **Figure 3.4**.

3.2.6 Statistics

Data were not normally distributed (Shapiro-Wilks test) and are therefore expressed throughout as medians with the 25th and 75th percentiles. Comparisons of the ascorbate depletion rates and metal concentrations across the patient groups were performed using the Kruskal–Wallis one-way analysis of variance by ranks, with post-hoc testing between specific groups performed using the Mann-Whitney U test. In all cases where ascorbate depletion rates were compared in a given subject group with or without co-incubation with metal chelators, post hoc testing was performed using the Wilcoxon-Signed Rank Test. In all cases significant differences were assumed at the 5% level. Correlation analysis for each individual group, plus compiled groups of COPD patients (current and ex-smokers) and smokers (both aged 'healthy' smokers and COPD smokers), were performed using the Spearman Rank Order Correlation. These analyses were restricted to parameters that had been shown to differ

significantly between groups to limit the likelihood of reporting spurious associations.

All analyses were performed using SPSS, version 17.0 (SPSS Inc., Chicago, IL).

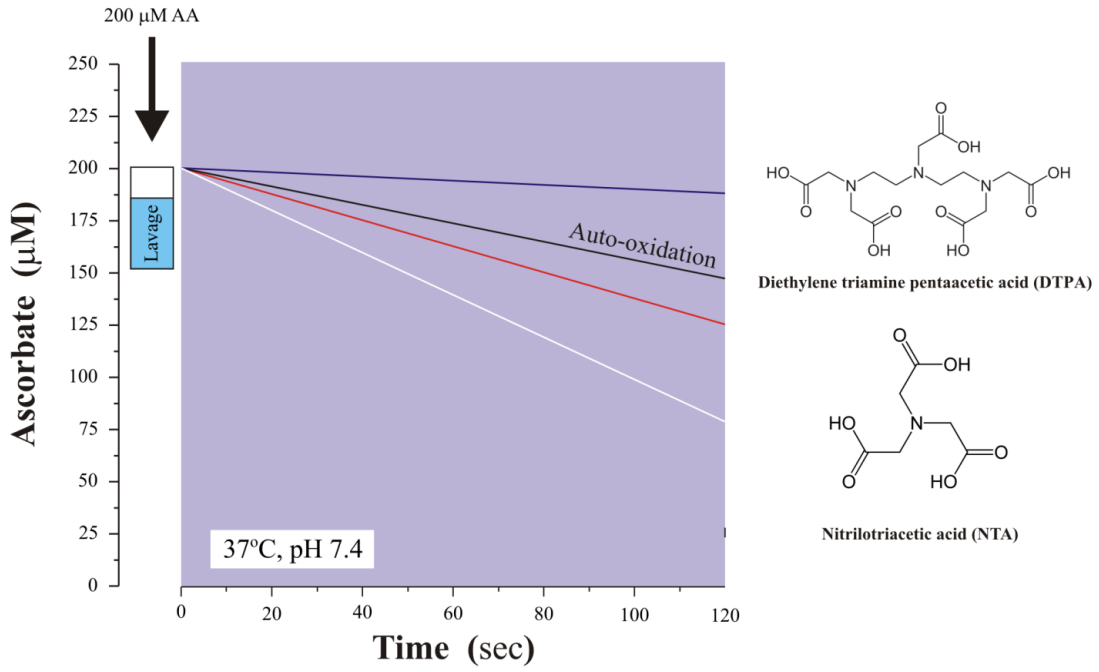

Figure 3.4: An illustration of the principle of the ascorbate depletion assay. Lavage samples are spiked with ascorbate to achieve a starting concentration of 200 µM. The loss of ascorbate is then monitored at 265 nm every 2 minutes for 2 hours. A typical profile for a lavage sample is shown above using the red line. All incubations are also performed parallel to a water blank, which accounts for the background rate of auto-oxidation occurring due to trace metal contamination (black line). Addition of the chelator DTPA in excess should completely abolish any metal dependent catalysis, including that contributing to the background oxidation (purple line). Co-incubation, conversely, may act to accelerate the oxidation of ascorbate, specifically in relation to the formation of Fe-NTA, as it is able to mobilise Fe from other biologic chelators in the biological media (white line).

3.3 Results and Discussion

To address the basis for the age-related increase in markers of oxidative damage (DHA and 4-HNE) observed in the previous chapter, I investigated the concentrations of the redox active metals Fe and Cu within the recovered BAL fluid samples. Direct measurements of these metals were made after a nitric acid digest by ICP-MS. Indirect assessment of their capacity to catalyse oxidation reactions was obtained using an ascorbate depletion assay, through the use of selective chelators, either to augment (NTA) or inhibit (DTPA) catalysis related to the non-transferrin bound Fe-pool i.e. that bound to low molecular weight anions, such as citrate and acetate, or associated with albumin (Hider, 2002). I hypothesised that ageing would be associated with a more pro-oxidant status within the airway lining fluids, characterised by an increase in catalytically active metals i.e. unchelated Fe and Cu concentrations. As a secondary hypothesis, I also tested the assumption that the concentration of these metals, as well as As and Cd, would be elevated in current smokers due to their presence in the cigarette smoke aerosol (See, 2007). Zinc was also examined in the lavage digests, both as a non-redox active metal but also due to its 1:1 stoichiometry with Cu in extracellular superoxide dismutase, which is known to be present in the airway lining fluids (Mudway, 2001). It was assumed that equivalence between Cu and Zn concentrations would therefore reflect their presence within this critical antioxidant enzyme, and deviation from this relationship due to alternate sources.

As outlined in the methods section, I was unable to obtain a valid measurement for BAL fluid Fe after the subtraction of the digestion blanks in any of the samples.

Previous studies have reported total and non-haem Fe concentrations to be broadly equivalent in lavage fluids harvested from healthy never-smokers, in the range of 0.01-0.03 μg/mL, with evidence of substantial increases in lavage samples obtained from patients with adult respiratory distress syndrome (Ghio, 2003) and pulmonary alveolar proteinosis (Ghio, 2008). Clearly, given the content of heam (catalase (Ulker, 2008), lactoperoxidase (Ratner, 2000), myeloperoxidase (Mudway, 1999), eosinophil peroxidase (Erpenbeck, 2003)) and non-haem Fe (transferrin, lactoferrin (Ghio, 2009)) proteins with the RTLF, the failure to detect measurable Fe was methodological. In the previous reports of non-haem Fe (Ghio, 2003; Ghio, 2008), quantification was achieved using inductively coupled plasma atomic emission spectroscopy following a somewhat more robust digestion protocol than I employed in the present analysis: 6 N HCl/20% trichloroacetic acid to 1.0mL of lavage supernatant, heating to 70°C for 18hrs. Whilst there is an acknowledged problem in quantifying the most abundant isotope of Fe (^{56}Fe) by ICP-MS, due to the polyatomic interference from ArO+, this should not have been a problem as I employed the dynamic reaction cell with NH_3 to eliminate this species. Therefore, most likely the failure to detect Fe reflected advantageous metal contamination, either during the bronchoscopy, or during the digestion protocol.

Whilst Fe and Cd were not possible to quantify, following the digestion blank subtraction, measureable concentrations of Cu, Zn and As were achieved in all of the analysed samples. The Cu concentrations measured in the lavage returns from each of the subject groups investigated are illustrated in **Figure 3.5**. Considering the COPD patient groups relative to their age and smoking status matched controls, I observed

no significant differences in total Cu. In contrast, the concentration of Cu was significantly lower in the lavages obtained from the young healthy adults and mild asthmatics, relative to all of the aged groups, irrespective of smoking or disease status. No difference in Cu concentrations was noted between the young asthmatic and control subjects. A similar pattern was observed with respect to the total Zn determinations in the lavage digests, with clearly elevated concentrations apparent in the aged groups (**Figure 3.6**). Notably, the concentration of Zn measured across all subject groups was 2.4-fold higher than the corresponding Cu measurements.

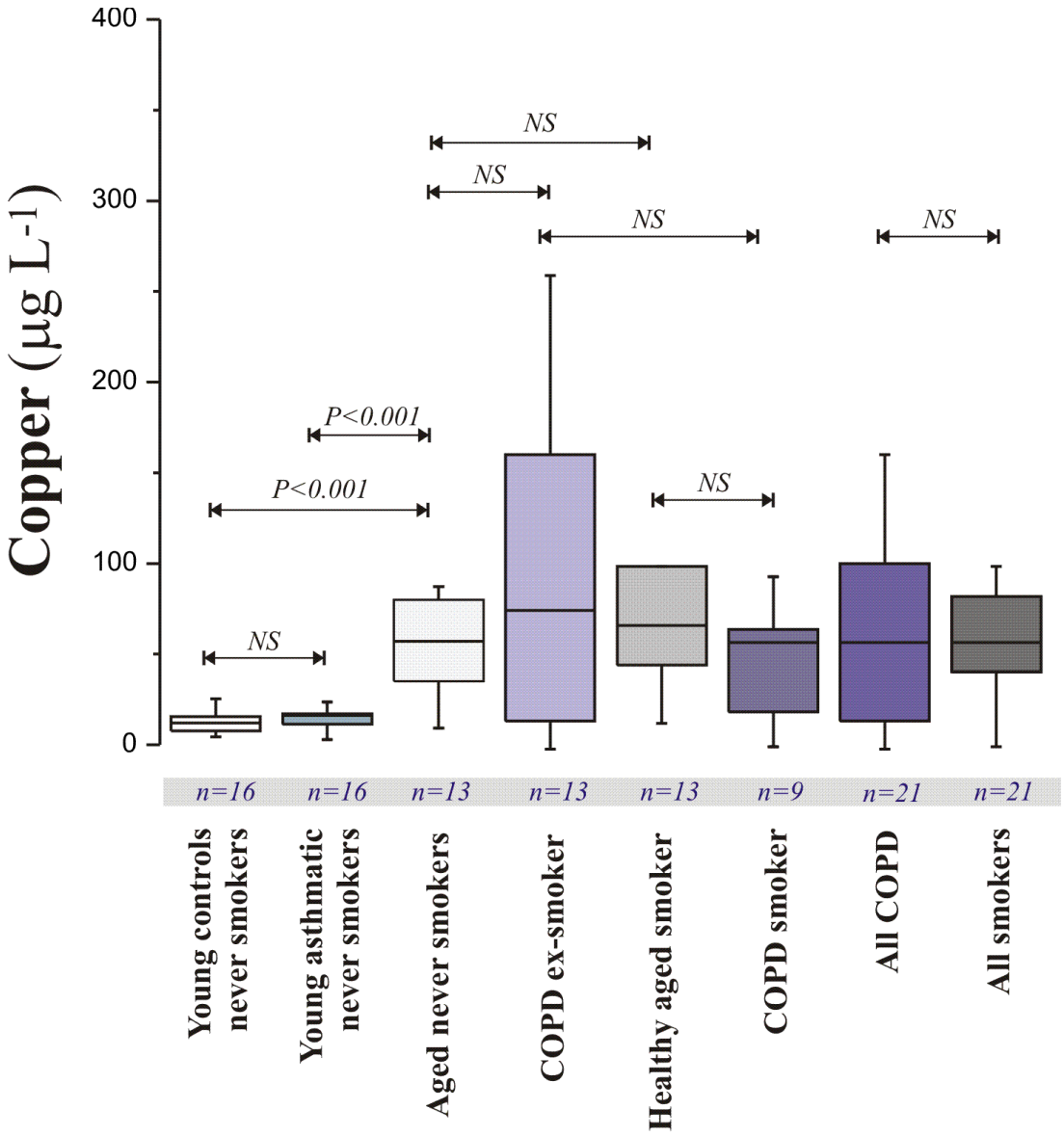

Figure 3.5: Total copper concentrations in BAL fluids samples obtained from COPD and asthmatic patients, plus aged and smoking history matched controls. Data are presented as box plots, with the central line indicating the median, the lower and upper boundaries of the box, the 25 and 75th percentiles and the whiskers the 95% confidence interval. Comparisons of the Cu concentrations between the patient groups were performed using the Kruskal–Wallis one-way analysis of variance by ranks, with post-hoc testing between specific groups performed using the Mann-Whitney U test.; P values are indicated where they were <5%.

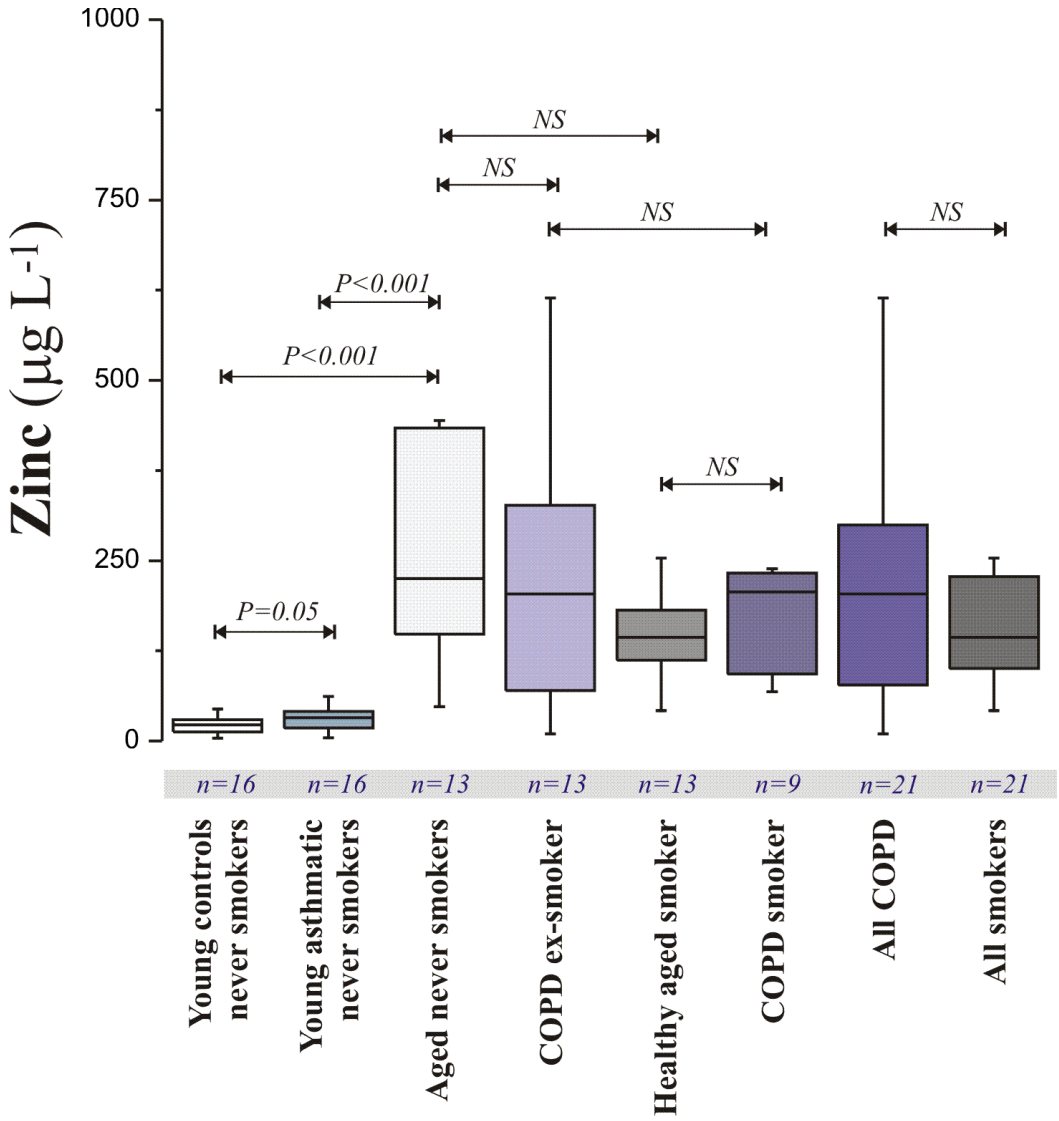

Figure 3.6: Total Zn concentrations in BAL fluids samples obtained from COPD and asthmatic patients, plus aged and smoking history matched controls. All other details are as outlined in the legend to Figure 3.5.

An examination of the RTLF proteome (Magi, 2006; Noël-Georis, 2002), indicates that the major Cu containing proteins within this extracellular compartment are extracellular Cu,Zn superoxide dismutase (ECSOD) and caeruloplasmin. The tetrameric metalloenzyme ECSOD contains 4 atoms of both Cu and Zn (Marklund, 1982), while the Cu transport protein and ferroxidase caeruloplasmin contains 6 six cupredoxin-type domains (Bento, 2007), plus a 7th labile surface copper binding site

that has been argued to attribute the protein a pro-oxidant state (Mukhopadhyay, 1997). Albumin has also been shown to loosely bind Cu and Zn at histidine residues (Masuoka, 1994). A comparison of the relative abundance of Cu and Zn in the lavage returns from each of the patient groups (**Figure 3.7**) clearly demonstrates a relationship between the two metals, but seems to support additional Zn sources. As the published proteome doesn't indicate any obvious candidates, it is probable that the additional Zn reflects a labile pool within this extracellular compartment.

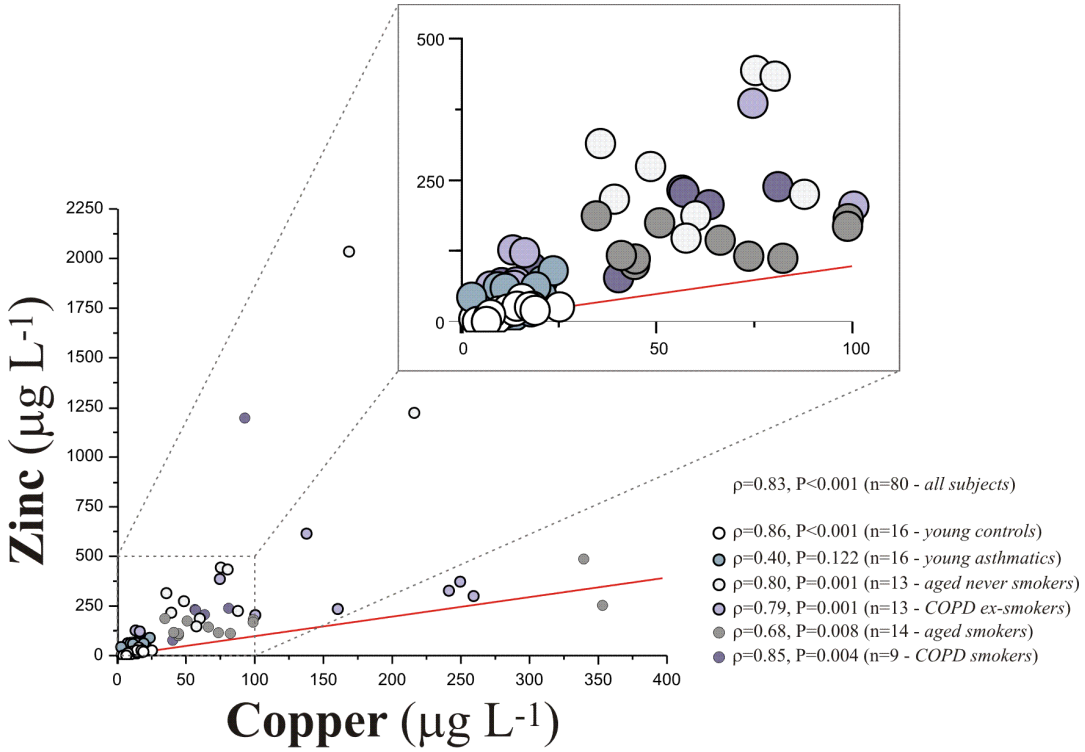

Figure 3.7: Association between the measured total (acid digested) BAL fluid Cu and Zn concentrations from all subjects, as well as broken down by each patient group (as illustrated in the above key). The strength of association was assessed using the Spearman Rank Order Correlation (Spearman's rho (ρ) and the associated P-values are illustrated). The red line represents the line of identity, with the data groups toward the intercept, blown up in the inset panel.

It was notable that neither Cu nor Zn was elevated in the lavage returns of current smokers. Similarly, As concentration was not enhanced in smokers relative to non-smokers (6.3 (5.3-7.2), n= 22 versus 7.9 (7.0 – 8.5) μg L^{-1}, n=26) and there was no evidence of an age-related increase, similar to that observed for Cu and Zn (data not shown).

To further explore whether the lavage returns from the aged subjects had a more pro-oxidant status, consistent with the increased concentration of oxidation markers reported in these subjects in chapter 2, I made use of the ascorbate depletion assay. In this assay the presence of an oxidant or redox catalyst, such as Fe or Cu promotes the oxidation of exogenous ascorbate added to the lavage samples (Welch, 2002). As the measured rate of ascorbate oxidation reflects the potential contribution of multiple oxidant/redox catalysts I employed selective synthetic chelators to isolate metal versus non-metal contributions to the observed oxidation rates, as well as to attempt to quantify the contribution of Fe and Cu. The ascorbate depletion rates observed in each of the patient groups, with and without co-incubation with DTPA or NTA are illustrated in **Figure 3.8**. Considering the total ascorbate depletion rate, illustrated in the uppermost panel, it was clear that the observed rates observed in the young volunteers (both healthy and mild asthmatic subjects) were significantly less than those seen in the aged groups, irrespective of COPD or smoking status, mirroring the earlier metal results. Perhaps counter-intuitively there was some evidence of a reduced rate of ascorbate depletion in the healthy current versus never-smokers (P=0.023).

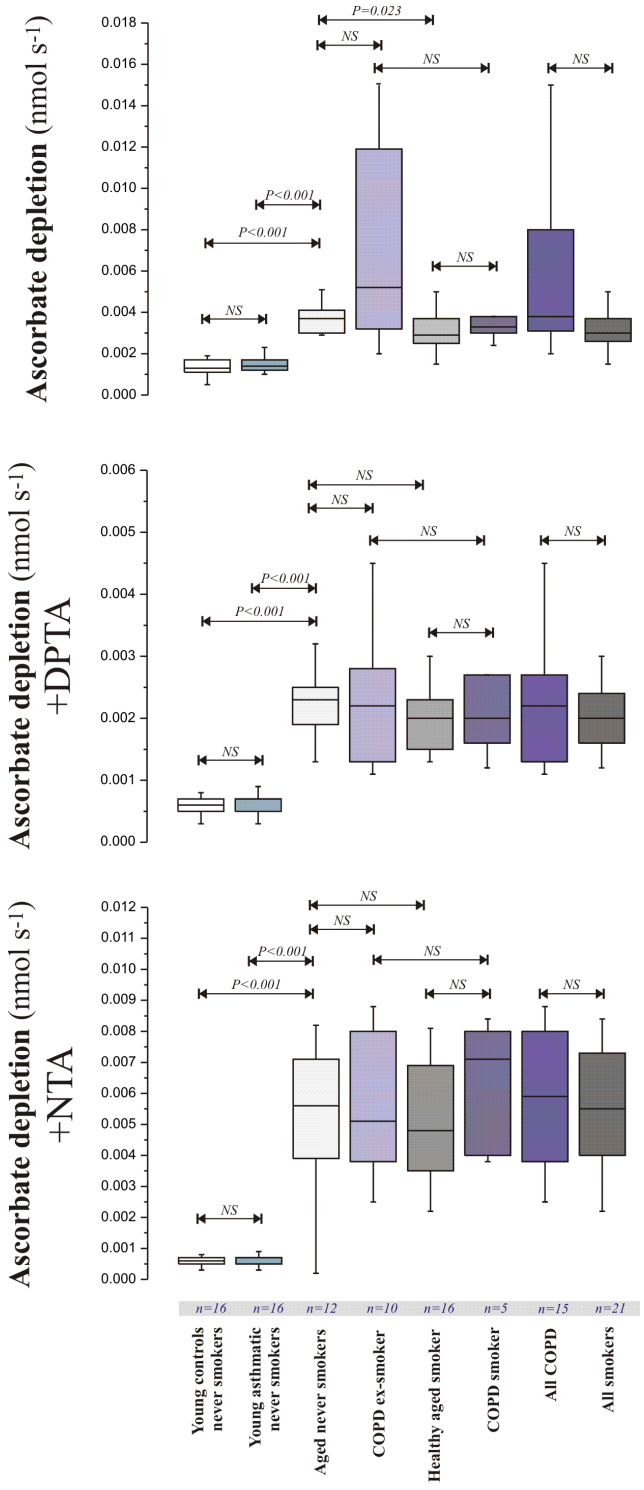

Figure 3.8: Ascorbate depletion rates, with and without chelators (DTPA and NTA), observed in lavage fluids obtained from young asthmatics, aged COPD patients, as well as age and smoking history matched controls. Data are presented and group comparisons performed as outlined in the legend to Figure 3.5.

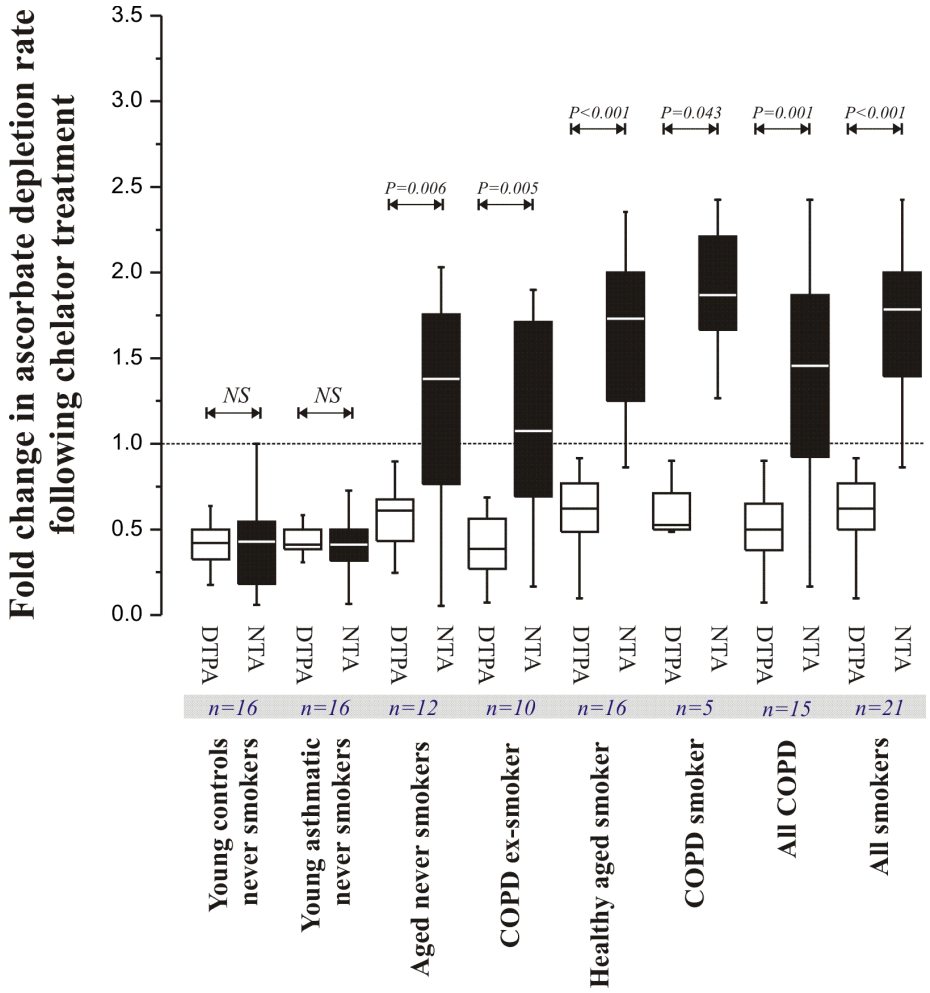

Figure 3.9: Fold change in the ascorbate depletion rate following co-incubation with DTPA (white boxes) or NTA (black boxes) relative to untreated rates. Paired comparisons between the DTPA and NTA treatments for each group were performed using the Wilcoxon-Signed Rank Test. P values are indicated where they were <5%.

The difference between the rates observed between the aged and young adults were maintained after DTPA (central panel, **Figure 3.8**), despite a significant decrease in the measured rate (**Figures 3.9** and **3.10**), as well as after NTA, which decreased the ascorbate depletion rate in the young adults but increased them in the aged populations (**Figure 3.9**). DTPA is a polyamino carboxylic acid consisting of a diethylenetriamine backbone with five carboxymethyl groups with the ability to bind to and fully redox-inactivate transition metals such as Fe and Cu. As such, any residual oxidation apparent after co-incubation with an excess of DTPA must reflect the

presence of other pro-oxidants, most likely peroxide species such as hydrogen peroxide, or lipid and protein peroxides. Hence, the data presented suggests both an increased content of catalytic metals within the RTLF with age but also implies that other pro-oxidant species are also increased in these groups. NTA has been shown to remove virtually all Fe from oligomeric iron complexes and albumin/low molecular weight ligand bound iron and therefore has the converse action of increasing the catalytic Fe pool, consistent with the evidence that Fe-NTA actually promotes the oxidation of biomolecules (Iqbal, 2009; Morel, 1997). As the Fe binding affinity of NTA does not permit it to remove bound Fe from ferritin, transferrin or lactoferrin it therefore has the effect of promoting oxidation in direct relation to the size of the NTBI pool.

A paper by Joyner *et al.* (2011) recently examined the influence of a panel of chelators (including NTA and DTPA) on the oxidative activity of redox active metals (Fe, Cu, Co and Ni) on the rate of ascorbate oxidation. These studies demonstrated that incubation with an excess of DTPA effectively prevented ascorbate oxidation by either Fe or Cu, consistent with the observations presented in this chapter. Notably, the rate of ascorbate oxidation by Fe (ferrous sulphate heptahydrate) in the absence of hydrogen peroxide was negligible, with the rate observed in the presence of H_2O_2 approximately 10-fold less than with Cu (cupric chloride dihydrate). This result highlights the importance of Cu as a redox catalyst in biological systems. They further observed that Cu catalysed oxidation of ascorbate was reduced 4-fold by NTA-chelation. This finding suggests that NTA can be used to discriminate between Fe and Cu dependent oxidative losses.

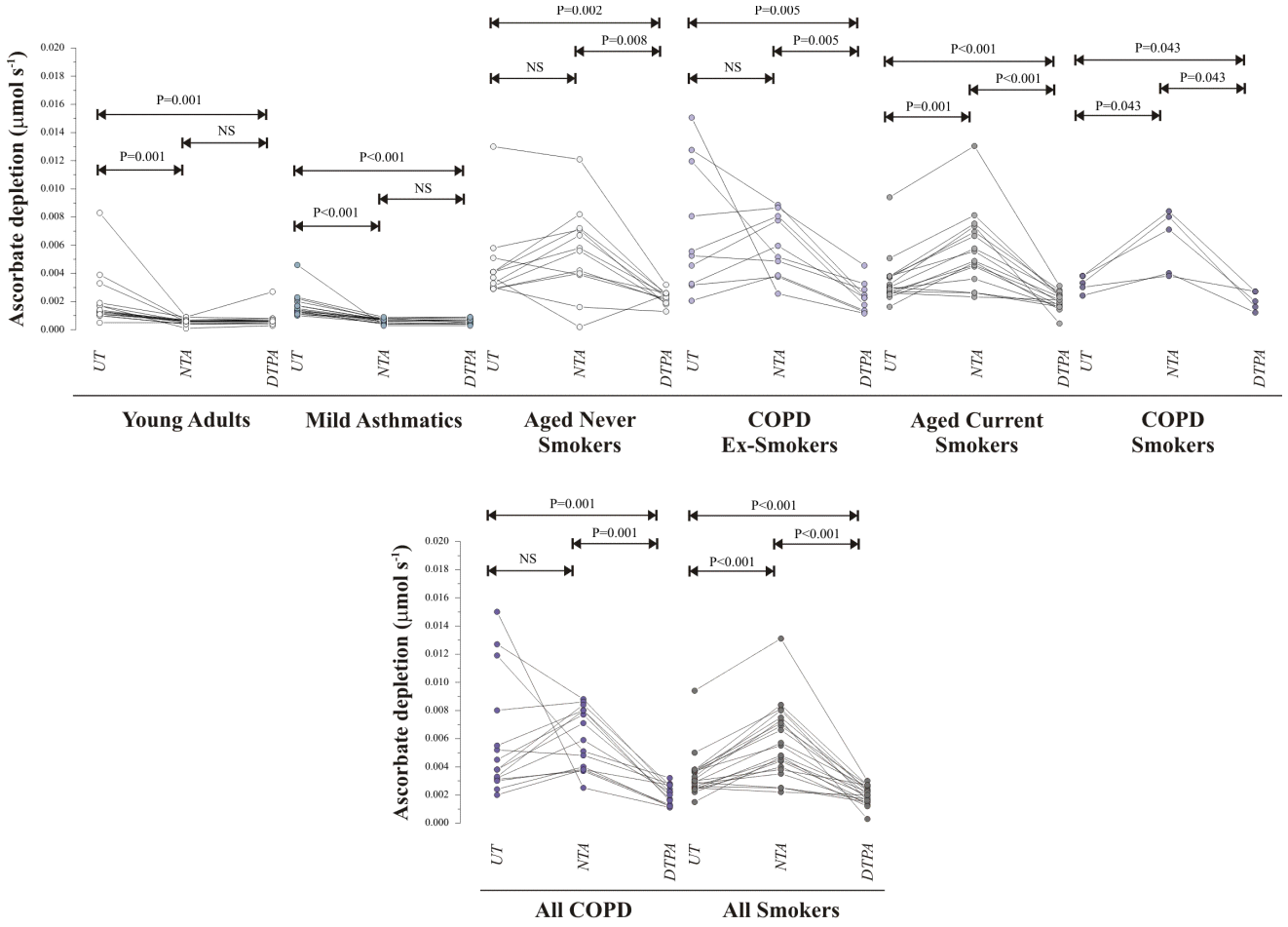

Figure 3.10: Individual ascorbate depletion rates, with and without chelation in each of the patient groups. Paired comparisons between the observed ascorbate depletion rates, with and without DTPA or NTA treatment for each group were performed using the Wilcoxon-Signed Rank Test. P values are indicated where they were <5%.

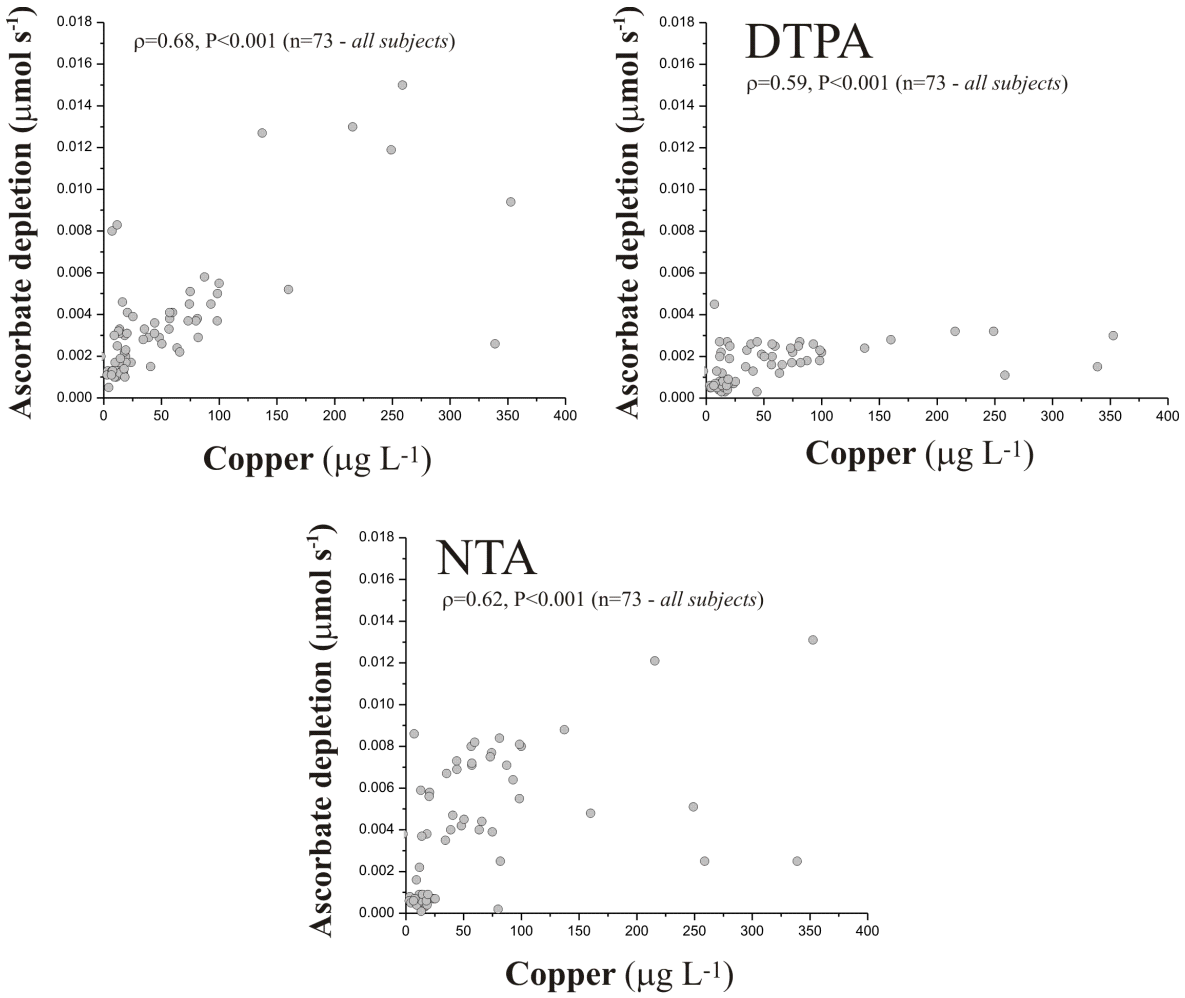

Figure 3.11: Associations between the observed ascorbate depletion rates (with and without chelators) with the measured total Cu concentrations in the lavage fluid samples. The strength of association was assessed using the Spearman Rank Order Correlation, with the Spearman's rho (ρ) and the associated P-values illustrated for all of the subject groups combined. The associations for each separate patient group are illustrated in Table 3.1.

Thus, the reduced rates of ascorbate oxidation observed in the young healthy and asthmatic groups following NTA treatment suggests the presence of a catalytically active Cu pool. Conversely, the increased oxidation rates observed with NTA co-incubation in the lavages from the aged groups (healthy, COPD and smokers) demonstrates the presence of a catalytically active NTBI pool. These data therefore represent the first evidence of an increased catalytic Fe pool in aged subjects and

though consistent with my previous observations on lavage metals and oxidation markers, this was not related to the presence of COPD or current smoking.

Table 3.1: Spearman correlation coefficients for BAL fluid total Cu and Zn content with the rate of ascorbate oxidation in the presence and absence of NTA or DTPA.

		All subjects	Healthy controls	Mild asthmatics	Age Control Never smoker	Aged Control Current smoker	COPD patients Ex-smokers	COPD patients Current smokers
Cu	AA depletion rate	ρ=0.69, *P*<0.001 (73)	NS (16)	ρ=0.51, *P*=0.04 (16)	ρ=0.70, *P*=0.01 (12)	ρ=0.67, *P*=0.009 (14)	ρ=0.73, *P*=0.016 (13)	NS (9)
Cu	AA depletion rate + dtpa	NS	NS (16)	NS (16)	NS (12)	NS (14)	NS (13)	NS (9)
Cu	AA depletion rate + nta	ρ=0.62, *P*<0.001 (73)	NS (16)	NS (16)	NS (12)	NS (14)	NS (13)	NS (9)
Zn	AA depletion rate	ρ=0.70, *P*<0.001 (73)	NS (16)	NS (16)	NS (12)	NS (14)	NS (13)	NS (9)
Zn	AA depletion rate + dtpa	ρ=0.70, *P*<0.001 (73)	NS (16)	NS (16)	NS (12)	NS (14)	NS (13)	NS (9)
Zn	AA depletion rate + nta	ρ=0.70, *P*<0.001 (73)	NS (16)	NS (16)	NS (12)	NS (14)	NS (13)	NS (9)

Correlation analysis demonstrated that the rates of ascorbate oxidation observed in the lavage returns from all subjects were significantly associated with the measured total Cu; with the association maintained with NTA co-incubation, but somewhat attenuated with DTPA (**Figure 3.11**). When these associations were examined on an individual group basis (**Table 3.1**) it was clear that only the overall rate was consistently associated with the pro-oxidant status of the lavage samples. Due to the underlying association between Zn and Cu (**Figure 3.7**), similar significant correlations were observed with the ascorbate depletion rate when all subjects were considered, but these associations were not robust across the individual groups (**Table 3.1**). Additional correlation analyses were performed between the measured lavage Cu content and the oxidation marker concentrations (GSSG, DHA and 4-HNE) reported in chapter 2 (**Figure 3.12**). In all cases significant associations were noted when all subjects were considered, most strongly for the measured DHA concentration. The

analysis by sub-group presented in **Table 3.2** was somewhat less consistent, with the most consistent associations observed in the aged current smokers and COPD ex-smokers. It should be noted however that the sub-group analysis was limited by the small group size in the COPD current smokers. Nevertheless, these data suggest that increased catalytic metal content at the surface of the lung related to age, gives rise to an increased pro-oxidant environment supported by evidence of antioxidant and lipid oxidation.

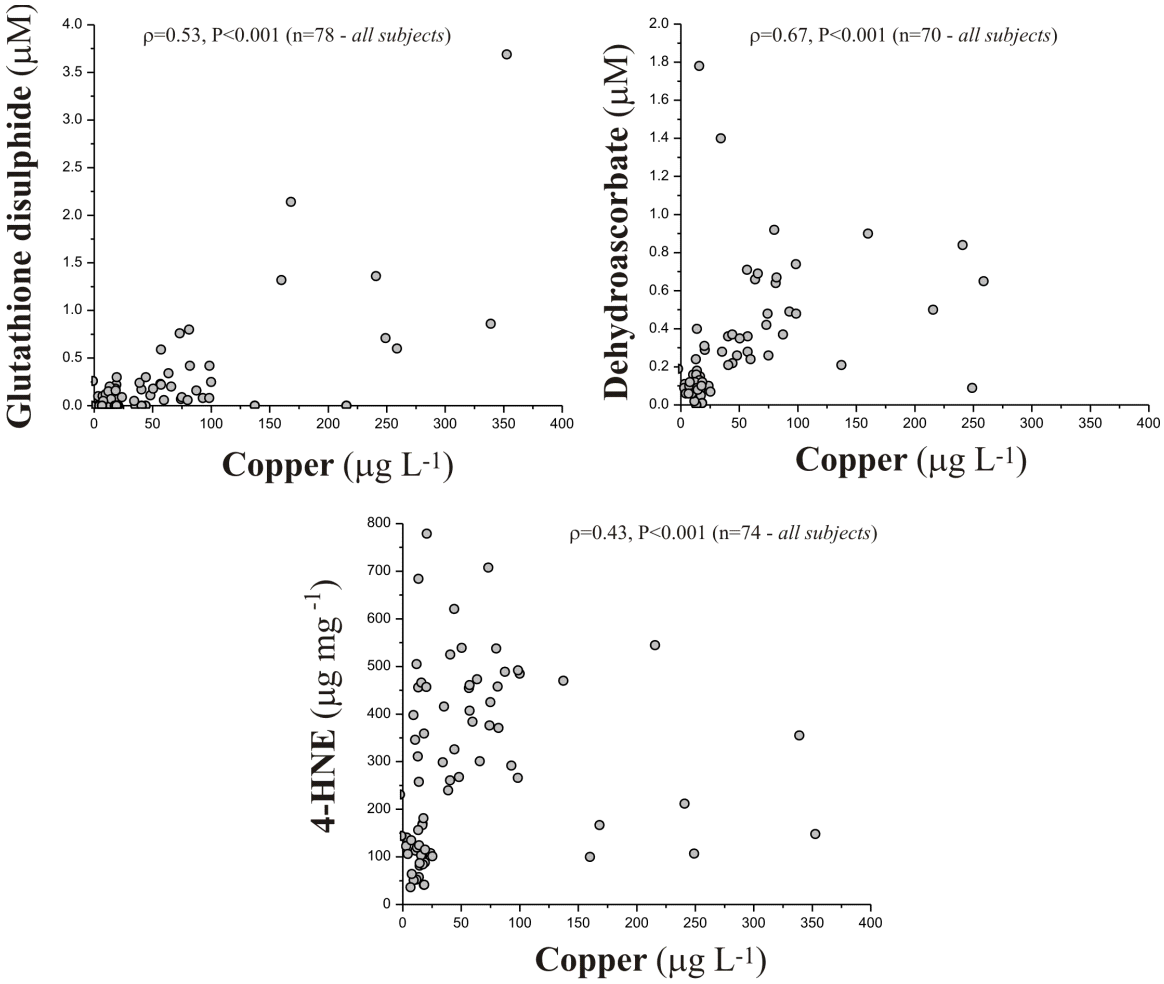

Figure 3.12: Associations between the measured total Cu concentrations in the lavage fluid samples with markers of oxidative stress. The strength of association was assessed using the Spearman Rank Order Correlation, with the Spearman's rho (ρ) and the associated P-values illustrated for all of the subject groups combined. The associations for each separate patient group are illustrated in Table 3.2.

Table 3.2: Spearman-Rank order correlations between BAL fluid total Cu and Zn, with glutathione (total, reduced and glutathione disulphide), Vitamin C (total, ascorbate, dehydroascorbate) and 4-HNE concentrations.

		All subjects	Healthy controls	Mild asthmatics	Age Control Never smoker	Aged Control Current smoker	COPD patients Ex-smokers	COPD patients Current smokers
Cu	**GSx**	ρ=0.30, *P*=0.008 (78)	NS (15)	NS (15)	NS (13)	NS (14)	ρ=0.63, *P*=0.02 (13)	NS (9)
Cu	**GSH**	NS (78)	ρ=-0.54, *P*=0.04 (15)	NS (15)	NS (13)	NS (14)	NS (13)	NS (9)
Cu	**GSSG**	ρ=0.53, *P*<0.001 (78)	NS (15)	NS (15)	NS (13)	ρ=0.77, *P*<0.001 (14)	ρ=0.81, *P*=0.001 (13)	NS (9)
Zn	**GSx**	NS (78)	NS (15)	NS (15)	NS (13)	NS (14)	NS (13)	NS (9)
Zn	**GSH**	NS (78)	NS (15)	NS (15)	NS (13)	NS (14)	NS (13)	NS (9)
Zn	**GSSG**	ρ=0.39, *P*<0.001 (78)	ρ=0.54, *P*=0.04 (15)	NS (15)	NS (13)	NS (14)	ρ=0.57, *P*=0.04 (13)	NS (9)
Cu	**Vit.C**	NS (71)	NS (15)	NS (14)	NS (11)	NS (12)	NS (12)	NS (8)
Cu	**AA**	ρ=-0.62, *P*<0.001 (71)	NS (15)	NS (14)	NS (11)	NS (12)	ρ=-0.58, *P*=0.04 (12)	NS (8)
Cu	**DHA**	ρ=0.67, *P*<0.001 (71)	NS (15)	NS (14)	NS (11)	ρ=0.77, *P*=0.01 (12)	NS (12)	NS (8)
Zn	**Vit.C**	NS (71)	NS (15)	NS (14)	NS (11)	NS (12)	NS (12)	NS (8)
Zn	**AA**	ρ=-0.70, *P*<0.001 (71)	NS (15)	NS (14)	NS (11)	NS (12)	ρ=-0.67, *P*=0.02 (12)	NS (8)
Zn	**DHA**	ρ=0.68, *P*<0.001 (71)	NS (15)	NS (14)	NS (11)	ρ=0.59, *P*=0.04 (12)	NS (12)	NS (8)
Cu	**4HNE**	ρ=0.43, *P*<0.001 (74)	NS (14)	NS (13)	NS (13)	NS (13)	ρ=0.53, *P*<0.001 (13)	NS (9)
Zn	**4HNE**	ρ=0.57, *P*<0.001 (74)	NS (14)	NS (13)	NS (13)	NS (13)	ρ=0.53, *P*<0.001 (13)	NS (9)

3.4 Conclusion

The results from the previous chapter did not support the presence of increased oxidative stress in the airways of patients with COPD, either current or ex-smokers. This was argued to reflect the fact that the studied COPD patients were well controlled, supported by the absence of neutrophilic inflammation. I did, however, note an increase in markers of oxidation in all of the aged groups (COPD ex- and current smoker, plus their aged matched controls) relative to the young healthy and asthmatic subjects. In this chapter I sought to investigate the basis for this age-related increase in oxidation at the air-lung interface, focusing on possible alterations in the airway handling of catalytic metals (Fe and Cu). As expanded upon in this chapter, the lung has evolved numerous mechanisms to limit the availability of 'free' unchelated metals, which would otherwise promote damaging biological oxidations or support bacterial growth. To achieve this, I attempted to quantify RTLF metals in lavage using ICP-MS and developed a novel method for assessing the pro-oxidant status of the recovered lavages. The use of this simple ascorbate oxidation assay, coupled to co-incubation with NTA and DTPA to isolate metal dependent oxidative catalysis and further define the relative contributions of Fe and Cu, is novel. The results obtained demonstrate for the first time an age-related increase in the NTBI pool in the lung. They are also suggestive of a labile and catalytically active Cu pool in young adults.

These observations are interesting not only because they provide a new explanation for the increased oxidation observed in numerous tissues with age, but also because they imply that the aged airway would display an increased sensitivity to oxidative injury, either due to the inhalation of oxidant gases/particulates, or acute

inflammation. In these scenarios, the presence of labile Fe or Cu pools would promote Fenton-like chemistry with the production of damaging hydroxyl radicals, as well as catalyse ongoing protein and lipid oxidation processes. This hypothesis needs to be tested, preferably in patients undergoing exacerbations, or of a more severe clinical state. The relationship of these endpoints with normal physiologic ageing also requires further exploration. In the present study, I did not examine the association between subject age and the endpoints studied due to the lack of subjects of intermediate age between the young controls and asthmatics. Given the nature of these observations, I believe there would be merit in examining a more complete age range to fully define the changes occurring with age.

Chapter 4:

Developing a novel Mass Spectrometry-based method for the quantification of 4-HNE adducts in complex biological fluids

4.1 Introduction

Oxidative stress reflects an oxidant–antioxidant imbalance, resulting from an excess oxidant production or depletion of antioxidants. Whilst there is a body of published evidence demonstrating increased markers of oxidative stress in the airspaces, breath and urine of patients with COPD, much of this is based on indirect measures and there is considerable inconsistency between various studies (reviewed in Chapter 2). In the previous two experimental chapters, I investigated whether there was evidence of oxidative stress or increased redox active metal concentrations in the alveolar lung lining fluids of COPD patients in BAL fluid samples. The data in these previous two chapters failed to demonstrate marked antioxidant deficiencies or altered metal concentrations in this extracellular compartment in patients with COPD, relative to age and smoking-history matched controls. Rather, the changes in these indices that were noted appeared to be a function either of smoking status, or the age of subjects.

Given the absence of global markers of oxidative stress the decision was made to focus on more subtle manifestations of increased ROS production, namely oxidative post-translational modifications to functionally important proteins. Previous studies

have demonstrated oxidations (cysteine and methionine oxidations, carbonylations, nitrations and adduct formation with reactive electrophiles) to specific proteins (plasma, airway lining fluid and in airway cells) in a range of airway diseases, resulting in altered protein function relevant to disease progression (Li, 2009; Wang, 2007; Starosta, 2006; Rottoli, 2005; Gole, 2000). In this study I decided to focus on 4-HNE adduct formation, as the concentrations of 4-HNE modified proteins have been shown to be increased in biopsies obtained from COPD patients, using immunohistochemical techniques (Rahman, 2002).

Michael adducts in proteins are yielded through the reaction of 4-HNE with sulfhydryl groups of cysteine residues, the ε-amino group of lysine residues and the imidazole moiety of histidine residues (Mendez, 2010). Previous publications have measured 4-HNE modifications most commonly through the use of immunological methods including: immunohistochemical staining using 4-HNE monoclonal antibodies (Toyoda, 2007; Waeg, 1996; Yoritaka, 1996); immunochemical detection (Hartley, 1999; Uchida, 1993); immunoblotting and SDS-PAGE electrophoresis (Mendez, 2010; Chen, 2007; Carbone, 2005; Li, 1997). Whilst immunological techniques offer rapid detection and kits are commercially available, the disadvantages are that they are expensive, some protocols require enrichment which prolongs analysis, specificity is only to the antibody/antigen that has been selected and false positives/negatives may occur. In addition, immunological approaches do not provide information on the chemical structure of the 4-HNE-protein adducts, nor do they allow absolute quantification of such derivatives in biological matrices. Alternative approaches have included the use of derivatising agents such as 2,4-dinitrophenylhydrazine (DNPH)

which reacts with carbonyl groups to generate 2,4-dinitrophenylhydrazones that are then characterised using UV spectroscopy (Levine, 1990). Limitations are also found with this technique as DNPH is not specific for 4-HNE and can react with any other carbonyl-modified proteins that have resulted from alternative oxidative pathways such as the metal-catalysed oxidation of amino acid side chains and covalent modification of protein by alternative reactive alkenals e.g. malondialdehyde and 4-oxononenal.

With proteins being one of the major targets of oxidative damage within the body, there is an urgent need for reliable and robust analytical methods that are capable of yielding absolute quantitative data, with particular emphasis on the accurate quantification of the extent of protein modification by 4-HNE (Hawkins, 2009). Many methods provide qualitative or semi-quantitative assessments on the degree of protein modification without unequivocally ascertaining the sites of modification or an absolute measurement. In the last 15 years, advances in ionisation and increases in the accessible mass ranges of modern mass spectrometry instruments have led to the fundamental improvements in the analysis of 4-HNE-modified proteins. Mass spectrometry-based proteomic techniques have sought to overcome the difficulties associated with specificity. These approaches include: GC-MS (Véronneau, 2002; Requena, 1997); MALDI-TOF (Mendez, 2010; Siegel, 2007; Bennaars-Eiden, 2002); LC-ESI-MS/MS with collision induced dissociation (Mendez, 2010; Zhu, 2007; Aldini, 2006; Carbone, 2005; Liu, 2003) and LC-ESI-MS/MS with electron-capture dissociation (Rauniyar, 2010; Rauniyar, 2009).

Mass spectrometry-based proteomics is a major tool used in the identification of proteins. Using the mass-to-charge ratio of analytes, a plethora of information can be gained including the measurement of: intact proteins and protein complexes; fragment ions produced from protein ions (known as top-down sequencing); peptides produced following enzymatic or chemical digestion of proteins (referred to as mass mapping) and fragment ions produced from mass-selected peptide ions (known as bottom-up sequencing) (Wysocki, 2005). Fragmentation can occur either "in-source" during the ionisation process or through purposeful induction of increased potential at the spray tip (usually by sources such as ESI) or "post-source" in a tandem mass spectrometry instrument (MS/MS by CID (collision-induced dissociation), ECD (electron-capture dissociation) or ETD (electron-transfer dissociation)). There is a continual expansion of genome and protein sequence data that is stored in databases and the application of mass spectrometry and MS/MS takes full advantage of this. Following digestion of a protein (either a model protein or complex matrix) and LC-MS/MS analysis, the resultant data of product ion peak intensities and their mass-to-charge ratios are compared with sequence data generated by the theoretical digestion of a protein. In the case of post-translational modifications, it is possible to define the instrument used, the protein that was digested, the type of digestion and the expected modifications to generate theoretical data.

As demonstrated in chapters 2 and 3, global measurements of oxidative stress are possible in relation to antioxidants and metals but do not evidence an increased level of oxidative stress that is directly related to disease severity and independent of smoking status. Therefore, the next logical step was to assess the extent of oxidative

stress at the molecular level. In order to achieve this, experiments were performed to demonstrate that Michael additions can be formed between 4-HNE and short-chain peptides followed by analysis of these adducts in a model protein and subsequently within a complex biological matrix (bronchoalveolar lavage samples). A novel approach was utilised to achieve this; LC-ESI-MS/MS (neutral-loss driven) with both CID and ETD. This approach is similar to that demonstrated by Rauniyar *et al.* (2009) but utilises ETD instead of ECD, which has previously been used to identify sites of post-translational modification by 4-HNE in peptides (Rauniyar, 2009).

4.2 Methodology

4.2.1 Synthesis of 4-hydroxy-2-nonenal

Reference 4-HNE material certified to a given purity is expensive and commonly purchased in milligram quantities prepared in organic solvent (ethanol is typical for such preparations). Given the number of preliminary experiments I wished to carry out and the expense associated with the purchase of 4-HNE, a decision was made to synthesise the material in-house. A method for the 3-step synthesis of 4-HNE was adapted from a paper by Gardner *et al.* (1992) with the expectation of yielding a large amount of the compound from relatively inexpensive materials.

4.2.1.1 Chemicals and reagents

Cis-3-Nonen-1-ol (97%) was purchased from Alfa Aesar (Lancashire, UK); 3-chloroperoxybenzoic acid (77% and also known as MCPBA) and Dess-Martin periodinane (97%) were purchased from Sigma Aldrich (Dorset, UK). All other chemicals and solvents were either reagent or HPLC grade. All the chemicals were used as received unless otherwise stated. Chloroform was purified by adding 100 mL of purified H_2O to 50 mL $CHCl_3$ in a separating funnel. The mixture was vigorously shaken and the bottom organic layer was collected. This organic layer was washed with H_2O a further 2 times after which excess di-potassium carbonate was added to the combined organic layers in order to remove any residual H_2O. The solution was then filtered and placed into a clean flask. This treatment was performed in order to remove potential traces of ethanol, which would have competed with the cis-3-nonenol in the formation of the epoxide.

4.2.1.2 Synthesis of 4-HNE

20 mL of ethanol-free $CHCl_3$ was placed into a round-bottom flask on ice and equilibrated for 5 mins with stirring. To this, 840 µL (5 mmol) of cis-3-nonenol was added and stirred for 5 mins. 1.5 g of MCPBA (8.7 mmol) was then added and the contents left to stir for 2 hrs. The solution was then removed from the ice bath, 20 mL of 10% $NaHCO_3$ was added and left to stir for 45 mins. A separating funnel was then used to decant the lower $CHCl_3$ layer into a clean flask. The organic layer was then washed a further 2 times with 20 mL of 10% $NaHCO_3$ followed by a final wash of the combined $CHCl_3$ layers with 20 mL of H_2O. The $CHCl_3$ layer was collected and placed into a beaker and excess anhydrous sodium sulphate was added to remove any residual H_2O. This solution (containing the 3,4-epoxynonanol) was then filtered and placed into a clean round-bottom flask and the solvent was removed *in vacuo* using a rotary evaporator. 280 mg of epoxide (2 mmol) was evident from weighing the flask to which 10 mL of ethanol-free $CHCl_3$ was added followed by the addition of a 2 molar excess of periodinane (2:1 periodinane : epoxide) which equated to 1.7 g of periodinane (4 mmol). This solution was left to stir at room temperature for 20 mins (forming the 3,4-epoxynonanal) and then 56 mL of diethylether and 16 mL of a 1.3 M NaOH solution were added and the mixture vigorously shaken for 30 seconds (breaking the oxygen bridge and subsequently forming the 4-hydroxy-2-nonenal). This solution was placed into a clean separating funnel and the aqueous NaOH (bottom layer) was removed. The organic diethylether layer was then washed a further 2 times with 20 mL of 1.3 M NaOH (each was left to stir vigorously for 10 mins before the aqueous layer was removed). The organic layer was then washed for a final time with 20 mL of H_2O after which, the diethylether layer was collected into a beaker and

excess anhydrous sodium sulphate was added. The organic layer was then filtered and placed into a clean round-bottom flask and the solvent removed *in vacuo* using a rotary evaporator. The simplified reaction scheme for this synthesis is shown in **Figure 4.1.**

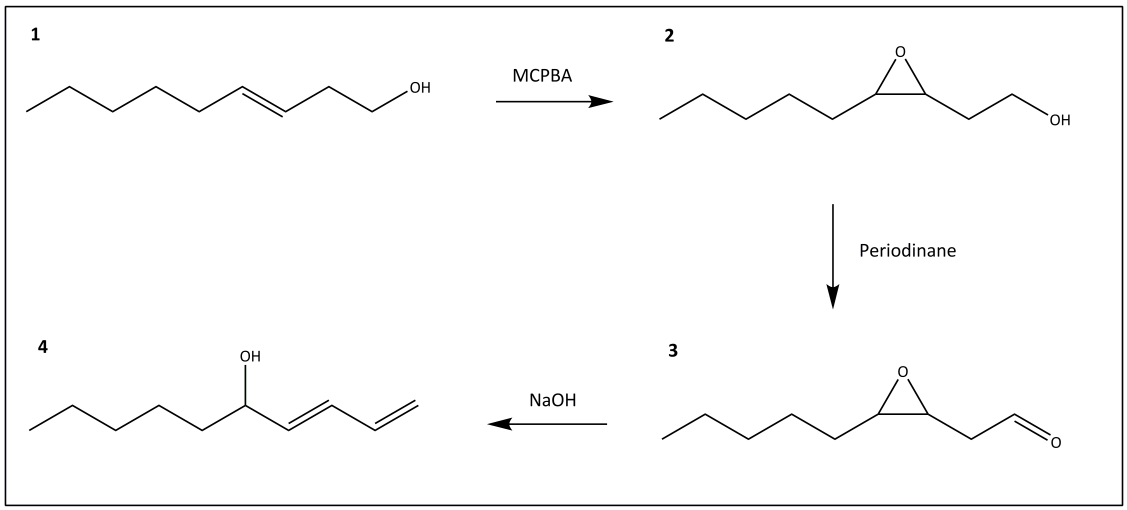

Figure 4.1: Reaction scheme of the synthesis of 4-HNE. The C3-C4 double bond of cis-3—nonenol (1) is oxidised to an oxygen bridge (2) by MCPBA. The hydroxyl group is then oxidised to form the aldehydic functional group on C1 (3) through the addition of periodinane. Treatment with the base NaOH breaks the oxygen bridge to form a hydroxyl group on C4 and a double bond between C2-C3 thus forming the product 4-hydroxy-2-nonenal (4).

The amount of product obtained was calculated by subtracting the weight of the empty flask from the weight of flask with product. A yield of 380 mg of 4-hydroxy-2-nonenal was obtained. From this the % yield of 4-HNE was calculated:

Theoretical yield = mmol x molecular weight

= 5 mmol (3(z)nonenol) x 156.22 (molecular weight of 4-HNE)

= 781.1 mg

Therefore:

Actual yield = (actual (mg) / expected (mg)) x 100

= (380mg / 781.1 mg) x 100

= 50% yield

The sample was finally flushed with nitrogen to displace any oxygen present in the flask, sealed with paraffin wrap and stored at -80 ˚C to prevent oxidative degradation.

4.2.1.3 Analysis by Nuclear Magnetic Resonance spectroscopy

The synthesised 4-hydroxy-2-nonenal was assessed for authenticity and purity by Nuclear Magnetic Resonance spectroscopy (NMR) using a Bruker 400 MHz instrument. A purified 4-HNE sample was purchased from Cayman Chemicals and used as the reference material. The preparation solvent used was $CDCl_3$ + 0.05% tetramethylsilane (TMS). The protons of the methyl groups of TMS are comparatively shielded compared with many other compounds and so serve as an internal standard (IS). TMS therefore marks one end of the range and the chemical shifts in ppm for

compounds are read in reference to how far downfield they have moved from zero ppm (TMS).

4.2.1.4 Analysis by Mass Spectrometry

Based upon the work published by Gioacchini *et al.* (1999) the synthesised 4-HNE was analysed using mass spectrometry to provide additional structural confirmation against the reference sample. In this reference paper, it was noted that 4-HNE can form a methyl-acetal structure when dissolved in methanol and so acetonitrile is recommended as the preferred solvent. All chemicals and solvents were either analytical or HPLC grade. All the chemicals were used as received unless otherwise stated.

A 50 µg/mL sample of purchased standard 4-HNE was prepared in a solution of 0.1 % formic acid in acetonitrile along with a 50 µg/mL sample of synthesised 4-HNE prepared in a solution of 0.1 % formic acid in acetonitrile. In addition, a 50 µg/mL sample of synthesised 4-HNE was prepared in a solution of 0.1 % formic acid in methanol. The instrument used was a Thermo-Fisher Accela UHPLC LTQ -MS linear ion-trap mass spectrometer system. A tune file was created for the purchased standard compound in which the electrospray voltage was set to 4 kV, the capillary temperature was set at 370˚C, capillary voltage at 15V and tube lens at 50V.

4.2.1.5 Analysis by Liquid Chromatography coupled with Mass Spectrometry

As a final step in confirming the authenticity of the synthesised 4-HNE compound against the reference material, chromatographic separations were carried

out using a Thermo-Fisher Accela UHPLC LTQ-MS system. A Waters XBridge BEH C18 3.5 µm (2.1 x 150 mm) column was used with a solvent system containing 0.1 % formic acid in water (A) and 0.1 % formic acid in acetonitrile (B). The column temperature was set at 40˚C and the tray temperature at 4˚C. The following chromatographic gradient conditions were used:

Table 4.1: Gradient conditions for the chromatographic separation of 4-HNE.

Time (minutes)	Solvent A (%)	Solvent B (%)	Flow (µL/min)
0	60	40	200
10	20	80	200
12	20	80	200
15	60	40	200

Parameters were also set to acquire two different scan events; full MS mode (*m/z* 50-200) and MS/MS by CID at a normalised collision energy of 35% (*m/z* 50-200) with parent mass *m/z* 157. Multiple injections (>3) of both the reference material and the synthesised material were performed.

4.2.2 Forming the peptide-4-HNE conjugate

It is widely regarded in the literature that 4-hydroxy-2-nonenal preferentially forms Michael additions with three amino acid residues; lysine, histidine and cysteine. As a proof of concept to determine that such additions could be observed, it was necessary to form a peptide-4-HNE conjugate. Neurotensin, a 13-amino acid neuropeptide, was selected as it contains a single lysine residue and no histidine or cysteine residues. This afforded the opportunity to show the Michael addition between the 4-HNE and the lysine residue in a short-chain peptide. The sequence of

neurotensin (NT) is as follows: pyroGlu-Leu-Tyr-Glu-Asn-Lys-Pro-Arg-Arg-Pro-Tyr-Ile-Leu-OH. In one letter notation the sequence is: pyro-QLYQNKPRRPYIL-OH with the K denoting the lysine residue.

4.2.2.1 Chemicals and reagents

Neurotensin (≥90%) was purchased from Sigma Aldrich (Dorset, UK). The synthesised 4-HNE was used to form the adduct. All other chemicals and solvents were either reagent or HPLC grade. All the chemicals were used as received unless otherwise stated.

4.2.2.2 Formation of the neurotensin-4-HNE adduct

A method was adapted from a paper by Rauniyar *et al.* (2009) and 4-HNE adducts of neurotensin were prepared by reaction of 1 mg/mL peptide with 2 mM 4-HNE in 0.1 M phosphate buffer (pH 7.4) at 37˚C for 2 hours. Phosphate buffer was prepared by the addition of 2.83 g potassium hydrogen orthophosphate (KH_2PO_4) and 0.6 g anhydrous disodium hydrogen orthophosphate (Na_2HPO_4) dissolved in 250 mL H_2O. The solution was adjusted to pH 7.4 using 1M sodium hydroxide (NaOH). After the incubation, 1 mL of diethylether (DEE) was added to the sample, vortexed for 30 seconds and spun for 1 minute in a centrifuge to extract the excess 4-HNE. The DEE layer was discarded and the extraction repeated a further 2 times.

4.2.2.3 Analysis of the neurotensin-4-HNE adduct by Mass Spectrometry

A 1 µg/mL solution of neurotensin (NT) in 0.1 % formic acid with 50:50 H_2O:ACN was used to create a tune file for the NT by direct infusion at a flow of 10 µL/min in full MS mode with a mass range of 50-2000 *m/z*. A 50 fold dilution (20 µg/mL) was prepared of the 4-HNE-NT adduct sample in 0.1 % formic acid with 50:50 H_2O:ACN. This solution was used to create a tune file for the product ion *m/z* 610.

4.2.2.4 Analysis of the neurotensin-4-HNE adduct by Liquid Chromatography coupled with Mass Spectrometry

Chromatographic separations were carried out using a Thermo-Fisher Accela UHPLC LTQ-MS system to provide detailed analyses on the synthesised adduct. A 5-fold dilution (4 µg/mL) of the original 50 fold dilution was prepared of the 4-HNE-NT adduct sample in 0.1 % formic acid with 50:50 H_2O:ACN. A Waters XBridge BEH C18 3.5 µm (2.1 x 150 mm) column was used with a solvent system containing 0.1 % formic acid in water (A) and 0.1 % formic acid in acetonitrile (B). The column temperature was set at 40˚C and the tray temperature at 4˚C. The chromatographic gradient conditions are illustrated in **Table 4.2**. Parameters were set to acquire three different scan events; MS^1 CID 35% (*m/z* 50-200) with parent mass *m/z* 157, MS^2 CID 35% (*m/z* 150-600) with parent mass *m/z* 559 and MS^3 CID 35% (*m/z* 165-2000) with parent mass *m/z* 610. Multiple injections (>3) were performed.

Table 4.2: Gradient conditions for the chromatographic separation of the peptide-4-HNE adduct.

Time (minutes)	Solvent A (%)	Solvent B (%)	Flow (µL/min)
0	90	10	200
2	90	10	200
20	30	70	200
22	30	70	200
22.5	90	10	200
30	90	10	200

4.2.2.5 Analysis of the neurotensin-4-HNE adduct by LC-MS/MS with Electron Transfer Dissociation

Direct infusions using the 50 fold dilution (20 µg/mL) NT-4-HNE adduct sample were carried out at a flow of 10 µL/min. MS/MS ETD with an activation energy of 500ms was used along with full MS scan of mass range 50-2000 *m/z*. The tune file from section *4.2.2.3* was used. Chromatographic separations were carried out using a Thermo-Fisher Accela UHPLC LTQ-MS system to provide detailed analyses on the synthesised adduct. A 5-fold dilution (4 µg/mL) of the original 50 fold dilution was prepared of the 4-HNE-NT adduct sample in 0.1 % formic acid with 50:50 H_2O:ACN. Chromatographic conditions were as described in section *4.2.2.4* above. Parameters were set to acquire two different scan events; MS^1 ETD 100ms (*m/z* 150-600) with parent mass *m/z* 559 and MS^2 ETD 100ms (*m/z* 165-2000) with parent mass *m/z* 610. Multiple injections (>3) were performed.

4.2.2.6 Assessment of the peptide-4-HNE adduct reaction completion time

Although Rauniyar *et al.* (2009) gave an estimated reaction completion time of 2 hours, I performed a series of adduct formations between neurotensin and 4-HNE

with variable incubation times. The adducts were formed as previously described with the variable incubation times of 2, 4 and 6 hours respectively. Minor changes to the protocol were made. Purchased 4-HNE was used instead of the synthesised compound in these formations as the reactions were scaled down and any possible hindrance from impurities needed to be avoided. In addition, a second set of reactions were completed substituting the purchased standard 4-HNE material with a purchased standard tri-deuterated form of 4-HNE (D_3-4-HNE). The tri-deuterated form was introduced as a means of creating an internal standard for later experiments, working towards the quantification of endogenous adducts in biological samples.

Chemicals and reagents were as described previously in section *4.2.2.1*. In addition, 4-HNE and tri-deuterated 4-HNE (D_3-4-HNE) were purchased from Cayman Chemicals (Europe). As the reference materials, in particular the deuterated 4-HNE compound were expensive, micro reactions were carried out to form the deuterated and undeuterated 4-HNE-neurotensin adducts. The deuterated 4-HNE came prepared as 100 µg in 200 µL methyl acetate. As the compound was expensive, it was deemed necessary to use as little as possible without compromising the reaction. With the original reaction requiring 300 ng to 1 mg peptide (a 3.33 excess peptide to aldehyde) it was decided that a 2x excess of the aldehyde to peptide should be used, eliminating the risk of insufficient aldehyde to react with the peptide and also allow the determination of reaction completion.

In order to satisfy equality between the D_3-4-HNE and 4-HNE standard materials, an appropriate dilution (100 µg in 200 µL ethanol) of the 4-HNE stock (1 mg

in 100 µL ethanol) was prepared. An appropriate dilution (100 µg in 1 mL H_2O) of the neurotensin stock solution (1 mg in 1 mL 0.1 M phosphate buffer) was also prepared. Phosphate buffer was prepared as described previously in section *4.2.2.2*.

Deuterated 4-HNE adducts of neurotensin were prepared by reaction of 250 ng peptide with 500 ng D_3-4-HNE in 96.5 µL of 0.1 M phosphate buffer (pH 7.4) at 37˚C for 2, 4 and 6 hours respectively (total volume 100 µL). Undeuterated 4-HNE adducts of neurotensin were prepared in the same way. For the internal standard calibration analyses, appropriate aliquots of the neurotensin stocks were taken to give the following peptide concentrations: 250 ng, 500 ng, 750 ng, 1 µg, 2 µg, 4 µg, 6 µg and 8 µg respectively. The concentration of the deuterated and undeuterated 4-HNE were further diluted to give 50 ng/µL. The adducts were formed as described above with the total volume remaining at 100 µL. Following incubation, 100 µL of diethylether (DEE) was added to each sample and gently vortexed for 30 seconds to extract the excess 4-HNE. The DEE layer was discarded and the extraction repeated once more. This method was adapted from a paper by Rauniyar *et al.* (2009). Chromatographic separations were carried out using a Thermo-Fisher Accela UHPLC LTQ-MS system to provide detailed analyses on the synthesised adducts. The chromatographic conditions used were as described in section *4.2.2.4* above. Parameters were also set to acquire two different scan events; MS^1 CID 35% (*m/z* 150-600) with parent mass *m/z* 559 and MS^2 CID 35% (*m/z* 165-2000) with parent mass *m/z* 611 (D_3-4-HNE) and *m/z* 610 (4-HNE). Multiple injections (>3) were performed.

4.2.2.7 Formation of an alternative peptide-4-HNE conjugate

As previously discussed, the literature states that 4-hydroxy-2-nonenal preferentially forms Michael additions with three amino acid residues; lysine, histidine and cysteine (Carini, 2004). Proof of concept in regards to the formation of a peptide-4-HNE conjugate has already been demonstrated with neurotensin. As an additional evidentiary piece of experimental work, an alternative short-chain peptide-4-HNE conjugate was formed. Human angiotensin 1, a 10-amino acid neuropeptide, was selected as it contains two histidine residues and no lysine or cysteine residues. This allowed exploration of the Michael additions between the 4-HNE and the histidine residues in a short-chain peptide. The amino acid sequence of angiotensin (AT) is as follows: Asp-Arg-Val-Tyr-Ile-His-Pro-Phe-His-Leu. In one letter notation the sequence is: DRVYIHPFHL with the H denoting the histidine residues. A mixture of both angiotensin and neurotensin was also incubated with 4-HNE to show the presence of both adducts in one solution. Chemicals and reagents were as described previously in section *4.2.2.1*. In addition, Human angiotensin 1 (≥90%) was purchased from Sigma Aldrich (Dorset, UK). The synthesised 4-HNE was used to form the adducts. Phosphate buffer was prepared as described previously in section *4.2.2.2*. 4-HNE adducts of angiotensin (AT) were prepared by reaction of 1 mg/mL peptide with 2 mM 4-HNE in 0.1 M phosphate buffer (pH 7.4) at 37˚C for 2 hours. 4-HNE adducts of angiotensin and neurotensin were prepared by reaction of 1 mg/mL of each peptide with 4 mM 4-HNE in 0.1 M phosphate buffer (pH 7.4) at 37˚C for 2 hours.

After the incubation, 1 mL (2mL for the AT/NT mixed solution) of diethylether (DEE) was added to each sample, vortexed for 30 seconds and spun for 1 minute in a

centrifuge to extract the excess 4-HNE. The DEE layer was discarded and the extraction repeated a further 2 times. This method was adapted from a paper by Rauniyar *et al.* (2009). A 50 fold dilution (20 µg/mL) was prepared from the original solution of AT-4-HNE in 0.1 % formic acid with 50:50 H_2O:ACN. This was used to create a tune file for the AT by direct infusion at a flow of 10 µL/min followed by direct infusion analysis of the sample. Full MS mode, with a mass range of 50-2000 *m/z* was applied.

To further characterise the AT-4-HNE conjugate in both its cleaved and preserved states, direct infusion analyses of the sample at a flow of 10 µL/min was carried out using the following scan events: MS/MS CID at a normalised collision energy of 35 (*m/z* 200-2000) with parent mass *m/z* 727 and MS/MS ETD 500ms (*m/z* 200-2000) with parent mass *m/z* 727.

4.2.3 Formation of protein-4-HNE adducts

Following the formation of short-chain peptide-4-HNE adducts for angiotensin and neurotensin, the next stage was to look at adduct formation using an intact protein. Bovine Serum Albumin (BSA) was selected as a model protein and incubated with either deuterated or undeuterated 4-HNE (purchased materials) and then subjected to a tryptic digest. The incubation period prior to the digestion of the protein allows Michael adducts to form with lysine, histidine and cysteine residues near to the outer surface of the BSA. Once these adducts have been formed, the protein is digested using trypsin, cleaving the peptide chain into smaller fragments. Trypsin possesses a high cleavage specificity, preferentially cleaving at arginine and

lysine residues and exerts its protease activity whilst remaining suitably stable in an array of conditions. The resultant peptide ion fragments are then processed through SEQUEST and MASCOT software (amino acid sequence databases and search algorithms) to establish the fragments exhibiting a 4-HNE-modified site.

4.2.3.1 Chemicals and reagents

Bovine Serum Albumin (BSA) was purchased from Sigma Aldrich (Dorset, UK). Deuterated and undeuterated 4-HNE were purchased from Cayman Chemicals (Europe). All other chemicals and solvents were either reagent or HPLC grade. All the chemicals were used as received unless otherwise stated.

4.2.3.2 Incubation and tryptic digestion protocol

A 50 µl sample (2 mg/ml protein concentration prepared in H_2O) was prepared and 1 uL of the relevant HNE stock (deuterated or undeuterated) was added. The solution was vortexed and incubated at 37˚C for 2 hours. Following incubation, 50 µl of trifluoroethanol (TFE) was added and the solution was vortexed again (protein concentrations may have varied as part of experiments, but the volume of 50 µl always remained the same). The addition of 11 µl of 150mM dithiothreitol (DTT) to give 15mM DTT was then carried out and the solution was heated to 55^{o}C for 45 min. The samples were cooled to room temperature (~5min) and then 12 µl of 550mM iodoacetamide (IAM) was added to achieve a final concentration of 55mM IAM. The solution was then incubated in the dark at room temperature for 30 min. The sample was diluted by adding 880 µl of 50mM Tris + 2mM $CaCl_2$ pH 8.0 (to achieve 5% TFE

concentration). 20 µl of trypsin (Promega sequencing grade) was then added to give a final concentration of 1:25-1:50 enzyme:protein and the solution was incubated at 37^{o}C overnight. Following overnight incubation, 10 µl of formic acid (to get 1% v/v total) was added to stop the digestion. The sample was then cleaned up using solid phase extraction to remove the digest reagents. A C18 extraction cartridge (Varian bond elut) was placed in a vacuum box and primed first by the addition of 2 ml of methanol (add 2 x 1 ml) and then 2ml of H_2O (add 2 x 1 ml). The sample was loaded using a glass pipette and allowed to pass through the column before adding 2 ml of water (2 x 1 ml) to wash through unwanted eluents. New tubes were then placed in the vacuum box and 2 ml of ACN (2 x 1ml) was added to elute the peptides. The samples were dried down in a water bath under nitrogen for approximately 20 min at 65^{o}C. The samples were then reconstituted into a solution of 200 µl of 90% H_2O 10% ACN.

Following the reduction step using DTT to reduce the disulphide bonds, the alkylation step (using IAM) adds an additional mass of 57 to cysteine residues prior to digestion. This carbamidomethyl modification prevents the cysteines from reforming disulphides and so modified peptide fragments will display an additional mass of 57 for carbamidomethylation and an additional 157 for 4-HNE. The carbamidomethyl modification is illustrated as:

$$-CH_2\text{-}SH + I\text{-}CH_2\text{-}CONH_2 \longrightarrow -CH_2\text{-}S\text{-}CH_2\text{-}CONH_2$$

Cysteine + IAM ⟶ S-carbamidomethyl cysteine

4.2.3.3 Data-dependent neutral-loss LC-MS/MS with ETD

Both the deuterated and undeuterated 4-HNE-BSA digests were analysed using LC-MS/MS. A neutral-loss driven data dependent method was used to characterise the HNE-modified peptides. In this approach, when a neutral loss of 4-HNE is produced following MS/MS of 4-HNE-modified peptides, MS/MS by ETD is triggered on the product ion which produces the neutral-loss. This generates peptide ion fragments with the 4-HNE still bonded to the amino acid. Whilst neutral-loss indicates the presence of 4-HNE-modification, it does not allow the elucidation of the actual site of the post-translational modification, that is, specificity is lost with respect to the identity of the amino acid residue (due to fragmentation). When more than one site is present that is susceptible to modification by 4-HNE, ETD can be used as it provides an alternative fragmentation technique that allows the modified sites to remain intact, thus enabling specificity and unequivocal identification of adduct sites. The digested samples were chromatographically separated using a Thermo-Fisher Accela UHPLC LTQ/ETD-MS system to provide MS/MS analyses. Multiple injections (>3) were performed. A Waters XBridge BEH C18 3.5 µm (2.1 x 150 mm) column was used with a solvent system containing 0.1 % (v/v) formic acid in water (A) and 0.1 % (v/v) formic acid in acetonitrile (B). The column temperature was set at 40˚C and the tray temperature at 4˚C. The chromatographic gradient conditions are outlined in **Table 4.3**.

Table 4.3: Gradient conditions for the chromatographic separation of the BSA-4-HNE adduct.

Time (minutes)	Solvent A (%)	Solvent B (%)	Flow (µL/min)
0	90	10	200
2	90	10	200
40	10	90	200
47	10	90	200
47.5	90	10	200
60	90	10	200

All MS measurements were made using the following instrumental parameters to acquire the MS scans: MS^1 full scan (*m/z* 350-1500) and MS^2 data-dependent CID with normalised collision energy of 35% with fragmentation of ions within the set thresholds given below. From both the deuterated and undeuterated digests, the peptide sequences SHCIAEVEK (average mass 1015.16) and FKDLGEEHFK (average mass 1249.39) were chosen as model peptide sequences due to their consistent appearance and reasonable signal across a number of preliminary digests. For undeuterated 4-HNE, the precursor ion mass list consisted of ions 470 *m/z* for triply charged FKDLGEEHFK with a 4-HNE modified site and 615 *m/z* for a doubly charged SHCIAEVEK with a carbamidomethylated cysteine and a 4-HNE modified site. The neutral loss of 4-HNE from the triply or doubly charged peptide corresponds to mass losses of *m/z* 52 and *m/z* 78 in the spectra. For deuterated 4-HNE, the precursor ion mass list consisted of the same peptide sequences with ions 471 *m/z* and 617 *m/z* for triply and doubly charged peptides with d_3-4-HNE, whilst the neutral loss list consisted of mass losses of *m/z* 53 and *m/z* 79 for the same respective charge states. The deuteration accounts for the m/z 1 difference between the values from the two digests.

Operating the instrument in *data-dependent* mode (as illustrated in **Figure 4.2**), the mass spectrometer performs a number of tandem MS scan events on ions that have been detected above a pre-set threshold (i.e. over a given intensity). The data-dependent analysis selects the most intense precursor ions from the MS scan with a minimum MS signal of 1000 counts. Scan event 1 is the MS full scan event over the range *m/z* 350-1500, which generates the precursor ions for scan event 2. Scan event 2 was an MS/MS product ion scan (CID) over the mass range *m/z* 200-2000 with a normalised collision energy of 35% and an activation time of 30 ms with an isolation width of 3.0 Da. Dynamic exclusion was applied with a repeat count of 3 and a repeat duration of 30 seconds in order to avoid oversampling the same ions. The peak exclusion list size was set at 100 with an exclusion duration of 2 minutes and a mass isolation width of 1.5 Da. Scan event 3 was triggered by scan event 2 following a neutral loss (pre-defined as described above) with spectra collected over the 200-2000 *m/z* mass range (precursor ion window). This activates the ETD source with an isolation width of 2.0 Da and activation time of 500 ms. Once again, dynamic exclusion was applied with same parameters of scan event 2.

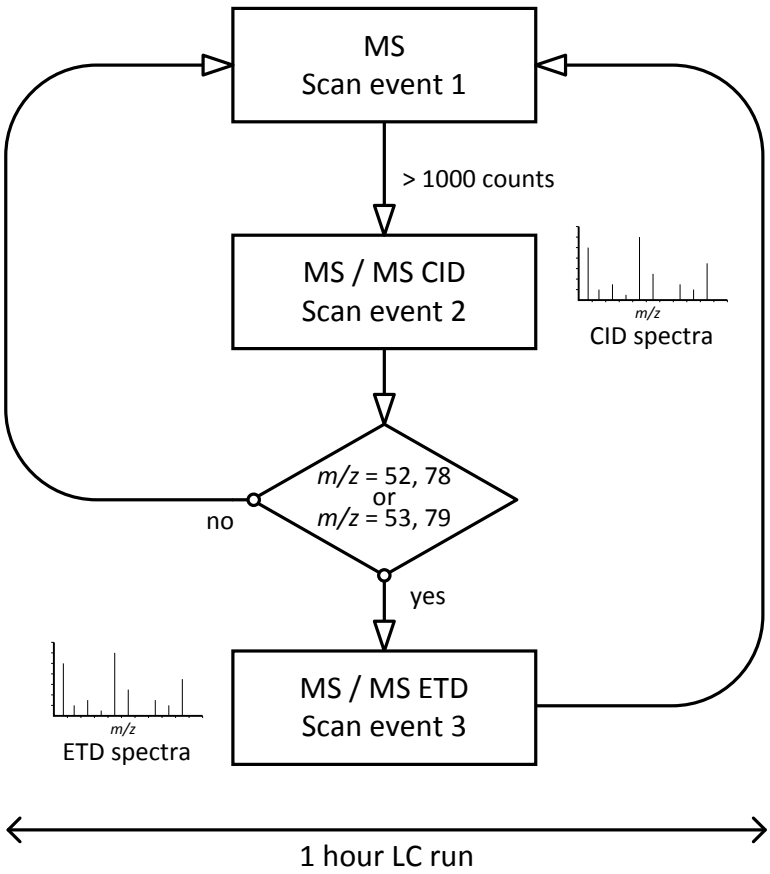

Figure 4.2: A flow diagram illustrating the various scan events and thresholds for data-dependent analysis using MS/MS CID and MS/MS ETD.

Peptide sequencing and protein precursor identification were carried out on the CID MS^2 data obtained from the chromatographic separation of the digests (both deuterated and undeuterated). The data was analysed using the SEQUEST Browser (v.3.0, ThermoFisher) to create DTA files of all of the MS^2 spectra obtained. This is a conversion from the Xcalibur software format to a generic ASCII file that can then be used across platforms. The following settings were used to generate the DTA files: bottom MW 500, top MW 2000, grouped scans 1, minimum number of ions 15 and minimum TIC 1000. The DTA files were merged using Mascot Daemon (Matrix Science, http://www.matrixscience.com) in order to upload a single file to the Mascot server. Correlations were then performed using the theoretical spectra from the Swiss Prot

protein database (accessed June 2010) against the bovine serum albumin digest and any mass spectra that exhibited an exact-match to a peptide sequence using the online available version of Mascot (Matrix Science, http://www.matrixscience.com) with the following algorithm parameters of; peptide tolerance ± 2.5 Da and MS/MS tolerance ± 1.0 Da. Mascot was also set to search for the variable modifications in peptide mass due to carbamidomethylation and the addition of 4-HNE. Sequences exhibiting a score that indicated homologies with greater than 95% probability were considered as confirmed by Mascot.

4.2.4 Formation of protein-4-HNE adducts in bronchoalveolar lavage

Following the tryptic digestion and neutral-loss LC-MS/MS (with CID and ETD) analysis of BSA-4-HNE adducts, the protocol was repeated using four BAL samples from selected COPD patients (as employed in Chapters 2 and 3), details outlined below:

1. Sample ID 33: *Female COPD current smoker, age 60 years, 14 pack years. Lavage recovery 39%, total protein concentration 0.02 mg/mL.*
2. Sample ID 38: *Female 'healthy' smoker, age 71 years, 30 pack years. Lavage recovery 9.4%, total protein concentration 0.06 mg/mL.*
3. Sample ID 39: *Male never-smoker, age 68 years. Lavage recovery 50%, total protein concentration 0.08 mg/mL.*
4. Sample ID 40: *Male COPD ex-smoker, age 70 years, 50 pack years. Lavage recovery 24%, total protein concentration 0.13 mg/mL.*

The four BAL samples were individually split into equal volumes between 2 vials, resulting in 8 sample vials. Of these newly-divided sets, half underwent protein precipitation, as described in section *4.2.4.2* whilst the other half remained untreated (**Figure 4.3**). The samples were then dried under nitrogen *in vacuo* and then reconstituted with water to provide 1 µg/µL equivalent concentrations of protein.

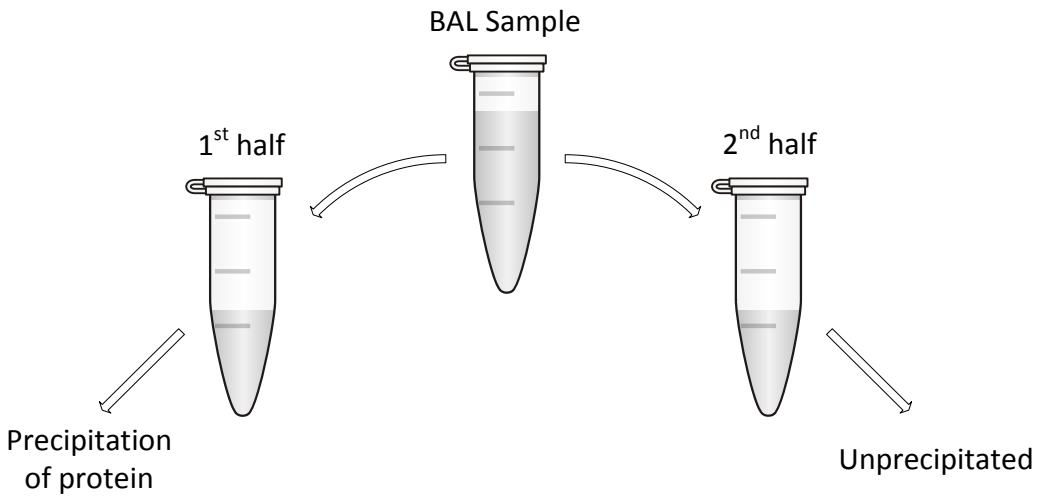

Figure 4.3: BAL fluid sample pre-treatment for 4-HNE adduction experiments.

4.2.4.1 Chemicals and reagents

Details of the clinical bronchoalveolar lavage are found in Chapter 2. All other chemicals and solvents were either reagent or HPLC grade. All the chemicals were used as received unless otherwise stated.

4.2.4.2 Precipitation of protein from the lavage samples

The protein precipitation protocol for the BAL samples was adapted from the method described by Kay *et al.* (2008); 180 µL of acetonitrile was added to an 80 µL

sample of BAL (containing 80 µg of protein), gently vortexed for 30 seconds and then sonicated for 10 minutes. The sample was then vortexed gently for another 30 seconds and sonicated for a further 10 minutes. Following this, the sample was centrifuged at 12,000 *g* at room temperature for 10 minutes. The supernatant (~250 µL) was transferred to a clean vial and dried with nitrogen at room temperature *in vacuo* for 30 minutes. The sample was then reconstituted in 50 µL of water.

4.2.4.3 Incubation and tryptic digestion protocol

The tryptic digestion of the lavage was carried out as described in section *4.2.3.2* with the following modifications: the starting concentration of protein in the lavage was 50 µg (estimated to be slightly lower in the precipitated samples) as opposed to 100 µg; no incubation with 4-HNE or d_3-4-HNE was performed. The digestion was performed on both the precipitated and unprecipitated BAL samples.

4.2.4.4 Data-dependent neutral-loss LC-MS/MS with ETD of the digested BAL

Data-dependent analyses was performed as described in section *4.2.3.3* with the exemption of neutral-loss scan events for deuterated 4-HNE. Only one injection for each sample was carried out due to volume constraints.

4.3 Results & Discussion

4.3.1 Assessing the purity of the 4-hydroxy-2-nonenal synthesis

Authenticity and purity of the synthesised 4-HNE were confirmed by Nuclear Magnetic Resonance (NMR) and mass spectrometry.

4.3.1.1 Assessing the synthesis using Nuclear Magnetic Resonance spectroscopy

Below is an estimation of the expected ^{1}H NMR values obtained by using ChemDraw software ver. 11.0 (Cambridgesoft) based upon the chemical structure of 4-HNE (**Figure 4.4**).

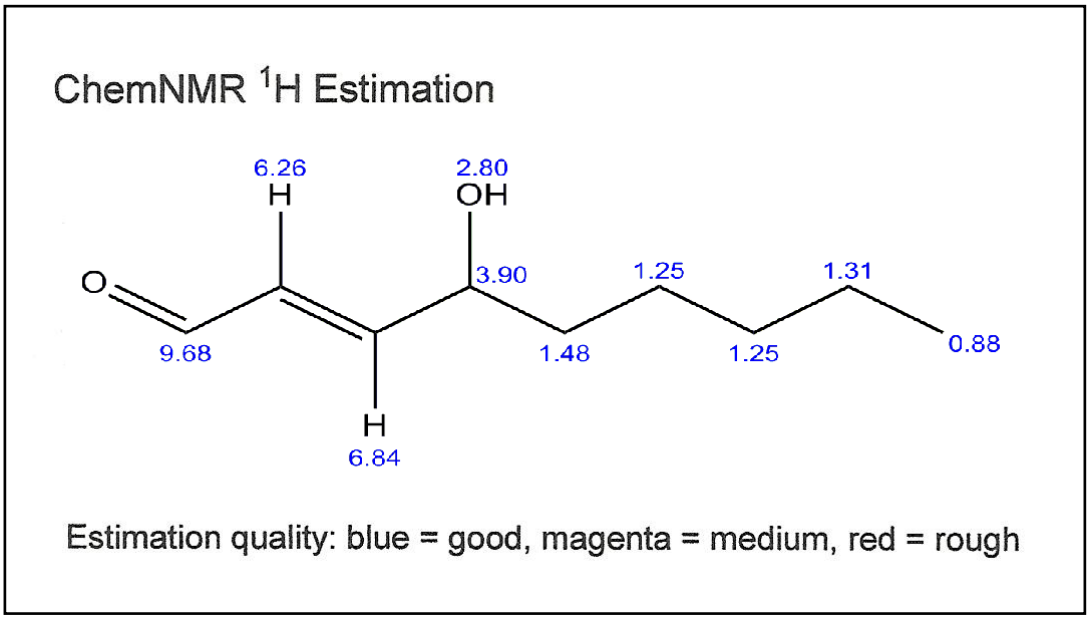

Figure 4.4: ChemDraw single proton NMR prediction of 4-hydroxy-2-nonenal based upon the structure.

The values in blue represent the predicted chemical shifts (ppm) downfield from TMS (internal standard, set at 0 ppm) that are expected for this compound. Below is the predicted ^{1}H NMR spectrum obtained by the same software (**Figure 4.5**).

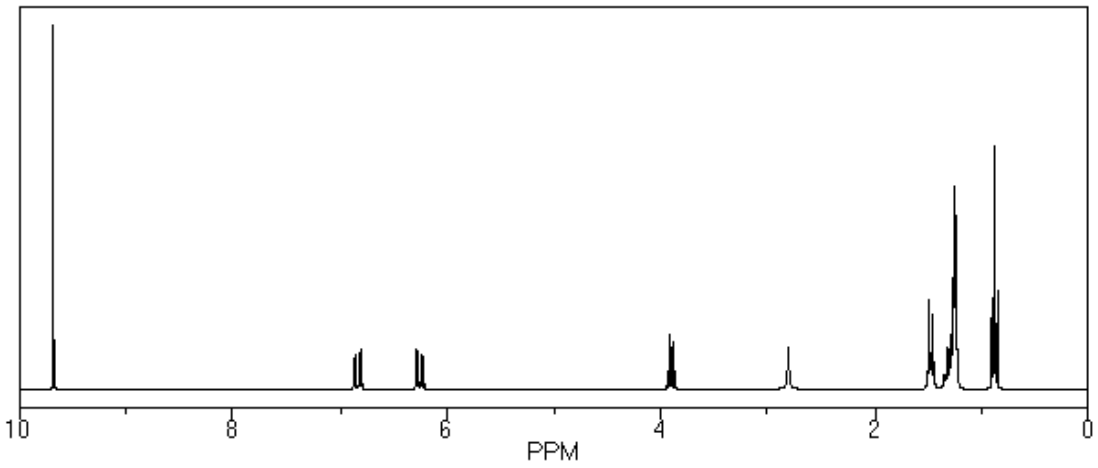

Figure 4.5: ChemDraw single proton NMR estimation for 4-hydroxy-2-nonenal.

Approximately 2 mg of reagent grade 4-HNE (purchased from Cayman Chemicals) was placed into solution with 700 µL of $CDCl_3$ (deuterated chloroform) + 0.05 % TMS. The sample was analysed via NMR and the spectrum obtained is illustrated in Figure 4.6**.** A scraping of the synthesised 4-HNE compound (approximately 25 mg) was placed into solution with 700 µL of $CDCl_3$ + 0.05 % TMS. The sample was analysed via ^1H NMR and the spectrum obtained is illustrated in **Figure 4.6**.

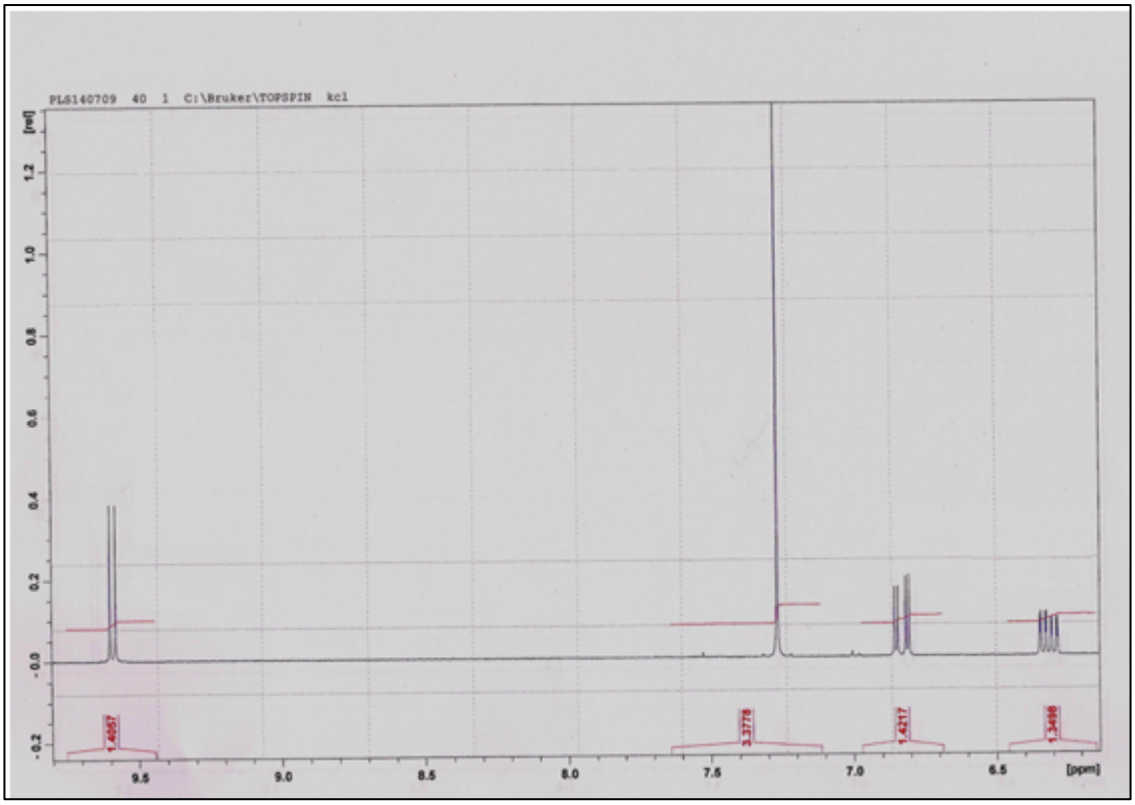

Figure 4.6: Single proton NMR spectrum of the reagent grade 4-HNE.

The original file for the reference HNE was unavailable and so a scanned version of the hard copy is shown. However, this spectrum was enhanced by the technician and so the range below 6.2 ppm is not presented. In addition, detailed information was not available to calculate the coupling constants for the enhanced areas although overlaying the two spectra (reference material and synthesised compound) showed that the values were identical. Therefore, for purposes of comparison this lower range for the synthesised compound will be assessed against the ChemDraw prediction and the values published by Gardner *et al.* (1992) where provided.

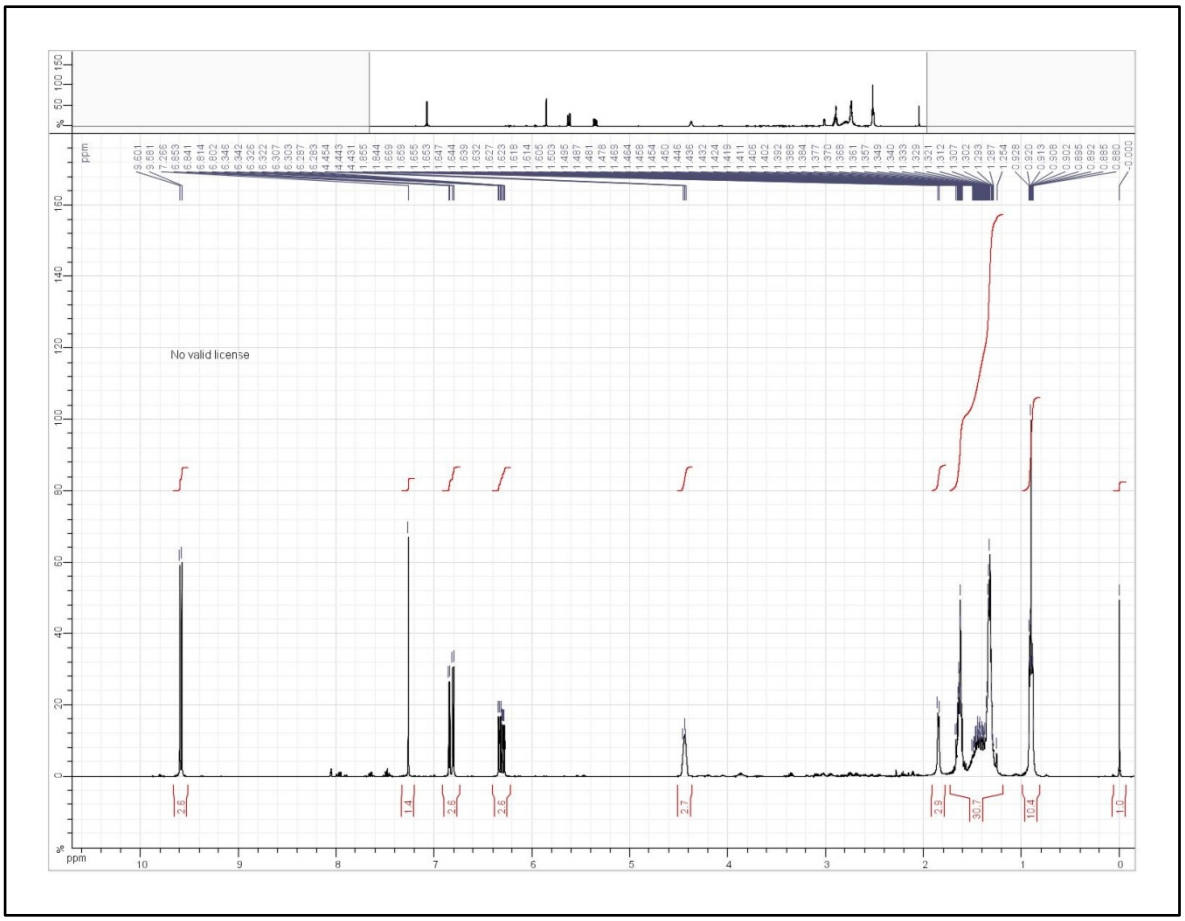

Figure 4.7: Single proton NMR spectrum of the synthesised 4-HNE.

The data from the predicted spectrum, the synthesis reference paper (method adapted from Gardner *et al.* 1992) and the in-house synthesised compound can be found in **Table 4.4** below. The coupling constant *J*, is calculated by the following formula:

$$J \text{ Hz} = \delta \text{ ppm} \times \text{MHz}$$

The reference paper characterised only from C1 to C4. The coupling constants for the synthesised compound satisfy the values of the reference paper and also the ChemDraw prediction. **Figures 4.8** to **4.11** are enhancements of the synthesised compound ^{1}H spectrum.

Table 4.4: NMR spectra data – chemical shifts (ppm) registered downfield from tetramethylsilane. 1H = single proton, *d* = doublet, *dd* = double doublet, *dddd* = quartet of doublets, *dtd* = doublet triplet doublet, *s* = singlet, *b* = broad, *m* = multiplet, *t* = triplet, *J* = coupling frequency.

ChemDraw 1H prediction	**Gardner *et. al* (1992) Lipids, 27, 9, 686-689**	**Synthesised 4-HNE**
CHO = 9.68 (*d*)	9.56 (1H, *d, J* = 7.9)	9.60 (1H, *d, J* = 7.8)
H on C-2 = 6.26 (*dddd*)	6.29 (1H, *dddd, J* = 15.7, 7.9, 1.6)	6.3 (1H, *dddd, J* = 15.6, 8, 1.6)
H on C-3 = 6.84 (*dd*)	6.81 (1H, *dd, J* = 15.7, 4.7)	6.8 (1H, *dd, J* = 15.6, 4.8)
H on C-4 = 3.9 (*dtd*)	4.42 (1H, *dtd, J* = 6.5, 4.7, 1.6)	4.44 (1H, *m*)
OH = 2.8 (*d*)		1.85 (1H, *d, J* = 4.4)
H on C-5 = 1.48 (*m*)		1.63 (1H, *m*)
C-6 to C8 = 1.27 (*m*)		1.33 (1H, *m*)
CH3 = 0.88 (*t*)		0.90 (1H, *t*)

Aldehyde groups typically exhibit a chemical shift of between 9.0-10.0 ppm. The hydrogen attached to the aldehyde is shifted further downfield based upon the anisotropy of the carbonyl group (C=O) in addition to the inductive effect of the oxygen which expresses electronegativity. Magnetic anisotropy can be explained as the effect of unsaturated π electrons upon protons within close proximity. In the case of aldehydes, the electronegativity of the oxygen in conjunction with the electron dense double bond cause significant deshielding and reduction of electron density of the attached hydrogen proton which results in a large downfield chemical shift. The doublet observed for the aldehyde is due to the weak coupling of the aldehydic hydrogen to the hydrogen present on the other side of the carbonyl group. **Figure 4.8** clarifies the presence of an aldehyde at 9.60 ppm with the characteristic doublet observed.

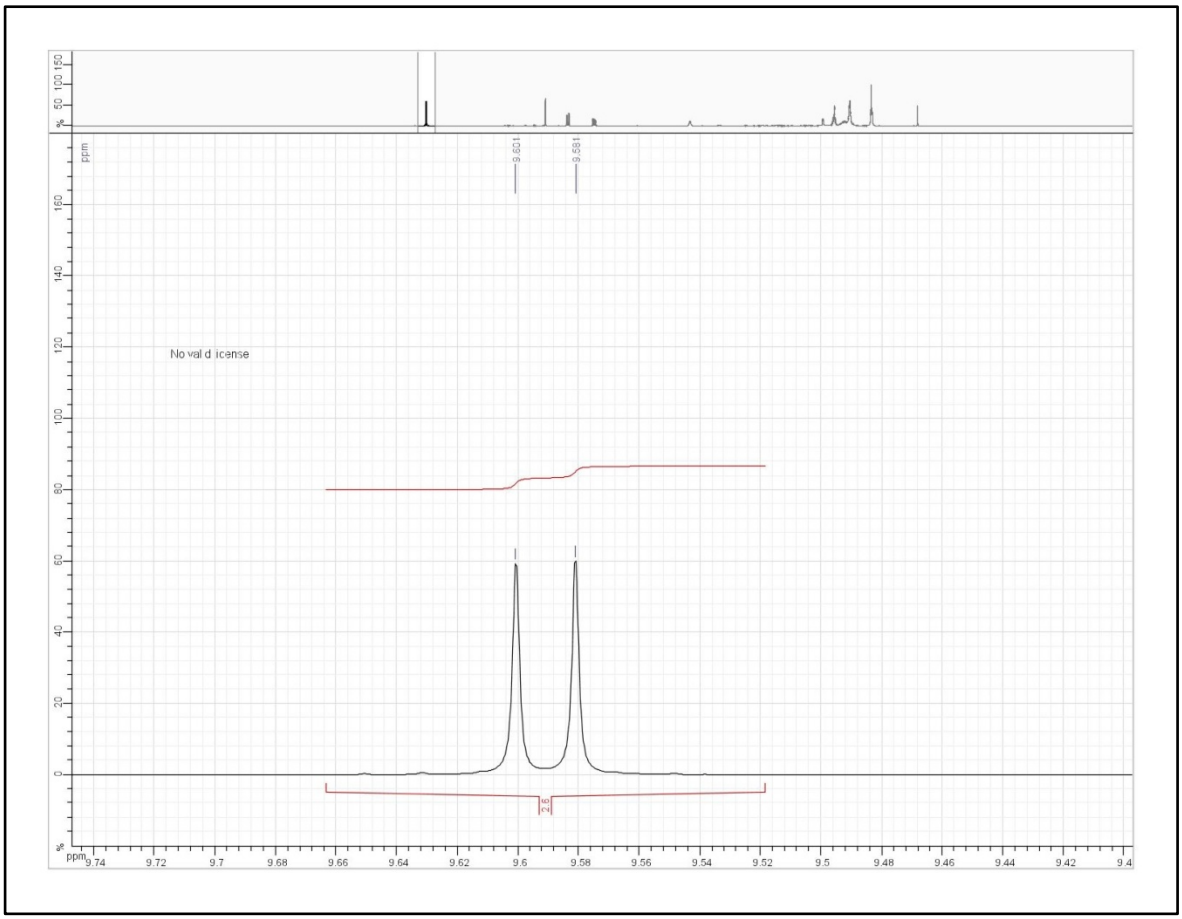

Figure 4.8: Enhancement of the aldehydic group (CHO) of the synthesised 4-HNE which exhibits a doublet formation.

Alkenes can exhibit two different types of absorptions; vinyl and allylic. Vinyl absorptions typically have a chemical shift of 4.5-6.5 ppm but the splitting patterns of vinyl protons are complicated as the protons on double bonds are rarely equivalent magnetically despite being located on the same carbon. Vinyl hydrogens become deshielded by the diamagnetic anisotropy caused by the π electrons in the double bond resulting in three distinct types of spin interactions in alkenes; cis, trans and geminal (terminal methylene). These splitting patterns cannot, therefore, be explained by the *n* + 1 rule (also known as spin-spin splitting). Cis coupling constants are typically between 6 – 15 Hz corresponding with the *cis*-formation of C2 and C3 of the

synthesised compound. C2 and C3 display unique splitting behaviour and chemical shifts in accordance with that of *cis*-alkenes (**Figure 4.9**).

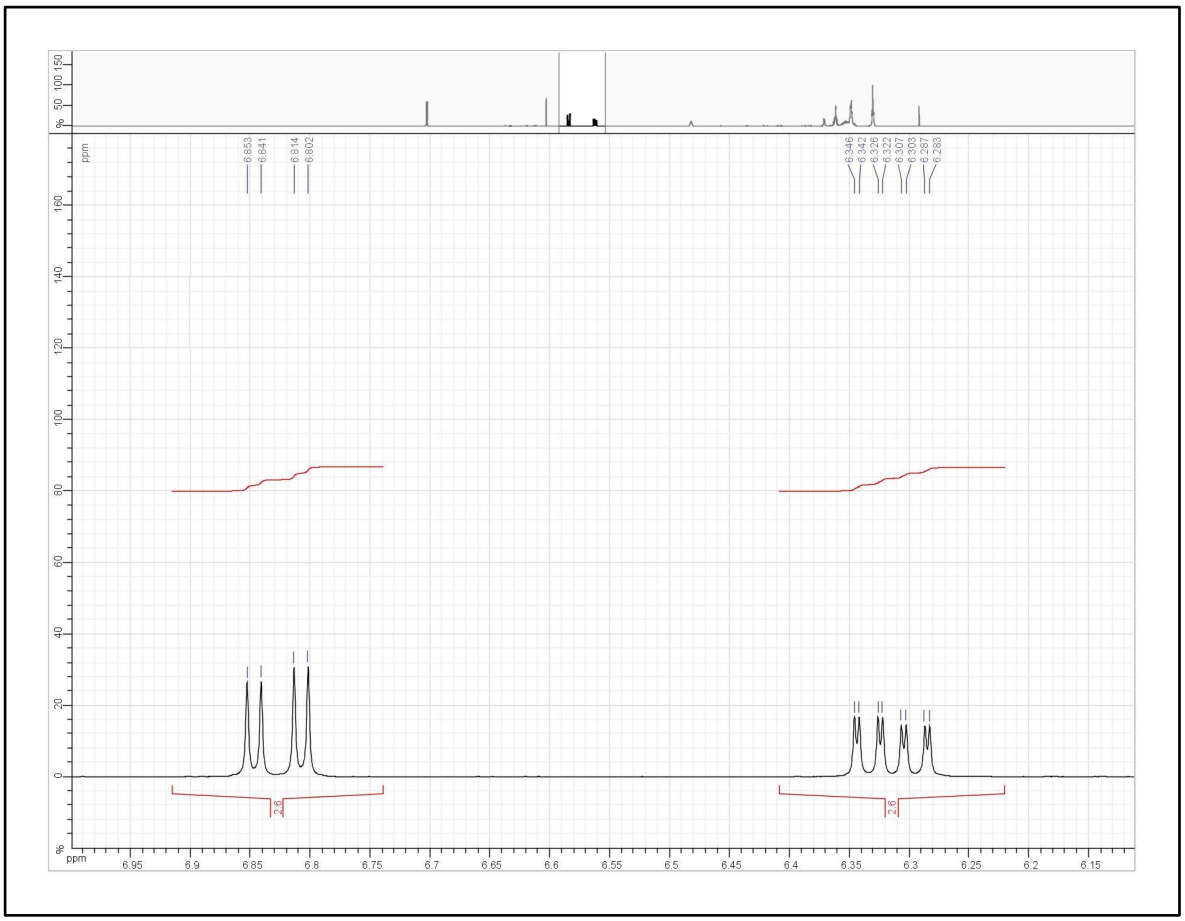

Figure 4.9: Enhancement of the *cis*-alkenes (vinyl hydrogens = hydrogens attached to a double bond) of C2 and C3 of the synthesised 4-HNE. C3 exhibits a double doublet and C2 exhibits a doublet of doublets, also referred to as a quartet of doublets.

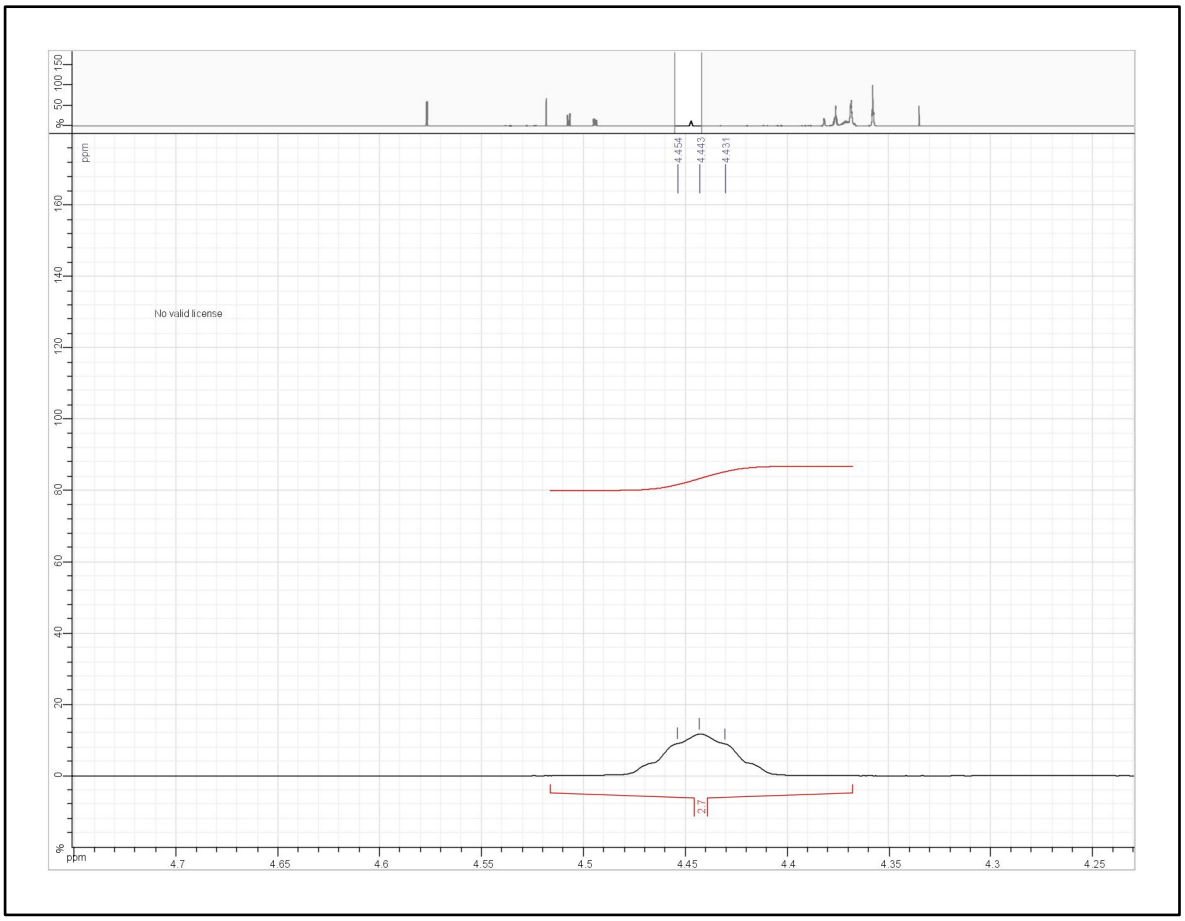

Figure 4.10: Enhancement of the C4 multiplet of the synthesised 4-HNE.

The C4 of the synthesised compound exhibited a multiplet at 4.44 ppm (**Figure 4.10**). The chemical shift δ value is identical to the value from the reference paper of 4.42 ppm. It is worth noting that as no chromatographic purification was carried out, this may have affected the resolution of the C4 multiplet which should have exhibited a doublet-triplet-doublet (*dtd*). However, no significant impurities were apparent following analyses and so it was decided that the compound was of a satisfactory purity for the research objectives.

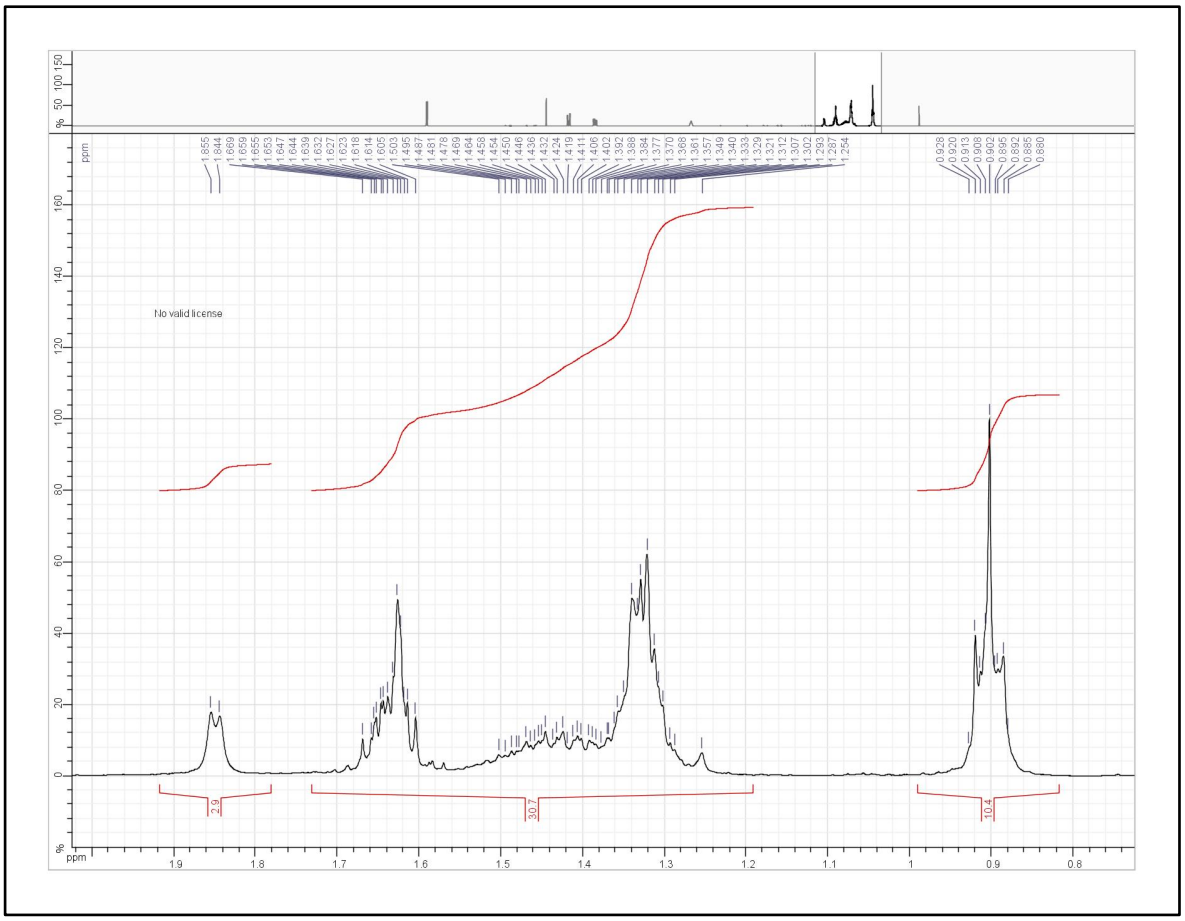

Figure 4.11: Enhancement of the aliphatic region of the synthesised 4-HNE. This encompasses the hydroxyl group on C4, followed by C5, C6-C8 and the methyl CH_3 group.

Hydroxyl protons demonstrate variable absorption positions with chemical shifts anywhere from 0.5–5.0 ppm. Concentrated solutions possess increased hydrogen bonding between molecules resulting in the increased deshielding of protons. Such deshielding will show absorption at the higher end of the range (4-5 ppm) whilst mildly concentrated solutions (with less hydrogen bonding) typically absorb at the lower end of the range (0.5-1.0 ppm). The reference paper did not give a value for the hydroxyl group and the predicted value fell at 2.80 ppm. However, as the hydroxyl group of the synthesised compound fell at 1.85 ppm and within the

described range, it was deemed an acceptable confirmation of its presence (**Figure 4.11**).

The C5 and C6-C8 regions exhibited multiplicity and low resolution rendering it difficult to calculate the coupling constants (*J*). However, the chemical shift values were similar to the predicted values; the C5 and C6-C8 predicted values were 1.48 and 1.27 ppm respectively and the synthesised compound values were 1.63 ppm for C5 and 1.33 ppm for C6-C8. Both sets of values displayed multiplet peaks (**Figure 4.11**).

The methyl group was characterised by a triplet conforming to the $n + 1$ rule of multiplicity as the resonance peak of the methyl protons is split by two equivalent protons on the adjacent carbon atom ($n = 2$ therefore $n + 1 = 3$). The synthesised compounds δ value for the methyl group (0.90 ppm) corresponds with the predicted value of 0.88 ppm in addition to the predicted triplet peaks (**Figure 4.11**).

4.3.1.2 Assessing the synthesis using Mass Spectrometry

The purchased standard 4-HNE was directly infused into the ESI source using a syringe pump at a rate of 10 µL/min. The instrument was set to acquire full scan spectra over the range *m/z* 105-200. The spectrum shown in **Figure 4.12** was obtained.

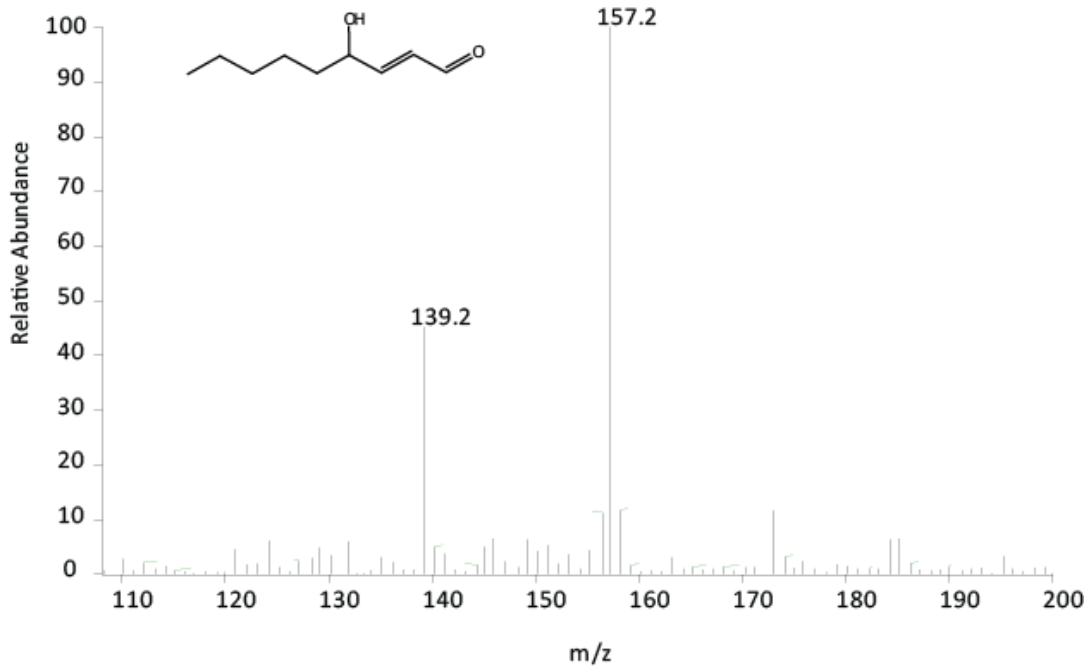

Figure 4.12: Direct infusion of purchased standard 4-HNE prepared in a solution of 0.1 % formic acid in acetonitrile (>3 injections). Parent ion of *m/z* 157.2 can be seen as well as *m/z* 139.1 which constitutes the common loss of water.

4-HNE has an average mass of 156.22 with the protonated molecule having a *m/z* 157.22 (i.e. $[M + H]^+$ = 157.22). An abundant ion at *m/z* 157.2 was seen in **Figure 4.12** which represents the 4-HNE protonated molecule. An ion at *m/z* 139.2 is also observed which is characteristic of the 4-HNE undergoing a loss of water (157.2 – 18) in the mass spectrometer due to the presence of the hydroxyl group on carbon-4. The direct infusion was repeated for this sample using tandem mass spectrometry (MS/MS). Tandem mass spectrometry by collision induced dissociation (CID) with helium as the collision gas at an energy of an arbitrary value of 35% was utilised over a mass range of *m/*z 50-200.

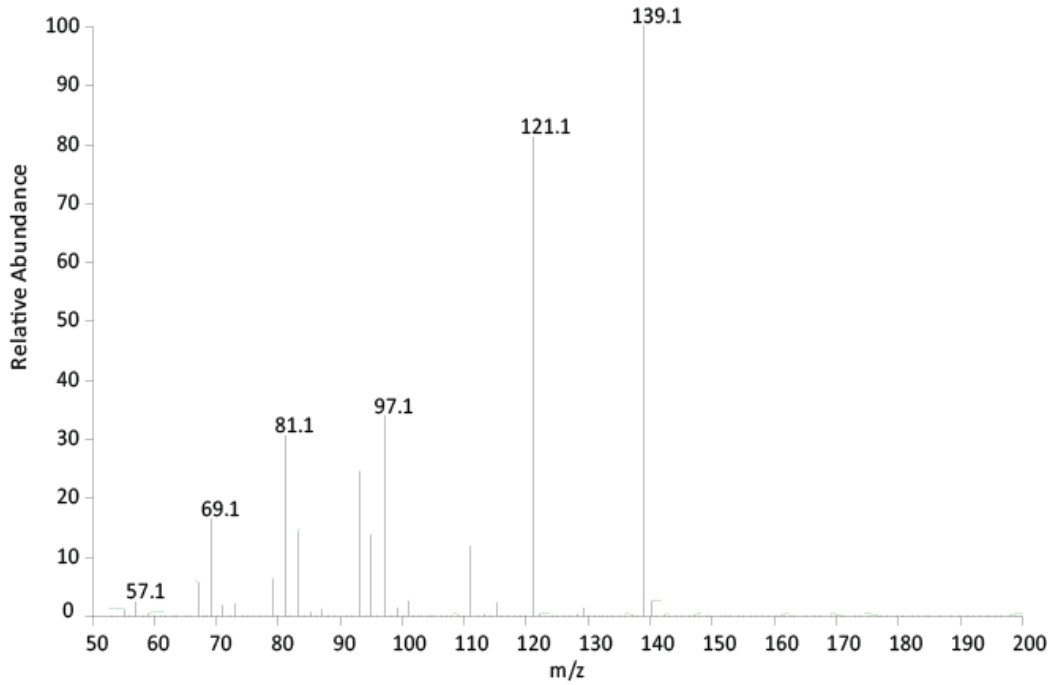

Figure 4.13: Direct infusion of purchased standard 4-HNE prepared in a solution of 0.1 % formic acid in acetonitrile with MS/MS collision induced dissociation of 35%, parent ion *m/z* 157 (>3 injections). Product ions of *m/z* 139.1, 121.1, 97.1, 81.1, 69.1 and 57.1 are observed.

The fragmentation pattern for the MS/MS by CID of the standard 4-HNE is shown in **Figure 4.13**. In addition to the water loss from *m/z* 157.2 resulting in *m/z* 139.1, further water loss is observed from this species forming *m/z* 121.1. The obtained spectra will serve as a reference against the spectra of the synthesised 4-HNE. The synthesised 4-HNE was directly infused into the ESI source using a syringe pump at a rate of 10 µL/min. The instrument was set to acquire full scan spectra over the range 108-200 *m/z*. The spectrum shown in **Figure 4.14** was obtained.

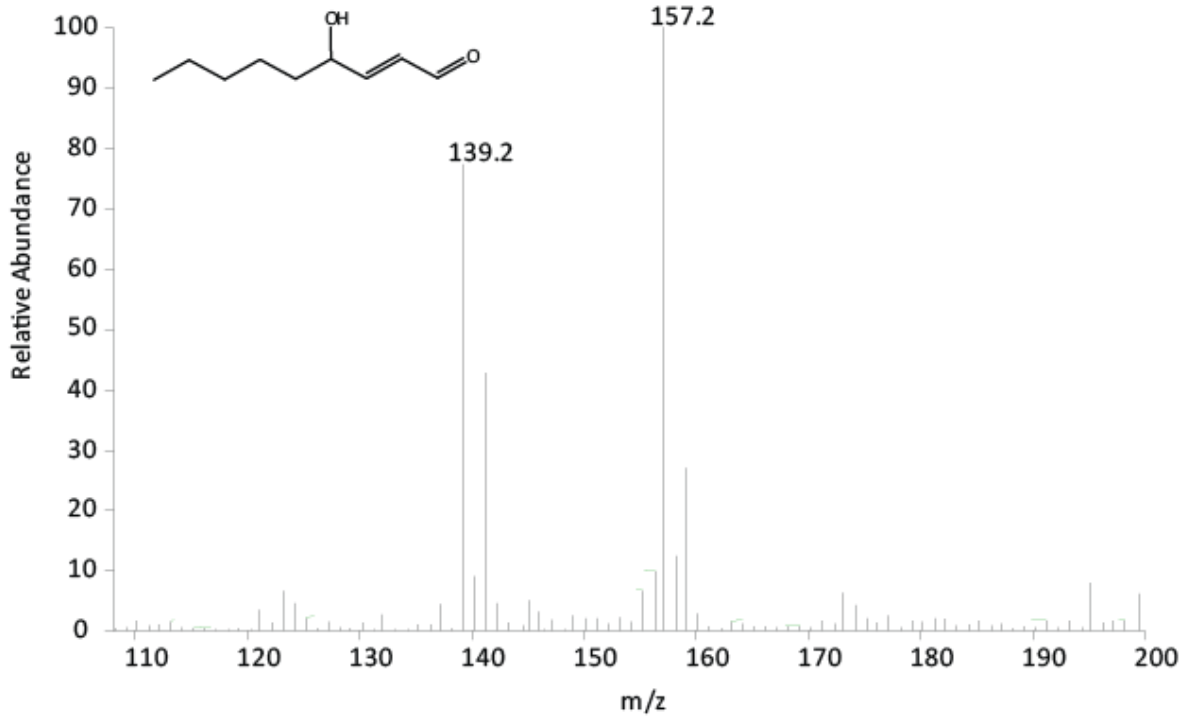

F**igure 4.14**: Direct infusion of synthesised 4-HNE prepared in a solution of 0.1 % formic acid in acetonitrile (>3 injections). Parent ion of *m/z* 157 can be seen as well as *m/z* 139.1 which constitutes the common loss of water.

The full MS spectrum for the synthesised 4-HNE shares great similarities with the full MS spectrum of the reference 4-HNE material. Both show the parent ion *m/z* 157 and the water loss resulting in *m/z* 139. Additional ions at 159.2 and 141.2 are also seen. The direct infusion was repeated for this sample with MS/MS performed using CID with a normalised collision energy of 35% over a mass range of *m/z* 50-200. Again, the spectrum for the MS/MS by CID of the reference material is identical to the spectrum obtained for the MS/MS by CID of the synthesised material, producing the same six ions; *m/z* 139.1, 121.1, 97.1, 81.1, 69.1 and 57.1 (**Figure 4.15**).

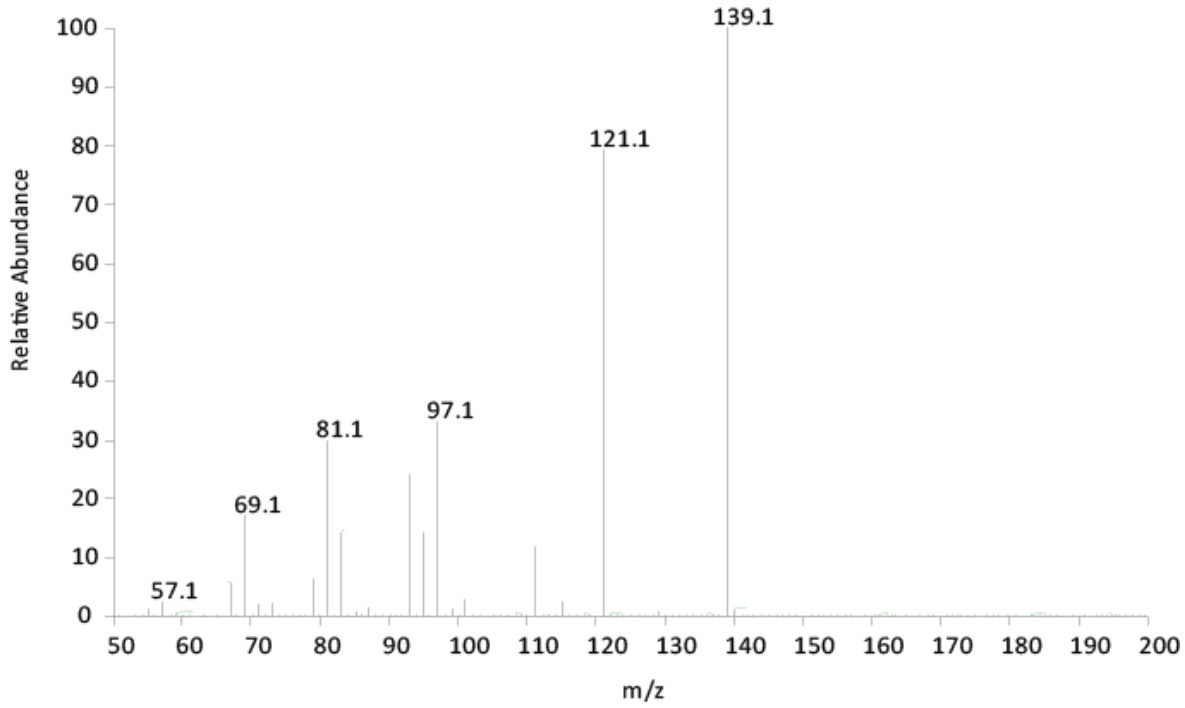

Figure 4.15: Direct infusion of synthesised 4-HNE prepared in a solution of 0.1 % formic acid in acetonitrile with MS/MS collision induced dissociation of 35%, parent ion *m/z* 157 (>3 injections). Product ions of *m/z* 139.1, 121.1, 97.1, 81.1, 69.1 and 57.1 are observed.

Following the direct infusion (MS full scan 100-200 *m/z*) of the synthesised sample prepared in methanol, as indicated by the reference paper (Gioacchini *et al*. 1999) an ion at *m/z* 171 was observed which corresponds to the addition of a methyl (CH_3^+) group as an adduct to the neutral 4-HNE molecule; specifically, the addition of a protonated methanol molecule to a neutral 4-HNE molecule followed by the loss of water (**Figure 4.16**). Methanol readily undergoes electrochemical oxidisation and is affected by the occurrence of electrochemical reactions taking place at the electrospray needle (Van Berkel *et al*. 1991). This is in contrast to the sample prepared in acetonitrile with an abundant ion at *m/z* 157 which corresponds to the 4-HNE molecule (**Figure 4.14**). This unfavourable adduct formation of the molecule in methanol confirms the preferred use of acetonitrile as the sample solvent for MS

analysis. This is of particular importance if quantitative analysis is to be performed as the degree of adduct formation is unknown.

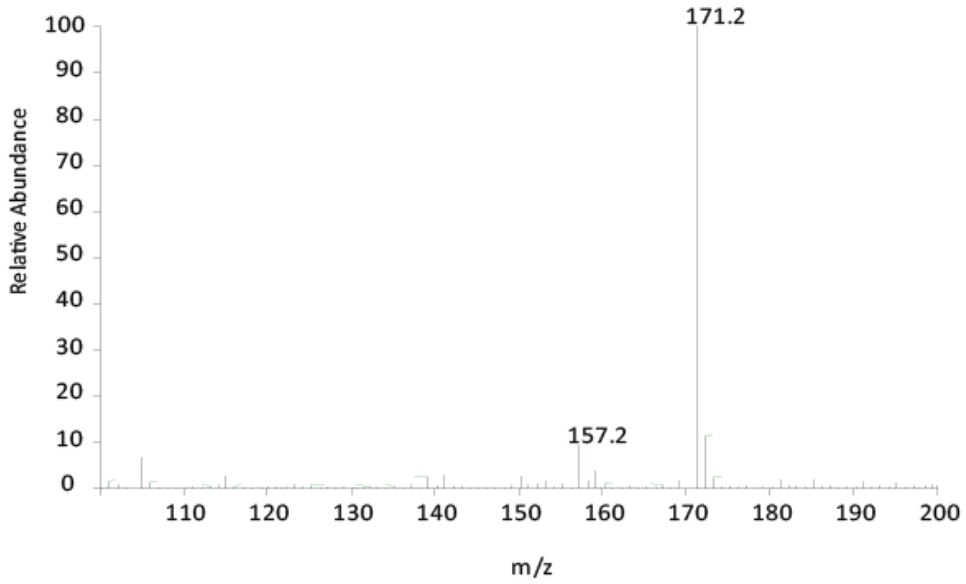

Figure 4.16: Direct infusion of synthesised 4-HNE prepared in a solution of 0.1 % formic acid in methanol (>3 injections). A dominant ion of *m/z* 171.2 due to methylation of the neutral 4-HNE molecule can be seen as well as the parent ion *m/z* 157.2.

4.3.1.3 Assessing the synthesis using Liquid Chromatography coupled with Mass Spectrometry

The previous spectra clearly demonstrate the similarities between the purchased standard 4-HNE and the synthesised 4-HNE. The introduction of the liquid chromatography sought to further characterise the compound to indicate the level of purity. **Figures 4.17** and **4.18** do not highlight any differences between the purchased and synthesised 4-HNE samples; the retention times are 4.26 and 4.29 minutes respectively with no other peaks present. Similarly, the MS and MS/MS CID spectra do not highlight any significant differences in the ions or fragmentation between the purchased and synthesised 4-HNE (**Figures 4.19** to **4.22**).

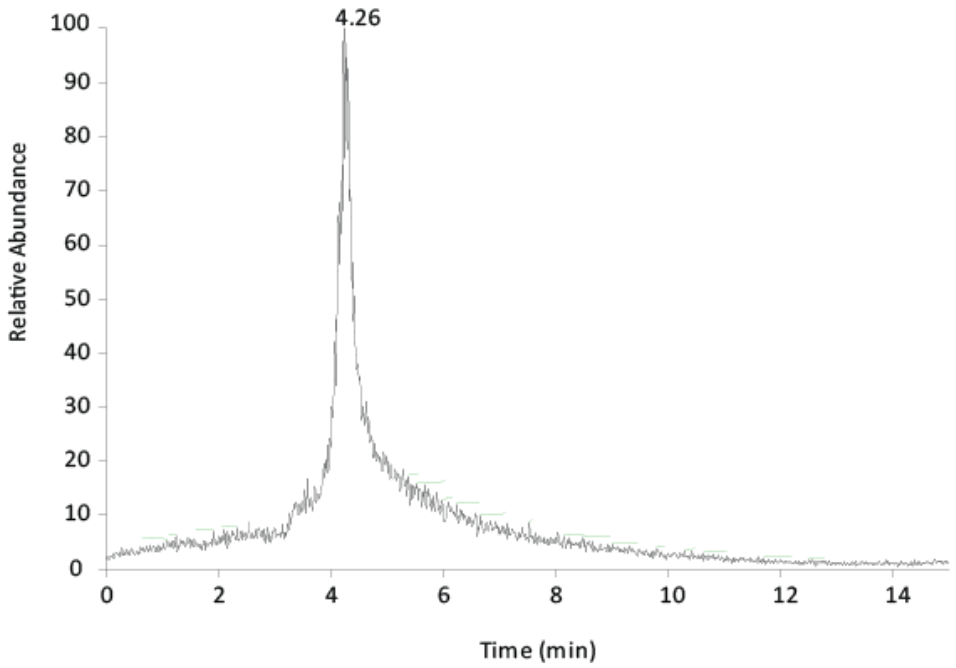

Figure 4.17: LC-MS separation of purchased standard 4-HNE prepared in a solution of 0.1 % formic acid in acetonitrile (>3 injections). A retention time was recorded of 4.26 mins.

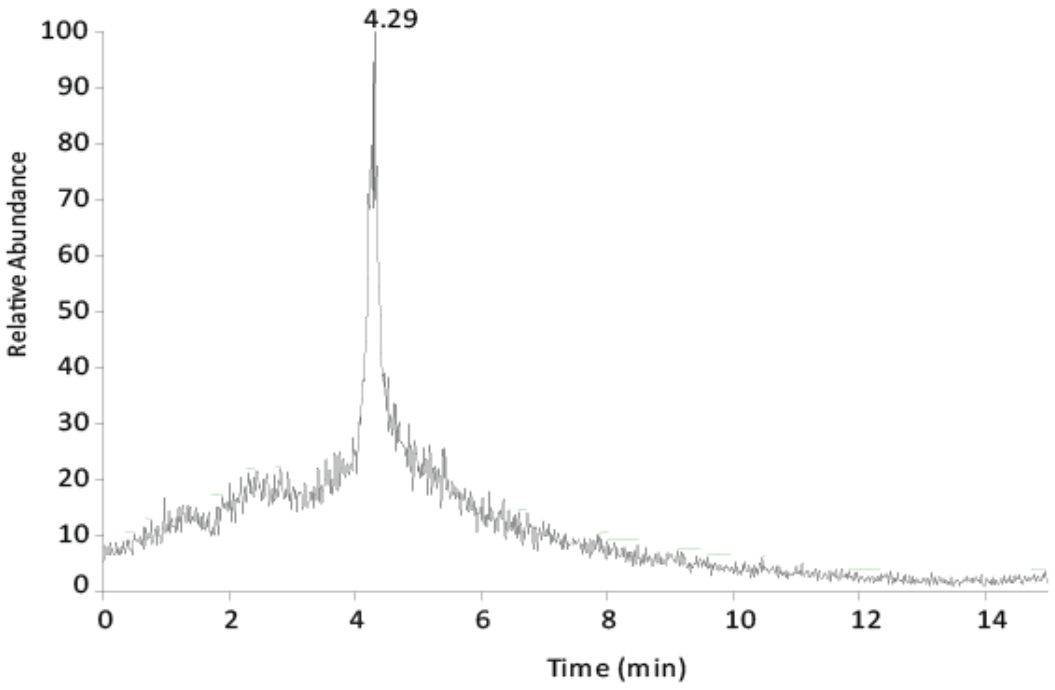

Figure 4.18: LC-MS separation of synthesised 4-HNE prepared in a solution of 0.1 % formic acid in acetonitrile (>3 injections). A retention time was recorded of 4.29 mins.

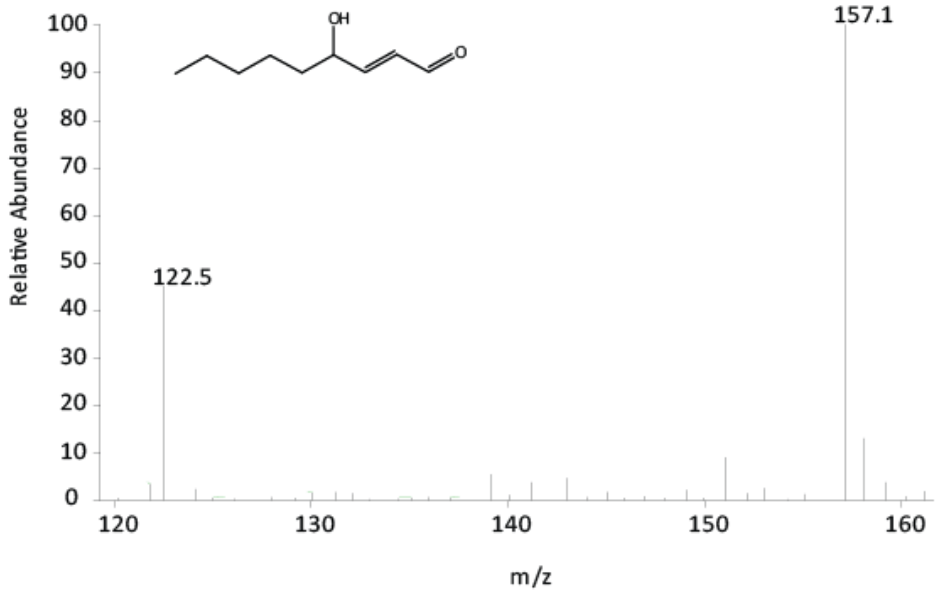

Figure 4.19: LC-MS separation of purchased standard 4-HNE prepared in a solution of 0.1 % formic acid in acetonitrile (>3 injections). Parent ion of *m/z* 157.1 can be seen as well as *m/z* 122.3. A retention time was recorded of 4.26 mins.

Figure 4.20: LC-MS separation of synthesised 4-HNE prepared in a solution of 0.1 % formic acid in acetonitrile (>3 injections). Parent ion of *m/z* 157.1 can be seen as well as *m/z* 122.3. A retention time was recorded of 4.29 mins.

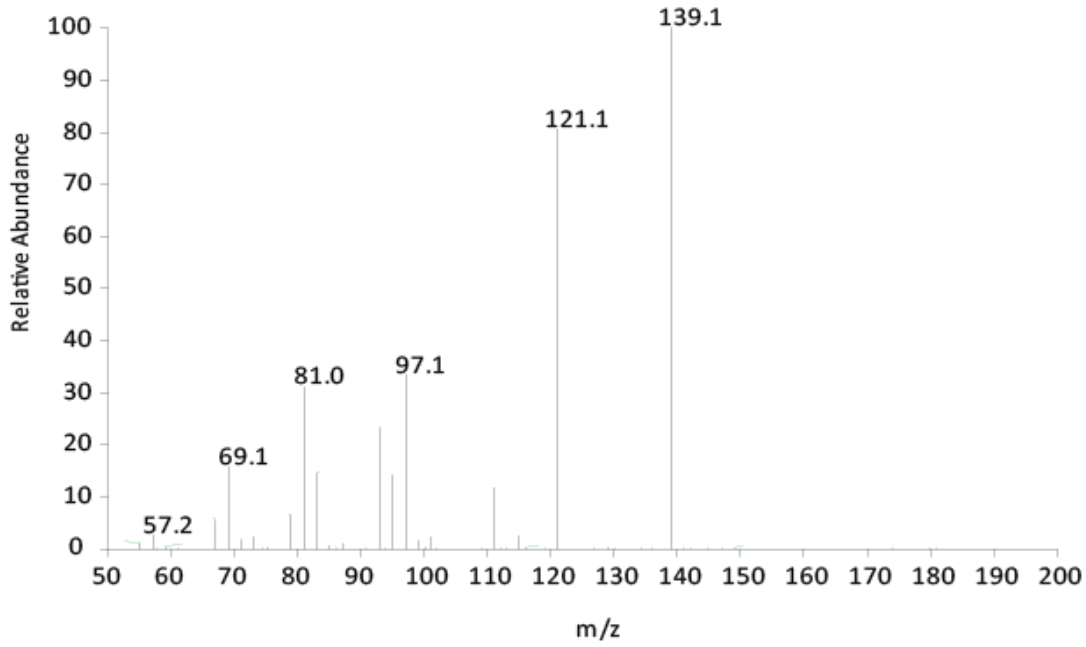

Figure 4.21: LC-MS separation of purchased standard 4-HNE prepared in a solution of 0.1 % formic acid in acetonitrile with MS/MS collision induced dissociation of 35%, parent ion *m/z* 157 (>3 injections). Product ions of *m/z* 139.1, 121.1, 97.1, 81.0, 69.1 and 57.2 are observed.

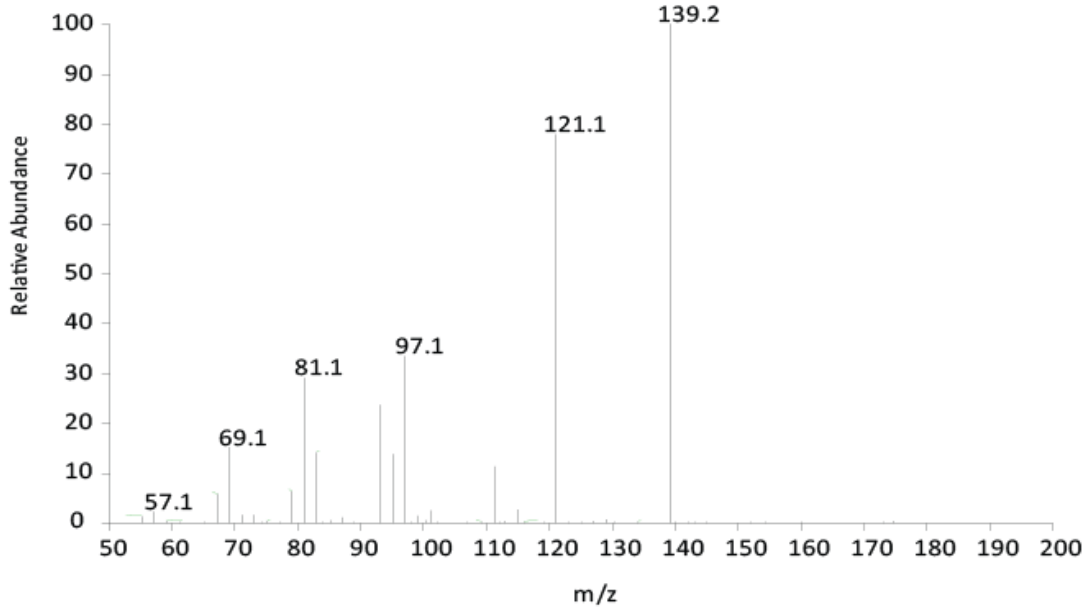

Figure 4.22: LC-MS separation of synthesised 4-HNE prepared in a solution of 0.1 % formic acid in acetonitrile with MS/MS collision induced dissociation of 35%, parent ion *m/z* 157 (>3 injections). Product ions of *m/z* 139.2, 121.1, 97.1, 81.1, 69.1 and 57.1 are observed.

In conclusion, the NMR, direct infusion MS and LC-MS/MS data of both the reference material 4-HNE and the synthesised material 4-HNE confirm the authenticity and therefore the successful synthesis of 4-hydroxy-2-nonenal. No significant impurities were noted and thus it can be concluded that a relatively pure compound was synthesised without the need to perform further fractional chromatographic purification.

4.3.2 Analysis of the 4-HNE-modified neurotensin

Preliminary experiments investigating the identification and quantification of 4-HNE adducts were performed with neurotensin as a simple model peptide. The average mass of neurotensin = 1672.92 and the average mass of 4-HNE = 156.22.

4.3.2.1 Analysis of the 4-HNE-modified neurotensin using mass spectrometry

The spectrum exhibited the dominant charge state of NT; a 3^+ charge state of *m/z* 558.8 and a 2^+ charge state of *m/z* 837.2. Given the increased intensity of the 558.8 ion, it was noted that this was the preferred charge state for the NT molecule (**Figure 4.23**). Using this value, the expected product ion (NT + 4-HNE) was calculated in order to create an appropriate tune file for its detection using mass spectrometry.

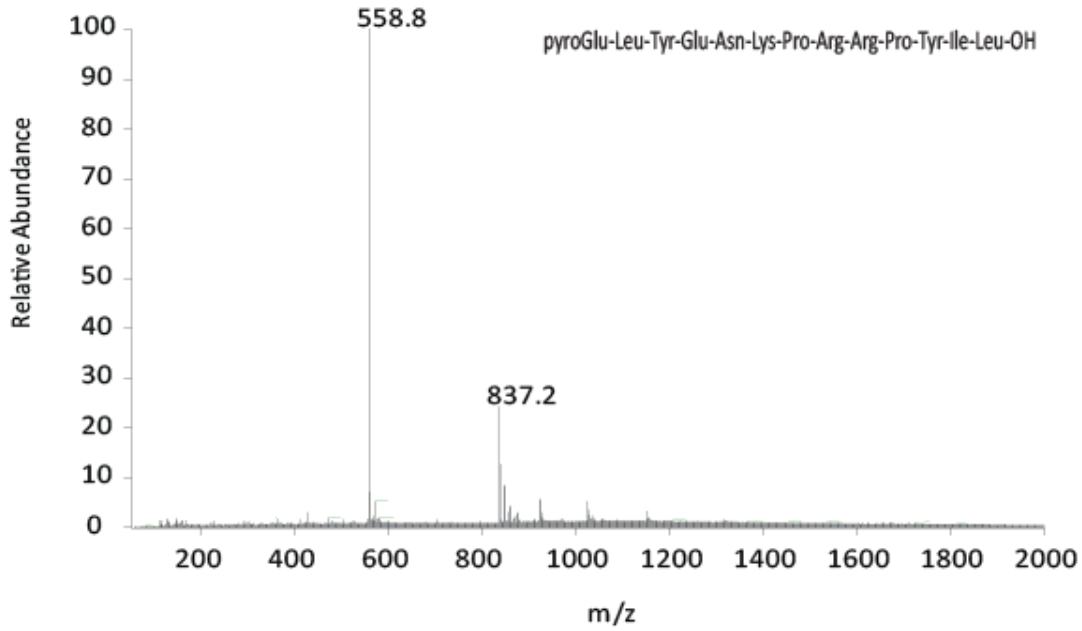

Figure 4.23: Direct infusion of neurotensin in a solution of 0.1 % formic acid in 50:50 H_2O:ACN (>3 injections). The dominant 3^+ charge state of *m/z* 558.8 can be seen as well as *m/z* 837.2 which constitutes the 2^+ charge state of the molecule.

The product ion for the 4-HNE-modified peptide was calculated as follows:

NT = 1672.92

+

4-HNE = 156.22

= 1829.14 combined

-1 (hydrogen) = 1828.14

+3 (3 protons) 1831.14

÷ 3 (3 charges) = *m/z* 610 i.e. $[M + 3H]^{3+}$

Following incubation of 4-HNE with neurotensin a 50-fold diluted sample was directly infused into the ESI source using a syringe pump at a rate of 10 µL/min. The instrument was set to acquire full scan spectra over the range *m/z* 50-2000 and the following spectrum was obtained (**Figure 4.24**).

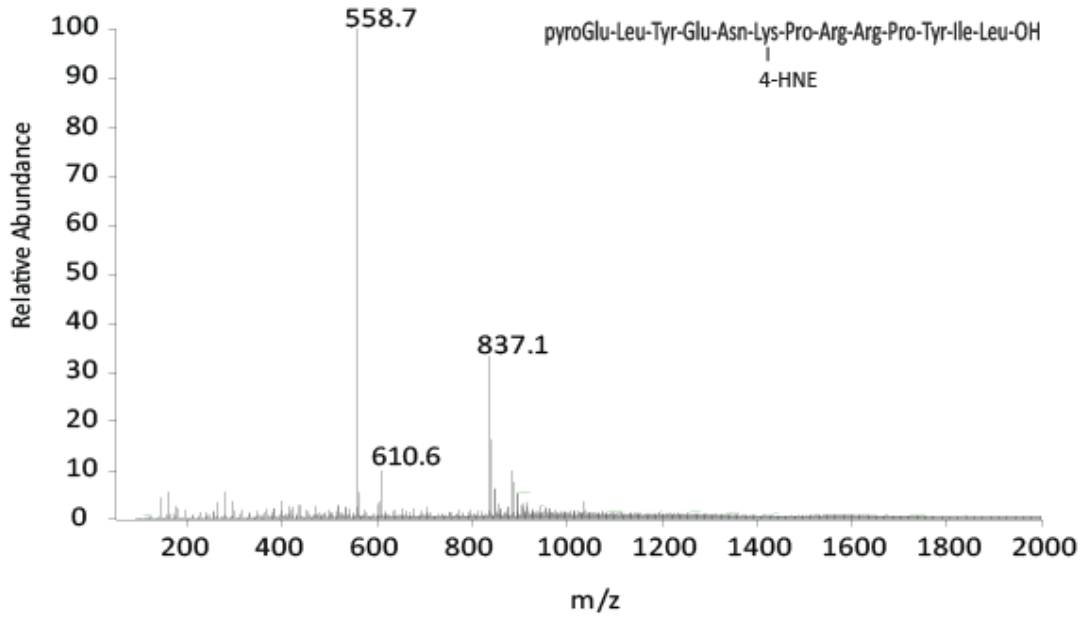

Figure 4.24: Direct infusion of 4-HNE-modified neurotensin prepared in a solution of 0.1 % formic acid in 50:50 H_2O:ACN (50x dilution, >3 injections). A strong ion of *m/z* 558.7 which reflects the 3^+ charge state of NT is observed along with *m/z* 837.1 reflecting the 2^+ charge state of NT. The product ion *m/z* 610.6 is also identified.

The product ion *m/z* 610.6 was observed in the sample. This product ion was further characterised by applying collision induced dissociation at a normalised collision energy of 35% to the direct infusion of the sample (MS/MS range of *m/z* 165-2000, parent ion *m/z* 610) which yielded a dominant ion of *m/z* 837. The *m/z* 837 ion is identified as the neurotensin-4-HNE adduct (NT 2^+ charge state) with the 4-HNE labile bond having been cleaved from the peptide, shown in **Figure 4.25**.

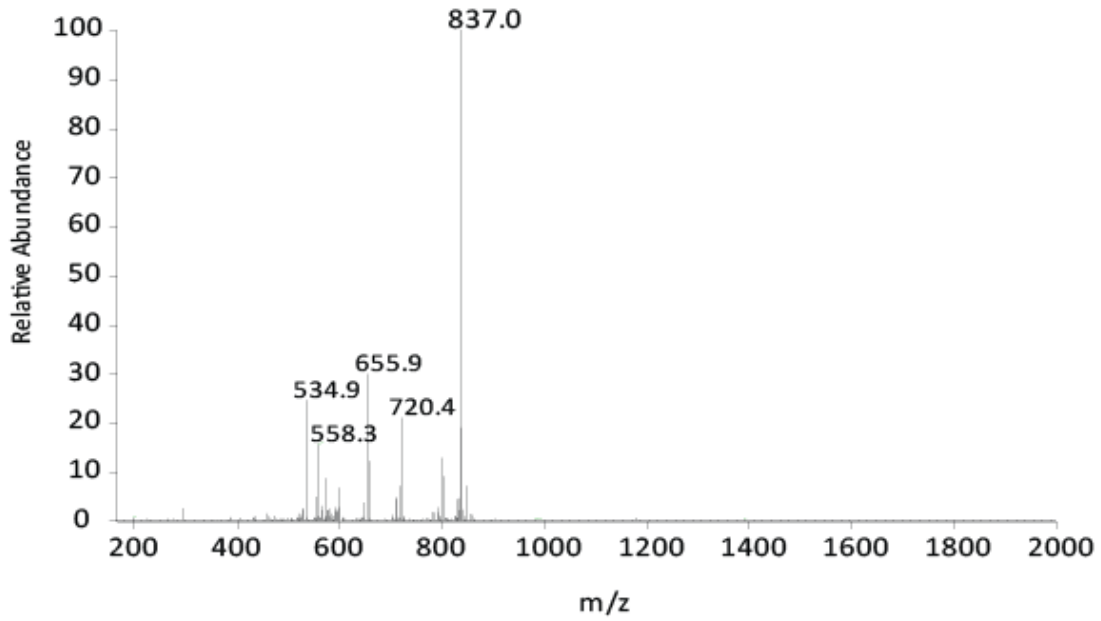

Figure 4.25: Direct infusion of 4-HNE-modified neurotensin prepared in a solution of 0.1 % formic acid in 50:50 H_2O:ACN (50x dilution) with MS/MS collision induced dissociation of 35%, parent ion *m/z* 610 (>3 injections). Product ions of *m/z* 837.0, 720.4, 655.9, 558.3 and 534.9 are observed.

4.3.2.2 Analysis of the 4-HNE-modified neurotensin by LC-MS/MS

The 5-fold dilution (4 µg/mL) of the 4-HNE-NT adduct sample (in 0.1 % formic acid with 50:50 H_2O:ACN) was analysed using LC-MS/MS. The 4-HNE M+H ion of *m/z* 157 was analysed utilising LC-MS/MS with collision induced dissociation at a normalised collision energy of 35% (**Figure 4.26**). The same was applied to the analysis of the NT 3^+ charge state of *m/z* 559 (**Figure 4.27**) and the NT-4-HNE^+ product ion *m/z* 610 (**Figure 4.28**).

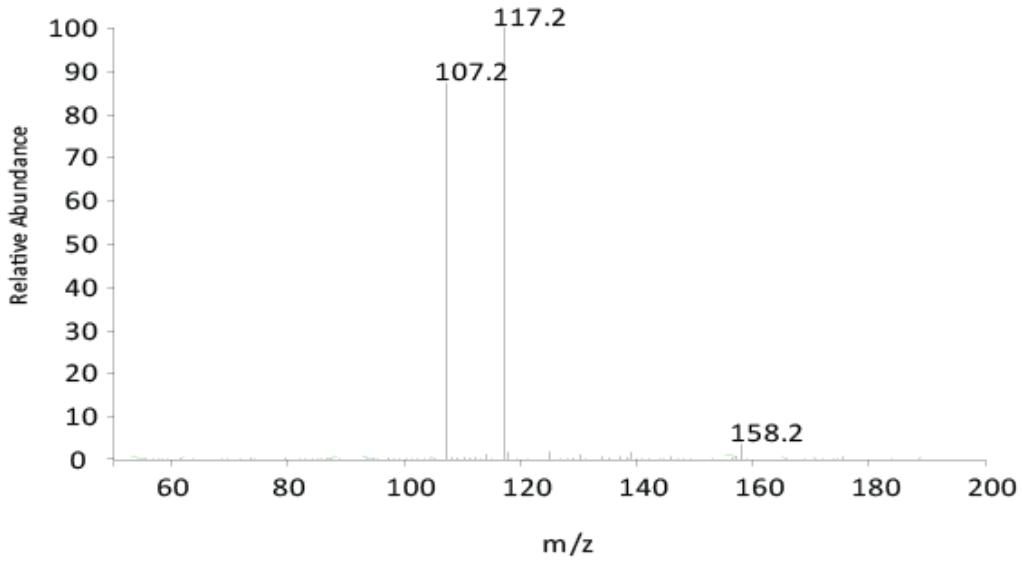

Figure 4.26: LC-MS separation of 4-HNE-modified neurotensin prepared in a solution of 0.1 % formic acid in 50:50 H_2O:ACN (5x dilution of original 50x dilution) with MS/MS collision induced dissociation of 35%, parent ion *m/z* 157 (>3 injections). Product ions of *m/z* 117.2, 107.2 and 158.2 are observed with a retention time of 1.40 mins.

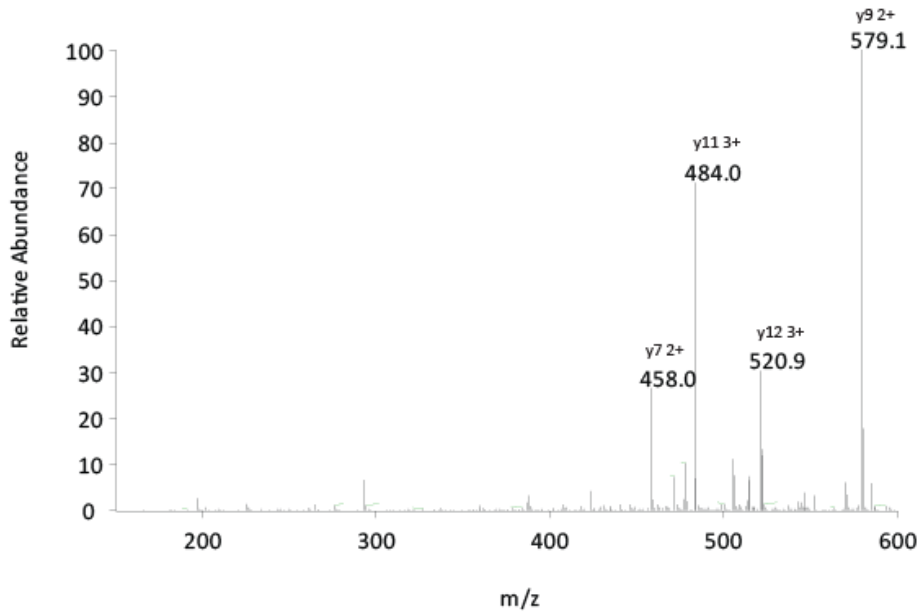

Figure 4.27: LC-MS separation of 4-HNE-modified neurotensin prepared in a solution of 0.1 % formic acid in 50:50 H_2O:ACN (5x dilution of original 50x dilution) with MS/MS collision induced dissociation of 35%, parent ion *m/z* 559 (>3 injections). Product ions of *m/z* 579.1, 520.9**,** 484.0 and 458.0 are observed with a retention time of 8.93 mins.

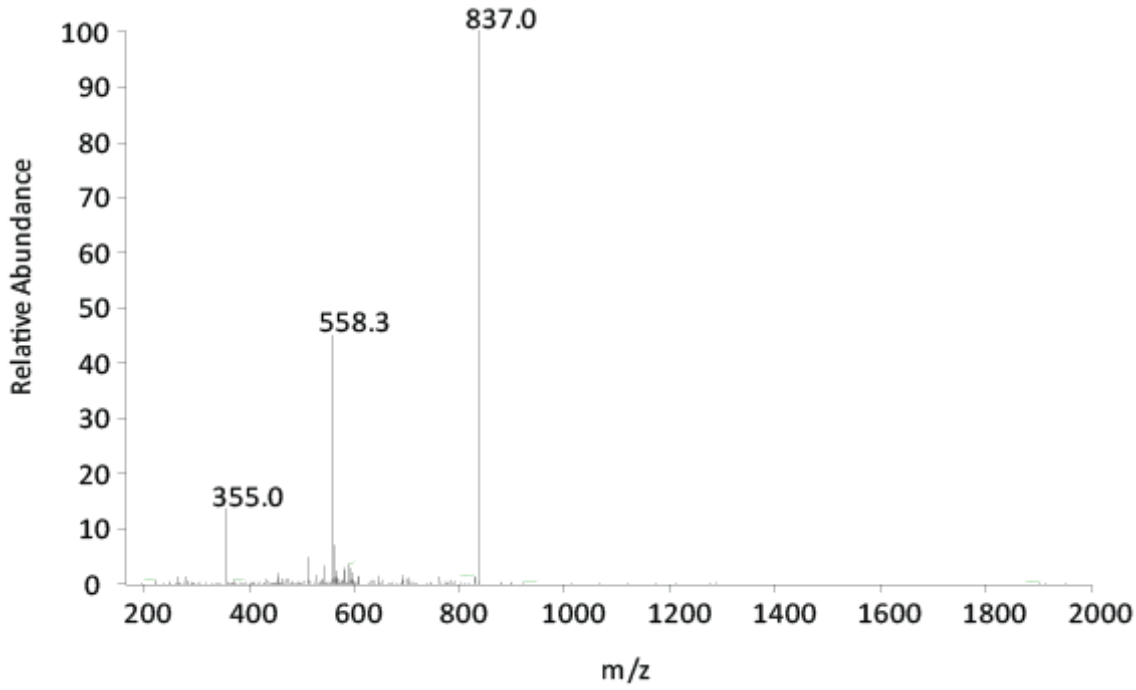

Figure 4.28: LC-MS separation of 4-HNE-modified neurotensin prepared in a solution of 0.1 % formic acid in 50:50 H_2O:ACN (5x dilution of original 50x dilution) with MS/MS collision induced dissociation of 35%, parent ion *m/z* 610 (>3 injections). Product ions of *m/z* 837.0, 558.3 and 355.0 are observed with a retention time of 10.56 mins.

A table was constructed (**Table 4.5**) containing the calculated y-ions for neurotensin which enabled the identification of the ions observed in **Figure 4.27**. The possible b-ions were also calculated, but the spectra did not exhibit any of these which indicate that the charge has been retained on the C-terminus of the peptide. The fragmentation process is influenced by the presence and position of basic amino acids within a peptide chain. Basic amino acids such as arginine, lysine, histidine and proline mainly induce the formation of y-ions when present and positioned near to the C-terminal side of the peptide (a fuller description of b- and y-ions is presented in **Appendix A1.1**).

Table 4.5: Calculated y-ions for neurotensin based upon the 1^+, 2^+ and 3^+ charge states.

y ion	Peptide sequence	Mass	1^+	2^+	3^+
y1	L-OH	130.2	131.2	66.6	44.7
y2	IL-OH	243.3	244.3	123.2	82.4
y3	YIL-OH	406.5	407.5	204.8	136.8
y4	PYIL-OH	503.6	504.6	253.3	169.2
y5	RPYIL-OH	659.8	660.8	331.4	221.3
y6	RRPYIL-OH	816.0	817.0	409.5	273.3
y7	PRRPYIL-OH	913.1	914.1	458.1	305.7
y8	KPRRPYIL-OH	1041.3	1042.3	522.2	348.4
y9	NKPRRPYIL-OH	1155.4	1156.4	579.2	386.5
y10	QNKPRRPYIL-OH	1283.5	1284.5	643.3	429.2
y11	YQNKPRRPYIL-OH	1446.7	1447.7	724.9	483.6
y12	LYQNKPRRPYIL-OH	1559.8	1560.8	781.4	521.3
y13	QLYQNKPRRPYIL-OH	1688.0	1689.0	845.5	564.0

The abundant ion *m/z* 837.0 was identified as the neurotensin-4-HNE adduct (NT 2^+ charge state) with the 4-HNE bond cleaved from the peptide. The second most abundant ion *m/z* 558.3 was also identified as the neurotensin-4-HNE adduct (NT 3^+ charge state), again with the 4-HNE bond cleaved. Collision induced dissociation induces ergodic processes where the commonly observed cleavages are of the weakest bonds of the precursor ions. For peptides, the lowest energy barrier to fragment is found in the backbone amide bond and so b- and y-ions are formed. In addition, post-translational modifications typically possess even lower energy barriers than those of backbone cleavages and as a result, they are also cleaved (see **Appendix A1.2**). This results in a loss of information with regard to the site of post-translational modification. For unequivocal identification of the adduct, it is necessary to preserve the labile 4-HNE bond and maintain its integrity with the peptide backbone.

4.3.2.3 Preservation of the adducted site utilising Electron Transfer Dissociation

4-HNE forms a labile bond with the lysine residue of the neurotensin and as such, the bond is easily broken upon the use of collision induced dissociation (CID). Although CID-generated spectra offer sufficient data for the determination of peptide sequences (forming b- and y- fragment ions), for proteins that have undergone a post translational modification, the weakly bound modification is preferentially cleaved from the peptide backbone during the high-energy collision event. This cleavage limits the structural identification of the peptide and the site of modification.

In order to effectively preserve the site of post translational modification of the peptide by 4-HNE, an alternative form of ion activation can be used called electron transfer dissociation (ETD). The Thermo LTQ-MS system used in this chapter has an ETD module attached that can ensure such preservation of the labile bond. In principle, the ions entering the ETD become subject to the transfer of an electron to the peptide ion via an ion-ion reaction (by reagent gas anions and gas phase ion/ion chemistry). This reaction results in the formation of singly charged radical anions which transfer a single electron to peptides that are multiply protonated. The peptide backbone is then fragmented in a sequence-independent manner; the fragmentation is independent of the bond-dissociation energy, forming c- and z- fragment ions with modifications remaining intact with the peptide chain. Direct infusions of the 50 fold dilution (20 μg/mL) of NT-4-HNE adduct sample were carried out with MS/MS ETD with an activation energy of 500ms. MS/MS ETD of the precursor ions *m/z* 559 and 610 displayed the following (**Figures 4.29** and **4.30**).

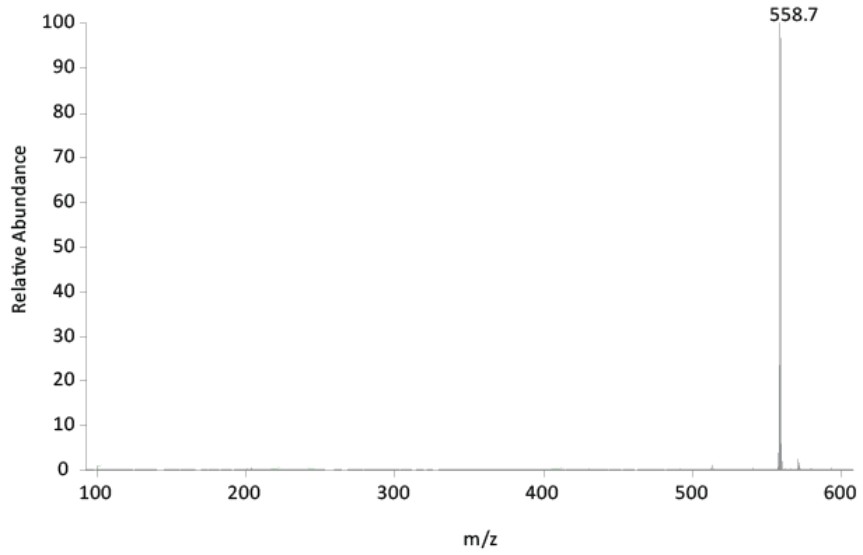

Figure 4.29: Direct infusion of 4-HNE-modified neurotensin prepared in a solution of 0.1 % formic acid in 50:50 H_2O:ACN (50x dilution) with MS/MS electron transfer dissociation of 500ms, parent ion *m/*z 559 (>3 injections). A product ion of *m/z* 558.7 is observed.

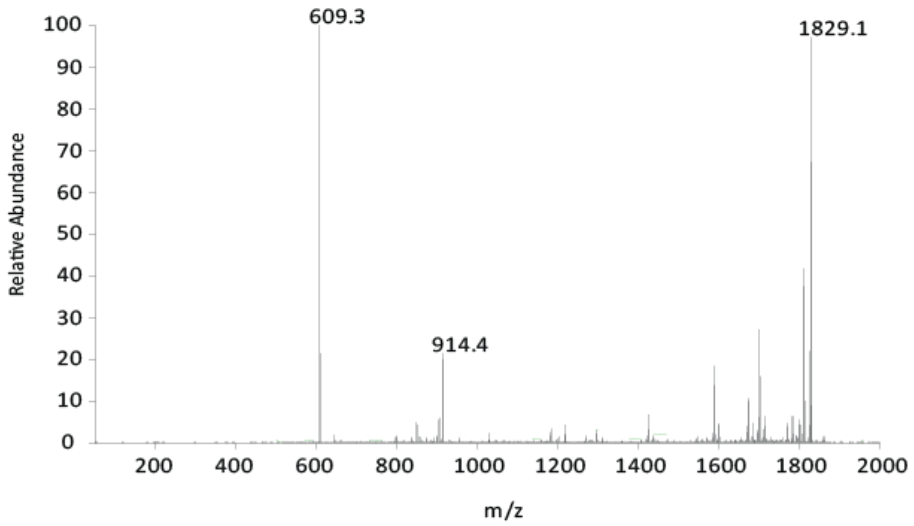

Figure 4.30: Direct infusion of 4-HNE-modified neurotensin prepared in a solution of 0.1 % formic acid in 50:50 H_2O:ACN (50x dilution) with MS/MS electron transfer dissociation of 500ms, parent ion *m/*z 610 (>3 injections). Product ions of *m/z* 1829.1, 914.4 and 609.3 are observed.

Three abundant ions of *m/z* 1829.1, 914.4 and 609.3 are of particular interest. Calculations were performed to identify these ions; *m/z* 1829.1 was identified as the m + H ion of the NT-4-HNE adduct, *m/z* 914.4 was identified as the adduct 2^+ charge state and *m/z* 609.3 was identified as the adduct 3^+ charge state. The 4-HNE bond remains intact for each of these ions therefore confirming the preservation of the adducted site.

The 5-fold dilution (4 µg/mL) of the 4-HNE-NT adduct sample (in 0.1 % formic acid with 50:50 H_2O:ACN) was further analysed using LC-MS/MS ETD. These chromatographic separations were exposed to a lower ETD activation energy of 100ms as an experimental measure to observe any differences in the fragmentation patterns. It was determined that an activation energy of 100ms was too low to induce appropriate fragmentation of the *m/z* 610 ion (**Figure 4.32**) and that 500ms (**Figure 4.30**) resulted in a more informative, conclusive fragmentation. However, for complex matrices a lower ETD energy is desirable given the very high number of ions that are yielded.

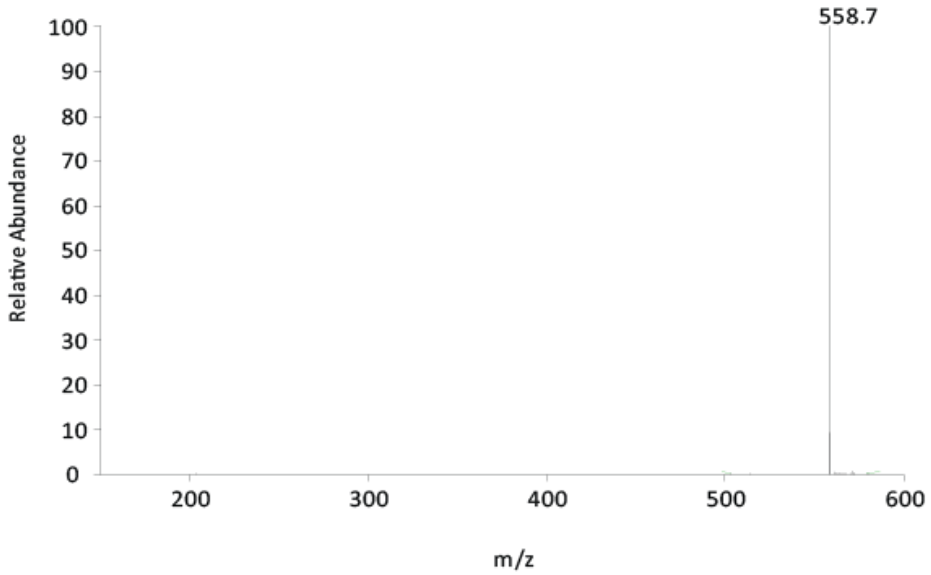

Figure 4.31: LC-MS separation of 4-HNE-modified neurotensin prepared in a solution of 0.1 % formic acid in 50:50 H_2O:ACN (5x dilution of original 50x dilution) with MS/MS electron transfer dissociation of 100ms, parent ion *m/*z 559 (>3 injections). Product ion of *m/z* 558.7 is observed with a retention time of 9.07 mins.

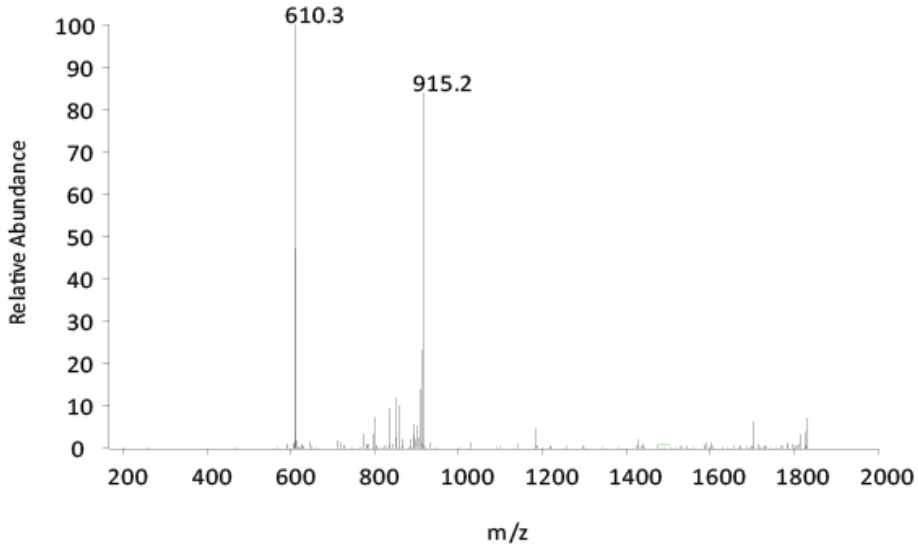

Figure 4.32: LC-MS separation of 4-HNE-modified neurotensin prepared in a solution of 0.1 % formic acid in 50:50 H_2O:ACN (5x dilution of original 50x dilution) with MS/MS electron transfer dissociation of 100ms, parent ion *m/*z 610 (>3 injections). Product ions of *m/z* 610.3 and 915.2 are observed with a retention time of 10.73 mins.

4.3.2.4 Determining the peptide-4-HNE adduct reaction completion time

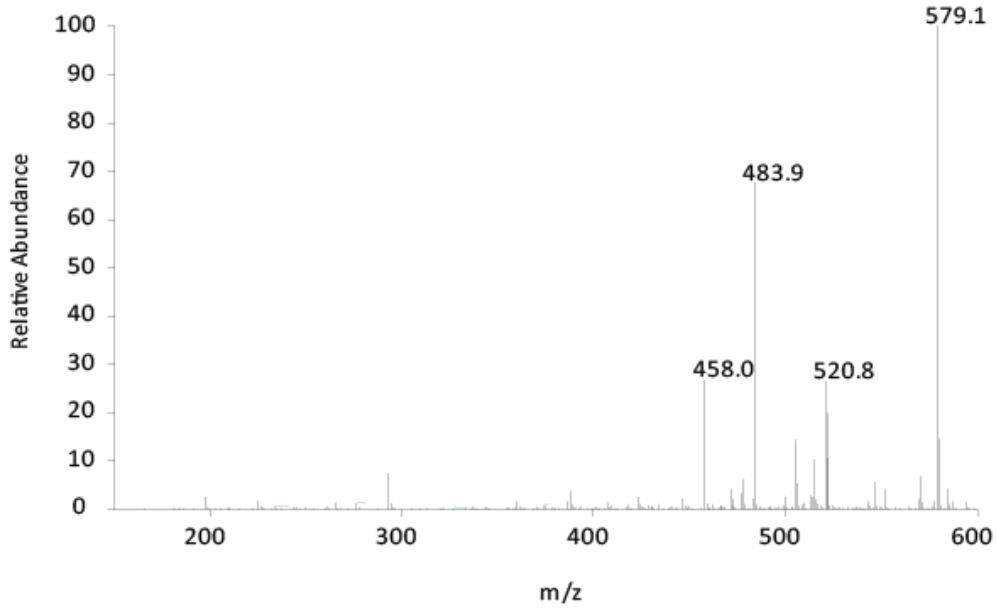

Figure 4.33: LC-MS separation of D_3-4-HNE-modified neurotensin with MS/MS collision induced dissociation of 35%, parent ion *m/*z 559 (>3 injections). Product ions of *m/z* 579.1, 520.8, 483.9 and 458.0 are observed with a retention time of 8.19 mins.

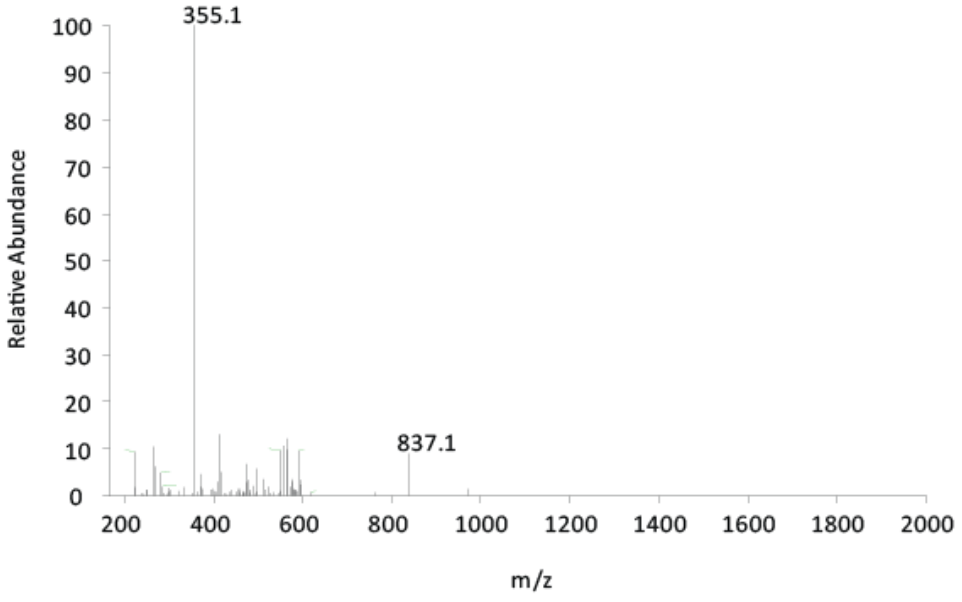

Figure 4.34: LC-MS separation of D_3-4-HNE-modified neurotensin with MS/MS collision induced dissociation of 35%, parent ion *m/*z 611 (>3 injections). Product ions of *m/z* 837.1 and 355.1 are observed with a retention time of 9.94 mins.

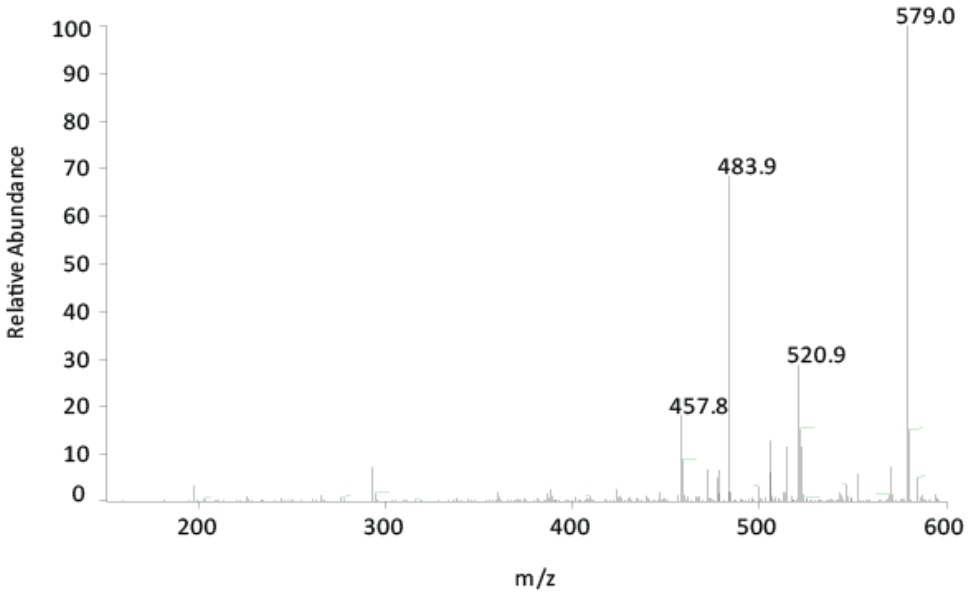

Figure 4.35: LC-MS separation of 4-HNE-modified neurotensin with MS/MS collision induced dissociation of 35%, parent ion *m/z* 559 (>3 injections). Product ions of *m/z* 579.0, 520.9, 483.9 and 457.8 are observed with a retention time of 8.20 mins.

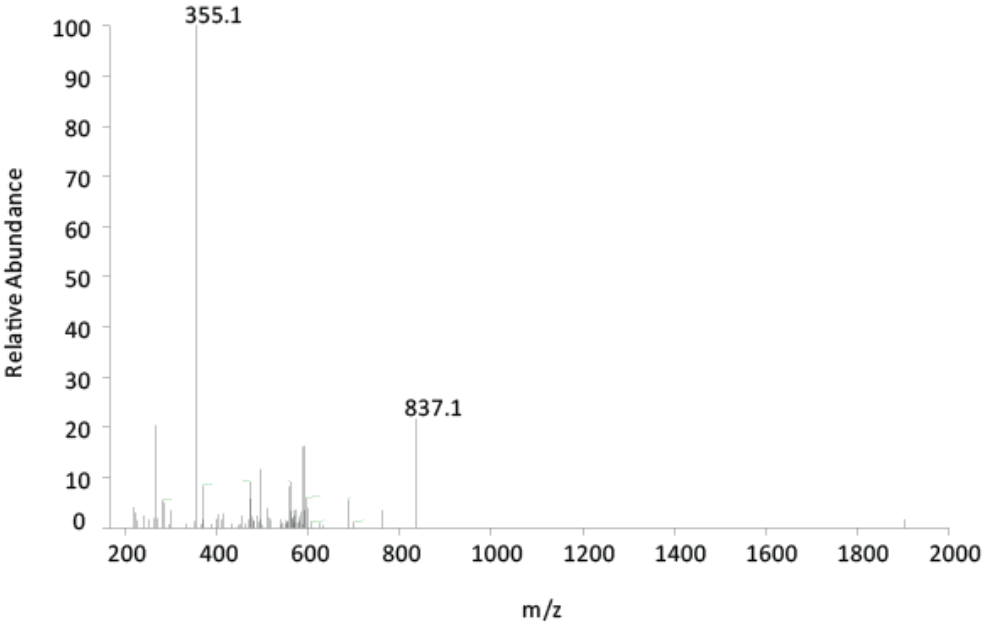

Figure 4.36: LC-MS separation of 4-HNE-modified neurotensin with MS/MS collision induced dissociation of 35%, parent ion *m/z* 610 (>3 injections). Product ions of *m/z* 837.1 and 355.1 are observed with a retention time of 9.91 mins.

There were no significant differences between the spectra for the variable timed incubation reactions of 2, 4 and 6 hours respectively. A general decrease in peak intensity was observed for the deuterated adducts when compared to the undeuterated adducts which may be due in part to ion suppression (**Figures 4.33-4.36**). However, as peak intensities did not increase for ions of interest in direct correlation with an increase in incubation time, it was concluded that the reaction had reached completion within 2 hours.

Analyses of varying peptide concentrations to a constant concentration of deuterated or undeuterated 4-HNE were conducted to explore the differences, if any, between the intensities of the peaks. Given the conclusive results that the incubation reaches completion at 2 hours, this incubation time was used to form the adducts. The calibration curves were calculated using the median values of the peak areas and heights of the relevant ion (*m/z* 610 or 611) taken from multiple injections (>3) and are shown below (**Figures 4.37**- **4.40**).

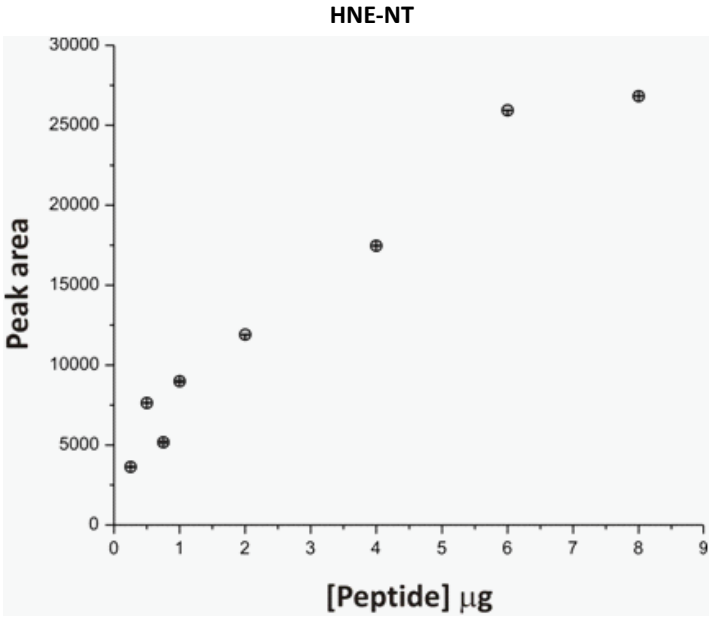

Figure 4.37: Calibration curve of the 4-HNE-NT adduct *m/z* 610 ion (peak area vs. concentration in μg).

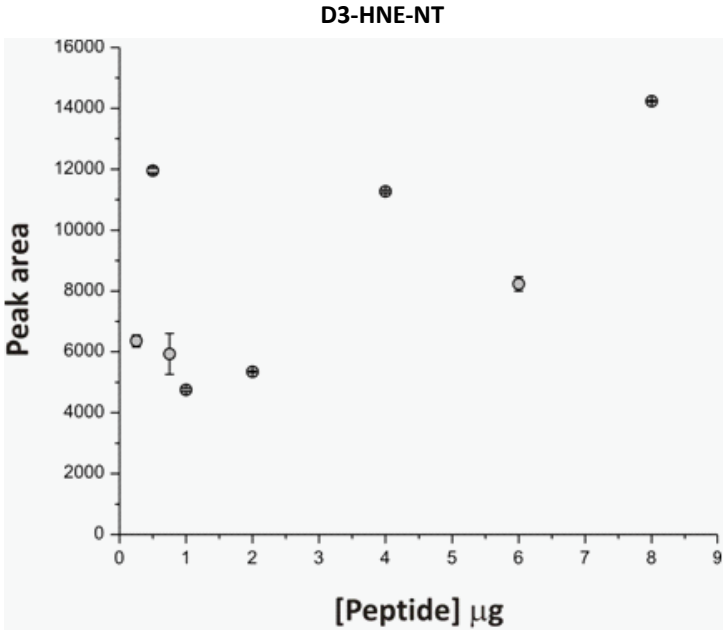

Figure 4.38: Calibration curve of the deuterated-4-HNE-NT adduct *m/z* 611 ion (peak area vs. concentration in μg).

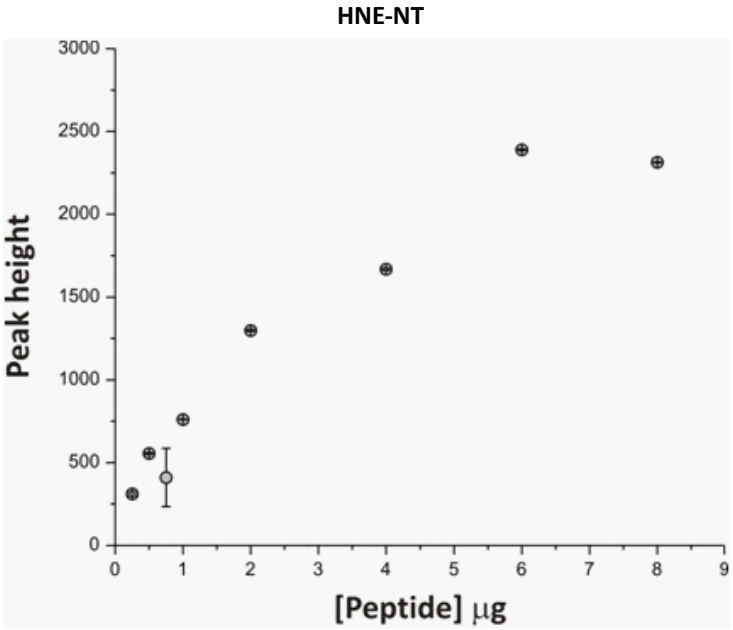

Figure 4.39: Calibration curve of the 4-HNE-NT adduct *m/z* 610 ion (peak height vs. concentration in μg).

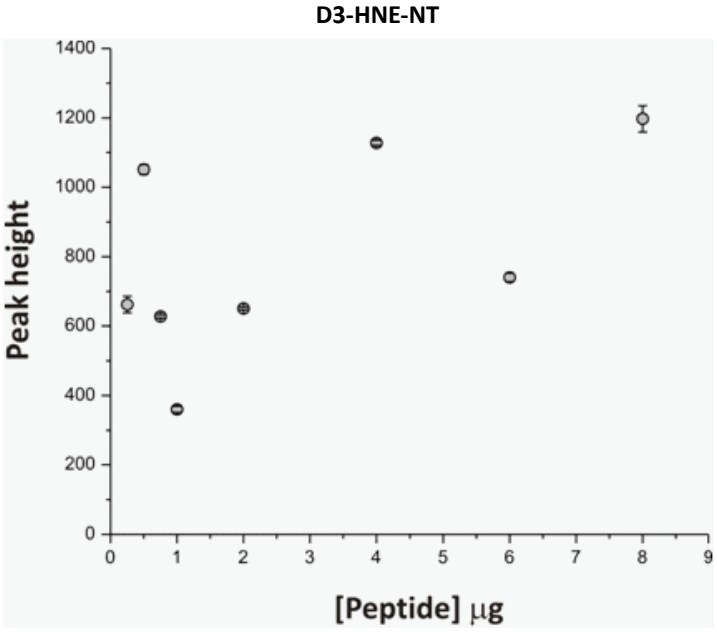

Figure 4.40: Calibration curve of the deuterated-4-HNE-NT adduct *m/z* 611 ion (peak height vs. concentration in μg).

The calibration curves for the 4-HNE-NT show a plateau effect at 6-8 µg of peptide (to a constant of 50 ng 4-HNE). This may indicate that there is no longer any residual 4-HNE available to form a conjugate with the peptide. If 8 µg is taken as the maximum amount of peptide needed to conjugate with the 4-HNE in its entirety leaving no residual 4-HNE, this equates to 5 nM of peptide to 0.03 nM of 4-HNE; 16.6 times the concentration of peptide to 4-HNE.

A great variability was observed in the calibration curves for the deuterated 4-HNE-NT; whilst the general curve is similar to that of the 4-HNE, the data lack consistency in both the peak areas and heights. In some instances, a 2-fold decrease is seen for the deuterated 4-HNE to the undeuterated 4-HNE but this was not demonstrated consistently across the concentration range. The median values taken from multiple injections (>3) of the standards for both the peak area and height are presented in **Tables 4.6** and **4.7**. The peak heights were measured as the intensity of signal from the detector (in this case a dynode) and as such, are taken as "counts". The peak area does not have a defined unit.

Table 4.6: Calibration data for 4-HNE-NT conjugates.

Neurotensin (ug)	HNE (ng)	Peak area	Peak height	Ion intensity
0.25	50	3638	312	3.18 E2
0.5	50	7639	555	5.55 E2
0.75	50	5180	410	4.13 E2
1	50	8987	761	7.62 E2
2	50	11908	1298	1.30 E3
4	50	17474	1668	1.67 E3
6	50	25939	2389	2.39 E3
8	50	26827	2313	2.31 E3

Table 4.7: Calibration data for the d_3-4-HNE-NT conjugates.

Neurotensin (ug)	d_3-HNE (ng)	Peak area	Peak height	Ion intensity
0.25	50	6359	662	6.34 E2
0.5	50	11957	1051	1.06 E3
0.75	50	5932	628	6.40 E2
1	50	4752	360	3.60 E2
2	50	5348	651	6.51 E2
4	50	11273	1128	1.13 E3
6	50	8231	740	7.44 E2
8	50	14236	1197	1.20 E3

A possible explanation for this variability is that a limiting effect is observed on the dynamic range of ion traps. When there are too many ions present in the trap, space-charge effects result in the diminished performance of the ion-trap analyzer. As a workaround solution, the use of automated scans allows the rapid counting of ions before they enter the trap, therefore limiting the number of ions gaining entry. Automatic gain control (AGC) allows the use of applied voltage amplitude to control the transmission of ions. However, given that the analysis is dynamic and the window of ions at a given time becomes a moving target, this limitation of ion entry results in an inconsistent number of ions entering the ion-trap consequently resulting in variable data. To overcome the variability observed in the analysis of the internal standards, it would be beneficial to analyse them using a triple quadrupole instrument. The fragmentation process of quadrupole instruments differs from that of linear ion-traps. The absence of any consistent measurable ratios between the deuterated and undeuterated 4-HNE may be explained further by the differences in electronegativity between the two compounds. Whilst CID at a normalised energy of 35% was sufficient to fragment the undeuterated 4-HNE adducts, the stronger covalent bonds of the deuterated 4-HNE adducts may require a higher CID energy to obtain reproducible

fragmentation. However, the deuterated compound was to be used as an internal standard against which endogenous 4-HNE adducts could be measured; hence if the CID energy is increased in order to reproducibly fragment the internal standard, this would lead to the sub-optimal fragmentation of the endogenous markers. The use of a triple quadrupole instrument would allow the circumvention of this inherent issue and facilitate the quantification of the endogenous modifications without compromising their fragmentation.

4.3.2.5 Analysis of the 4-HNE-modified peptides using mass spectrometry

As modification by 4-HNE of the lysine residue had been demonstrated in the short-chain peptide neurotensin, it was necessary to demonstrate this could also occur in an alternative short-chain peptide with more than one binding site and so angiotensin was used due to the two histidine residues within its sequence. Histidine is another of the targeted amino acid residues as described previously in section *4.2.2.7*. The average mass of angiotensin = 1296.48, neurotensin = 1672.92 and the average mass of 4-HNE = 156.22.

A 50 fold dilution (20 µg/mL) was prepared from the original solution of AT-4-HNE (in 0.1 % formic acid with 50:50 H_2O:ACN). Direct infusions of this sample produced the following representative spectra (**Figure 4.41**). In addition, a mixture of both angiotensin and neurotensin was also incubated with 4-HNE to show the presence of both adducts within one solution (**Figure 4.42**).

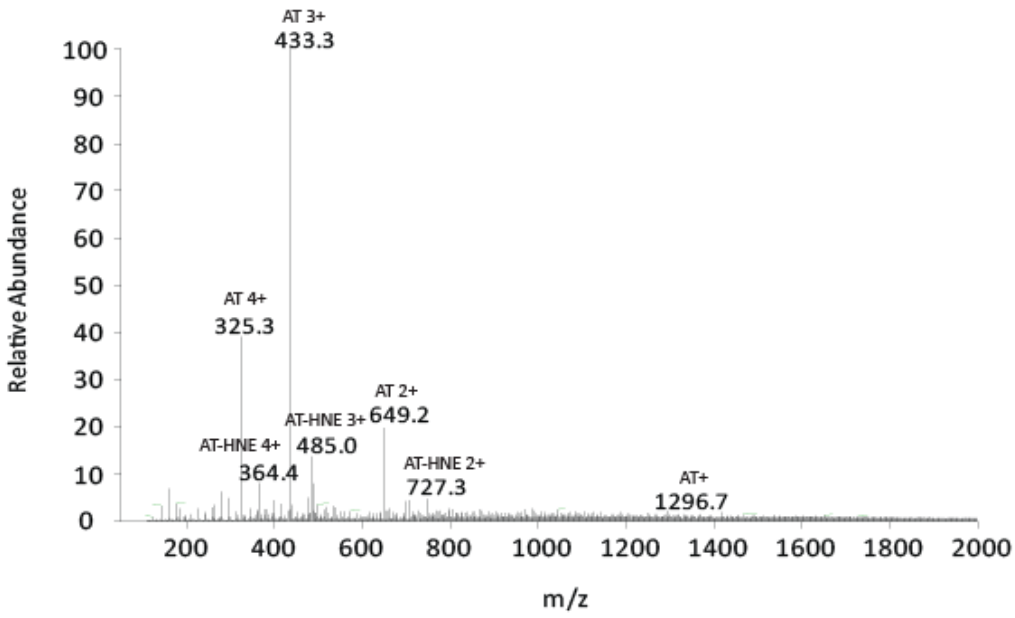

Figure 4.41: Direct infusion of 4-HNE-modified angiotensin prepared in a solution of 0.1 % formic acid in 50:50 H_2O:ACN (50x dilution) with full MS 50-2000 (>3 injections). Product ions of *m/z* 433.3, 485.0, 364.4, 325.3, 649.2, 727.3 and 1296.7 were observed.

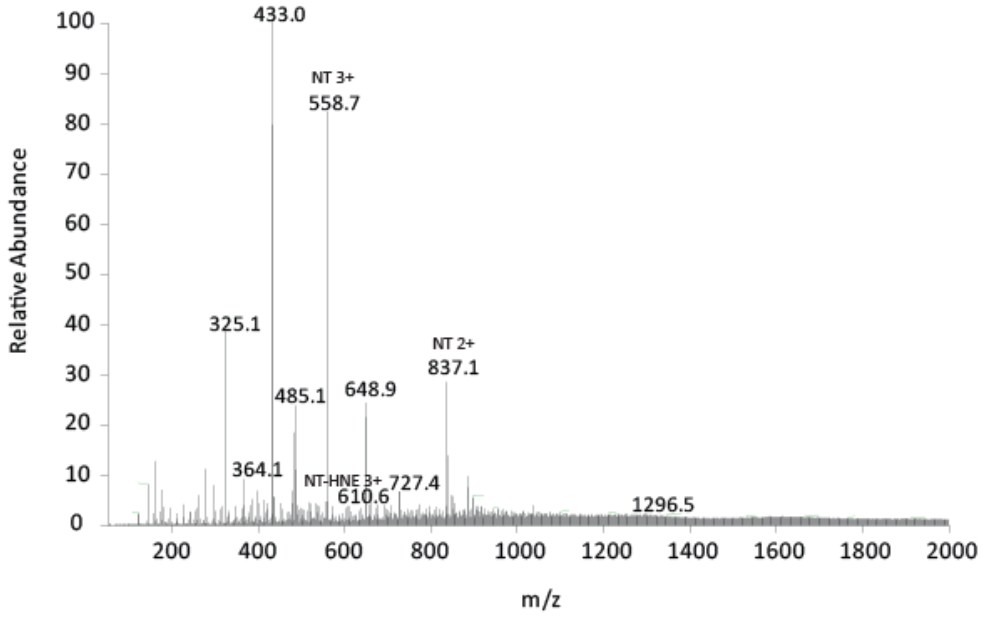

Figure 4.42: Direct infusion of 4-HNE-modified angiotensin and neurotensin prepared in a solution of 0.1 % formic acid in 50:50 H_2O:ACN (50x dilution) with full MS 50-2000 (>3 injections). Additional ions of *m/z* 558.7, 837.1 and 610.6 are observed.

These spectra exhibit the dominant charge states of AT; a 3^+ charge state of *m/z* 433.0, a 4^+ charge state of *m/z* 325.0 and a 2^+ charge state of *m/z* 648.9. Given the increased intensity of the *m/z* 433.0 ion, it was noted that this was the dominant charge state for the AT molecule. From these values, the expected product ions were calculated as; $(AT\text{-}4\text{-}HNE)^{2+}$ =727, $(AT\text{-}4\text{-}HNE)^{3+}$ = 485 and $(AT\text{-}4\text{-}HNE)^{4+}$ = 363. The AT-NT-4-HNE mixed solution gave an additional three ions of *m/z* 558.7 and *m/z* 837.1 (which are characteristic of the NT 3^+ and 2^+ charge states respectively) and an *m/z* 610.6 ion which has been identified as the NT-4-HNE 3^+ product ion (figure 4.41). One can assume that the labile bond has been cleaved in the case of NT (a neutral loss of 156). The AT-4-HNE conjugate was further characterised in both its cleaved and preserved states through direct infusion analyses of the sample carrying out both MS/MS CID at a normalised collision energy of 35 and MS/MS ETD 500ms on the AT-4-HNE^{2+} (727) ion (**Figures 4.43-4.44**).

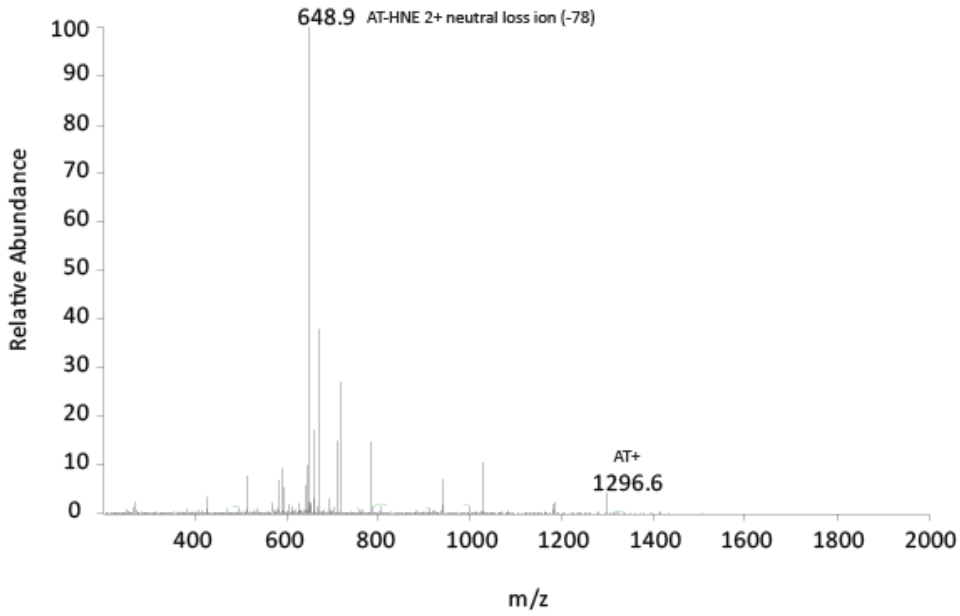

Figure 4.43: Direct infusion of 4-HNE-modified angiotensin prepared in a solution of 0.1 % formic acid in 50:50 H_2O:ACN (50x dilution) with MS/MS collision induced dissociation of 35%, parent ion *m/z* 727 (>3 injections). Product ions of *m/z* 648.9 and 1296.6 are observed.

Figure 4.43 shows the neutral loss ion *m/z* 648.9 (identified as the AT-HNE 2+ ion) which has undergone a neutral loss of *m/z* 78, equivalent to a doubly-charged 4-HNE molecule. In addition, the angiotensin singly-protonated molecule ion was seen at *m/z* 1296.6. Upon the activation of ETD, the neutral loss no longer occurs and the labile 4-HNE bond remains intact as demonstrated in **Figure 4.44** by ions *m/z* 726.7 and 1453.5.

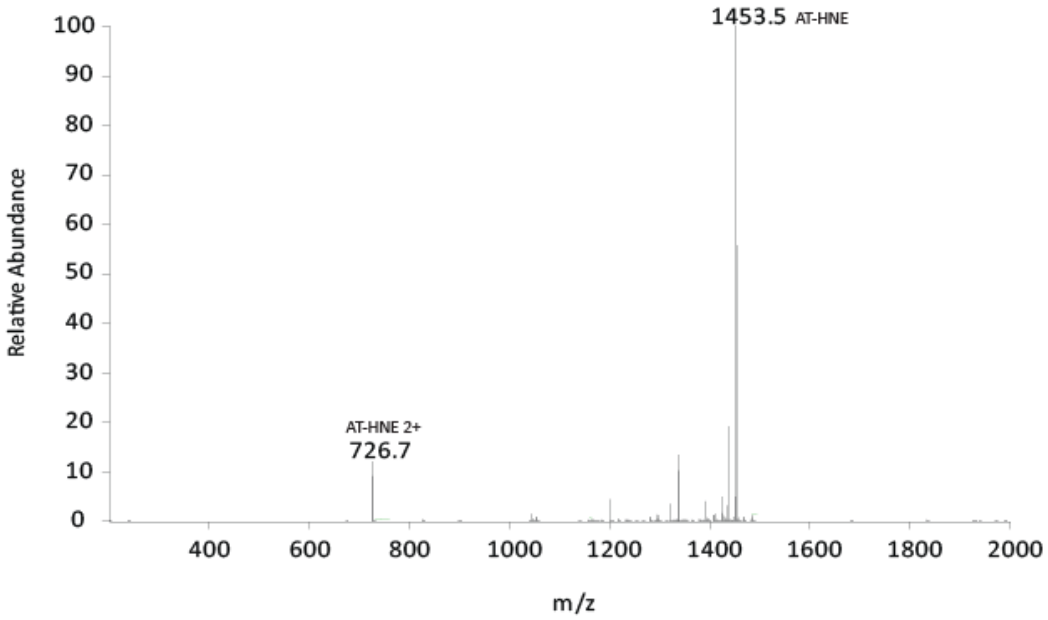

Figure 4.44: Direct infusion of 4-HNE-modified angiotensin prepared in a solution of 0.1 % formic acid in 50:50 H_2O:ACN (50x dilution) with MS/MS electron transfer dissociation of 500ms, parent ion *m/z* 727 (>3 injections). Product ions of *m/z* 726.7 and 1453.5 are observed.

4.3.3 Analysis of the protein-4-HNE conjugates

Data-dependent analyses were conducted as outlined in the methods section *4.2.3.3*. Incubation and digestion of the model protein BSA was carried out in order to assess the degree of post-translational modification by 4-HNE and to identify the modified fragments against those held on the Mascot database. The spectra obtained from the LC-MS/MS CID at a normalised collision energy of 35% for both *m/z* 469.8 and 615.1 are presented in **Figures 4.45** and **4.46**. The deuterated 4-HNE digest only exhibited data for the *m/z* 616 ion (**Figure 4.47**).

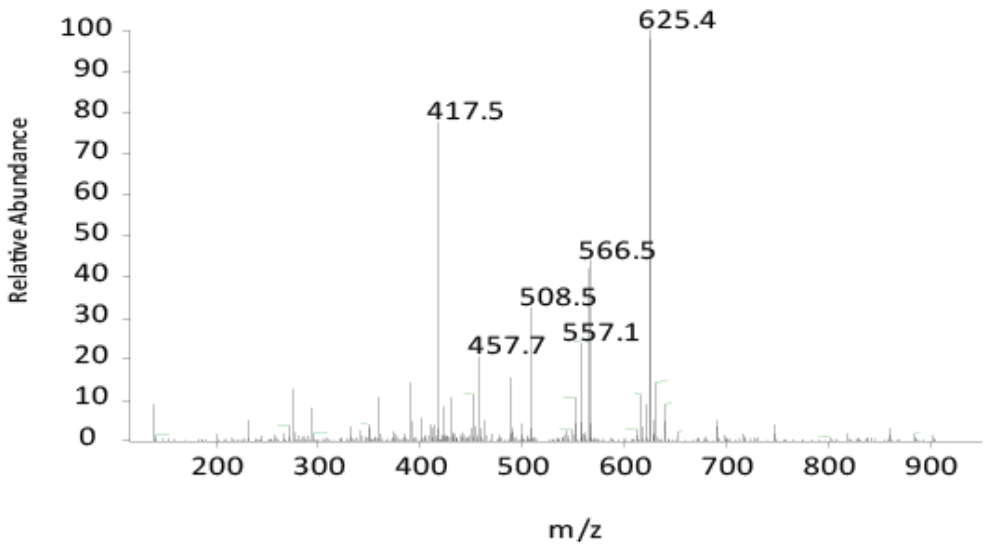

Figure 4.45: LC-MS separation of 4-HNE-BSA digest (full ms *m/*z 350-1500) with data-dependent collision induced dissociation of 35% for ion *m/*z 469.8 (>3 injections). Dominant product ions of *m/z* 625.4, 566.5, 557.1, 508.5, 457.7 and 417.5 are observed.

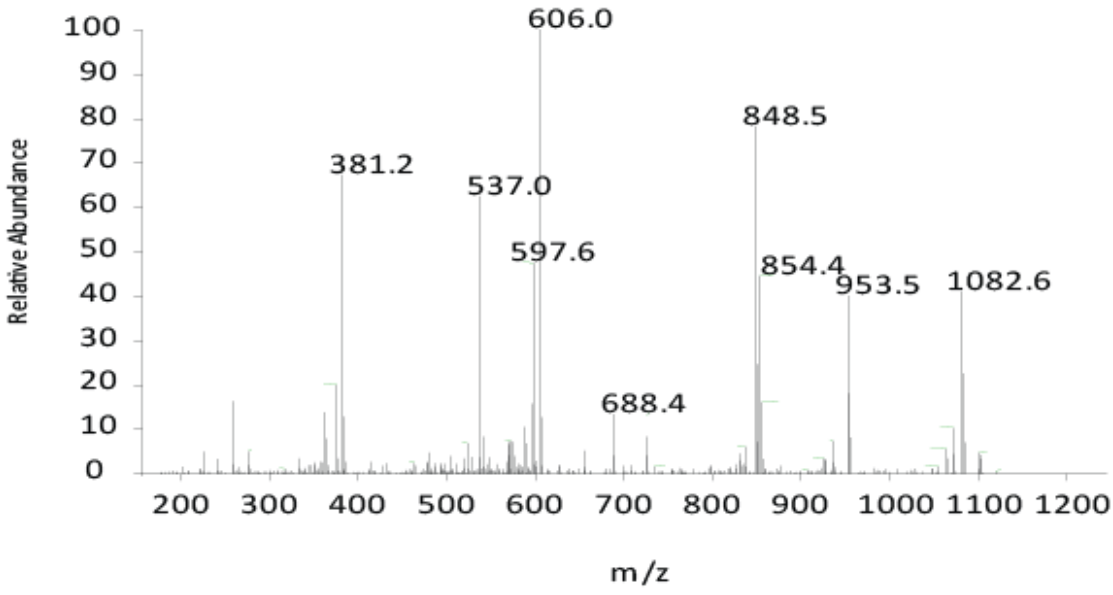

Figure 4.46: LC-MS separation of 4-HNE-BSA digest (full ms *m/*z 350-1500) with data-dependent collision induced dissociation of 35% for ion *m/*z 615.1 (>3 injections). Dominant product ions of *m/z* 1082.6, 953.5, 854.4, 848.5, 688.4, 606.0, 597.6, 537.0 and 381.2 are observed.

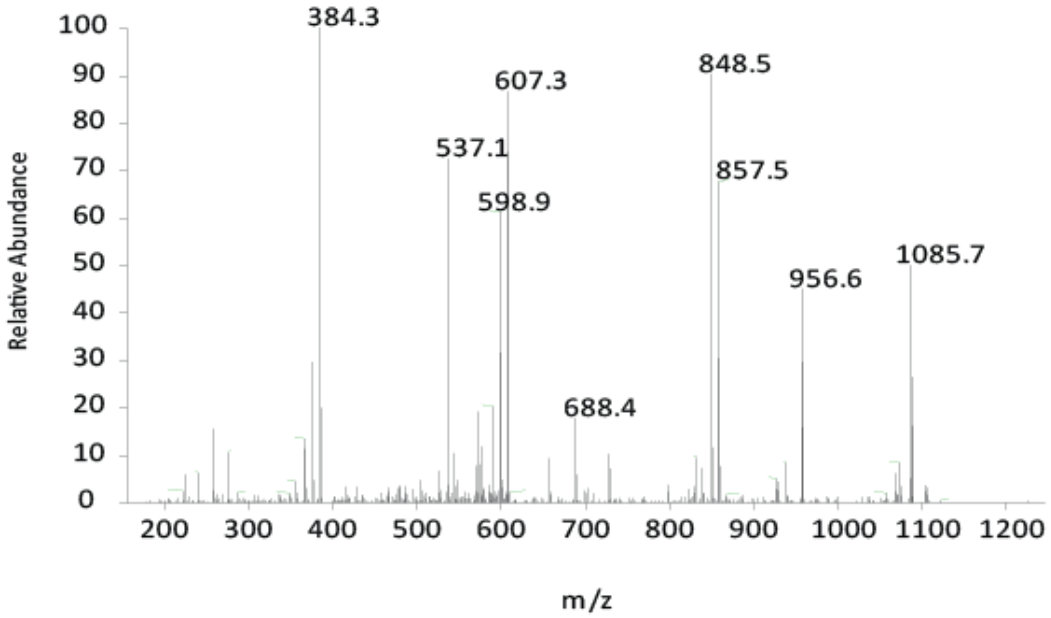

Figure 4.47: LC-MS separation of deuterated 4-HNE-BSA digest (full ms *m/z* 350-1500) with data-dependent collision induced dissociation of 35% for ion *m/z* 616.7 (>3 injections). Dominant product ions of *m/z* 1085.7, 956.6, 857.5, 848.5, 688.4, 607.3, 598.9, 537.1 and 384.3 are observed.

The digested samples were then analysed using the data-dependent neutral-loss parameters in which the additional ETD scan event was activated if a neutral loss of either *m/z* 52 or 78 was detected (*m/z* 53 or 79 for deuterated digests). **Figures 4.48** and **4.49** show the spectra for the peptide fragment precursor ion *m/z* 469 arising from the 4-HNE BSA digests. Under CID conditions, the neutral-loss ion is shown as *m/z* 417.5, resulting from a neutral-loss of *m/z* 52; this ion is shown intact as *m/z* 469.6 under ETD conditions therefore demonstrating the intact post-translational modification.

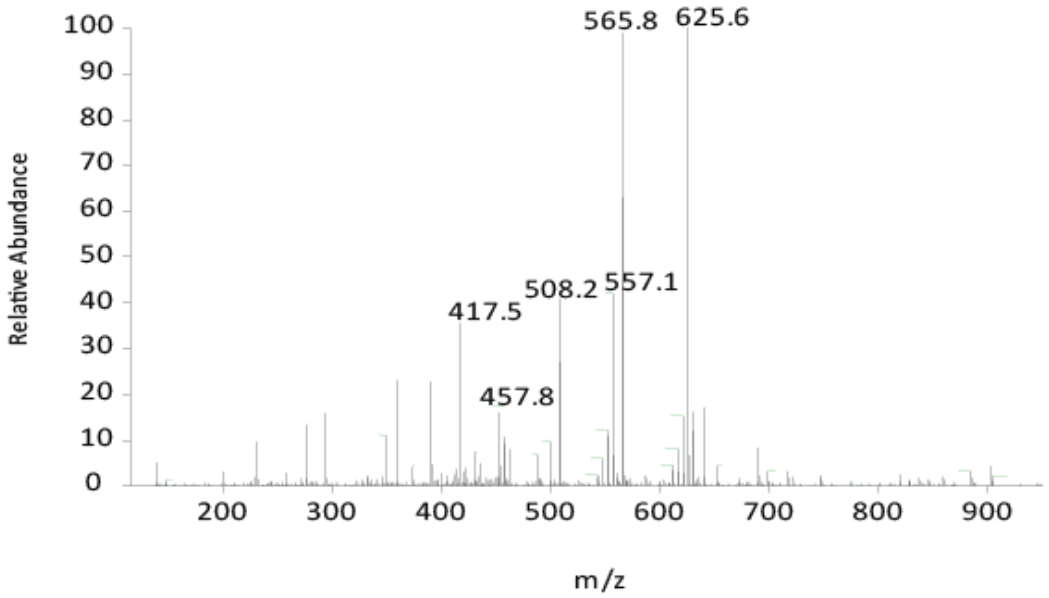

Figure 4.48: LC-MS separation of 4-HNE-BSA digest (full ms *m/z* 350-1500) with data-dependent collision induced dissociation of 35% for ion *m/z* 469.7 (>3 injections). Dominant product ions of *m/z* 625.6, 565.8, 557.1, 508.2, 457.8 and 417.5 are observed.

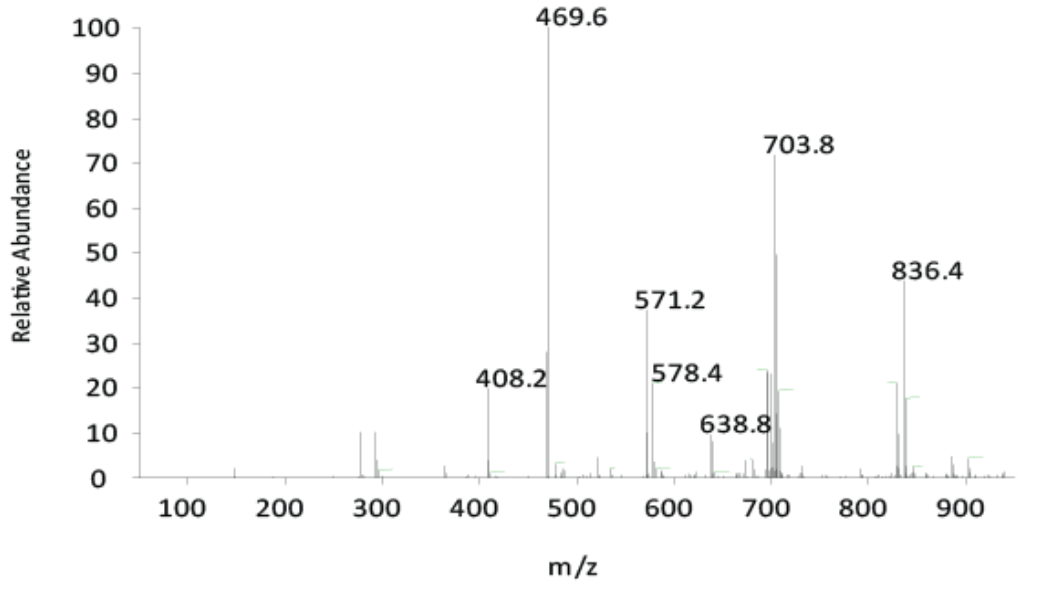

Figure 4.49: LC-MS separation of 4-HNE-BSA digest (full ms *m/z* 350-1500) with data-dependent electron transfer dissociation of 100ms for ion *m/z* 469.9 (>3 injections). Dominant product ions of *m/z* 836.4, 703.8, 638.8, 578.4, 571.2, 469.6 and 408.2 are observed.

Figures 4.50 and **4.51** show the spectra for the peptide fragment precursor ion *m/z* 615 arising from the 4-HNE BSA digests. Under CID conditions, the neutral-loss ion is shown as *m/z* 536.9, resulting from a neutral-loss of *m/z* 78; this ion is shown intact as *m/z* 615.0 under ETD conditions therefore demonstrating the intact post-translational modification.

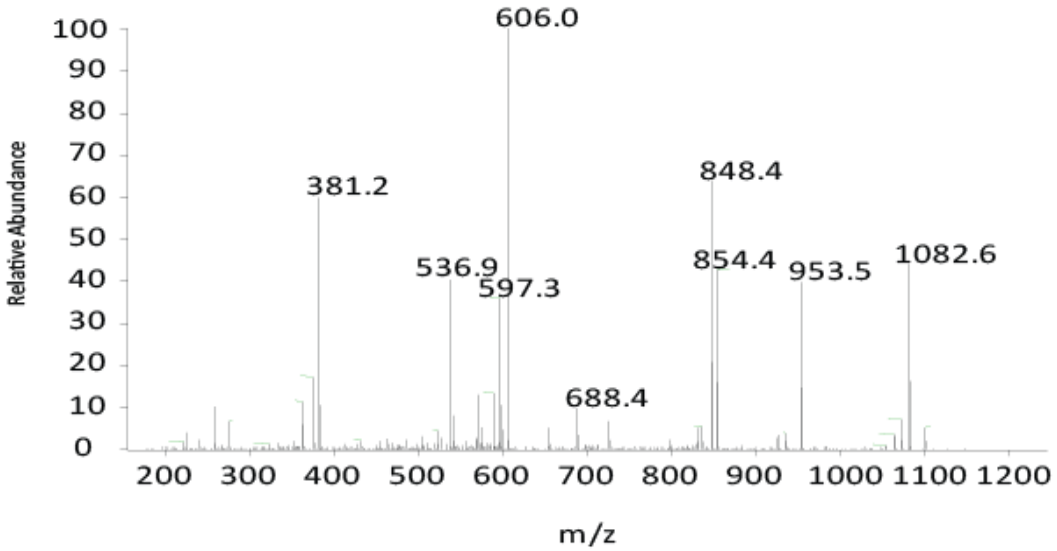

Figure 4.50: LC-MS separation of 4-HNE-BSA digest (full ms *m/*z 350-1500) with data-dependent collision induced dissociation of 35% for ion *m/*z 615.2 (>3 injections). Dominant product ions of *m/z* 1082.6, 953.5, 854.4, 848.4, 688.4, 606.0, 597.3, 536.9 and 381.2 are observed.

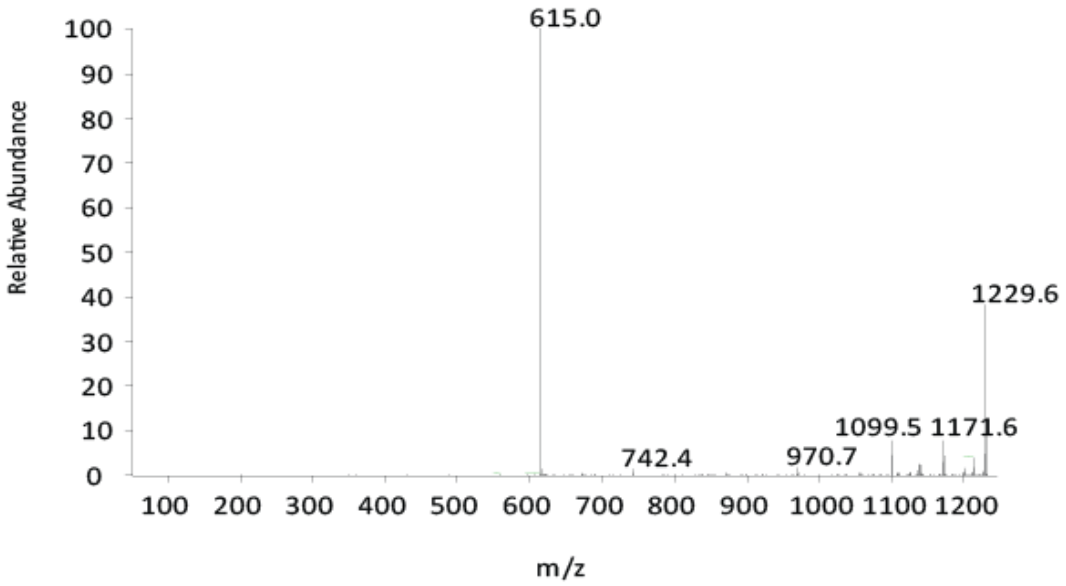

Figure 4.51: LC-MS separation of 4-HNE-BSA digest (full ms *m/z* 350-1500) with data-dependent electron transfer dissociation of 100ms for ion *m/z* 615.2 (>3 injections). Dominant product ions of *m/z* 1229.6, 1171.6, 1099.5, 970.7, 742.4 and 615.0 are observed.

Figures 4.52 and **4.53** show the spectra for the peptide fragment precursor ion *m/z* 470 arising from the deuterated 4-HNE BSA digests. Under CID conditions, the neutral-loss ion is shown as *m/z* 417.5, resulting from a neutral-loss of *m/z* 53; this ion is shown intact as *m/z* 470.6 under ETD conditions therefore demonstrating the intact post-translational modification.

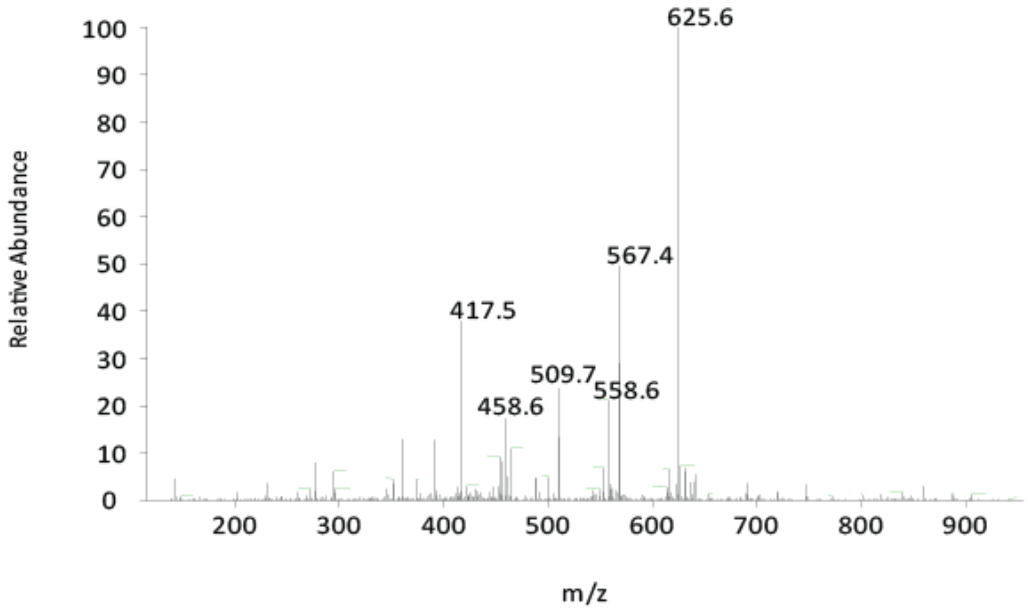

Figure 4.52: LC-MS separation of deuterated 4-HNE-BSA digest (full ms *m/z* 350-1500) with data-dependent collision induced dissociation of 35% for ion *m/z* 470.7 (>3 injections). Dominant product ions of *m/z* 625.6, 567.4, 558.6, 509.7, 458.6 and 417.5 are observed.

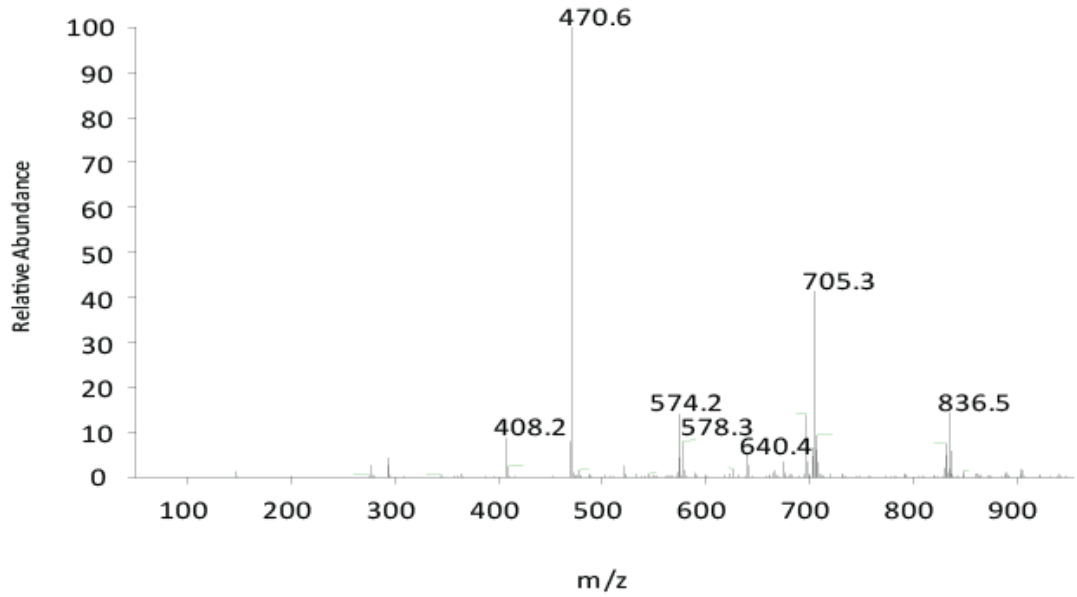

Figure 4.53: LC-MS separation of deuterated 4-HNE-BSA digest (full ms *m/z* 350-1500) with data-dependent electron transfer dissociation of 100ms for ion *m/z* 470.7 (>3 injections). Dominant product ions of *m/z* 836.5, 705.3, 640.4, 578.3, 574.2, 470.6 and 408.2 are observed.

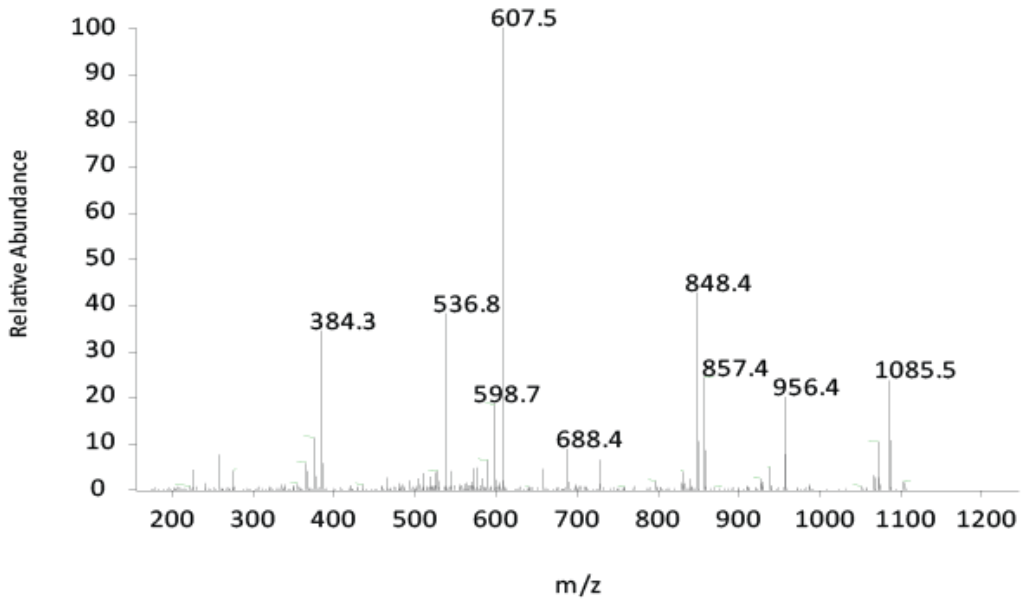

Figure 4.54: LC-MS separation of deuterated 4-HNE-BSA digest (full ms *m/z* 350-1500) with data-dependent collision induced dissociation of 35% for ion *m/z* 616.6 (>3 injections). Dominant product ions of *m/z* 1085.5, 956.4, 857.4, 848.4, 688.4, 607.5, 598.7, 536.8 and 384.3 are observed.

Figure 4.54 shows the spectra for the peptide fragment precursor ion *m/z* 616 arising from the deuterated 4-HNE BSA digests. Under CID conditions, the neutral-loss ion is shown as *m/z* 536.8, resulting from a neutral-loss of *m/z* 79. A data-dependent electron transfer dissociation at 100ms for *m/z* 616.6 was not observed in the deuterated 4-HNE-BSA digest. However, based upon the neutral-loss data the intact ion would have been shown by *m/z* 616 demonstrating the intact post-translational modification.

These data-dependent neutral-loss experiments demonstrated the ability to locate sites of post-translational modification in simple protein digests, following incubation with 4-HNE (either deuterated or undeuterated). To investigate whether this could be applied to a more complex and heterogeneous biological matrix, the

experiment was repeated using selected human bronchoalveolar lavage samples obtained from patients with COPD and aged matched controls; both current and ex-smokers.

4.3.4 Analysis of the lavage-4-HNE conjugates

The analysis of the data generated from the 4 BAL digests revealed that those that had undergone protein precipitation yielded some identifiable fragments. No peptide matches were obtained from the 'native' unprecipitated samples. Peptide modifications that were identified are shown in **Table 4.8**, and reflect a panel of proteins one would not expect in this extracellular compartment. Individual samples were only injected once due to the limited sample volume, so these data should be viewed as purely illustrative and not as a definitive assessment of the methodology. The dynamic range of protein concentrations within bronchoalveolar lavage is extensive with albumin being the dominant protein content followed by Immunoglobulin (Ig) G, IgA and transferrin (Hatch, 1993). These species account for in excess of 80% of lavage total protein. Although the unprecipitated samples did not yield any identifiable data, modified fragments were identified in the precipitated samples. It should be noted that the precipitation protocol was relatively 'soft' and that it should be viewed as reducing the concentration of the dominant protein species within the RTLF, rather than eliminating them. Thus one would have expected to have obtained peptide fragments following the tryptic digest corresponding to these dominant protein species, particularly albumin, in both the native and protein precipitated samples. This was not the case suggesting that the digest conditions were

not optimal and further work would be required to optimise the methodology for more complex biological matrices.

Table 4.8: Protein identification of BAL samples from a panel of COPD patients following protein precipitation. The "protein hit" refers to the accession entry from Mascot and the underlined residues within a given sequence indicate that the residue has been modified.

BAL #	Sample details	Protein hit	Observed ion *m/z*	Sequence	Modification	Identified protein
33	Female COPD current smoker	nil	-	-	-	-
38	Female healthy smoker	RPOC_ALKMQ	447.98	R.SALAC<u>R</u>SK.H	carbamidomethyl	DNA-directed RNA polymerase subunit beta
			403.98	K.<u>H</u>GVCGTCYGR.N	HNE	
			493.02	R.RGKPVTGPGNRPLK.S		
		NO66_CAEBR	440.94	K.SASVSHYK.E		hypothetical protein CBG11988
			440.93	K.SASVSHYKEPSK.E		
		RSMG_DINSH	520.23	M.DAASR.C		methyltransferase GidB
			622.19	K.VIDLGSGGGLPVVVLGVLAK.H		
		KDPD_CLOAB	450.12	K.SIVEAHGGK.I		sensor protein KdpD
			525.43	K.LLSAVGTSEVVSIGIK.Y		
		LEPA_MYCMO	424.68	K.IDLPSSDPEAVK.K		GTP-binding protein LepA (mycoplasma)
		Y4645_ARATH	564.64	R.SGSIGMGMSGSR.I		unknown protein
			556.78	K.VSEGSSSLSAGSGEM<u>K</u>.G	HNE	
		GA2L2_HUMAN	480.94	R.ERGAGTGASR.E		GAS2-like protein 2
			537.65	K.AI<u>Q</u>ELAQGSPSLLK.V	HNE	
			541.25	R.SFPGATSGSPRTELGR.D		
39	Male non-smoker	GLR24_ARATH	532.67	K.GGPVAY<u>Q</u>RDSFVLGK.L		Glutamate receptor 2.4
			533.03	R.DDVVGAAAAALDLIK.N	HNE	
		PUB18_ARATH	436.14	K.AGAVTPLLK.L		ubiquitin-protein ligase
			436.19	K.AGAVTPLLK.L		
		IYD1_HUMAN	436.14	K.EATVPDLK.R		iodotyrosine dehalogenase 1 isoform 2
			436.19	K.EATVPDLK.R		
40	Male COPD ex-smoker	COX4_ONCMY	615.17	K.NLSPSV.-		Cytochrome coxidase polypeptide 4, mitochondrial
			617.04	K.NLSPSV.-		
			629.39	K.NLSPVV.-		
			630.95	K.NLSPCV.-		
			631.07	K.NLSPTV.-		
			657.34	K.NLSPKV.-		
		ATPF_PEDPA	764.52	K.DSGAKER.E		F0F1-type ATP synthase, subunit b
			486.31	R.ELIIGNA<u>Q</u>NEA<u>K</u>.S	HNE	
		LIG_DROME	470.63	R.GDRGSGGPGGAYGSGR.G		MIP15115p
			596.85	R.EPWSG<u>Q</u>NAG<u>Q</u>DRGDDR.A		
		MT1_CASGL	597.02	-.MSSCGCGSGCSCGSGCN<u>C</u>K.N	carbamidomethyl	Metallothionein-like protein 1
			643.32	M.SS<u>C</u>G<u>C</u>GSG<u>C</u>S<u>C</u>GSGCNCK.N	3 x carbamidomethyl and 1 x HNE	
		TTC3_HUMAN	541.24	K.FSSSSPLTLPADL<u>K</u>.N	HNE	Isopentenyl diphosphate

Proteins that were identified from the lavage samples were unique to each of the four distinct sample groups. Sample ID 33 (female COPD current smoker) did not yield any identifiable protein fragments. However, this sample contained the lowest total protein concentration of the four samples (0.02 mg/mL) and so endogenous protease activity may have contributed towards degradation of the sample, therefore

affecting the identification of peptide sequences. Sample ID 38 (female healthy smoker) yielded seven protein hits from Mascot with three of the fifteen resulting peptide sequences exhibiting modification by 4-HNE and one sequence with a carbamidomethyl modification. Sample ID 39 (male never-smoker) yielded three protein hits from Mascot. Of the six resulting peptide sequences, only one exhibited modification by 4-HNE. Sample ID 40 (male COPD ex-smoker) yielded five protein hits from Mascot. Of the thirteen resulting peptide sequences, two exhibited modification by 4-HNE only, one displayed carbamidomethylation and one possessed three carbamidomethylations in addition to a single modification by 4-HNE. The identified proteins from the samples (fifteen proteins in total) were not representative of expected proteins associated with the respiratory tract lining fluid from individuals with COPD. Sample ID 39 (male non-smoker) was identified as containing ubiquitin-protein ligase which can both alter cellular function and target proteins for degradation by the proteosome. Sample ID 40 (male COPD ex-smoker) was identified as containing metallothionein, an important intracellular endogenous cysteine-rich antioxidant protein with metal-chelating properties. An increased presence of such a protein may be induced by oxidative stress. The only identifiable trend across the sample groups (excluding sample ID 33) was the apparent increase of protein hits for the healthy current and COPD ex-smoker compared to the healthy non-smoker (7, 5 and 3 respective hits).

4.4 Conclusion

The aim of this chapter was to develop a method that would permit the identification and quantification of proteins that had undergone oxidative post-translational modification via 4-HNE adduction in bronchoalveolar lavage samples (or other complex biological matrices). The rationale for focusing specifically on oxidative post-translation protein modifications was based on the absence of global indicators of the presence of oxidative stress in the airway lining fluids of COPD patients (Chapters 2 and 3). I therefore hypothesised that more subtle changes might be occurring within this compartment leading to functional changes in proteins relevant to disease pathology, either reflecting increased oxidative damage to specific proteins or a reduced capacity to eliminate modified proteins.

Whilst in Chapter 2 I saw no change in 4-HNE measured by immunoassay in lavage fluids, total or per unit protein, there is an existing literature in COPD demonstrating increased 4-HNE adduct formation in biopsies from COPD patients by immunohistochemistry (Rahman, 2002), with evidence that this is associated with the degree of airway obstruction. The stable lipid peroxidation product 4-HNE is a potent alkylating agent that has been shown to react with DNA and proteins, generating adducts with cysteine, lysine, and histidine residues (Esterbauer, 1991) that are capable of inducing specific cellular stress responses such as cell signalling and apoptosis (Uchida, 1993; Uchida, 1999). It was therefore an appealing marker to pursue, allied to a technology with the potential to identify modified proteins, as well as the site of oxidative modification.

In order to accomplish this significant task, a series of pilot experiments were performed with the aim of developing a suitable validated analytical method based upon mass spectrometry. A typical approach for quantitative analysis involves the use of reliable and stable internal standards. In mass spectrometry, deuterated compounds are typically employed as internal standards as they are equivalent in every way to their analogue, with the exception that a sufficient number of hydrogen (or carbon) atoms are deuterated to give a measurable mass shift. In the first part of this chapter I looked at whether there was any difference in signal intensity for a short-chain peptide (neurotensin) modified by deuterated and undeuterated 4-HNE (0.25-8 µg peptide incubated with 50 ng of relevant 4-HNE). The undeuterated adducts demonstrated a linear response, effectively forming a plateau between 6-8 µg. However, variability was noted for the deuterated adducts and the linear response that was observed for the undeuterated 4-HNE adducts was not reproducible to the same extent over a series of injections carried out on different days. In order that the deuterated adduct can be employed as an internal standard for quantification, this variability must be eliminated. Therefore, analysis using a quadrupole MS instrument would have been desirable to overcome the limitations of ion-trap instruments (further explained in Chapter 5).

Having demonstrated the formation of 4-HNE adducts with simple peptides the next logical step was to attempt modifying and then digesting a typical representative protein. BSA was used as the model protein and was subsequently incubated with deuterated and undeuterated 4-HNE. The protein was then digested with trypsin and an attempt was made to locate peptides from the protein which were modified by 4-

HNE and a comparison of the two sample types was made. Quantitative protein mass spectrometry typically involves two types of approach known as “bottom up” and “top down”. With the top down approach, the proteins are left intact and the intact protein intensity is measured for a given concentration. This is often a difficult approach due to the very large masses involved and the difficulty in chromatographically separating out the intact proteins. The bottom up approach circumvents these difficulties by digesting the protein into smaller peptides and separating and measuring these peptide fragments instead. However, this introduces the significant problem of understanding which peptides can be treated as being representative of the intact protein in terms of their signal intensity. In order to get around this issue, a number of peptides from the digested protein are typically used as the quantitative markers. The peptide sequences SHCIAEVEK (average mass 1015.16) and FKDLGEEHFK (average mass 1249.39) were chosen as model peptide sequences for both the deuterated and undeuterated digests due to their consistent appearance and reasonable signal across a number of preliminary digests.

The work was successful in locating the post translational modifications for both the deuterated and undeuterated 4-HNE peptides (from the model protein) but failed to find consistency in signal intensities across the two digest types. This meant that tackling the biological sample was feasible but not quantifiable at this stage. Human bronchoalveolar lavage samples from 4 subjects were either subjected to precipitation methods or left untreated and digested prior to quantification of 4-HNE adducts. Several modifications were identified for the precipitated samples however, no identifiable data was found for the untreated samples. Whilst identification of

some modifications were made, their origins cannot be assured at the present time and so further work will be required to confirm their authenticity before progressing onto their quantification. As the digests produce a very large number of peptides in a complex matrix there is always the problem of peptide identification by random chance and therefore a more significant finding might be deemed to be the absence of modified peptides from the most abundant proteins in airway lining fluids namely: albumin, immunoglobulin (A and G) heavy and light chains and transferrin (Hatch, 1993), especially within the 'native' unprecipitated samples. At this time and given the preliminary nature of these pilot studies it is safer to conclude that the method has not worked in the lavage samples. A diagrammatic illustration of the experiments conducted along with the experiments that are further required can be found in **Figure 4.55** below.

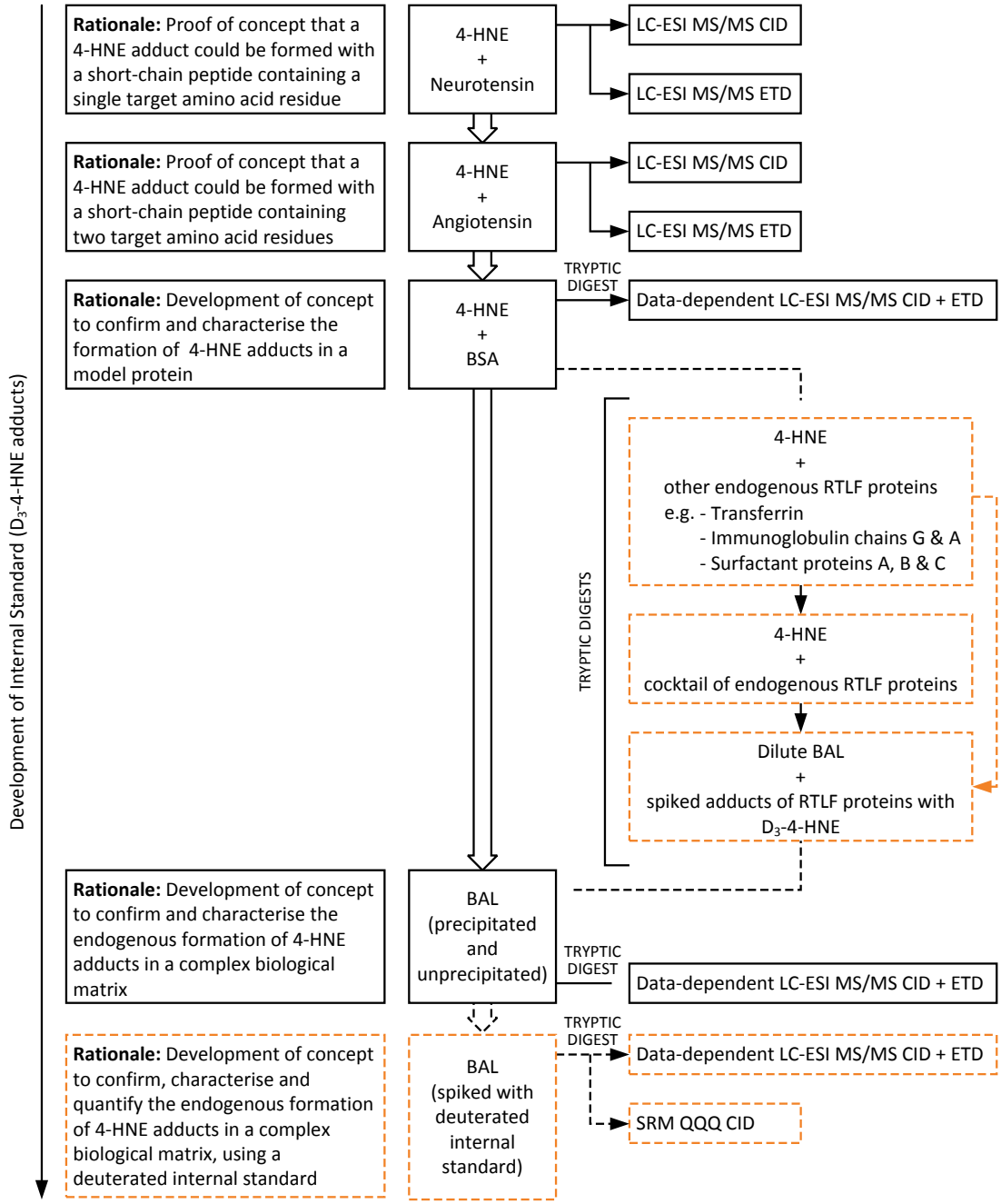

Figure 4.55: A flow diagram of the mass spectrometry experiments conducted in Chapter 4. Proof of concept was required for the formation and characterisation of 4-HNE adducts in a short-chain peptide (neurotensin) with a single binding site followed by an alternative short-chain peptide (angiotensin) with two binding sites. This was then applied to a model protein (BSA) followed by tryptic digestion and data-dependent analysis. The analysis of BAL samples was premature and did not yield any significant results. This diagram illustrates the experiments that are further required for progression towards the identification and quantification of endogenous 4-HNE adducts in lavage samples.

Due to time constraints, the decision to examine adduct formation in lavage samples was probably premature and there would have been considerable merit in working through a variety of major airway lining fluid proteins, singularly and in combination, before progressing to human lavage samples. In addition, in these preliminary studies no account was made of the potential formation of peptides through the action of endogenous proteases within the lavage samples, which would have the potential to significantly affect the ultimate peptide population within the digest. Therefore, pre-treatment of the lavage samples with a commercially available protease inhibitor cocktail may have been appropriate to prevent proteolytic degradation by endogenous proteases and to inhibit the protease activity from lysates through repetitive freeze-thaw cycles prior to analysis. Nevertheless, there is a sufficient body of preliminary data to suggest there is merit in pursuing this method further. Whilst absolute quantification of protein bound 4-HNE remains an extremely challenging objective by MS techniques, the semi-quantitative identification of adduction sites within protein remains a feasible target and one with the potential to identify functional oxidative post-translation modifications relevant to disease pathology.

Chapter 5:

PhD synopsis, critique and suggestions for future work

It has been argued that oxidative stress plays a significant role in the aetiology and progression of COPD; however the published data demonstrating this are scant and largely based on indirect measurements of antioxidants and oxidative damage markers in plasma, exhaled breath condensate and induced sputum (as reviewed in chapter 1). There is a paucity of data actually addressing oxidative stress in the regions of the lung directly affected by this disorder, particularly the distal airways and alveoli which undergo significant destruction and remodelling in emphysema. In the study described in chapter 2 we attempted to address this gap in the published literature by examining the concentrations of antioxidant and oxidative damage markers in alveolar lavage samples obtained from COPD patients, both ex- and current smokers.

5.1 Oxidative stress and inflammation in COPD – Chapter 2

I hypothesised that COPD would be associated with increased oxidative stress in the airway lumen, specifically, within the respiratory tract lining fluids sampled by bronchoalveolar lavage. Further, we anticipated that any oxidative signals observed in the COPD ex-smokers would be magnified in those patients who had continued to smoke post-diagnosis. In contrast to this view I observed an absence of clear signals of oxidative stress; either in terms of decreased antioxidant concentrations, or increased levels of protein and lipid oxidation products in COPD patients, relative to their aged matched controls. Increased concentrations of GSH and decreased concentrations of

vitamin C were observed in smokers, either 'healthy' subjects or COPD patients, relative to their age and smoking status matched controls. In addition, the endogenous metal chelators transferrin, lactoferrin and ferritin were measured in the lavage samples with only the latter being significantly increased in current smokers. These data do not therefore support the contention that oxidative stress is elevated in the distal airways of stable COPD patients. They do however, support the previously published evidence for increased airway GSH in current smokers (Rahman, 1996). The association with increased ferritin concentrations however, would tend to suggest that this reflects leakage from injured cells rather than a regulated adaptation to the cigarette smoke insult.

One potential explanation for the lack of contrast between the aged controls and the COPD patients is that age-related declines in antioxidant status have occurred that limited the capacity to discriminate clear disease-related signals. The concentration of low molecular weight antioxidants and enzymatic antioxidant activities has been shown to decrease with age in human populations, though many of these measurements have been restricted to plasma and circulating blood lymphocytes (Rizvi, 2007). An additional group of young healthy adults were therefore recruited to permit me to examine potential age-related declines in respiratory tract lining fluid antioxidant concentrations. I found evidence of increased vitamin C oxidation with age, in the absence of an equivalent increase in the concentration of GSSG, suggesting some evidence that the RTLF antioxidant network is impaired with age.

In addition, the pattern of inflammation we observed in the COPD patients was characterised by an increase in the numbers of macrophages and lymphocytes, consistent with a chronic inflammatory profile. In pulmonary conditions with established evidence of oxidative stress, such as asthma, adult respiratory distress syndrome and cystic fibrosis there is often a more neutrophilic/eosinophilic inflammatory profile. We therefore investigated an additional group of young mild asthmatics to examine whether the lack of oxidative stress in COPD reflected the absence of a disease related increase in PMNs. Contrary to the published literature (Kelly, 1999), I found no evidence of increased oxidative stress in this group who were largely indistinguishable from the young healthy controls in terms of their antioxidant levels. This may have reflected their mild clinical status and underlying absence of neutrophilia in comparison with previous studies (as discussed in detail in chapter 2). Nevertheless, neither the examination of ageing or alternative inflammatory profiles fully explained the absence of oxidative stress in the COPD patient groups.

These data therefore failed to confirm the original hypothesis and appeared to suggest that there is not a significant oxidative burden in the lungs of stable COPD patients in the absence of concurrent smoking. It should be acknowledged that this does not preclude the possibility that oxidative stress is restricted in this population to periods of exacerbation, or that this group may have a restricted capacity to mount protective adaptations to acute oxidative insults, as has been suggested by other authors (Goven, 2008). A recent paper by Behndig (2009), has shown that cellular enzymatic antioxidants in asthmatics (Cu, Zn, superoxide dismutase, glutathione peroxidase, glutathione disulphide reductase and catalase) are up-regulated, relative

to aged matched young adults. These same antioxidant enzymes are significantly decreased with age, but not further impaired in COPD patients, consistent with the data in the current study. This study did not however, include a group of young healthy smokers so it was not possible to evaluate whether a protective adaptive response would occur in these subjects relative to aged COPD current smokers.

5.2 Metal homeostasis in COPD – Chapter 3

Having failed to demonstrate the presence of oxidative stress in COPD, I decided to examine whether the age-related increase in oxidation markers could be attributed to increased concentrations of catalytic metals at the air-lung interface, specifically Cu and Fe. Under normal conditions these metals are rapidly and efficiently sequestered into cells in ferritin (Fe) or metallothionein (Cu, Zn, Cd) to prevent them promoting damaging oxidation reactions. Failure of these mechanisms can result in the presence of unchelated pools of Fe and Cu, referred to as the non-transferrin and non-caeruloplasmin bound pools respectively, which would promote oxidative stress. Increases in these metals in the RTLFs could reflect either increased necrotic cell death, or the inhalation of exogenous sources such as cigarette smoke, particularly of relevance to COPD.

To address this question I adopted two approaches. The first involved the determination of metal concentrations within BAL fluid digests following a relatively mild nitric acid digest. For these analyses I focused on Fe and Cu, for the reasons outlined above, but also As and Cd, as markers of cigarette smoke inhalation and Zn, as a major non-catalytic metal. Zn was studied due to its presence with Cu at a 1:1

stoichiometry in extracellular superoxide dismutase. It was assumed that a proportionate increase in Cu and Zn would likely reflect an increased expression of this critical antioxidant enzyme, whilst deviations from this relationship would be reflective of alternative sources. The second approach was based on an indirect assessment of 'free' Fe and Cu within the lavage fluids, i.e. that unbound by transferrin, lactoferrin or caeruloplasmin. The assay examined the catalytic oxidation of ascorbate added to the lavage fluids with time, in the presence or absence of the exogenous chelators DTPA and NTA, to either inhibit or promote metal dependent oxidations. In this assay, the role of NTA further allowed the potential contribution of Fe and Cu to ascorbate oxidation to be discriminated, as Fe-NTA sponsors increased oxidation whilst Cu-NTA is inhibitory.

Due to the reasons discussed at length in chapter 3, I was unable to obtain a robust measurement of Fe. Nevertheless, I did observe increased concentrations of both Cu and Zn with age. No differences were apparent in any of the measured metals between the COPD patient groups, with their respective age and smoking matched controls. The age-related increase in Cu was associated with an increased rate of ascorbate oxidation, which was inhibited by DTPA and augmented by NTA in the aged population. This latter observation provided some, albeit indirect, evidence for a non-transferrin Fe pool in the RTLFs of aged subjects. Further, the presence of increased Cu and Zn, or enhanced rates of ascorbate oxidation appeared correlated with the markers of oxidation reported in chapter 2. These data therefore represent the first reported evidence of an increase in catalytic metal activities in the aged population, specifically within the lung. There was however, consistent with the results from

chapter 2, no evidence of increased oxidative stress or altered metal handling related to disease status.

5.3 Discussion of mass spectrometry analysis – Chapter 4

The previous two experimental chapters failed to demonstrate any substantive evidence of oxidative stress in the airways of stable COPD patients. As argued above, this picture may be somewhat altered during periods of disease exacerbation, when the age-related degradation of cellular antioxidant defences might result in transient increases in oxidative damage and tissue injury. This however, remains to be determined. One might argue that whilst the data in chapters 2 and 3 examined gross indicators of oxidative stress, or altered metal handling, the role of biological oxidation/reduction reactions in COPD pathogenesis may be rather more subtle, acting through functional oxidative post translational modifications of enzymes and cell signalling molecules. A classic example being the oxidative inactivation of alpha-1-antitrypsin in lavage fluids recovered from smokers (Carp, 1980), reflecting the oxidation of critical methionine residues at the active site of the enzyme (Taggart, 2000). Over recent years the methods for examining 'functional' oxidations or reductions in proteins have advanced considerably (Burgoyne, 2011), with the role of thiolation (Antelmann, 2011), nitration (Monteiro, 2008) and protein adduction reviewed extensively (Ferrington, 2004).

The aim of this chapter was to develop a method to permit the identification of proteins that had undergone post translational modification via 4-HNE adduction in bronchoalveolar lavage samples. Such an approach, targeted at identifying specific

proteins and protein regions adducted by 4-HNE rather than the overall level of oxidation within the RTLF, was thought to be valuable in examining the pathogenesis of COPD rather than simply the presence of oxidative stress. In order to accomplish this significant task, a suitable semi-validated analytical method based upon mass spectrometry had to be established and well characterised.

A typical approach for such a quantitative analysis involves the use of reliable and stable internal standards. In mass spectrometry deuterated compounds are used as internal standards, which are equivalent in every way to their analogue, with the exception that a sufficient number of hydrogen (or carbon) atoms are deuterated to give a measurable mass shift. In order to quantify proteins in complex biological samples, a suitable internal standard had to be employed. Quantitative protein mass spectrometry typically involves two types of approach known as *bottom up* and *top down*. With the top down approach, the proteins are left intact and the intact protein intensity is measured for a given concentration. This is often a difficult approach due to the very large masses involved and the difficulty in chromatographically separating out the intact proteins. The bottom up approach circumvents these difficulties by digesting the protein into smaller peptides and separating and measuring these peptide fragments instead. However, this introduces the significant problem of understanding which peptides can be treated as being representative of the intact protein in terms of their signal intensity. In order to get around this issue, a number of peptides from the digested protein are used as the quantitative markers.

The first part of this chapter looked at whether there was any difference in signal intensity for a short chain peptide (angiotensin and neurotensin) modified by deuterated and undeuterated 4-HNE. Having determined that there is no difference in signal for deuterated versus undeuterated 4-HNE modified peptides, the next logical step was to attempt modifying and then digesting a typical representative protein. BSA was used as the model protein and was subsequently incubated with deuterated and undeuterated 4-HNE in parallel. The protein was then digested with trypsin and an attempt was made to locate peptides from the protein which were modified by 4-HNE and a comparison of the two sample types was made. The work was successful in locating the post-translational modifications (PTMs) for both the deuterated and undeuterated 4-HNE peptides (from the protein) but failed to find consistency in signal intensities across the two digest types. This meant that tackling the biological sample was not feasible at this stage.

To take this work forward, which was not possible in this project, the variability between the deuterated and undeuterated 4-HNE modified digests would need to be eliminated. To do this, I would first look to identify suitable peptide sequences that are consistently observed in the undeuterated digests and then go on to confirm whether these are also observed in the deuterated digests. If the variability was not eliminated, I would then look to the original digest protocol to see whether sample losses are occurring during the different stages of the protocol (denaturing, reducing, alkylating and drying down steps), which could be indicative of signal variability. If this was the case, then various aspects of the digestion protocol would have to be investigated. If reproducible results could then be obtained, the next stage

would be to use the human lavage as the biological matrix/proteins to undergo digestion and apply the same approach to quantify the PTMs. Prior to injection onto the LC-MS system, a set of varying concentrations of deuterated digest would be mixed with a set of lavage digest samples and following MS analysis, a comparison of the signal intensities of the deuterated 4-HNE peptides could be compared to the lavage peptide signals to relatively quantify the amount of protein that has undergone post-translational modification by 4-HNE in varying disease severity. This would serve as a molecular measure of the extent of oxidative stress observed in varying COPD and control samples and could be a more selective and sensitive approach in comparison to current immunological-based methods.

There are other factors which should also be considered in order to mitigate the limitations of the current work undertaken. It is possible that the protein precipitation method utilised may have affected the recovery of BAL proteins and negatively affected the proteomic analysis. In attempting to reduce/remove albumin as the large dominating protein in the BAL samples, it is possible that other smaller proteins were also removed in the process. The addition of organic solvents, in this case acetonitrile, precipitates high molecular weight proteins and leaves behind low molecular weight proteins (<30 kDa) in the solution; immuno-depletion methods were avoided due to disadvantages such as low sample throughput, specificity issues and the potential for non-specific albumin-bound protein loss. However, whilst acetonitrile may have allowed the dissociation of albumin-bound molecules, these lower molecular weight proteins may have been inadvertently removed from the sample through ‘trapping’ in the web-like structure created by the denatured larger proteins

(Merrell *et al.* 2004). These acknowledged difficulties led to the development of an in-tube chromatographic absorbent method to enrich low molecular weight proteins by the group of Wu *et al.* (2010) which has sought to eliminate such losses. Alternatively, precipitation plates can be used. The volume of acetonitrile and the centrifugal force applied during the precipitation method in the experimental work may have been too aggressive for the low volume BAL samples used and so this should be considered in future work where an in-tube absorbent method or precipitation plates could instead be employed.

In addition to possible precipitation issues, false discovery rates in database searches may have been apparent, affecting the specificity of protein identification. Computational analysis is performed by correlating the acquired MS/MS spectra with predicted theoretical fragmentation spectra contained within a protein sequence database such as Mascot. Due to the potential of false-positives, decoy databases should be used for large scale experiments. Such decoy searches consist of repeating the search using identical parameters against a database with reversed or randomised sequences; thus the number of positive matches found is an efficient way of estimating the validity of the matches found from the target database. It has also been suggested in the literature that multiple search tools and multi-stage strategies (iterative analysis) should be used to increase the overall rate of peptide identification (Bern *et al.* (2011); Ma, (2010); Larsen *et al.* (2006)).

The mass accuracy and resolution capabilities of the mass spectrometry equipment used in proteomic research can have a significant effect on the resultant

spectral data which in turn impacts subsequent peptide identification. In terms of analytical sensitivity, the merits of utilising a triple quadrupole instrument instead of a linear ion trap have already been acknowledged. Sensitivity can be further increased by using nanoelectrospray ionisation LC/MS which, when coupled with a quadrupole, results in increased sample concentrations (on column), lower flow rates (limiting dilution by the mobile phase) and increased ionisation efficiency (Cutillas, 2005). There are other mass analysers available which afford higher mass accuracy and resolution such as the Orbitrap which traps ions in an electrostatic field and causes them to oscillate in complex spiral patterns (much like a satellite in orbit) followed by Fourier transformation to generate accurate mass spectra. The ability to resolve and measure *m/z* values with greater accuracy can reduce the number of false positives from database searching algorithms and provide greater confidence in determining the amino acid sequence of peptide/proteins together with any ligands that may be present.

5.4 Final conclusion and suggestions for future work

I found no simplistic relationship between COPD and the presence of oxidative stress. Rather, I uncovered evidence of age-related changes at the air-lung interface suggestive of the presence of a non-transferrin bound Fe pool. These data are the first evidence of disturbances in the antioxidant network and metal handling capacity in the aged healthy lung. Whilst these changes could not be related to disease state they may imply that the aged airway is more susceptible to injury during periods of inflammation, i.e. as would be observed during airway infections and COPD exacerbations. As mentioned previously, the results presented within this thesis build

upon earlier observations in this group of patients demonstrating age-related decreases in cellular enzymatic antioxidants. Further, there is an emerging literature suggesting that adaptive stress pathways in COPD are impaired. These observations further support the view that the aged airway would be more sensitive to oxidative stress arising from airway inflammation. The presence of an unchelated pool of Fe at the lung surface also raises the possibility that the aged air-lung interface would be a more hospitable environment for bacterial infection, which would further augment airway injury.

Taken as a whole, the literature on oxidative stress in COPD is unconvincing and insufficiently robust. By focusing on airway responses in this study with appropriate age and smoking matched controls, I had hoped to have overcome many of the more obvious limitations of the published literature. Despite this, the role of oxidative stress in the pathogenesis and progression of COPD remains oblique. As discussed above, there would be merit in extending these analyses into patients with more advanced COPD or those undergoing acute exacerbations; however such studies raise significant ethical concerns. There is also the question as to whether the approach of looking at global markers of oxidation, in one-off samples, is somewhat naïve and whether a more targeted approach is required, for example, focusing on oxidative post-translational modifications to proteases and antiproteases. In the final chapter of this thesis, I attempted to develop a methodology that would permit the identification of such adducts within the RTLF. I was only able to progress this methodology to establish proof of principle and clearly this method still requires further development. However, the requirement for robust adductomic approaches is

now widely acknowledged and the preliminary work presented within this thesis represents a significant step in this direction.

References

Aldini G, Gamberoni L, Orioli M, Beretta G, Regazzoni L, Maffei Facino R, Carini M. (2006). “Mass spectrometric characterization of covalent modification of human serum albumin by 4-hydroxy-trans-2-nonenal.” J Mass Spectrom. 41(9): 1149-1161.

Aldridge RE, Chan T, van Dalen CJ, et al. (2002). “Eosinophil peroxidase produces hypobromous acid in the airways of stable asthmatics.” Free Radic Biol Med 33(6): 847-56.

Allwright S, Paul G, et al. (2005). “Legislation for smoke-free workplaces and health of bar workers in Ireland: before and after study.” BMJ. 331(7525): 1117.

Aniwidyaningsih W, Varraso R, Cano N, Pison C. (2008). “Impact of nutritional status on body functioning in chronic obstructive pulmonary disease and how to intervene.”Curr Opin Clin Nutr Metab Care. 11(4): 435–442.

Ansarin K, Chatkin JM, Ferreira IM, et al. (2001). “Exhaled nitric oxide in chronic obstructive pulmonary disease: respiratory to pulmonary function.” Eur Respir J. 17(5): 934-38.

Antczak A, Piotrowski W, Marczak J, Ciebiada M, Gorski P, Barnes PJ. (2011). “Correlation between eicosanoids in bronchoalveolar lavage fluid and in exhaled breath condensate.” Dis Markers. 30(5): 213-20.

Antelmann H, Helmann JD. (2011). “Thiol-based redox switches and gene regulation. Antioxid Redox Signal.” Mar 15;14(6): 1049-63.

Arcaroli, J. and J. Hokanson (2009). "Extracellular Superoxide Dismutase Haplotypes Are Associated with Acute Lung Injury and Mortality." American Journal of Respiratory and Critical Care Medicine 179: 105-112.

Aruoma OI, Bomford A, Polson RJ, Halliwell B. (1988). “Non-transferrinbound iron in plasma from haemochromatosis patients: Effects of phlebotomy therapy. Blood, 72: 1416–9.

ATS American Thoracic Society (1996). “Cigarette smoking and health.” Am. J. Respir. Crit. Care Med. 153: 861-865.

Attfield MD, Hodous TK. (1992). “Pulmonary function of U.S. coal miners related to dust exposure estimates.” Am Rev Respir Dis. 145(3): 605-609.

Avissar, N. and C. Reed (2000). "Ozone, but not nitrogen dioxide, exposure decreases glutathione peroxidases in epithelial lining fluid of human lung." American Journal of Respiratory and Critical Care Medicine 162: 1342-1347.

Ayo, D. and G. Aughenbaugh (2007). "Cystic lung disease in Birt-Hogg-Dube syndrome." Chest 132: 679-684.

Babusyte A, Stravinskaite K, Jeroch J, Lötvall J, Sakalauskas R, Sitkauskiene B. (2007). “Patterns of airway inflammation and MMP-12 expression in smokers and ex-smokers with COPD.” Respir Res. Nov 14;8: 81.

Bai, T. and J. Vonk (2007). "Severe exacerbations predict excess lung function decline in asthma." European Respiratory Journal 30: 452-456.

Baker MA, Cerniglia GJ, Zaman A. (1990). “Microtiter plate assay for the measurement of glutathione and glutathione disulfide in large numbers of biological samples.” Anal Biochem. Nov 1;190(2): 360-5.

Ballatori N, Hammond CL, Cunningham JB, Krance SM, Marchan R. (2005). “ Molecular mechanisms of reduced glutathione transport: role of the MRP/CFTR/ABCC and OATP/SLC21A families of membrane proteins.” Toxicol Appl Pharmacol. May 1;204(3): 238-55.

Baraldo S, Turato G, Badin C, Bazzan E, Beghé B, Zuin R, Calabrese F, Casoni G, Maestrelli P, Papi A, Fabbri LM, Saetta M. (2004). “Neutrophilic infiltration within the airway smooth muscle in patients with COPD.” Thorax. 59(4): 308-12.

Barbers RG, Evans MJ, Gong H, Tashkin DP. (1991). “Enhanced alveolar monocytic phagocyte (macrophage) proliferation in tobacco and marijuana smokers.” Am Rev Respir Dis 143: 1092–1095.

Barcelo B, Pons J, Ferrer J M, Sauleda J, Fuster A, Agusti A G. (2008). “Phenotypic characterisation of T-lymphocytes in COPD: abnormal CD4+CD25+ regulatory T-lymphocyte response to tobacco smoking.” Eur Respir J Mar 31: 555–562.

Barnes NC. (1998). “Inhaled steroids in COPD.” Lancet. 351(9105): 766-7.

Barnes PJ, Shapiro SD, Pauwels RA. (2003). “Chronic obstructive pulmonary disease: molecular and cellular mechanisms.” Eur Respir J. 22(4): 672-88.

Barnes, P. J. and B. R. Celli (2009). "Systemic manifestations and comorbidities of COPD." The European Respiratory Journal 33: 1165-1185.

Barnett, M. (2006). Chronic Obstructive Pulmonary Disease in Primary Care. Chichester, Whurr Publishers Limited (a subsidiary of John Wiley & Sons Ltd).

Beeh KM, Beier J, Koppenhoefer N, et al. (2004). “Increased glutathione disulphide and nitrosothiols in sputum supernatant of patients with stable COPD.” Chest. 126(4): 1116-22.

Behndig AF, Blomberg A, Helleday R, Kelly FJ, Mudway IS. (2009). “Augmentation of respiratory tract lining fluid ascorbate concentrations through supplementation with vitamin C.” Inhal Toxicol. Feb;21(3): 250-8.

Behndig, AF, A. Blomberg, E. Roos-Engstrand, I.S. Mudway. (2009). “Intracellular antioxidant enzyme differency in COPD reflects age-related declines in function, rather than disease state.” Respiratory Medicine, Volume 103, Supplement 1, August, Page S4.

Bellamy, D. and R. Booker (2005). Chronic Obstructive Pulmonary Disease in Primary Care. London, Class Publishing (London) Ltd.

Bennaars-Eiden A, Higgins L, Hertzel AV, Kapphahn RJ, Ferrington DA, Bernlohr DA. (2002). “Covalent modification of epithelial fatty acid-binding protein by 4-hydroxynonenal in vitro and in vivo. Evidence for a role in antioxidant biology.” J Biol Chem. 277(52): 50693-50702.

Bento I, Peixoto C, Zaitsev VN, Lindley PF. (2007). “Ceruloplasmin revisited: structural and functional roles of various metal cation-binding sites.” Acta Crystallogr D Biol Crystallogr. Feb;63(Pt 2): 240-8.

Berenson CS, Garlipp MA, Grove LJ, et al. (2006). “Impaired phagocytosis of nontypeable haemophilus influenzae by human alveolar macrophages in chronic obstructive pulmonary disease.” J Infect Dis 194: 1375–1384.

Biljak VR, Rumora L, Cepelak I, Pancirov D, Popović-Grle S, Sorić J, Grubisić TZ. (2010). “Glutathione cycle in stable chronic obstructive pulmonary disease.” Cell Biochem Funct. Aug;28(6): 448-453.

Biswas SK, Rahman I. (2009). “Environmental toxicity, redox signaling and lung inflammation: the role of glutathione. Mol Aspects Med. Feb-Apr; 30(1-2): 60-76.

Bitterman PB, Saltzman LE, Adelberg S, Ferrans VJ, Crystal RG. (1984). “Alveolar macrophage replication: one mechanism for the expansion of the mononuclear phagocyte population in the chronically inflamed lung.” J Clin Invest 74: 460–469.

Black, L. and F. Kueppers (1978). "Alpha-1 antitrypsin deficiency in nonsmokers." American Review of Respiratory Disease 117: 421-428.

Black, P. and R. Scragg (2005). "Relationship between serum 25-hydroxyvitamin D and pulmonary function in the Third National Health and Nutrition Examination Survey." Chest 128: 3792-3798.

Blank V. (2008). “Small Maf proteins in mammalian gene control: mere dimerization partners or dynamic transcriptional regulators?” J. Mol. Biol. 376: 913-925.

Boezen HM. (2009). “Genome-wide association studies: what do they teach us about asthma and chronic obstructive pulmonary disease?” Proc Am Thorac Soc. 6(8): 701-3.

Bonner JC, Rice AB, Moomaw CR, Morgan DL. (2000). “Airway fibrosis in rats induced by vanadium pentoxide.” Am J Physiol Lung Cell Mol Physiol. 278(1): L209-216.

Bossé Y. (2009). “Genetics of chronic obstructive pulmonary disease: a succinct review, future avenues and prospective clinical applications.” Pharmacogenomics. 10(4): 655-67.

Bournazou, I. and K. Mackenzie (2010). "Inhibition of eosinophil migration by lactoferrin." Immunology and Cell Biology 88: 220-223.

Boutten A, Goven D, Artaud-Macari E, Boczkowski J, Bonay M. (2011). “NRF2 targeting: a promising therapeutic strategy in chronic obstructive pulmonary disease.” Trends Mol Med. Apr 1. [Epub ahead of print].

Braman, S. and J. Kaemmerlen (1991). "Asthma in the elderly: a comparison between patients with recently acquired and long-standing disease." The American Review of Respiratory Disease 143: 336-340.

Brightling CE, Alaina J. Ammit, Davinder Kaur, Judith L. Black, Andrew J. Wardlaw, J. Margaret Hughes and Peter Bradding. (2005). “The CXCL10/CXCR3 axis mediates human lung mast cell migration to asthmatic airway smooth muscle.” Am J Respir Crit Care Med Vol. 171 pp. 1103–1108.

Brightling CE, McKenna S, Hargadon B, Birring S, Green R, Siva R, Berry M, Parker D, Monteiro W, Pavord ID, Bradding P. (2005). “Sputum eosinophilia and the short term response to inhaled mometasone in chronic obstructive pulmonary disease.” Thorax. 60(3): 193-8.

Britton JR, Pavord ID, Richards KA, Knox AJ, Wisniewski AF, Lewis SA, Tattersfield AE, Weiss ST. (1995). “Dietary antioxidant vitamin intake and lung function in the general population.” Am J Respir Crit Care Med. 151(5): 1383–7.

Brody AR, Craighead JE. (1975). “Cytoplasmic inclusions in pulmonary macrophages of cigarette smokers.” Lab Invest 32: 125–132.

Brown V, Elborn JS, Bradley J, et al. (2009). “Dysregulated apoptosis and NFkappaB expression in COPD subjects.” Respir Res 10: 24–35.

Buist AS, McBurnie MA, et al. (2007). “International variation in the prevalence of COPD (the BOLD Study): a population-based prevalence study.” Lancet. 370(9589): 741-750.

Burgoyne JR, Eaton P. (2011). “Contemporary techniques for detecting and identifying proteins susceptible to reversible thiol oxidation.” Biochem Soc Trans. Oct;39(5): 1260-7.

Caballero A, Torres-Duque CA, Jaramillo C, et al. (2008). “Prevalence of COPD in five Colombian cities situated at low, medium, and high altitude (PREPOCOL study).” Chest. 133(2): 343-349.

Calverley, P. (2004). "The GOLD Classification Has Advanced Understanding of COPD." American Journal of Respiratory and Critical Care Medicine 170: 211.214.

Cannon MJ, Openshaw PJ, Askonas BA. (1988). “Cytotoxic T cells clear virus but augment lung pathology in mice infected with respiratory syncytial virus.” J Exp Med. 168(3): 1163-8.

Cantin AM, et al. (1987). “Normal alveolar epithelial lung fluid contains high levels of glutathione.” J Appl Physiol. 63: 152–157.

Capelli A, Di Stefano A, Gnemmi I, Balbo P, Cerutti C G, Balbi B, Lusuardi M, Donner C F. (1999). “Increased MCP-1 and MIP-1β in bronchoalveolar lavage fluid of chronic bronchitis.” Eur Respir J 14: 160–165.

Carbone DL, Doorn JA, Kiebler Z, Petersen DR. (2005). “Cysteine modification by lipid peroxidation products inhibits protein disulfide isomerase.” Chem Res Toxicol. 18(8): 1324-1331.

Carini, M., Aldini, G., Facino, R. (2004). "Mass spectrometry for detection of 4-hydroxy-trans-2-nonenal (HNE) adducts with peptides and proteins." Mass Spectrometry Reviews 23: 281-305.

Carlsson, L.M, J. Jonsson, T. Edlund and S.L. Marklund. (1995). “Mice lacking extracellular superoxide dismutase are more sensitive to hyperoxia.” Proc. Natl. Acad. Sci. U. S. A. 92: 6264–6268.

Carp H, Janoff A. (1980). “Potential mediator of inflammation. Phagocyte-derived oxidants suppress the elastase-inhibitory capacity of alpha 1-proteinase inhibitor in vitro.” J Clin Invest. Nov;66(5): 987-95.

Chapman HA, Campbell EJ, et al. (2002). “Genome-wide linkage analysis of severe, early-onset chronic obstructive pulmonary disease: airflow obstruction and chronic bronchitis phenotypes.” Hum Mol Genet 11: 623–632.

Chapman RS, He X, Blair AE, Lan Q. (2005). “Improvement in household stoves and risk of chronic obstructive pulmonary disease in Xuanwei, China: retrospective cohort study.” BMJ. 331(7524): 1050.

Chen K, Kazachkov M, Yu PH. (2007). “Effect of aldehydes derived from oxidative deamination and oxidative stress on beta-amyloid aggregation; pathological implications to Alzheimer's disease.” J Neural Transm. 114(6): 835-839.

Cheng SL, Yu CJ, Chen CJ, Yang PC. (2004). “Genetic polymorphism of epoxide hydrolase and glutathione S-transferase in COPD.” Eur Respir J 23: 818–824.

Cho HY, Reddy SP, Kleeberger SR. (2006). “Nrf2 defends the lung from oxidative stress.” Antioxid Redox Signal. 8(1-2): 76-87.

Cho HY, Kleeberger SR. (2010). “Nrf2 protects against airway disorders.” Toxicol Appl Pharmacol. Apr 1;244(1): 43-56.

Chrysofakis G, Tzanakis N, Kyriakoy D, Tsoumakidou M, Tsiligianni I, Klimathianaki M, Siafakas NM. (2004). “Perforin expression and cytotoxic activity of sputum CD8+ lymphocytes in patients with COPD.” Chest. 125(1): 71-6.

Churg A, Hobson J, Wright J. (1989) “Functional and morphologic comparison of silica- and elastase-induced airflow obstruction.” Exp Lung Res. 15(6): 813-822.

Churg A, Tai H, Coulthard T, Wang R, Wright JL (2006). “Cigarette smoke drives small airway remodeling by induction of growth factors in the airway wall.” Am J Respir Crit Care Med 174(12): 1327–1334.

Chuwers P, Barnhart S, Blanc P, Brodkin CA, et al. (1997). “The protective effect of beta-carotene and retinol on ventilatory function in an asbestos-exposed cohort.” Am J Respir Crit Care Med. 155(3): 1066-1071.

Clarke L, R.L. Clifford, S. Jindarat, D. Proud, L. Pang and M. Belvisi et al. (2010). “TNFα and IFNγ synergistically enhance transcriptional activation of CXCL10 in human airway smooth muscle cells via STAT-1, NF-κB, and the transcriptional coactivator CREB-binding protein.” J Biol Chem 285 (38) Sep 17, pp. 29101–29110.

Codreanu SG, Zhang B, Sobecki SM, Billheimer DD, Liebler DC. (2009). “Global analysis of protein damage by the lipid electrophile 4-hydroxy-2-nonenal.” Mol Cell Proteomics. 8(4): 670-680.

Cohen, S. B., P. D. Pare, et al. (2007). "The Growing Burden of Chronic Obstructive Pulmonary Disease and Lung Cancer in Women." American Journal of Respiratory and Critical Care Medicine 176: 113-120.

Corhay JL, Henket M, Nguyen D, et al. (2009). “Leukotriene B4 contributes to exhaled breath condensate and sputum neutrophil chemotaxis in COPD.” Chest 136: 1047–1054.

Costabel U, Maier K, Teschler H, Wang YM. (1992). “Local immune components in chronic obstructive pulmonary disease.” Respiration. 59 Suppl 1: 17-9.

Cross, C. and P. Motchnik (1992). "Oxidative damage to plasma constituents by ozone." FEBS letters 298(2-3): 269-272.

Cross, C., A. van der Vliet, et al. (1994). "Oxidants, Antioxidants and Respiratory Tract Lining Fluids." Environmental Health Perspectives Supplements 102(Supplement 10): 185-191.

Crystal, R. (1991). "Oxidants and Respiratory Tract Epithelial Injury: Pathogenesis and Strategies for Therapeutic Intervention." The American Journal of Medicine 91(Supplement 3C): 39-44.

Cueto R, Pryor WA. (1994). “Cigarette smoke chemistry: conversion of nitric oxide to nitrogen dioxide and reactions of nitrogen oxides with other smoke components as studied by fourier transform infrared spectroscopy.” Vib Spectrosc 7: 97-111.

Currie, G. (2007). ABC of COPD. Oxford, Blackwell Publishing Ltd.

Cutillas, P (2005). “Principles of Nanoflow Liquid Chromatography and Applications to Proteomics.” Current Nanoscience 1: 65-71.

Dahl M, Tybjaerg-Hansen A, Lange P, Vestbo J, Nordestgaard BG. (2002). “Change in lung function and morbidity from chronic obstructive pulmonary disease in α1-antitrypsin MZ heterozygotes: a longitudinal study of the general population.” Ann Intern Med 136: 270–279.

Dam TT, Harrison S, Fink HA, Ramsdell J, Barrett-Connor E. (2010). “Osteoporotic Fractures in Men (MrOS) Research Group. Bone mineral density and fractures in older men with chronic obstructive pulmonary disease or asthma.” Osteoporos Int. 21(8): 1341-9.

Davies KJ, Sevanian A, Muakkassah-Kelly SF, Hochstein P. (1986). “Uric acid-iron ion complexes. A new aspect of the antioxidant functions of uric acid.” Biochem J. May 1;235(3): 747-54.

De Boer W I, Sont J K, van Schadewijk A, Stolk J, van Krieken J H, Hiemstra P S. (2000). “Monocyte chemoattractant protein 1, interleukin 8, and chronic airways inflammation in COPD.” J Pathol 190: 619–626.

DeMeo DL, Mariani TJ, Lange C *et al.* (2006). “The SERPINE2 gene is associated with chronic obstructive lung disease.” Am J Hum Genet. 78: 253-264.

De Raeve HR, Thunnissen FBJM, Kaneko FT, et al. (1997). “Decreased Cu, Zn-SOD activity in asthmatic airway epithelium: correction by inhaled corticosteroid in vivo.” Am J Physiol. 272(1Pt1): L148-54.

Deutsch, J.C. (2000). Dehydroascorbic acid. J Chromatogr A. 881(1-2): 299-307.

De Valk B, Addicks MA, Gosriwatana I, Lu S, Hider RC, Marx JJ. (2000). “Non-transferrin-bound iron is present in serum of hereditary haemochromatosis heterozygotes.” Eur J Clin Invest. Mar;30(3): 248-51.

Devereux, G. (2006). "ABC of chronic obstructive pulmonary disease: Definition, epidemiology and risk factors." British Medical Journal 332: 1142-1144.

Dinkova-Kostova, A. T., W. D. Holtzclaw, et al. (2002). "Direct evidence that sulfhydryl groups of Keap1 are the sensors regulating induction of phase 2 enzymes that protect against carcinogens and oxidants." Proc Natl Acad Sci U S A **99**(18): 11908-11913.

Di Stefano A, Capelli A, Lusuardi M, Balbo P, Vecchio C, Maestrelli P, et al. (1998). “Severity of airflow limitation is associated with severity of airway inflammation is smokers.” Am J Respir Crit Care Med. 158: 1277–1285.

Di Stefano A, Capelli A, Lusuardi M, Caramori G, Balbo P, Ioli F, et al. (2001). “Decreased T-lymphocyte infiltration in bronchial biopsies of subjects with severe chronic obstructive pulmonary disease.” Clin Expir Allergy. 31: 893–902.

Di Stefano A, Caramori G, Gnemmi I, Contoli M, Vicari C, Capelli A, Magno F, D'Anna SE, Zanini A, Brun P, Casolari P, Chung KF, Barnes PJ, Papi A, Adcock I, Balbi B. (2009). “T helper type 17-related cytokine expression is increased in the bronchial mucosa of stable chronic obstructive pulmonary disease patients.” Clin Exp Immunol. 157(2): 316-24.

Di Stefano A, Caramori G, Oates T, Capelli A, Lusuardi M, Gnemmi I, Ioli F, Chung KF, Donner CF, Barnes PJ, Adcock IM. (2002). “Increased expression of nuclear factor-kappaB in bronchial biopsies from smokers and patients with COPD.” Eur Respir J. Sep;20(3): 556-63.

Di Stefano A, Turato G, Maestrelli P, Mapp CE, Ruggieri MP, Roggeri A, Boschetto P, Fabbri LM, Saetta M. (1996). “Airflow limitation in chronic bronchitis is associated with T-lymphocyte and macrophage infiltration of the bronchial mucosa.” Am J Respir Crit Care Med. 153(2): 629-32.

Doumas, S. and A. Kolokotronis (2005). "Anti-inflammatory and antimicrobial roles of secretory leukocyte protease inhibitor." Infection and Immunity 73(3): 1271-1274.

Douwes J, Gibson P, Pekkanen J, Pearce N. (2002). “Non-eosinophilic asthma: importance and possible mechanisms.” Thorax. 57(7): 643-8.

Downs SH, Schindler C, et al. (2007) “Reduced exposure to PM10 and attenuated age-related decline in lung function.” N Engl J Med. 357(23): 2338-2347.

Dowton, S. and S. Pincott (1996). "Respiratory complications of Ehlers-Danlos syndrome type IV." Clinical Genetics 50: 510-514.

Drost, E. and K. Skwarski (2005). "Oxidative stress and airway inflammation in severe exacerbations of COPD." Thorax 60: 293-300.

Eggler AL, Liu G, Pezzuto JM, van Breemen RB, Mesecar AD. (2005). “Modifying specific cysteines of the electrophile-sensing human Keap1 protein is insufficient to disrupt binding to the Nrf2 domain Neh2.” Proc Natl Acad Sci U S A. 102(29): 10070-5.

Eisner MD, Blanc PD, Yelin EH, Katz PP, Sanchez G, Iribarren C, Omachi TA. (2010). “Influence of anxiety on health outcomes in COPD.” Thorax. 65(3): 229-34.

Eisner MD, Balmes J. et al. (2005) “Lifetime environmental tobacco smoke exposure and the risk of chronic obstructive pulmonary disease.” Environ Health. 4(1): 7.

Ekeowa UI, Marciniak SJ, Lomas DA. (2011). “α(1)-antitrypsin deficiency and inflammation.” Expert Rev Clin Immunol. 7(2): 243-52.

Erpenbeck VJ, Hohlfeld JM, Petschallies J, Eklund E, Peterson CG, Fabel H, Krug N. (2003). “Local release of eosinophil peroxidase following segmental allergen provocation in asthma.” Clin Exp Allergy. Mar;33(3): 331-6.

Esterbauer H, Schaur RJ, Zollner H. (1991). “Chemistry and biochemistry of 4-hydroxynonenal, malonaldehyde and related aldehydes.” Free Radic Biol Med. 11: 81–128.

Ezzati M and Lopez AD. (2003) “Estimates of global mortality attributable to smoking in 2000.” Lancet. 362(9387): 847-852.

Fattman, C.L, R.J. Tan, J.M. Tobolewski and T.D. Oury. (2006). “Increased sensitivity to asbestos-induced lung injury in mice lacking extracellular superoxide dismutase.” Free Radic. Biol. Med. 40: 601–607.

Favier, A. (1995). Analysis of free radicals in biological sysytems. Germany, Birkhauser Verlag AG.

Ferrington DA, Kapphahn RJ. (2004). “Catalytic site-specific inhibition of the 20S proteasome by 4-hydroxynonenal.” FEBS Lett. Dec 17;578(3): 217-23.

Filosa, S., A. Fico, et al. (2003). "Failure to increase glucose consumption through the pentose-phosphate pathway results in the death of glucose-6-phosphate dehydrogenase gene-deleted mouse embryonic stem cells subjected to oxidative stress." Biochem J 370(Pt 3): 935-43.

Finkelstein, R., R. S. Fraser, H. Ghezzo, and M. G. Cosio. (1995). “Alveolar inflammation and its relation to emphysema in smokers.” Am. J. Respir. Crit. Care Med. 152: 1666–1672.

Finlay GA, O'Driscoll LR, Russell KJ, D'Arcy EM, Masterson JB, FitzGerald MX, O'Connor CM. (1997). “Matrix metalloproteinase expression and production by alveolar macrophages in emphysema.” Am J Respir Crit Care Med. 156(1): 240-7.

Fiorini G, Crespi S, Rinaldi M, Oberti E, Vigorelli R, Palmieri G. (2000). “Serum ECP and MPO are increased during exacerbations of chronic bronchitis with airway obstruction.” Biomed Pharmacother. Jun;54(5): 274-8.

Fischbach MA, Lin H, Liu DR, Walsh CT. (2006). “How pathogenic bacteria evade mammalian sabotage in the battle for iron.” Nat Chem Biol. Mar;2(3): 132-8.

Fletcher C, Peto R. (1977). “The natural history of chronic airflow obstruction.” Br Med J. 1(6077): 1645-8.

Folz R.J, A.M. Abushamaa and H.B. Suliman. (1999). “Extracellular superoxide dismutase in the airways of transgenic mice reduces inflammation and attenuates lung toxicity following hyperoxia.” J. Clin. Invest. 103: 1055–1066.

Fowles, J., M. Bates, et al. (2000) The Chemical Constituents in Cigarettes and Cigarette Smoke: Priorities for Harm Reduction - A Report to the New Zealand Ministry of Health. 1-67.

Frischer T, Studnicka M, Gartner C, et al. (1999) “Lung function growth and ambient ozone: a three-year population study in school children.” Am J Respir Crit Care Med. 160(2): 390-396.

Frye C, Hoelscher B, et al. (2003) “Association of lung function with declining ambient air pollution.” Environ Health Perspect. 111(3): 383-387.

Fujimoto K, Yasuo M, Urushibata K, Hanaoka M, Koizumi T, Kubo K. (2005). “Airway inflammation during stable and acutely exacerbated chronic obstructive pulmonary disease.” Eur Respir J. 25: 640–646.

Fujita J, Nelson NL, Daughton DM, Dobry CA, Spurzem JR, Irino S, Rennard SI. (1990). “Evaluation of elastase and anti-elastase balance in patients with chronic bronchitis and pulmonary emphysema.” Am Rev Respir Dis. 142(1): 57-62.

Fullerton DG, Bruce N, Gordon S. (2008). “Indoor air pollution from biomass fuel smoke is a major health concern in the developing world.” Trans R Soc Trop Med Hyg. 102(9): 843–851.

Furst, J.; Gschwentner, M.; Ritter, M.; Botta, G.; Jakab, M.; Mayer, M.; Garavaglia, L.; Bazzini, C.; Rodighiero, S.; Meyer, G.; Eichmuller, S.; Woll, E.; Paulmichl, M. (2002). “Molecular and functional aspects of anionic channels activated during regulatory volume decrease in mammalian cells.” Pflugers Arch. 444(1-2): 1-25.

Gadek JE, Fells GA, Crystal RG. (1979). “Cigarette smoking induces functional antiprotease deficiency in the lower respiratory tract of humans.” Science. 206(4424): 1315-6.

Gao F, J.R. Koenitzer, J.M. Tobolewski, D. Jiang, J. Liang, P.W. Noble and T.D. Oury. (2008). “Extracellular superoxide dismutase inhibits inflammation by preventing oxidative fragmentation of hyaluronan.” J. Biol. Chem. 283: 6058–6066.

Gao L, Kim KJ, Yankaskas JR, Forman HJ. (1999). “Abnormal glutathione transport in cystic fibrosis airway epithelia.” Am J Physiol. Jul;277(1 Pt 1): L113-8.

Garcia-Pachon E, Padilla-Navas I, Shum C. (2007). “Serum uric acid to creatinine ratio in patients with chronic obstructive pulmonary disease.” Lung 185(1): 21–24.

Garcia-Sanz JA, Velotti F, MacDonald HR, Masson D, Tschopp J, Nabholz M. (1988). “Appearance of granule-associated molecules during activation of cytolytic T-lymphocyte precursors by defined stimuli.” Immunology. 64(1): 129-34.

Gardner, H., R. Bartelt, et al. (1992). "A Facile Synthesis of 4-Hydroxy-2(E)-nonenal." LIPIDS 27(9): 686-689.

Gauderman WJ, McConnell R, et al. (2000). “Association between air pollution and lung function growth in southern California children.” Am J Respir Crit Care Med. 162(4 Pt 1): 1383-1390.

Gauderman WJ, Vora H, et al. (2007). “Effect of exposure to traffic on lung development from 10 to 18 years of age: a cohort study.” Lancet. 369(9561): 571-577.

Ghio AJ. (2009). “Disruption of iron homeostasis and lung disease.” Biochim Biophys Acta. Jul;1790(7): 731-9.

Ghio, A. and J. Carter (1998). "Disruption of normal iron homeostasis after bronchial instillation of an iron-containing particle." American Journal Physiology (Lung Cellular & Molecular Physiology) 274(18): L396-L403.

Ghio AJ, Carter JD, Richards JH, Richer LD, Grissom CK, Elstad MR. (2003). “Iron and iron-related proteins in the lower respiratory tract of patients with acute respiratory distress syndrome.” Crit Care Med. Feb;31(2): 395-400.

Ghio AJ, Carter JD, Samet JM, Reed W, Quay J, Dailey LA, Richards JH, Devlin RB. (1998). “Metal-dependent expression of ferritin and lactoferrin by respiratory epithelial cells.” Am J Physiol. May;274(5 Pt 1): L728-36.

Ghio AJ, Hilborn ED, Stonehuerner JG, Dailey LA, Carter JD, Richards JH, Crissman KM, Foronjy RF, Uyeminami DL, Pinkerton KE. (2008). “Particulate matter in cigarette smoke alters iron homeostasis to produce a biological effect.” Am J Respir Crit Care Med. Dec 1;178(11): 1130-8.

Ghio, A. and J. Stonehuerner (2008). "Iron homeostasis and oxidative stress in idiopathic pulmonary alveolar proteinosis: a case-control study." Respiratory Research 9(10): 1-10.

Ghio AJ, Wang X, Silbajoris R, Garrick MD, Piantadosi CA, Yang F. (2003). “DMT1 expression is increased in the lungs of hypotransferrinemic mice.” Am J Physiol Lung Cell Mol Physiol. Jun;284(6): L938-44.

Gilmour PS, Brown DM, Lindsay TG, Beswick PH, MacNee W, Donaldson K. (1996). “Adverse health effects of PM10 particles: involvement of iron in generation of hydroxyl radical.” Occup Environ Med. Dec;53(12): 817-22.

Gioacchini, A. M. and N. Calonghi (1999). "Determination of 4-Hydroxy-2-nonenal at Cellular Levels by Means of Electrospray Mass Spectrometry." Rapid Communications in Mass Spectrometry 13: 1573-1579.

GOLD (2008). Global strategy for the diagnosis, management and prevention of Chronic Obstructive Pulmonary Disease, Global Initiative for Chronic Obstructive Lung Disease.

Gole MD, Souza JM, Choi I, Hertkorn C, Malcolm S, Foust RF 3rd, Finkel B, Lanken PN, Ischiropoulos H. (2000). “Plasma proteins modified by tyrosine nitration in acute respiratory distress syndrome.” Am J Physiol Lung Cell Mol Physiol. 278(5): L961-967.

Gorska K, Krenke R, Domagala-Kulawik J, Korczynski P, Nejman-Gryz P, Kosciuch J, Hildebrand K, Chazan R. (2008). “Comparison of cellular and biochemical markers of airway inflammation in patients with mild-to-moderate asthma and chronic obstructive pulmonary disease: an induced sputum and bronchoalveolar lavage fluid study.” J Physiol Pharmacol. Dec;59 Suppl 6: 271-83.

Gosriwatana I, Loréal O, Lu S, Brissot P, Porter J, Hider RC. (1999). “Quantification of non-transferrin-bound iron in the presence of unsaturated transferrin.” Anal Biochem. 273: 212–20.

Goven D, Boutten A, Leçon-Malas V, Marchal-Sommé J, Amara N, Crestani B, Fournier M, Lesèche G, Soler P, Boczkowski J, Bonay M. (2008). “Altered Nrf2/Keap1-Bach1 equilibrium in pulmonary emphysema.” Thorax. Oct;63(10): 916-24.

Graham G, Bates GW, Rachmilewitz EA, Hershko C. (1979). “Non-specific serum iron in thalassaemia: quantitation and chemical reactivity.” Am J Hematol. 6: 207–17.

Grievink L, Smit HA, Ocké MC, van 't Veer P, Kromhout D. (1998). “Dietary intake of antioxidant (pro)-vitamins, respiratory symptoms and pulmonary function: the MORGEN study.” Thorax. 53(3): 166–71.

Gross P, Pfitzer E A, Toker A, et al. (1965). “Experimental emphysema: its production with papain in normal and silicotic rats.” Arch Environ Health 11: 50–58.

Gudmundsson, G., T. Gislason, et al. (2006). "Mortality in COPD patients discharged from hospital: the role of treatment and co-morbidity." Respiratory Research 7(109).

Guenegou, A. and B. Leynaert (2006). "Serum carotenoids, vitamins A and E, and 8 year lung function decline in a general population." Thorax 61: 320-326.

Gumral, N. and M. Nazirolglu (2009). "Antioxidant enzymes and melatonin levels in patients with bronchial asthma and chronic obstructive pulmonary disease during stable and exacerbation periods." Cell Biochemistry and Function 27: 276-283.

Gutteridge, J.M.; Mumby, S.; Quinlan, G.J.; Chung, K.F.; Evans, T.W. (1996). “Pro-oxidant iron is present in human pulmonary epithelial lining fluid: implications for oxidative stress in the lung.” Biochem. Biophys. Res. Commun. 220(3):1024-7.

Gutteridge JMC, Rowley DA, Griffiths E, Halliwell B. (1995). “Low-molecular-weight iron complexes and oxygen radical reactions in idiopathic haemochromatosis.” Clin Sci. 68: 463– 7.

Gutteridge JMC, Rowley DA, Halliwell B. (1982). “Superoxide-dependent formation of hydroxyl radicals in the presence of iron salts. Detection of “free” iron in biological systems by using bleomycin-dependent degradation of DNA.” Biochem J. 199: 263-265.

Hacievliyagil SS, Gunen H, Mutlu LC, Karabulut AB, Temel I. (2006). “Association between cytokines in induced sputum and severity of chronic obstructive pulmonary disease.” Respir Med. 100: 846–854.

Hageman GJ, Larik I, Pennings HJ, Haenen GR, Wouters EF, Bast A. (2003). “Systemic poly(ADP-ribose) polymerase-1 activation, chronic inflammation, and oxidative stress in COPD patients.” Free Radic Biol Med 35(2): 140–148.

Halbert, R. J., J. L. Natoli, et al. (2006). "Global Burden of COPD: systematic review and meta-analysis." The European Respiratory Journal 28: 523-532.

Halliwell B. (2000). “The antioxidant paradox.” Lancet. Apr 1;355(9210): 1179-80.

Halliwell, B. and J. Gutteridge (2007). Free Radicals in Biology and Medicine. Oxford, Oxford University Press.

Halliwell, B. and J. Gutteridge (1984). "Oxygen toxicity, oxygen radicals, transition metals and disease." Biochemical Journal 219: 1-14.

Hammond CL, Marchan R, Krance SM, Ballatori N. (2007). “Glutathione export during apoptosis requires functional multidrug resistance-associated proteins.” J Biol Chem. May 11;282(19): 14337-47.

Happo MS, Hirvonen MR, Halinen AI, Jalava PI, Pennanen AS, Sillanpaa M, Hillamo R, Salonen RO. (2008). “Chemical compositions responsible for inflammation and tissue damage in the mouse lung by coarse and fine particulate samples from contrasting air pollution in Europe.” Inhal Toxicol. Nov;20(14): 1215-31.

Harkema JR, Hotchkiss JA. (1993). “Ozone- and endotoxin-induced mucus cell metaplasias in rat airway epithelium: novel animal models to study toxicant-induced epithelial transformation in airways.” Toxicol Lett. 68(1-2): 251-263.

Harman D. (2006). “Free radical theory of aging: an update: increasing the functional life span.” Ann N Y Acad Sci. 1067: 10-21.

Hart LA, Krishnan VL, Adcock IM, et al. (1998). “Activation and localization of transcription factor, nuclear factor-kappaB, in asthma.” Thorax. 53(7): 563-71.

Hartley DP, Kolaja KL, Reichard J, Petersen DR. (1999). “4-Hydroxynonenal and malondialdehyde hepatic protein adducts in rats treated with carbon tetrachloride: immunochemical detection and lobular localization.” Toxicol Appl Pharmacol. Nov 15; 161(1): 23-33.

Haslam, P. and R. P. Baughman. (1999). "Report of ERS Task Force: guidelines for measurement of acellular components and standardisation of BAL." The European Respiratory Journal 14: 245-248.

Hatch GE. (1992). “Comparative biochemistry of the airway lining fluid.” In Parent RA (ed) Treatise on Pulmonary Toxicology. CRC Press, Boca Raton, pp 617-632.

Hawkins CL, Morgan PE, Davies MJ. (2009). “Quantification of protein modification by oxidants.” Free Radic Biol Med. 46(8): 965-988.

He JQ, Connett JE, Anthonisen NR, Sandford AJ. (2003). “Polymorphisms in the IL13, IL13RA1, and IL4RA genes and the rate of decline in lung function in smokers.” Am J Respir Cell Mol Biol 28: 379–385.

He S, Aslam A, Gaça MD, He Y, Buckley MG, Hollenberg MD, Walls AF. (2004). “Inhibitors of tryptase as mast cell-stabilizing agents in the human airways: effects of tryptase and other agonists of proteinase-activated receptor 2 on histamine release.” J Pharmacol Exp Ther. 309(1): 119-26.

He X, Lin GX, Chen MG, Zhang JX, Ma Q. (2007). “Protection against chromium (VI)-induced oxidative stress and apoptosis by Nrf2. Recruiting Nrf2 into the nucleus and disrupting the nuclear Nrf2/Keap1 association.” Toxicol Sci. 98(1): 298-309.

Heart Protection Study Collaborative Group. (2002). “MRC/BHF Heart Protection Study of antioxidant vitamin supplementation in 20,536 high-risk individuals: a randomised placebo-controlled trial.” Lancet. 360(9326): 23-33.

Hersh, C. and D. Demeo (2005). "Attempted replication of reported chronic obstructive pulmonary disease candidate gene associations." American Journal of Respiratory Cell and Molecular Biology 33: 71-78.

Hider R.C. (2002). “Nature of nontransferrin-bound iron.” Eur. J. Clin. Invest. 32 (Suppl. 1): 50–54.

Hnizdo E, Baskind E, Sluis-Cremer GK. (1990). “Combined effect of silica dust exposure and tobacco smoking on the prevalence of respiratory impairments among gold miners.” Scand J Work Environ Health. 16(6): 411-422.

Hodge SJ, Hodge GL, Holmes M, Reynolds PN. (2004). “Flow cytometric characterization of cell populations in bronchoalveolar lavage and bronchial brushings from patients with chronic obstructive pulmonary disease.” Cytometry B Clin Cytom. Sep;61(1): 27-34.

Hodge S, Hodge G, Scicchitano R, et al. (2003). “Alveolar macrophages from subjects with chronic obstructive pulmonary disease are deficient in their ability to phagocytose apoptotic airway epithelial cells.” Immunol Cell Biol 81:289–296.

Hogervorst JG, de Kok TM, et al. (2006) “Relationship between radical generation by urban ambient particulate matter and pulmonary function of school children.” J Toxicol Environ Health A. 69(3-4): 245-262.

Hogg JC, Chu F, Utokaparch S, Woods R, Elliott WM, Buzatu L, Cherniack RM, Rogers RM, Sciurba FC, Coxson HO, Paré PD. (2004). “The nature of small-airway obstruction in chronic obstructive pulmonary disease.” N Engl J Med. 350(26): 2645-53.

Hogg JC, Macklem PT, Thurlbeck WM. (1968). “Site and nature of airway obstruction in chronic obstructive lung disease.” N Engl J Med. 278(25): 1355-60.

Holguin F, Flores S, et al. (2007). “Traffic-related exposures, airway function, inflammation, and respiratory symptoms in children.” Am J Respir Crit Care Med. 176(12): 1236-1242.

Holman CD, Psaila-Savona P, Roberts M, McNulty JC. (1987). “Determinants of chronic bronchitis and lung dysfunction in Western Australian gold miners.” Br J Ind Med. 44(12): 810-818.

Horak F Jr, Studnicka M, et al. (2002). “Particulate matter and lung function growth in children: a 3-yr follow-up study in Austrian schoolchildren.” Eur Respir J. 19(5): 838-845.

Horváth I, Donnelly LE, Kiss A, et al. (1998). “Raised levels of exhaled carbon monoxide are associated with an increased expression of heme oxygenase 1 in airway macrophages in asthma: a new marker of oxidative stress.” Thorax. 53(8): 668-72.

Hunt, J. and K. Fang (2000). "Endogenous airway acidification." American Journal of Respiratory and Critical Care Medicine 161(3): 694-699.

Ihorst G, Frischer T, et al. (2004) “Long- and medium-term ozone effects on lung growth including a broad spectrum of exposure.” Eur Respir J. 23(2): 292-299.

Iriyama K, Yoshiura M, Iwamoto T, Ozaki Y. (1984). “Simultaneous determination of uric and ascorbic acids in human serum by reversed-phase high-performance liquid chromatography with electrochemical detection.” Anal Biochem. Aug 15;141(1): 238-43.

Ito K, Barnes PJ. (2009). “COPD as a disease of accelerated lung aging.” Chest. 135(1): 173-80.

Ito K, Barnes PJ, Adcock IM. (2000). “Glucocorticoid receptor recruitment of histone deacetylase 2 inhibits interleukin-1beta-induced histone H4 acetylation on lysines 8 and 12.” Mol Cell Biol 20: 6891–6903.

Ito K, Yamamura S, Essilfie-Quaye S, Cosio B, Ito M, Barnes PJ, Adcock IM. (2006). “Histone deacetylase 2-mediated deacetylation of the glucocorticoid receptor enables NF-kappaB suppression.” J Exp Med. 203(1): 7-13.

Ito K, Ito M, Elliott WM, Cosio B, Caramori G, Kon OM, Barczyk A, Hayashi S, Adcock IM, Hogg JC, Barnes PJ. (2005). “Decreased histone deacetylase activity in chronic obstructive pulmonary disease.” N Engl J Med. 352(19): 1967-76.

Itoh K, Mimura J, Yamamoto M. (2010). “Discovery of the negative regulator of Nrf2, Keap1: a historical overview.” Antioxid Redox Signal. 13(11): 1665-78.

Iqbal M, Okazaki Y, Okada S. (2009). “Curcumin attenuates oxidative damage in animals treated with a renal carcinogen, ferric nitrilotriacetate (Fe-NTA): implications for cancer prevention.“ Mol Cell Biochem. Apr;324(1-2): 157-64.

Janus, E. and N. Phillips (1985). "Smoking, lung function and alpha-1 antitrypsin deficiency." Lancet 1: 152-154.

Jayet PY, Schindler C, et al. (2005). “Passive smoking exposure among adults and the dynamics of respiratory symptoms in a prospective multicenter cohort study.” Scand J Work Environ Health. 31(6): 465-473.

Jeong WS, Jun M, Kong AN. (2006). “Nrf2: a potential molecular target for cancer chemoprevention by natural compounds.” Antioxid Redox Signal. 8(1-2): 99-106.

Jiang R, Paik DC, Hankinson JL, Barr RG. (2007). “Cured meat consumption, lung function, and chronic obstructive pulmonary disease among United States adults.” Am J Respir Crit Care Med. 175(8): 798-804.

Jiang, R. and C. Camargo (2008). "Consumption of cured meats and prospective risk of chronic obstructive pulmonary disease in women." The American Journal of Clinical Nutrition 87: 1002-1008.

Jimenez, I. and H. Speisky (2000). "Effects of copper ions on the free radical-scavenging properties of reduced gluthathione: implications of a complex formation." J Trace Elem Med Biol 14(3): 161-7.

Jin, S.N.; Mun, G.H.; Lee, J.H.; Oh, C.S.; Kim, J.; Chung, Y.H.; Kang, J.S.; Kim, J.G.; Hwang, D.H.; Hwang, Y.I.; Shin, D.H.; Lee, W.J. (2005). “Immunohistochemical study on the distribution of sodium-dependent vitamin C transporters in the respiratory system of adult rat.” Microsc Res Tech. 68(6): 360-7.

Jomova K, Valko M. (2011). “Advances in metal-induced oxidative stress and human disease.” Toxicology. May 10;283(2-3): 65-87.

Joos L, He J-Q, Shepherdson MB, Connett JE, Anthonisen NR, Pare PD, Sandford AJ. (2002). “The role of matrix metalloproteinase polymorphisms in the rate of decline in lung function.” Hum Mol Genet 11: 569–576.

Joos L, McIntyre L, Ruan J, Connett JE, Anthonisen NR, Weir TD, Pare PD, Sandford AJ. (2002). “Association of IL-1beta and IL1 receptor antagonist haplotypes with rate of decline in lung function in smokers.” Thorax 57: 863–866.

Joost O, Wilk JB, Cupples A, Harmon M, Shearman AM, Baldwin CT, O’Conner GT, Myers RH, Gottlieb DJ. (2002). “Genetic loci influencing lung function: a genome-wide scan in the Framingham study.” Am J Respir Crit Care Med 165: 795–799.

Joyner JC, Reichfield J, Cowan JA. (2011). “Factors influencing the DNA nuclease activity of iron, cobalt, nickel, and copper chelates.” J Am Chem Soc. Oct 5;133(39): 15613-26.

Kalenderian R, Raju L, Roth W, Schwartz LB, Gruber B, Janoff A. (1988). “Elevated histamine and tryptase levels in smokers' bronchoalveolar lavage fluid. Do lung mast cells contribute to smokers' emphysema?” Chest. 94(1): 119-23.

Kauffmann F, Drouet D, Lellouch J, Brille D. (1982). “Occupational exposure and 12-year spirometric changes among Paris area workers.” Br J Ind Med. 39(3): 221-232.

Kaur, H. and B. Halliwell (1990). "Action of biologically-relevant oxidising species upon uric acid. Identification of uric acid oxidation products." Chem Biol Interact 73: 235-247.

Kay R, Barton C, Ratcliffe L. (2008). “Enrichment of low molecular weight serum proteins using acetonitrile precipitation for mass spectrometry based proteomic analysis.” Rapid Communications in Mass Spectrometry 20: 3255-3260.

Kelly FJ, Blomberg A, Frew A, Holgate ST, Sandstrom T. (1996). “Antioxidant kinetics in lung lavage fluid following exposure of humans to nitrogen dioxide.” Am J Respir Crit Care Med. Dec; 154(6 Pt 1): 1700-5.

Kelly FJ, Dunster C, Mudway I. (2003). “Air pollution and the elderly: oxidant/antioxidant issues worth consideration.” Eur Respir J Suppl. May;40: 70s-75s.

Kelly, F. J. and I. S. Mudway (2003). "Protein oxidation at the air-lung interface." Amino Acids 25(3-4): 375-96.

Kelly, F., I. Mudway, et al. (1999). "Altered lung antioxidant status in patients with mild asthma." Lancet 354(9177): 482-483.

Kelly Y, Sacker A, Marmot M. (2003). “Nutrition and respiratory health in adults: findings from the health survey for Scotland.” Eur Respir J. 21(4): 664-671.

Kharitonov SA, Barnes PJ. (2001). “Exhaled markers of pulmonary disease.” Am J Respir Crit Care Med. Jun;163(7): 1693-722.

Kikuchi I, Kikuchi S, Kobayashi T, Hagiwara K, Sakamoto Y, Kanazawa M, Nagata M. (2006). “Eosinophil trans-basement membrane migration induced by interleukin-8 and neutrophils.” Am J Respir Cell Mol Biol. 34(6): 760-5.

Kim, H., X. Liu, et al. (2004). "Cigarette Smoke Stimulates MMP-1 Production by Human Lung Fibroblasts Through the ERK1/2 Pathway." COPD 1: 13-23.

Kinnula VL, Ilumets H, Myllärniemi M, et al. (2007). “8-isoprostane as a marker of oxidative stress in nonsymptomatic cigarette smokers and COPD.” Eur Respir J. 29(1): 51-55.

Kiraz K, Kart L, Demir R, Oymak S, et al. (2003). “Chronic pulmonary disease in rural women exposed to biomass fumes.” Clin Invest Med. 26(5): 243-248.

Kirkil G, Hamdi Muz M, Seçkin D, Sahin K, Küçük O. (2008). “Antioxidant effect of zinc picolinate in patients with chronic obstructive pulmonary disease.” Respir Med. 102(6): 840-4.

Kirkwood TB. (2005). “Understanding the odd science of aging.” Cell. 120(4): 437-47.

Kobayashi A, Kang MI, Okawa H, Ohtsuji M, Zenke Y, Chiba T, Igarashi K, Yamamoto M. (2004). “Oxidative stress sensor Keap1 functions as an adaptor for Cul3-based E3 ligase to regulate proteasomal degradation of Nrf2.” Mol Cell Biol. 24(16): 7130-9.

Koh YH, Yoon SJ, Park JW (1997). “Lipid Peroxidation Product-Mediated DNA Damage and Mutagenicity.” J. Biochem. Mol. Biol. 30(3): 188-19

Kon, O. M., T. Hansel, et al. (2008). Chronic Obstructive Pulmonary Disease (COPD). Oxford, Oxford University Press.

Kondoh, Y. and H. Taniguchi (1990). "Emphysematous change in chronic asthma in relation to cigarette smoking: assessment by computed tomography." Chest 97: 845-849.

Kongerud J, Crissman K, Hatch G, et al. (2003). “Ascorbic acid is decreased in induced sputum of mild asthmatics.” Inhalation Toxicology. 15: 101-109.

Kulkarni N, Pierse N, Rushton L, Grigg J. (2006). “Carbon in airway macrophages and lung function in children.” N Engl J Med. 355(1): 21-30.

Kumagai K, Ohno I, Okada S. (1999). “Inhibition of matrix metalloproteinases prevents allergen-induced airway inflammation in a murine model of asthma.” J Immunol. 162(7): 4212-9.

Lacoste JY, Bousquet J, Chanez P, Van Vyve T, Simony-Lafontaine J, Lequeu N, Vic P, Enander I, Godard P, Michel FB. (1993). “Eosinophilic and neutrophilic inflammation in asthma, chronic bronchitis, and chronic obstructive pulmonary disease.” J Allergy Clin Immunol. 92(4): 537-48.

Lange, P. and J. Parner (1998). "A 15-year follow-up study of ventilatory function in adults with asthma." New England Journal of Medicine 339: 1194-1200.

Lapperre TS, Postma DS, Gosman MM, Snoeck-Stroband JB, ten Hacken NH, Hiemstra PS, Timens W, Sterk PJ, Mauad T. (2006). “Relation between duration of smoking cessation and bronchial inflammation in COPD.” Thorax. 61(2): 115-21.

Larsson, C. (1978). "Natural history and life expectancy in severe alpha-1 antitrypsin deficiency." Acta medica Scandinavica 204: 345-351.

Laurell C B, Eriksson S. (1963). “The electrophoretic alpha-1-globulin pattern of serum in alpha-1-antitrypsin deficiency. Scand J Clin Invest 15: 132–140.

Leuenberger P, Schwartz J, et al. (1994). “Passive smoking exposure in adults and chronic respiratory symptoms (SAPALDIA Study). Swiss Study on Air Pollution and Lung Diseases in Adults, SAPALDIA Team.” Am J Respir Crit Care Med. 150(5 Pt 1): 1222-1228.

Levine RL, Garland D, Oliver CN, Amici A, Climent I, Lenz AG, Ahn BW, Shaltiel S, Stadtman ER (1990). “Determination of carbonyl content in oxidatively modified proteins.” Methods Enzymol. 186: 464-478.

Li CJ, Nanji AA, Siakotos AN, Lin RC. (1997). “Acetaldehyde-modified and 4-hydroxynonenal-modified proteins in the livers of rats with alcoholic liver disease.” Hepatology 26(3): 650-657.

Li N, Hao M, Phalen RF, Hinds WC, Nel AE. (2003). “Particulate air pollutants and asthma. A paradigm for the role of oxidative stress in PM-induced adverse health effects.” Clin Immunol. Dec;109(3): 250-65.

Li Z, Alam S, Wang J, Sandstrom CS, Janciauskiene S, Mahadeva R. (2009). “Oxidized {alpha}1-antitrypsin stimulates the release of monocyte chemotactic protein-1 from lung epithelial cells: potential role in emphysema.” Am J Physiol Lung Cell Mol Physiol. 297(2): L388-400.

Liang, W.J.; Johnson, D.; Jarvis, S.M. (2001). “Vitamin C transport systems of mammalian cells.” Mol. Membr. Biol. 18(1): 87-95.

Linden, M., L. Hakansson, et al. (1989). "Glutathione in bronchoalveolar lavage fluid from smokers is related to humoral markers of inflammatory cell activity." Inflammation 13: 651-658.

Linden M, Rasmussen JB, Piitulainen E, Tunek A, Larson M, Tegner H, Venge P, Laitinen LA, Brattsand R. (1993). “Airway inflammation in smokers with nonobstructive and obstructive chronic bronchitis.” Am Rev Respir Dis. 148(5): 1226-32.

Liu Z, Minkler PE, Sayre LM. (2003). “Mass spectroscopic characterization of protein modification by 4-hydroxy-2-(E)-nonenal and 4-oxo-2-(E)-nonenal.” Chem Res Toxicol. 16(7): 901-911.

Lokke, A., P. Lange, et al. (2006). "Developing COPD: a 25 year follow up study of the general population." Thorax 61: 935-939.

Louhelainen N, Rytilä P, Haahtela T, et al. (2009). “Persistence of oxidant and protease burden in the airways after smoking cessation.” BMC Pulm Med 9: 25–33.

Loukides S, Bouros D, Papatheodorou G, et al. (2002). “The relationships among hydrogen peroxide in expired breath condensate, airway inflammation and asthma severity.” Chest 121(2): 338-46.

Lowe CR. (1956). “An association between smoking and respiratory tuberculosis.” Br Med J. 2(5001): 1081-1086.

Ma, B (2010). “Challenges in computational analysis of mass spectrometry data for proteomics”. Journal of Computer Science and Technology 25(1): 1.

MacNee, W. (2000). "Oxidants/Antioxidants and COPD." CHEST 117: 303s-317s.

MacNee W. (2001). “Oxidants/antioxidants and chronic obstructive pulmonary disease: pathogenesis to therapy.” Novartis Found Symp. 234: 169-188.

Magi B, Bargagli E, Bini L, Rottoli P. (2006). “Proteome analysis of bronchoalveolar lavage in lung diseases.” Proteomics. Dec;6(23): 6354-69.

Majo J, Ghezzo H, Cosio MG. (2001). " Lymphocyte population and apoptosis in the lungs of smokers and their relation to emphysema." Eur Respir J. 17(5): 946-53.

Mak, J. (2008). "Pathogenesis of COPD Part II: Oxidative-antioxidative imbalance." The International Journal of Tuberculosis and Lung Disease 12(4): 368-374.

Malhotra D, Thimmulappa R, Navas-Acien A, Sandford A, Elliott M, Singh A, Chen L, Zhuang X, Hogg J, Pare P, Tuder RM, Biswal S. (2008). "Decline in NRF2-regulated antioxidants in chronic obstructive pulmonary disease lungs due to loss of its positive regulator, DJ-1." Am J Respir Crit Care Med. 178(6): 592-604.

Mannino DM, Aguayo SM, Petty TL, Redd SC. (2003). "Low lung function and incident lung cancer in the United States: data From the First National Health and Nutrition Examination Survey follow-up." Arch Intern Med 163: 1475–1480.

Marchan R, Hammond CL, Ballatori N. (2008). "Multidrug resistance-associated protein 1 as a major mediator of basal and apoptotic glutathione release." Biochim Biophys Acta. Oct;1778(10): 2413-20.

Marklund SL (1982). "Human copper-containing superoxide dismutase of high molecular weight." Proc Natl Acad Sci U S A. Dec;79(24): 7634-8.

Markowetz B, Van Snick JL, Masson PL. (1979). "Binding and ingestion of human lactoferrin by mouse alveolar macrophages." Thorax. Apr;34(2): 209-12.

Marques LJ, Teschler H, Guzman J, Costabel U. (1997). "Smoker's lung transplanted to a nonsmoker: long-term detection of smoker's macrophages." Am J Respir Crit Care Med 156: 1700–1702.

Marshall Bern and Yong J. Kil (2011). "Unbiased Statistical Analysis for Multi-Stage Proteomic Search Strategies". *J. Proteome Res. 10* (4): 2123–2127.

Martin R. Larsen, Morten B. Trelle, Tine E. Thingholm, and Ole N. Jensen (2006). "Analysis of posttranslational modifications of proteins by tandem mass spectrometry." BioTechniques 40: 790-798.

Marzec JM, Christie JD, Reddy SP, Jedlicka AE, Vuong H, Lanken PN, Aplenc R, Yamamoto T, Yamamoto M, Cho HY, Kleeberger SR. (2007). "Functional polymorphisms in the transcription factor NRF2 in humans increase the risk of acute lung injury." FASEB J. 21(9): 2237-46.

Masuoka J, Saltman P. (1994). "Zinc(II) and copper(II) binding to serum albumin. A comparative study of dog, bovine, and human albumin." J Biol Chem. Oct 14;269(41): 25557-61.

Mateos, F. and J. Brock (1998). "Iron metabolism in the lower respiratory tract." Thorax 53: 594-600.

May, J. M., Z. Qu, et al. (2001). "Requirement for GSH in recycling of ascorbic acid in endothelial cells." Biochem Pharmacol 62(7): 873-81.

McKeever TM, Lewis SA, Smit HA, Burney P, Cassano PA, Britton J. (2008). “A multivariate analysis of serum nutrient levels and lung function.” Respir Res. 9: 67.

Meijer E, Kromhout H, Heederik D. (2001). “Respiratory effects of exposure to low levels of concrete dust containing crystalline silica.” Am J Ind Med. 40(2): 133-140.

Mendez D, Hernaez ML, Diez A, Puyet A, Bautista JM. (2010). “Combined proteomic approaches for the identification of specific amino acid residues modified by 4-hydroxy-2-nonenal under physiological conditions.” J Proteome Res. Nov 5; 9(11): 5770-5781.

Menezes AM, Hallal PC, Perez-Padilla R, et al. (2007). “Tuberculosis and airflow obstruction: evidence from the PLATINO study in Latin America.” Eur Respir J. 30(6): 1180-1185.

Menezes AM, Perez-Padilla, R. et al. (2005). “Chronic obstructive pulmonary disease in five Latin American cities (the PLATINO study): a prevalence study.” Lancet. 366(9500):1875-81.

Menzies D, Nair A, et al. (2006). “Respiratory symptoms, pulmonary function, and markers of inflammation among bar workers before and after a legislative ban on smoking in public places.” JAMA. 296(14): 1742-1748.

Merrell K, Southwick K, et al. (2004). “Analysis of Low-Abundance, Low-Molecular-Weight Serum Proteins Using Mass Spectrometry.” Journal of Biomolecular Techniques 15: 238-248.

Meyer KC, Rosenthal NS, Soergel P, Peterson K. (1998). “Neutrophils and low-grade inflammation in the seemingly normal aging human lung.” Mech Ageing Dev. 104(2): 169-81.

Miedema, I. and E. Feskens (1993). "Dietary determinants of long-term incidence of chronic non-specific lung diseases: the Zutphen Study." American Journal of Epidemiology 138: 37-45.

Mishra VK, Retherford RD, Smith KR. (1999). “Biomass cooking fuels and prevalence of tuberculosis in India.” Int J Infect Dis. 3(3): 119-129.

Molet S, Belleguic C, Lena H, Germain N, Bertrand CP, Shapiro SD, Planquois JM, Delaval P, Lagente V. (2005). “Increase in macrophage elastase (MMP-12) in lungs from patients with chronic obstructive pulmonary disease.” Inflamm Res. 54(1): 31-6.

Montaño M, Beccerril C, Ruiz V, Ramos C, Sansores RH, González-Avila G. (2004). “Matrix metalloproteinases activity in COPD associated with wood smoke.” Chest. 125(2): 466-72.

Monteiro HP, Arai RJ, Travassos LR. (2008). “Protein tyrosine phosphorylation and protein tyrosine nitration in redox signaling. Antioxid Redox Signal. May;10(5): 843-89.

Montuschi P, Collins JV, Ciabattoni G, Lazzeri N, Corradi M, Kharitonov SA, Barnes PJ. (2000). “Exhaled 8-isoprostane as an in vivo biomarker of lung oxidative stress in patients with COPD and healthy smokers.” Am J Respir Crit Care Med. Sep;162(3 Pt 1): 1175-7.

Montuschi P, Corradi M, Ciabattoni G, et al. (1999). “Increased 8-isoprostane, a marker of oxidative stress, in exhaled condensate of asthma patients.” Am J Respir Crit Care Med 160(1): 216-20.

Montuschi P, Kharitonov SA and Barnes PJ. (2001). “Exhaled carbon monoxide and nitric oxide in COPD.” Chest 120(2); 496-501.

Morel I, Hamon-Bouer C, Abalea V, Cillard P, Cillard J. (1997). “Comparison of oxidative damage of DNA and lipids in normal and tumor rat hepatocyte cultures treated with ferric nitrilotriacetate.” Cancer Lett. Oct 28;119(1): 31-6.

Morgan, W. and D. Stern (2005). "Outcome of asthma and wheezing in the first 6 years of life: follow-up through adolescence." American Journal of Respiratory and Critical Care Medicine 172: 1253-1258.

Morlá M, Busquets X, Pons J, Sauleda J, MacNee W, Agustí AG. (2006). “Telomere shortening in smokers with and without COPD.” Eur Respir J. 27(3): 525-8.

Morrison D, et al. (1999). “Epithelial permeability, inflammation, and oxidant stress in the air spaces of smokers.” Am J Respir Crit Care Med. 159: 473–479.

Morrison HM, Kramps JA, Burnett D, Stockley RA. (1987). “Lung lavage fluid from patients with alpha 1-proteinase inhibitor deficiency or chronic obstructive bronchitis: anti-elastase function and cell profile.” Clin Sci (Lond). 72(3): 373-81.

Morrison HM, Welgus HG, Stockley RA, Burnett D, Campbell EJ. (1990). “Inhibition of human leukocyte elastase bound to elastin: relative ineffectiveness and two mechanisms of inhibitory activity.” Am J Respir Cell Mol Biol. 2(3): 263-9.

Mortaz E, Folkerts G, Redegeld F. (2011). “Mast cells and COPD.” Pulm Pharmacol Ther. 24(4): 367-72.

Mudway IS, Behndig AF, Helleday R, Pourazar J, Frew AJ, Kelly FJ, Blomberg A. (2006). “Vitamin supplementation does not protect against symptoms in ozone-responsive subjects.“ Free Radic Biol Med. May 15;40(10): 1702-12.

Mudway IS, Blomberg A, Frew AJ, Holgate ST, Sandström T, Kelly FJ. (1999). "Antioxidant consumption and repletion kinetics in nasal lavage fluid following exposure of healthy human volunteers to ozone." Eur Respir J. Jun;13(6): 1429-38.

Mudway I, Duggan S, Venkataraman C, Habib G, Kelly F, Grigg J. (2005). "Combustion of dried animal dung as biofuel results in the generation of highly redox active fine particulates." Part Fibre Toxicol. 2: 6.

Mudway IS, Kelly FJ. (2000). "Ozone and the lung: a sensitive issue." Mol Aspects Med. Feb-Apr;21(1-2): 1-48.

Mudway IS, Krishna MT, Frew AJ, MacLeod D, Sandstrom T, Holgate ST, Kelly FJ. (1999). "Compromised concentrations of ascorbate in fluid lining the respiratory tract in human subjects after exposure to ozone." Occup Environ Med. Jul;56(7): 473-81.

Mudway IS, Stenfors N, Duggan ST, Roxborough H, Zielinski H, Marklund SL, Blomberg A, Frew AJ, Sandström T, Kelly FJ. (2004). "An in vitro and in vivo investigation of the effects of diesel exhaust on human airway lining fluid antioxidants." Arch Biochem Biophys. Mar 1;423(1): 200-12.

Mudway IS, Stenfors N, Blomberg A, Helleday R, Dunster C, Marklund SL, Frew AJ, Sandström T, Kelly FJ. (2001). "Differences in basal airway antioxidant concentrations are not predictive of individual responsiveness to ozone: a comparison of healthy and mild asthmatic subjects." Free Radic Biol Med. Oct 15;31(8): 962-74.

Mukhopadhyay CK, Mazumder B, Lindley PF, Fox PL. (1997). "Identification of the prooxidant site of human ceruloplasmin: a model for oxidative damage by copper bound to protein surfaces." Proc Natl Acad Sci U S A. Oct 14;94(21): 11546-51.

Müller KC, Welker L, Paasch K, Feindt B, Erpenbeck VJ, Hohlfeld JM, Krug N, Nakashima M, Branscheid D, Magnussen H, Jörres RA, Holz O. (2006). "Lung fibroblasts from patients with emphysema show markers of senescence in vitro." Respir Res. Feb 21;7:32.

Mulley T, Wiebel M, Schulz V, Ebert W. (1994). "Elastinolytic activity of alveolar macrophages in smoking-associated pulmonary emphysema." Clin Investig. 72(4): 269-76.

Nadeem A, Raj HG, Chhabra SK. (2005). "Increased oxidative stress and altered levels of antioxidants in chronic obstructive pulmonary disease." Inflammation. 29(1): 23-32.

Nel A, Xia T, Madler L, Li N. (2006). "Toxic potential of materials at the nanolevel." Science 311: 622-627.

Neurohr C, Lenz AG, Ding I, Leuchte H, Kolbe T, Behr J. (2003). "Glutamate-cysteine ligase modulatory subunit in BAL alveolar macrophages of healthy smokers." Eur Respir J. Jul;22(1): 82-7.

Nguyen NB, Callaghan KD, Ghio AJ, Haile DJ, Yang F (2006). “Hepcidin expression and iron transport in alveolar macrophages.” Am J Physiol Lung Cell Mol Physiol. Sep;291(3): L417-25.

Nicks ME, O'Brien MM, Bowler RP. (2011). “Plasma Antioxidants Are Associated with Impaired Lung Function and COPD Exacerbations in Smokers.” COPD. Jun 1. [Epub ahead of print]

Niewoehner DE, Kleinerman J, Rice DB. (1974). “Pathologic changes in the peripheral airways of young cigarette smokers.” N Engl J Med. 291(15): 755-8.

Nilsson UA, Bassen M, Sävman K, Kjellmer I. (2002). “A simple and rapid method for the determination of "free" iron in biological fluids.” Free Radic Res. Jun;36(6): 677-84.

Noël-Georis I, Bernard A, Falmagne P, Wattiez R. (2002) “Database of bronchoalveolar lavage fluid proteins.” J Chromatogr B Analyt Technol Biomed Life Sci. May 5;771(1-2): 221-36.

Nowak D, Kasielski M, Antczak A, Pietras T, Bialasiewicz P. (1999). “Increased content of thiobarbituric acid-reactive substances and hydrogen peroxide in the expired breath condensate of patients with stable chronic obstructive pulmonary disease: no significant effect of cigarette smoking.” Respir Med. Jun;93(6): 389-96.

Nualart, F.J.; Rivas, C.I.; Montecinos, V.P.; Godoy, A.S.; Guaiquil, V.H.; Golde, D.W.; Vera, J.C. (2003). “Recycling of vitamin C by a bystander effect.” J Biol Chem. 278(12): 10128-33.

Oberley-Deegan R.E, E.A. Regan, V.L. Kinnula and J.D. Crapo (2009). “Extracellular superoxide dismutase and risk of COPD.” COPD 6: 307–312.

Ochs-Balcom HM, Grant BJ, Muti P, Sempos CT, Freudenheim JL, Browne RW, McCann SE, Trevisan M, Cassano PA, Lacoviello L, Schunemann HJ. (2006). “Antioxidants, oxidative stress, and pulmonary function in individuals diagnosed with asthma or COPD.” Eur J. Clin Nutr. 60(8): 991–999.

O’Donnell R, Breen D, Wilson S. (2006). “Inflammatory cells in the airways in COPD.” Thorax 61: 448-454.

Ogilvie CM, Forster RE, Blakemore WS, Morton JW. (1954). “A standardized breath holding technique for the clinical measurement of the diffusing capacity of the lung for carbon monoxide.” J Clin Invest 36: 1-17.

Ohnishi, K, Takagi, M, Kurokawa, Y, et al. (1998). “ Matrix metalloproteinase-mediated extracellular matrix protein degradation in human pulmonary emphysema.” Lab Invest 78: 1077-1087.

Oppenheimer SJ. (2001). “Iron and its relation to immunity and infectious disease.” J Nutr. Feb;131(2S-2): 616S-633S.

Orozco-Levi M, Garcia-Aymerich J, Villar J, et al. (2006). “Wood smoke exposure and risk of chronic obstructive pulmonary disease.” Eur Respir J. 27(3): 542-546.

O'Shaughnessy TC, Ansari TW, Barnes NC, Jeffery PK. (1997). “Inflammation in bronchial biopsies of subjects with chronic bronchitis: inverse relationship of CD8+ T lymphocytes with FEV1.” Am J Respir Crit Care Med. 155(3): 852-7.

Osoata GO, Yamamura S, Ito M, Vuppusetty C, Adcock IM, Barnes PJ, Ito K. (2009). “Nitration of distinct tyrosine residues causes inactivation of histone deacetylase 2.” Biochem Biophys Res Commun. Jul 3;384(3): 366-71.

Papaioannou AI, Loukides S, Minas M, Kontogianni K, Bakakos P, Gourgoulianis KI, Alchanatis M, Papiris S, Kostikas K. (2011). “Exhaled breath condensate pH as a biomarker of COPD severity in ex-smokers.” Respir Res. May 22; 12:67.

Pappas RS. (2011). “Toxic elements in tobacco and in cigarette smoke: inflammation and sensitization.” Metallomics. Nov 1;3(11): 1181-98.

Park, J.B.; Levine, M. (1996). “Purification, cloning and expression of dehydroascorbic acid-reducing activity from human neutrophils: identification as glutaredoxin.” Biochem J. 315(Pt 3): 931-8.

Parmar JS, Mahadeva R, Reed BJ, Farahi N, Cadwallader KA, Keogan MT, Bilton D, Chilvers ER, Lomas DA. (2002). “Polymers of alpha(1)-antitrypsin are chemotactic for human neutrophils: a new paradigm for the pathogenesis of emphysema.” Am J Respir Cell Mol Biol. 26(6): 723-30.

Pérez-Padilla R, Pérez-Guzmán C, Báez-Saldaña R, Torres-Cruz A. (2001). “Cooking with biomass stoves and tuberculosis: a case control study.” Int J Tuberc Lung Dis. 5(5): 441-447.

Peters JM, Avol E, Gauderman WJ, et al. (1999). “A study of twelve Southern California communities with differing levels and types of air pollution. II. Effects on pulmonary function.” Am J Respir Crit Care Med. 159(3): 768-775.

Pillai SG, Ge D, Zhu G, Kong X, Shianna KV, Need AC, Feng S, Hersh CP, Bakke P, Gulsvik A, Ruppert A, Lødrup Carlsen KC, Roses A, Anderson W, Rennard SI, Lomas DA, Silverman EK, Goldstein DB;ICGN Investigators. (2009). “A genome-wide association study in chronic obstructive pulmonary disease (COPD): identification of two major susceptibility loci.” PLoS Genet. 5(3): e1000421.

Pillai SG, Kong X, Edwards LD, Cho MH, Anderson WH, Coxson HO, Lomas DA, Silverman EK; ECLIPSE and ICGN Investigators. (2010). “Loci identified by genome-wide association studies influence different disease-related phenotypes in chronic obstructive pulmonary disease.” Am J Respir Crit Care Med. 182(12): 1498-505.

Pizzichini E, Pizzichini MM, Gibson P, Parameswaran K, Gleich GJ, Berman L, Dolovich J, Hargreave FE. (1998). “Sputum eosinophilia predicts benefit from prednisone in smokers with chronic obstructive bronchitis.” Am J Respir Crit Care Med. 158(5 Pt 1): 1511-7.

Ponka, P. (1999). "Cellular iron metabolism." Kidney International 55(Supp. 69): s2-s11.

Pons AR, Sauleda J, Noguera A, Pons J, Barceló B, Fuster A, Agustí AG. (2005). “Decreased macrophage release of TGF-beta and TIMP-1 in chronic obstructive pulmonary disease.” Eur Respir J. 26(1): 60-6.

Praticò D, Basili S, Vieri M, Cordova C, Violi F, Fitzgerald GA. (1998). “Chronic obstructive pulmonary disease is associated with an increase in urinary levels of isoprostane F2-alpha-III, an index of oxidant stress.” Am J Respir Crit Care Med. Dec;158(6): 1709-14.

Prieto A, Reyes E, Bernstein ED, et al. (2001). “Defective natural killer and phagocytic activities in chronic obstructive pulmonary disease are restored by glycophosphopeptical (immunoferon).” Am J Respir Crit Care Med 163: 1578–1583.

Pryor WA. (1997). “Cigarette smoke radicals and the role of free radicals in chemical carcinogenicity.” Environ Health Perspect. Jun;105 Suppl 4: 875-82.

Pryor WA, Prier DG, Church DF. (1983). “Electron-spin resonance study of mainstream and sidestream cigarette smoke: nature of the free radicals in gas-phase smoke and in cigarette tar.” Environ Health Perspect 47: 345-355.

Pugh C, Hathwar V, Richards JH, Stonehuerner J, Ghio AJ (2005). “Disruption of iron homeostasis in the lungs of transplant patients.” J Heart Lung Transplant. Nov;24(11): 1821-7.

Rabe, K., S. Hurd, et al. (2007). "Global Strategy for the Diagnosis, Management, and Prevention of Chronic Obstructive Pulmonary Disease." American Journal of Respiratory and Critical Care Medicine 176: 532-555.

Raherison, C. and P. Girodet (2009). "Epidemiology of COPD." European Respiratory Review 18(114): 213-221.

Rahman, I. and S. Biswas (2006). "Oxidant and antioxidant balance in the airways and airways diseases." European Journal of Pharmacology 533: 222-239.

Rahman I, Biswas SK, Jimenez LA, Torres M, Forman HJ. (2005). “Glutathione, stress responses, and redox signaling in lung inflammation.” Antioxid Redox Signal. Jan-Feb;7(1-2): 42-59.

Rahman I, Gilmour PS, Jimenez LA, MacNee W. (2002). “Oxidative stress and TNF-alpha induce histone acetylation and NF-kappaB/AP-1 activation in alveolar epithelial cells: potential mechanism in gene transcription in lung inflammation.” Mol Cell Biochem. 234-235(1-2): 239-48.

Rahman I, MacNee W. (1999). “Lung glutathione and oxidative stress: implications in cigarette smoke-induced airway disease.” Am J Physiol. Dec;277(6 Pt 1): L1067-88.

Rahman, I. and W. MacNee (1996). "Role of Oxidants/Antioxidants in Smoking-Induced Lung Diseases." Free Radical Biology & Medicine 21(5): 669-681.

Rahman, I. and W. MacNee (1996). "Oxidant/antioxidant imbalance in smokers and chronic obstructive pulmonary disease." Thorax. Apr;51(4): 348-50.

Rahman I, Smith CA, Lawson MF, Harrison DJ, MacNee W. (1996). “Induction of gamma-glutamylcysteine synthetase by cigarette smoke is associated with AP-1 in human alveolar epithelial cells.” FEBS Lett. Oct 28;396(1): 21-5.

Rahman I, van Schadewijk AA, Crowther AJ, Hiemstra PS, Stolk J, MacNee W, De Boer WI. (2002). “4-Hydroxy-2-nonenal, a specific lipid peroxidation product, is elevated in lungs of patients with chronic obstructive pulmonary disease.” Am J Respir Crit Care Med. Aug 15;166(4): 490-5.

Rajendrasozhan S, Yang SR, Kinnula VL, Rahman I. (2008). “SIRT1, an anti-inflammatory and anti-aging protein, is decreased in lungs of patients with chronic obstructive pulmonary disease.” Am J Respir Crit Care Med. 177(8): 861-70.

Rappaport SM, Li H, Grigoryan H, Funk WE, Williams ER. (2011). “Adductomics: Characterizing exposures to reactive electrophiles.” Toxicol Lett. Apr 8.

Ratner AJ, Prince A. (2000). “Lactoperoxidase. New recognition of an "old" enzyme in airway defenses.” Am J Respir Cell Mol Biol. Jun;22(6): 642-4.

Rauniyar N, Prokai-Tatrai K, Prokai L. (2010). “Identification of carbonylation sites in apomyoglobin after exposure to 4-hydroxy-2-nonenal by solid-phase enrichment and liquid chromatography-electrospray ionization tandem mass spectrometry.” J Mass Spectrom. 45(4): 398-410.

Rauniyar N, Stevens SM, Prokai-Tatrai K, Prokai L. (2009). “Characterization of 4-hydroxy-2-nonenal-modified peptides by liquid chromatography-tandem mass spectrometry using data-dependent acquisition: neutral loss-driven MS3 versus neutral loss-driven electron capture dissociation.” Anal Chem. 81(2): 782-789.

Rautalahti M, Virtamo J, Haukka J, et al. (1997). “The effect of alpha-tocopherol and beta-carotene supplementation on COPD symptoms.” Am J Respir Crit Care Med. 156(5): 1447-1452.

Regalado J, Pérez-Padilla R, Sansores R, et al. (2006). “The effect of biomass burning on respiratory symptoms and lung function in rural Mexican women.” Am J Respir Crit Care Med. 174(8): 901-905.

Regan EA, Mazur W, Meoni E, Toljamo T, Millar J, Vuopala K, Bowler RP, Rahman I, Nicks ME, Crapo JD, Kinnula VL. (2011). “Smoking and COPD increase sputum levels of extracellular superoxide dismutase.” Free Radic Biol Med. Aug 1;51(3): 726-32.

Requena JR, Fu MX, Ahmed MU, Jenkins AJ, Lyons TJ, Baynes JW, Thorpe SR. (1997). “Quantification of malondialdehyde and 4-hydroxynonenal adducts to lysine residues in native and oxidized human low-density lipoprotein.” Biochem J. 322 (Pt 1): 317-325.

Ricciardolo FL, Caramori G, Ito K, Capelli A, Brun P, Abatangelo G, Papi A, Chung KF, Adcock I, Barnes PJ, Donner CF, Rossi A, Di Stefano A. (2005). “Nitrosative stress in the bronchial mucosa of severe chronic obstructive pulmonary disease.” J Allergy Clin Immunol. Nov;116(5): 1028-35.

Ricciardolo, F. and A. Di Stefano (2006). "Reactive nitrogen species in the respiratory tract." European Journal of Pharmacology 533: 240-252.

Rizvi SI, Maurya PK. (2007). “Alterations in antioxidant enzymes during aging in humans.” Mol Biotechnol. Sep;37(1): 58-61.

Rodriguez-Revenga, L. and P. Iranzo (2004). "A novel elastin gene mutation resulting in an autosomal dominant form of cutis laxa." Archives of Dermatology 140: 1135-1139.

Roginsky, V. and H. Stegmann (1994). "Ascorbyl radical as natural indicator of oxidative stress: quantitative regularities." Free Radical Biology & Medicine 17(2): 93-103.

Rojas-Martinez R, Perez-Padilla R, et al. (2007). “Lung function growth in children with long-term exposure to air pollutants in Mexico City.” Am J Respir Crit Care Med. 176(4): 377-384.

Romieu, I. and C. Trenga (2001). "Diet and obstructive lung diseases." Epidemiologic Reviews 23: 268-287.

Roos-Engstrand E, Ekstrand-Hammarström B, Pourazar J, Behndig AF, Bucht A, Blomberg A. (2009). “Influence of smoking cessation on airway T lymphocyte subsets in COPD.” COPD. 6(2): 112-20.

Roos-Engstrand E, Pourazar J, Behndig AF, Blomberg A, Bucht A. (2010). “Cytotoxic T cells expressing the co-stimulatory receptor NKG2 D are increased in cigarette smoking and COPD.” Respir Res. Sep 24;11: 128.

Roos-Engstrand E, Pourazar J, Behndig AF, Bucht A, Blomberg A. (2011). “Expansion of CD4+CD25+ helper T cells without regulatory function in smoking and COPD.” Respir Res. Jun 8; 12:74.

Rottoli P, Magi B, Cianti R, Bargagli E, Vagaggini C, Nikiforakis N, Pallini V, Bini L. (2005). “Carbonylated proteins in bronchoalveolar lavage of patients with sarcoidosis, pulmonary fibrosis associated with systemic sclerosis and idiopathic pulmonary fibrosis.” Proteomics. 5(10): 2612-2618.

Rubin, E., & Reisner, H. M. (2009). Essentials of Rubin’s Pathology (5th ed.). Philadelphia: Lippincott Williams & Wilkins.

Rumsey, S.C.; Kwon, O.; Xu, G.W.; Burant, C.F.; Simpson, I.; Levine, M. (1997). “Glucose transporter isoforms GLUT1 and GLUT3 transport dehydroascorbic acid.” J. Biol. Chem. 272(30): 18982-9.

Russell RE, Culpitt SV, DeMatos C, Donnelly L, Smith M, Wiggins J, Barnes PJ. (2002). “Release and activity of matrix metalloproteinase-9 and tissue inhibitor of metalloproteinase-1 by alveolar macrophages from patients with chronic obstructive pulmonary disease.” Am J Respir Cell Mol Biol. 26(5): 602-9.

Rutgers SR, Postma DS, ten Hacken NH, Kauffman HF, van Der Mark TW, Koëter GH, Timens W. (2000). “Ongoing airway inflammation in patients with COPD who do not currently smoke.” Thorax. Jan;55(1): 12-8.

Saetta M, Baraldo S, Corbino L, Turato G, Braccioni F, Rea F, Cavallesco G, Tropeano G, Mapp CE, Maestrelli P, Ciaccia A, Fabbri LM. (1999). “CD8+ve cells in the lungs of smokers with chronic obstructive pulmonary disease.” Am J Respir Crit Care Med. 160(2): 711-7.

Saetta M, Di Stefano A, Maestrelli P, Turato G, Ruggieri MP, Roggeri A, Calcagni P, Mapp CE, Ciaccia A, Fabbri LM. (1994). “Airway eosinophilia in chronic bronchitis during exacerbations.” Am J Respir Crit Care Med. 150(6 Pt 1): 1646-52.

Saetta M, Di Stefano A, Turato G, et al. (1998). “CD8+ T-lymphocytes in peripheral airways of smokers with chronic obstructive pulmonary disease.” Am J Respir Crit Care Med 157(3 pt 1): 822–826.

Saetta M, Di Stefano A, Maestrelli P, Ferraresso A, Drigo R, Potena A, Ciaccia A, Fabbri LM. (1993). “Activated T-lymphocytes and macrophages in bronchial mucosa of subjects with chronic bronchitis.” Am Rev Respir Dis. 147(2): 301-6.

Saetta M, Turato G, Facchini FM, Corbino L, Lucchini RE, Casoni G, Maestrelli P, Mapp CE, Ciaccia A, Fabbri LM. (1997). “Inflammatory cells in the bronchial glands of smokers with chronic bronchitis.” Am J Respir Crit Care Med. Nov;156(5): 1633-9.

Saha S, Brightling CE. (2006). “Eosinophilic airway inflammation in COPD.” Int J Chron Obstruct Pulmon Dis. 1(1): 39-47.

Sandford AJ, Chagani T, Weir TD, Connett JE, Anthonisen NR, Pare PD. (2001). “Susceptibility genes for rapid decline of lung function in the Lung Health Study.” Am J Respir Crit Care Med 163: 469–473.

Sandford AJ, Weir TD, Spinelli JJ, Pare PD. (1999). “Z and S mutations of the 1-antitrypsin gene and the risk of chronic obstructive pulmonary disease.” Am J Respir Cell Mol Biol 20: 287–291.

Sapey E, Stockley RA. (2006). “COPD exacerbations. 2: aetiology.” Thorax. 61: 250–258.

Sargeant LA, Jaeckel A, Wareham NJ . (2000). “Interaction of vitamin C with the relation between smoking and obstructive airways disease in EPIC Norfolk.” European Prospective Investigation into Cancer and Nutrition. Eur Respir J. 16(3): 397–403.

Sarir H, Mortaz E, Karimi K, et al. (2009). “Cigarette smoke regulates the expression of TLR4 and IL-8 production by human macrophages.” J Inflamm 6: 12–19.

Sato A, Hirai T, Imura A, Kita N, Iwano A, Muro S, Nabeshima Y, Suki B, Mishima M. (2007). “Morphological mechanism of the development of pulmonary emphysema in Klotho mice.” Proc Natl Acad Sci USA 104: 2361–2365.

Sato T, Seyama K, Sato Y, Mori H, Souma S, Akiyoshi T, Kodama Y, Mori T, Goto S, Takahashi K, Fukuchi Y, Maruyama N, Ishigami A. (2006). “Senescence marker protein-30 protects mice lungs from oxidative stress, aging and smoking.” Am J Respir Crit Care Med 174: 530–537.

Schikowski T, Sugiri D, et al. (2005). “Long-term air pollution exposure and living close to busy roads are associated with COPD in women.” Respir Res. 6: 152.

Schock, B.C.; Koostra, J.; Kwack, S.; Hackman, R.M.; Van Der Vliet, A.; Cross, C.E. (2004). “Ascorbic acid in nasal and tracheobronchial airway lining fluids.” Free Radic.Biol.Med. 37(9): 393-401.

Schunemann, H. and J. Freudenheim (2001). "Epidemiologic evidence linking antioxidant vitamins to pulmonary function and airway obstruction." Epidemiologic Reviews 23: 248-267.

Schwartz J, Weiss ST. (1994). “Relationship between dietary vitamin C intake and pulmonary function in the First National Health and Nutrition Examination Survey (NHANES I).” Am J Clin Nutr. 59(1): 110–4.

Schwartz J, Weiss ST. (1990). “Dietary factors and their relation to respiratory symptoms.” The Second National Health and Nutrition Examination Survey. Am J Epidemiol. 132(1): 67–76.

See SW, Wang YH, Balasubramanian R. (2007). “Contrasting reactive oxygen species and transition metal concentrations in combustion aerosols.” Environ Res. Mar;103(3): 317-24.

Segura-Valdez L, Pardo A, Gaxiola M, Uhal BD, Becerril C, Selman M. (2000). “Upregulation of gelatinases A and B, collagenases 1 and 2, and increased parenchymal cell death in COPD.” Chest. 117(3): 684-94.

Seixas NS, Robins TG, Attfield MD, Moulton LH. (1993). “Longitudinal and cross sectional analyses of exposure to coal mine dust and pulmonary function in new miners.” Br J Ind Med. 50(10): 929-937.

Sethi, S. (1999). "Infectious exacerbations of chronic bronchitis: diagnosis and management." Journal of Antimicrobial Chemotherapy 43(Supplement A): 97-105.

Sezer H, Akkurt I, et al. (2006). “A case-control study on the effect of exposure to different substances on the development of COPD.” Ann Epidemiol. 16(1): 59-62.

Shao MX, Nakanaga T, Nadel JA. (2004). “Cigarette smoke induces MUC5AC mucin overproduction via tumor necrosis factor-alpha-converting enzyme in human airway epithelial (NCI-H292) cells.” Am J Physiol Lung Cell Mol Physiol. 287(2): L420-7.

Shapiro SD. (2000). “Animal models for COPD.” Chest. 117(5 Suppl 1): 223S-227S.

Shigemura, M. and Y. Nasuhara (2010). "Levels of Transferrin in Bronchoalveolar Lavage Fluid in Sarcoidosis." Lung 188: 151-157.

Siegel SJ, Bieschke J, Powers ET, Kelly JW. (2007). “The oxidative stress metabolite 4-hydroxynonenal promotes Alzheimer protofibril formation.” Biochemistry. 46(6): 1503-1510.

Silverman, E. (2006). "Progress in chronic obstructive pulmonary disease genetics." Proceedings of the American Thoracic Society 3: 405-408.

Silverman EK, Mosley JD, Palmer LJ, Barth M, Senter JM, Brown A, Darzen JM, Kwiatkowski DJ,

Silverman EK, Speizer FE. (1996). “Risk factors for the development of chronic obstructive pulmonary disease.” Med Clin North Am. 80(3): 501-22.

Sin DD, Man SF. (2005). “Chronic obstructive pulmonary disease as a risk factor for cardiovascular morbidity and mortality.“ Proc Am Thorac Soc. 2(1): 8-11.

Sin DD, Wu L, Man SF. (2005). “The relationship between reduced lung function and cardiovascular mortality: a population-based study and a systematic review of the literature.” Chest 127: 1952–1959.

Sinden NJ, Stockley RA. (2010). “Systemic inflammation and comorbidity in COPD: a result of 'overspill' of inflammatory mediators from the lungs? Review of the evidence.” Thorax. 65(10): 930-6.

Skogstad M, Kjaerheim K, et al. (2006) “Cross shift changes in lung function among bar and restaurant workers before and after implementation of a smoking ban.” Occup Environ Med. 63(7): 482-487.

Smith K, Samet J, Romieu I, Bruce N. (2000). “Indoor air pollution in developing countries and acute lower respiratory infections in children.” Thorax 55: 518–532.

Smith, K.R., Biofuels, air pollution and health. A global review. Plenum Press, New York, 1987.

Smith LJ, Shamsuddin M, Sporn PH, Denenberg M, Anderson J. (1997). “Reduced superoxide dismutase in lung cells of patients with asthma.” Free Radic Biol Med. 1997;22(7): 1301-7.

Smith PK, Krohn RI, Hermanson GT, Mallia AK, Gartner FH, Provenzano MD, Fujimoto EK, Goeke NM, Olson BJ, Klenk DC. (1985). “Measurement of protein using bicinchoninic acid.” Anal Biochem. Oct;150(1): 76-85.

Smyth LJ, Starkey C, Vestbo J, Singh D. (2007). “CD4-regulatory cells in COPD patients. Chest.” Jul;132(1): 156-63.

Sommerhoff CP, Nadel JA, Basbaum CB, Caughey GH. (1990). “Neutrophil elastase and cathepsin G stimulate secretion from cultured bovine airway gland serous cells.” J Clin Invest. 85(3): 682-9.

Song Y, Klevak A, Manson JE, Buring JE, Liu S. (2010). “Asthma, chronic obstructive pulmonary disease, and type 2 diabetes in the Women's Health Study.” Diabetes Res Clin Pract. 90(3): 365-71.

Soriano, J., W. Maier, et al. (2000). "Recent trends in physician diagnosed COPD in women and men in the UK." Thorax 55: 789-794.

Spitz MR, Amos CI, Dong Q, Lin J, Wu X. (2008). “The CHRNA5-A3 region on chromosome 15q24-25.1 is a risk factor both for nicotine dependence and for lung cancer.” J Natl Cancer Inst. 100: 1552-1556.

Stanescu D, Sanna A, Veriter C, Kostianev S, Calcagni P, Fabbri L, et al. (1996). “Airways obstruction, chronic expectoration and rapid decline in FEV1 in smokers are associated with increased levels of sputum in neutrophils.” Thorax. 51: 267–271.

Starosta V, Griese M. (2006). “Oxidative damage to surfactant protein D in pulmonary diseases.” Free Radic Res. 40(4): 419-425.

Stavrides JC. (2006). “Lung carcinogenesis: pivotal role of metals in tobacco smoke.” Free Radic Biol Med. Oct 1;41(7): 1017-30.

Stemmler S, Arinir U, Klein W, Rohde G, Hoffjan S, Wirkus N, Reinitz-Rademacher K, Bufe A, Schultze-Werninghaus G, Epplen JT. (2005). “Association of intereukin-8 receptor polymorphisms with chronic obstructive pulmonary disease and asthma.” Genes Immun 6: 225–230.

Stites SW, Plautz MW, Bailey K, O'Brien-Ladner AR, Wesselius LJ. (1999). “Increased concentrations of iron and isoferritins in the lower respiratory tract of patients with stable cystic fibrosis.” Am J Respir Crit Care Med. Sep;160(3): 796-801.

Stone PJ, Calore JD, McGowan SE, Bernardo J, Snider GL, Franzblau C. (1983). “Functional alpha 1-protease inhibitor in the lower respiratory tract of cigarette smokers is not decreased.” Science. 221(4616): 1187-9.

Sugiri D, Ranft U, Schikowski T, Krämer U. (2006) “The influence of large-scale airborne particle decline and traffic-related exposure on children's lung function.” Environ Health Perspect. 114(2): 282-288.

Sundh J, Ställberg B, Lisspers K, Montgomery SM, Janson C. (2011). “Co-Morbidity, Body Mass Index and Quality of Life in COPD Using the Clinical COPD Questionnaire. COPD. 8(3): 173-81.

Sunyer J. (2001) “Urban air pollution and chronic obstructive pulmonary disease: a review.” Eur Respir J. 17(5): 1024-1033.

Syed BA, Sargent PJ, Farnaud S, Evans RW. (2006). “An overview of molecular aspects of iron metabolism.” Hemoglobin. 30(1): 69-80.

Sykiotis GP, Bohmann D. (2010). “Stress-activated cap'n'collar transcription factors in aging and human disease.” Sci Signal. 3(112): re3.

Szulakowski P, Crowther AJL, Jiménez LA, et al. (2006). “The effect of smoking on the transcriptional regulation of lung inflammation in patients with chronic obstructive pulmonary disease.” Am J Respir Crit Care Med. 174: 41-50.

Taggart C, Cervantes-Laurean D, Kim G, McElvaney NG, Wehr N, Moss J, Levine RL. (2000). “Oxidation of either methionine 351 or methionine 358 in alpha 1-antitrypsin causes loss of anti-neutrophil elastase activity.” J Biol Chem. Sep 1;275(35): 27258-65.

Taylor AE, Finney-Hayward TK, Quint JK, Thomas CM, Tudhope SJ, Wedzicha JA, Barnes PJ, Donnelly LE. (2010). “Defective macrophage phagocytosis of bacteria in COPD.” Eur Respir J. 35(5): 1039-47.

Tennant, P. and G. Gibson (2008). "Lifecourse predictors of adult respiratory function: results from the Newcastle Thousand Families Study." Thorax 63: 823-830.

Tetley TD. (1993). “New perspectives on basic mechanisms in lung disease. 6. Proteinase imbalance: its role in lung disease.” Thorax 48(5): 560-5.

Tietze F. (1969). “Enzymic method for quantitative determination of nanogram amounts of total and oxidized glutathione: applications to mammalian blood and other tissues.” Anal Biochem. Mar;27(3): 502-22.

Tkacova R, Kluchova Z, Joppa P, Petrasova D, Molcanyiova A. (2007). “Systemic inflammation and systemic oxidative stress in patients with acute exacerbations of COPD.” Respir Med. Aug;101(8): 1670-6.

Tobin, M. and P. Cook (1983). "Alpha-1 antitrypsin deficiency: the clinical and physiological features of pulmonary emphysema in subjects homozygous for Pi type Z." British Journal of Diseases of the Chest 77: 14-27.

Tollefson A.K, Oberley-Deegan R.E, Butterfield K.T, Nicks M.E, Weaver M.R, Remigio L.K, Decsesznak J, Chu H.W, Bratton, D.L, Riches D.W, Bowler R.P. (2010). “Endogenous enzymes (NOX and ECSOD) regulate smoke-induced oxidative stress.” Free Radic. Biol. Med. 49: 1937–1946.

Tomita K, Caramori G, Lim S, Ito K, Hanazawa T, Oates T, Chiselita I, Jazrawi E, Chung K F, Barnes P J, Adcock I M. (2002). “Increased p21CIP1/WAF1 and B cell lymphoma leukemia-xL expression and reduced apoptosis in alveolar macrophages from smokers.” Am J Respir Crit Care Med 166: 724–731.

Toyoda K, Nagae R, Akagawa M. (2007). “Protein-bound 4-hydroxy-2-nonenal: an endogenous triggering antigen of anti-DNA response.” J Biol Chem. 282(35): 25769-25778.

Tsuji T, Aoshiba K, Nagai A. (2006). “Alveolar cell senescence in patients with pulmonary emphysema.” Am J Respir Crit Care Med. 174(8): 886-93.

Tsukaguchi, H.; Tokui, T.; Mackenzie, B.; Berger, U.V.; Chen, X.Z.; Wang, Y.; Brubaker, R.F.; Hediger, M.A. (1999). “A family of mammalian Na+-dependent L-ascorbic acid transporters.” Nature. 399(6731): 70-5.

Traves S L, Culpitt S, Russell R EK, Barnes P J, Donnelly L E. (2002). “Elevated levels of the chemokines GRO-α and MCP-1 in sputum samples from COPD patients.” Thorax 57: 590–595.

Turato G, Zuin R, Miniati M, Baraldo S, Rea F, Beghé B, Monti S, Formichi B, Boschetto P, Harari S, Papi A, Maestrelli P, Fabbri LM, Saetta M. (2002). “Airway inflammation in severe chronic obstructive pulmonary disease: relationship with lung function and radiologic emphysema.” Am J Respir Crit Care Med. 166(1): 105-10.

Turner-Stokes, L. and C. Turton (1983). "Emphysema and cutis laxa." Thorax 38: 790-792.

Uchida K, Shiraishi M, Naito Y, Torii Y, Nakamura Y, Osawa T. (1999). “Activation of stress signaling pathways by the end product of lipid peroxiation.” J Biol Chem. 274: 2234–2242.

Uchida K, Szweda LI, Chae HZ, Stadtman ER. (1993). “Immunochemical detection of 4-hydroxynonenal protein adducts in oxidized hepatocytes.” Proc Natl Acad Sci U S A. 90(18): 8742-8746.

Ulker O, Yucesoy B, Demir O, Tekin I, Karakaya A. (2008). “Serum and BAL cytokine and antioxidant enzyme levels at different stages of pneumoconiosis in coal workers.” Hum Exp Toxicol. Dec;27(12): 871-7.

Ulrik, C. and P. Lange (1994). “Decline of lung function in adults with bronchial asthma.” American Journal of Respiratory and Critical Care Medicine 150: 629-634.

Ulrik, C. and V. Backer (1992). “A 10 year follow up of 180 adults with bronchial asthma: factors important for the decline in lung function.” Thorax 47: 14-18.

Ulrik, C. and V. Backer (1999). “Nonreversible airflow obstruction in life-long nonsmokers with moderate to severe asthma.” European Respiratory Journal 14: 892-896.

Ulvestad B, Bakke B, Eduard W, Kongerud J, Lund MB. (2001). “Cumulative exposure to dust causes accelerated decline in lung function in tunnel workers.” Occup Environ Med. 58(10): 663-669.

Van Berkel, G. J., McLuckey, S. A., Glish, G. L. (1991). “Preforming Ions in Solution via Charge-Transfer Complexation for Analysis by Electrospray Ionization Mass Spectrometry.” *Anal. Chem. 63*: 2064-2068.

Van den Dobbelsteen DJ, Nobel CS, Schlegel J, Cotgreave IA, Orrenius S, Slater AF. (1996). “Rapid and specific efflux of reduced glutathione during apoptosis induced by anti-Fas/APO-1 antibody.” J Biol Chem. Jun 28;271(26): 15420-7.

Van der Pouw Kraan TCTM, Kucukaycan M, Bakker AM, Baggen JMC, van der Zee JS, Dentener MA, Wouters EFM, Verweij CL. (2002). “Chronic obstructive pulmonary disease is associated with the –1055 IL-13 promoter polymorphism.” Genes Immun 3: 436–439.

Van der Vliet, A., C. O'Neill, et al. (1999). “Determination of low-molecular-mass antioxidant concentrations in human respiratory tract lining fluids.” American Journal Physiology (Lung Cellular & Molecular Physiology) 276: L289-296.

Van Maldergem, L. and E. Vamos (1988). “Severe congenital cutis laxa with pulmonary emphysema: a family with three affected siblings.” American Journal of Medical Genetics 31: 455-464.

Van Schayck, C. and E. Dompeling (1991). "Interacting effects of atopy and bronchial hyperresponsiveness on the annual decline in lung function and the exacerbation rate in asthma." The American Review of Respiratory Disease 144: 1297-1301.

Varraso R, Jiang R, Barr RG, Willett WC, Camargo CA Jr. (2007). “Prospective study of cured meats consumption and risk of chronic obstructive pulmonary disease in men.” Am J Epidemiol. 166(12): 1438-1445.

Vatrella A, Bocchino M, Perna F, Scarpa R, Galati D, Spina S, Pelaia G, Cazzola M, Sanduzzi A. (2007). “Induced sputum as a tool for early detection of airway inflammation in connective diseases-related lung involvement.” Respir Med. Jul;101(7): 1383-9.

Vera, J.C.; Rivas, C.I.; Fischbarg, J.; Golde, D.W. (1993). “Mammalian facilitative hexose transporters mediate the transport of dehydroascorbic acid.” Nature. 364(6432): 79-82.

Véronneau M, Comte B, Des Rosiers C. (2002). “Quantitative gas chromatographic-mass spectrometric assay of 4-hydroxynonenal bound to thiol proteins in ischemic/reperfused rat hearts.” Free Radic Biol Med. 33(10): 1380-1388.

Vignola, A. and F. Paganin (2004). “Airway remodelling assessed by sputum and high-resolution computed tomography in asthma and COPD.” European Respiratory Journal 24: 910-917.

Vogelmeier, C. and A. Gillissen (1996). “Use of secretory leukoprotease inhibitor to augment lung antineutrophil elastase activity.” CHEST 110: 261s-266s.

Vuppusetty C, Ito M, Elliot M, et al. (2007). “Expression of SIRT1, an anti-aging molecule, decreases with an increasing severity of COPD” [abstract]. Am J Respir Crit Care Med A553

Waeg G, Dimsity G, Esterbauer H. (1996). “Monoclonal antibodies for detection of 4-hydroxynonenal modified proteins.” Free Radic Res. 25(2): 149-159.

Wallace WA, Gillooly M, Lamb D. (1992). “Intra-alveolar macrophage numbers in current smokers and non-smokers: a morphometric study of tissue sections.” Thorax 47: 437–440.

Wally J, Buchanan SK. (2007). “A structural comparison of human serum transferrin and human lactoferrin.” Biometals. Jun;20(3-4): 249-62.

Wang X, Ghio AJ, Yang F, Dolan KG, Garrick MD, Piantadosi CA. (2002). “Iron uptake and Nramp2/DMT1/DCT1 in human bronchial epithelial cells.” Am J Physiol Lung Cell Mol Physiol. May;282(5): L987-95.

Walshe JM. (2012). “Serum 'free' copper in Wilson disease.” QJM. Feb 1. [Epub ahead of print]

Wang Y, Rosen H, Madtes DK, Shao B, Martin TR, Heinecke JW, Fu X. (2007). “Myeloperoxidase inactivates TIMP-1 by oxidizing its N-terminal cysteine residue: an oxidative mechanism for regulating proteolysis during inflammation.” J Biol Chem. 2;282(44): 31826-31834

Wang, Y.; Russo, T.A.; Kwon, O.; Chanock, S.; Rumsey, S.C.; Levine, M. (1997). “Ascorbate recycling in human neutrophils: induction by bacteria.” Proc. Natl. Acad. Sci. USA. 94(25): 13816-9.

Weinreich UM, Korsgaard J. (2008). “Bacterial colonisation of lower airways in health and chronic lung disease.” Clin Respir J. 2(2): 116-22.

Welch KD, Davis TZ, Van Eden ME, Aust SD. (2002). “Deleterious iron-mediated oxidation of biomolecules.” Free Radic Biol Med. Apr 1;32(7): 577-83.

Weldon, S. and P. McNally (2009). "Decreased levels of secretory leucoprotease inhibitor in the Pseudomonas-infected cystic fibrosis lung are due to neutrophil elastase degradation." The Journal of Immunology 183: 8148-8156.

Wen, D.W. Reid, D. Zhang, C. Ward, R. Wood-Baker and E.H. Walters. (2010). “Assessment of airway inflammation using sputum, BAL, and endobronchial biopsies in current and ex-smokers with established COPD.” Int J Chron Obstruct Pulmon Dis 5 pp. 327–334.

Wenzel, S. and L. Schwartz (1999). "Evidence that severe asthma can be divided pathologically into two inflammatory subtypes with distinct physiologic and clinical characteristics." American Journal of Respiratory and Critical Care Medicine 160: 1001-1008.

Whiteman M, Ketsawatsakul U, Halliwell B. (2002). “A reassessment of the peroxynitrite scavenging activity of uric acid.” Ann NY Acad Sci 962: 242–259.

WHO (2008). The top 10 causes of death (2004).

Wilk, J. and A. Herbert (2007). "Secreted modular calcium-binding protein 2 haplotypes are associated with pulmonary function." American Journal of Respiratory and Critical Care Medicine 175: 554-560.

Wilson, J.X. (2005). “Regulation of vitamin C transport.” Annu. Rev. Nutr. 25: 105-25.

Wilson, J.X. (2002). “The physiological role of dehydroascorbic acid. FEBS Lett. 527(1-3): 5-9.

Winkler, B.S.; Orselli, S.M.; Rex, T.S. (1994). “The redox couple between glutathione and ascorbic acid: a chemical and physiological perspective. Free Radic. Biol. Med. 17(4): 333-49.

Winterbourn, C. (1985). "Comparative reactivities of various biological compounds with myeloperoxidase-hydrogen peroxide-chloride, and similarity of the oxidant to hypochlorite." Biochim Biophys Acta 840(2): 204-210.

Wood, J. and D. Bellamy (1984). "Pulmonary disease in patients with Marfan syndrome." Thorax 39: 780-784.

Wood LG, Garg ML, Simpson JL, et al. (2005). “Induced sputum 8-isoprostane concentrations in inflammatory airway disease.” Am J Respir Crit Care Med 171(5): 426-30.

Wu J, An Y, Pu H, Shan Y, Ren X, An M, Wang Q, Wei S, Ji J. (2010). “Enrichment of serum low-molecular-weight proteins using C18 absorbent under urea/dithiothreitol denatured environment.” Anal Biochem. Mar; 398(1): 34-44.

Wysocki VH, Resing KA, Zhang Q, Cheng G. (2005). “Mass spectrometry of peptides and proteins.” Methods. 35(3): 211-222.

Xie J, Zhang Q, Zhong N, et al. (2009). “BAL fluid 8-isoprostane concentrations in eosinophilic bronchitis and asthma.” J Asthma. 46(7): 712-5.

Yamamoto C, Yoneda T, Yoshikawa M, Fu A, Tokuyama T, Tsukaguchi K, Narita N. (1997). “Airway inflammation in COPD assessed by sputum levels of interleukin-8.” Chest. 112(2): 505-10.

Yao H, Arunachalam G, Hwang J.W, Chung S, Sundar I.K, Kinnula V.L, Crapo, J.D, Rahman, I. (2010). “Extracellular superoxide dismutase protects against pulmonary emphysema by attenuating oxidative fragmentation of ECM.” Proc. Natl. Acad. Sci. U.S.A. 107: 15571–15576.

Yigla M, Berkovich Y, Nagler RM. (2007). “Oxidative stress indices in COPD - Bronchoalveolar lavage and salivary analysis.” Arch Oral Biol. Jan;52(1): 36-43.

Yin P, Jiang CQ, et al. (2007) “Passive smoking exposure and risk of COPD among adults in China: the Guangzhou Biobank Cohort Study.” Lancet. 370(9589): 751-757.

Yin Y, Solomon G, Deng C, Barrett JC. (1999). “Differential regulation of p21 by p53 and Rb in cellular response to oxidative stress.” Mol Carcinog 24: 15–24.

Yoritaka A, Hattori N, Uchida K, Tanaka M, Stadtman ER, Mizuno Y. (1996). “Immunohistochemical detection of 4-hydroxynonenal protein adducts in Parkinson disease.” Proc Natl Acad Sci U S A. Apr 2; 93(7): 2696-2701.

Yoshikawa M, Hiyama K, Ishioka S, Maeda H, Maeda A, Yamakido M. (2000). “Microsomal epoxide hydrolase genotypes and chronic obstructive pulmonary disease in Japanese.” Int J Mol Med 5: 49–53.

Young R, Hopkins R, Black P, Eddy C, Wu L, Gamble G, Mills G, Garrett J, Eaton T, Rees M. (2006). “Functional variants of antioxidant genes in smokers with COPD and in those with normal lung function.” Thorax. 61(5): 394–399.

Zanconato S, Carraro S, Corradi M, et al. (2004). “Leukotrienes and 8-isoprostane in exhaled breath condensate of children with stable and unstable asthma.” J Allergy Clin Immunol. 113(2): 257-263.

Zandvoort A, Postma DS, Jonker MR, Noordhoek JA, Vos JT, Timens W (2008). “ Smad gene expression in pulmonary fibroblasts: indications for defective ECM repair in COPD.” Respir Res 9: 83–93.

Zayasu K, Sekizawa K, Okinaga S, et al. (1997). “Increased carbon monoxide in exhaled air of asthmatic patients.” Am J Respir Crit Care Med. 156(4Pt1): 1140-43.

Zeng M, Wen Y, Liu LY, Wang H, Guan KP, Huang X. (2009). “Role of TNF-alpha, sTNF-R55 and sTNF-R75 in inflammation of acute exacerbations of chronic obstructive pulmonary disease.” Respiration 78(4): 399-403.

Zhou X, Jin Y, He X. (1995). “A study on the relationship between in-door air pollution and chronic obstructive pulmonary disease in Xuanwei County.” Zhonghua Yu Fang Yi Xue Za Zhi. 29(1): 38-40.

Zhu G, Warren L, Aponte J, Gulsvik A, Bakke P, Anderson WH, Lomas DA, Silverman EK, Pillai SG; International COPD Genetics Network (ICGN) Investigators. (2007). “The SERPINE2 gene is associated with chronic obstructive pulmonary disease in two large populations.” Am J Respir Crit Care Med. 176(2): 167-73.

Zhu X, Sayre LM. (2007). “Long-lived 4-oxo-2-enal-derived apparent lysine michael adducts are actually the isomeric 4-ketoamides.” Chem Res Toxicol. 20(2): 165-170.

Appendices

Appendix 1:

A1.1 Peptide ion fragmentation

Identification of peptide sequences by mass spectrometry involves the fragmentation of a peptide into smaller *m/z* fragments. The cleavage of a peptide occurs primarily through charge-directed pathways with the cleavage being initiated by a charge that is transferred to the locality of the cleavage site (Wysocki, 2005). Such transfers are facilitated by heteroatomic proton affinity, for example carbonyl oxygen situated along the backbone of a peptide. Traditional methods of activation result in differing cleavages; CID produces b- and y-ion pairs following cleavage across amide bonds whilst ECD and ETD activation produce c- and z-ion pairs following extensive cleavage along the backbone of the peptide for precursor ions with multiple charges. The scheme in Figure A1:1 below illustrates where these differing ions types occur in a model peptide.

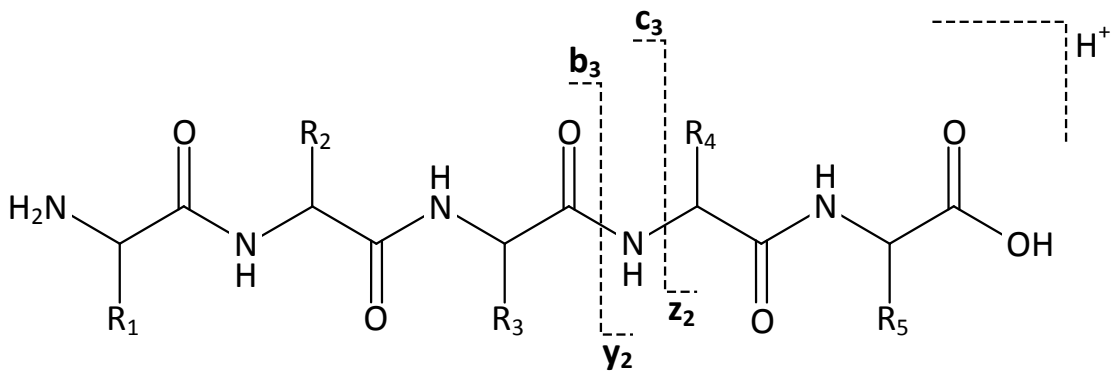

Figure A1.1: Fragmentation of the peptide main chain giving rise to the nomenclature of b/y and c/z ion types.

Cleavages of the backbone that occur at the amide bond result in b- and y-ions; retention of the charge at the N-terminus produces b-ions whilst retention of the charge at the C-terminus produces y-ions. When homolytic cleavage occurs at the N-C_α bond, c- and z-ions result; retention of the charge at the N-terminus produces c-ions whilst retention of the charge at the C-terminus produces z-ions.

A1.2 Ergodic and non-ergodic processes

Depending upon the activation method used, fragmentation will occur either in a sequence-dependent or sequence-independent manner. CID is described as an "ergodic" ion activation method in which fragmentation is sequence-dependent. As the rate of dissociation is slower than the rate of energy randomisation, the energy is redistributed in the vibrational modes of the ion. The energy is distributed among the internal modes of the ion in equal probability, leading to preferential cleavage of the weakest bonds. Under these conditions, the fragmentation is dependent upon the energy that is deposited and so for higher molecular-weight compounds an increased

energy transfer is desirable. ECD and ETD are described as “non-ergodic” ion activation methods in which fragmentation is sequence-independent. As the rate of dissociation is faster than the rate of energy randomisation, bond cleavage can be induced with minimal energy as the rapid dissociation occurs before the energy is randomised over the vibrational modes of the ion – a highly desirable feature for the fragmentation of high molecular-weight compounds. As a consequence the weakest bonds, such as post-translational modifications, remain intact and the sequence-independent fragmentation allows for greater characterisation of the peptide.